CHARLES UNIVERSITY

Faculty of Science

Study program: Developmental and Cell Biology

Mgr. Jakub Novák

Virulence of *Bordetella pertussis* from an Omics Perspective

Virulence *Bordetella pertussis* perspektivou omics přístupů

Dissertation thesis

Supervisor: Prof. Ing. Peter Šebo, CSc.

Institute of Microbiology of the ASCR, v.v.i.

Prague, 2021

Prohlašuji, že jsem tuto práci zpracoval samostatně, veškeré použité informační zdroje a literatura jsou citovány a uvedeny v seznamu citované literatury. Tato práce, ani její podstatná část, nebyla doposud předložena k získání jiného nebo stejného akademického titulu.

I hereby declare that I have elaborated and written this thesis independently, with the use of properly cited literature. All the resources used for writing of this thesis are listed in the reference list. Neither this thesis, nor its significant part, has been previously submitted for the purpose of obtaining another, or the same academic degree.

Praha, 21.02.2021

Mgr. Jakub Novák

I would like to thank my supervisor Prof. Peter Šebo for giving me the opportunity to work in his laboratory, for his ideas, scientific enthusiasm and the support of all what I was doing. I also wish to gratefully acknowledge all members of the Laboratory of Molecular Biology of Bacterial Pathogens and of the Laboratory of Post-Transcriptional Control of Gene Expression from the Institute of Microbiology ASCR, for the stimulating and highly cooperative environment and their friendly support and collaborations, which were of great help in accomplishing of this work. I am further grateful to our collaborators and friends from the Department of Molecular Pathology and Biology from the Faculty of Military Health Sciences, University of Defence in Hradec Kralove.

My apologies for the time when I was not available and my very special thanks for all the patience and support belong to my family.

1. Abstract

The Gram-negative aerobic coccobacillus *Bordetella pertussis* is one of the few exclusively human pathogens and the main causative agent of the respiratory infectious disease called pertussis, or whooping cough. Despite global vaccination programs, pertussis remains an important public-health burden and still accounts for over 100,000 infant deaths and over a dozen of millions of whooping cough cases every year. Substantial effort is devoted to studies on the mechanisms of action of virulence factors of *B. pertussis*, but the biology of interactions of *B. pertussis* with its human host remains largely underexplored. Evolution, genetics and adaptation of *B. pertussis* to the complex environment of human nasopharynx and the mechanisms enabling *B. pertussis* to overcome host innate and adaptive mucosal immune defenses, remain poorly understood. In such situations, unbiased exploratory omics approaches represent valuable tools for uncovering of unknown aspects of host-pathogen interactions and open the path to detailed analysis of virulence-underlying processes by mechanistic studies.

In this thesis, I am presenting the results of three omics projects on *B. pertussis* biology that involved high-throughput proteomics. In the inital phosphoprotemics project, we analyzed the kinase signaling pathways hijacked in murine dendritic cells upon elevation of cytosolic cAMP levels by the cell-invasive adenylyl cyclase enzyme activity of the adenylate cyclase toxin (CyaA) of *B. pertussis*. In the second project, we identified and characterized Bkd1, a novel bacterial lysine deacetylase enzyme and characterized the acetylome of *B. pertussis*. By serendipity, we isolated a *B. pertussis* mutant exhibiting an intriguing pleiotropic phenotype that we characterized in depth in the third project, using a combination of proteomic and transcriptomic approaches. We showed that a point mutation, that deregulates expression of a ribosomal protein operon and increases production of the alpha subunit of RNA polymerase, provokes global *B. pertussis* genome expression deregulation and suppresses virulence factor production through reduced production of the key virulence regulating transcription factor BvgA~P. This work led to exploration of intracellular survival of *B. pertussis* inside primary human macrophage cells and revealed that downregulation of virulence factor production may represent an adaptation strategy of *B. pertussis* towards persistence within an intracellular niche.

2. Abstrakt

Gram-negativní aerobní kokobacilus *Bordetella pertussis* je jedním z nemnoha výhradně lidských patogenů a hlavním původcem respiračního onemocnění zvaného pertuse, nebo také černý kašel. Navzdory globálním vakcinačním programům představuje pertuse stále významný problém pro veřejné zdraví - ročně padne za oběť tomuto onemocnění po celém světě na sto tisíc dětí a celkové počty hlášených případů dosahují desítek milionů. Také proto je výzkumu mechanismů působení faktorů virulence bakterie *B. pertussis* věnována významná pozornost. Navzdory tomu však zůstává biologie interakcí této bakterie se svým lidským hostitelem z velké části neznámá nebo jen málo prozkoumaná. Evoluce, genetika a adaptace *B. pertussis* komplexnímu prostředí lidského nosohltanu spolu s procesy umožňujícími této bakterii obejít hostitelské obranné mechanismy, ať už vrozené, tak i získané imunity, jsou doposud jen částečně popsány a pochopeny. V tomto kontextu představují omics přístupy velmi cenné nástroje k odhalení doposud neznámých aspektů interakcí mezi hostitelem a patogenem a otevírají tak cestu detailnější analýze regulace virulence pomocí mechanistických studií.

V této práci představuji výsledky tří omics projektů věnovaných biologii *B. pertussis*, postavených alespoň zčásti na tzv. high-throughput proteomických přístupech. V rámci prvního fosfoproteomického projektu jsme analyzovali kinázové signalizační dráhy v myších dendritických buňkách deregulovaných v důsledku zvýšení koncentrace cytosolického cAMP v důsledku aktivity adenylyl cyklázové aktivity adenylát-cyklázového toxinu (CyaA) bakterie *B. pertussis*. V rámci druhého projektu jsme identifikovali a charakterizovali Bkd1, novou bakteriální lyzinovou deacetylázu a charakterizovali acetylom *B. pertussis*. Zároveň jsme, šťastnou shodou okolností, izolovali mutantní kmen této bakterie, který vykazoval velmi zajímavý a pleiotropní fenotyp, který jsme následně charakterizovali v rámci třetího projektu a to za pomoci kombinace proteomických a transkriptomických přístupů. Ukázali jsme zde, že bodová mutace, která vedla k deregulaci exprese genů jednoho z operonů kódujících ribosomální proteiny a ke zvýšení produkce alfa-podjednotky RNA polymerázy, způsobila ve svém důsledku globální deregulaci genomu *B. pertussis* a snížení produkce virulenčních faktorů prostřednictvím snížené produkce klíčového regulačního faktoru BvgA~P. Tato práce také vedla k výzkumu

vnitrobuněčného přežívání *B. pertussis* uvnitř primárních lidských makrofágů a ukázala, že snížení produkce virulenčních faktorů může představovat jeden z mechanismů adaptace *B. pertussis* vedoucí k perzistentnímu přežívání uvnitř hostitelských buněk.

3. Contents

4. List of abbreviations

4E-BP1 eukaryotic translation initiation factor 4E (eIF4E)-binding protein 1

ACT adenylate cyclase toxin-hemolysin

AC adenylyl-cyclase enzyme (domain)

Ac-CoA acetyl-coenzyme A

AcK acetyl-lysine

AcP acetyl phosphate

AcuC acetoin utilization protein

APAHs acetylpolyamine amidohydrolases

ArnT glycosyl transferase ortholog

ATP adenosine triphosphate

BAL bronchoalveolar lavage

bhu *Bordetella* heme utilization

Bkd1 *Bordetella* lysine deacetylase (encoded by BP0960 gene)

bsc locus encoding components of the type III secretion injectosome

btr locus encoding type III regulatory proteins

BvgA response regulator protein of the BvgAS two-component regulatory system

BvgA~P phosphorylated BvgA

BvgS polydomain sensor histidine kinase BvgAS two-component regulatory system

cAMP 3′,5′-cyclic adenosine monophosphate

CD circular dichroism

CD- cluster of differentiation-

CDC Centers for Disease Control and Prevention

CoA Coenzyme A

CobB NAD+-dependent lysine deacetylase, sirtuin

COPD chronic obstructive pulmonary disease

CR3 complement receptor 3, the $\alpha_M\beta_2$ integrin CD11b/CD18, known also as Mac-1

CREB cAMP-response element binding protein

CRTC3 CREB-regulated transcription coactivator 3

CyaA adenylate cyclase toxin-hemolysin

DCs dendritic cells

DMEM Dulbecco's Modified Eagle Medium

DNT dermonecrotic toxin

EDTA ethylenediaminetetraacetic acid

EPAC Exchange Protein directly Activated by cAMP

FACS Fluorescence-Activated Cell Sorting

FBS/FCS fetal bovine/calf serum

FEP fluorinated ethylene propylene

FHA filamentous hemagglutinin

FIM fimbriae

FMLP N-formyl-L-methionyl-L-leucyl-L-phenylalanine

Giα α-subunit of the inhibitory G-protein

GNATs Gcn5-related N-acetyltransferases

GPCRs G-protein-coupled receptors

HDAC histone deacetylase

HDAH histone-like amidohydrolase

HIV Human Immunodeficiency Virus

HliD transcriptional regulator of *Salmonella* Pathogenicity Island 1

HK histidine kinase (domain)

HLA-DR human leucocyte antigen DR/MHC class II antigen

Hly hemolysin (moiety)

Hpt histidine phosphoryl transfer (domain)

hrp hypersensitive response and pathogenicity

HS human serum

hTECs human tracheobronchial epithelial cells

HTH helix–turn–helix (domain)

CheY response regulator of the chemotaxis

IAP islets-activating protein

IFN-γ interferon gamma

IL- interleukin-

IS insertion sequence

KATs lysine acetyltransferases

KDACs lysine deacetylases

LOS lipooligosaccharides

LPF lymphocytosis-promoting factor

LPS lipopolysaccharide

LpxA acyltransferase

LpxH pyrophosphohydrolase

LRT lower respiratory tract

M molar

MAPK mitogen-activated protein kinase

MASP2 mannose-binding protein-associated serine protease 2

M-CSF macrophage colony-stimulating factor

MDDCs monocyte-derived dendritic cells

MET methyltransferase

mTOR mammalian target of rapamycin

NAD nicotinamide adenine dinucleotide

NETs neutrophil extracellular traps

NF-κB nuclear factor kappa-light-chain-enhancer of activated B cells

NO nitric oxide

ORF open reading frame

PAS Per-ARNT-Sim domain

Pat protein acetyltransferase

PBMCs human peripheral blood mononuclear cells

PBS phosphate-buffered saline

PhoP/Q two-component system from *Salmonella* Typhimurium

PKA protein kinase A

PlrSR persistence in the lower respiratory tract sensor kinase/response regulator

PMLN polymorphonuclear leukocytes

(p)ppGpp guanosine tetra-/penta-phosphate

PRN pertactin

PRR proline-rich region

ptl secretion system locus for PTX

PTM post-translational modification

PTX pertussis toxin

Rpd3/Hda1 "classical" zinc-dependent deacetylases

Rec receiver (domain)

RGD Arg-Gly-Asp motif

RisA response regulator of RisAK two-component regulatory system

RisK cognate histidine kinase of RisA

RNAP RNA polymerase holoenzyme

rplN gene encoding 50S ribosomal protein L14

RPMI Roswell Park Memorial Institute Medium

RpoA alpha subunit of the DNA-dependent RNA polymerase

rpsD gene encoding 30S ribosomal protein S4

RTX Repeats-in-toxin (family)

SAXS small angle X-ray scattering

SHP Src homology domain 2 containing protein tyrosine phosphatase

SILAC stable isotope labelling by amino acids in cell culture

Sir2 NAD+-dependent deacetylases of Sir2 family

SNPs single nucleotide polymorphisms

SSM Stainer-Scholte medium

T1SS type 1 secretion system

T3SS type 3 secretion system

T4SS type 4 secretion system

TCS two-component regulatory system

TcfA tracheal colonization factor

TCT tracheal cytotoxin

TEER transepithelial electrical resistance

TGFβ transforming growth factor beta

TLR4 Toll-like receptor 4

TNF-α tumor necrosis factor α

UTR untranslated region

vag *vir* (/*bvg*)-activated gene

Vag8 *vir* (/*bvg*)-activated gene 8

VASP vasodilator-stimulated phosphoprotein

VFT Venus flytrap

VLA-5 very late antigen-5

VBNC viable but non-culturable

vrg *vir* (/*bvg*)-repressed gene

WHO World Health Organization

YfiQ acetyltransferase in E. coli

YopJ Yersinia outer protein J, acetyltransferase

5. Introduction

5.1 *Bordetellae*

Members of the *Bordetella* genus are mostly strictly aerobic Gram-negative bacteria with non-fermentative, asaccharolytic metabolism, due to the lack of genes for glycolytic enzymes, such as glucokinase, phosphofructokinase and fructose-1,6-bisphosphatase (Parkhill et al., 2003; von Wintzingerode et al., 2002). Together with the *Achromobacter* and *Alcaligenes* genera, *Bordetella* form a closely related group of species of β-Proteobacteria. To date, around 16 species of the *Bordetella* genus have been described and named, some of which being known animal pathogens or environmental colonizers (Weigand et al., 2019; von Wintzingerode et al., 2002). The current *Bordetella* phylogenetic tree is shown in Figure 1.

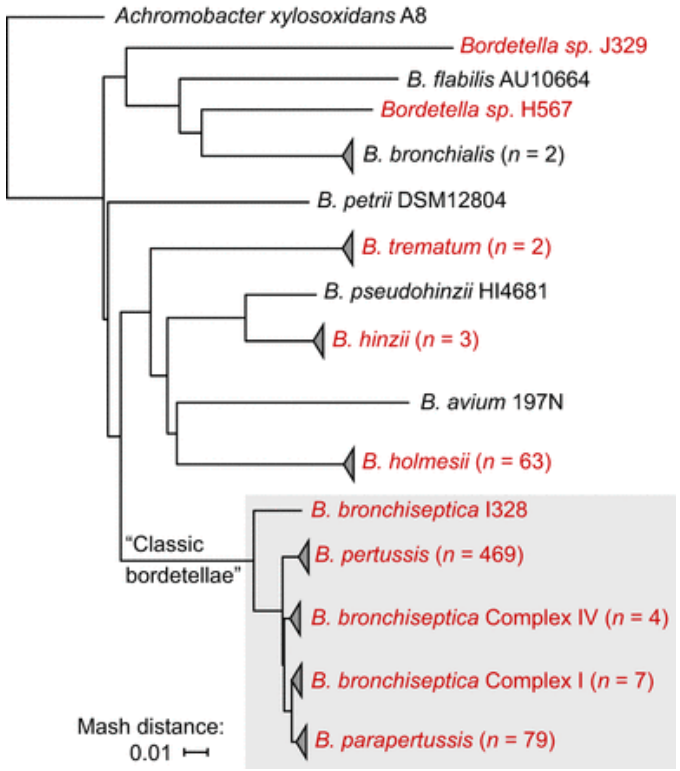

Figure 1: Phylogenetic tree of the *Bordetella* genus. Neighbor-joining tree of named and provisional *Bordetella* species for which the complete-genome sequences are available. The phylogenetic tree is based on pairwise mash distances and is rooted with *Achromobacter xylosoxidans*. Species that were sequenced at the CDC are listed in red. Triangles indicate collapsed nodes. Reprinted from Weigand et al. (Weigand et al., 2019)

The *Bordetella* genus includes species that are known human and animal pathogens. Other species of this genus can be found in the environment, including soil, water, sediments or plants, where soil and water seem to be the original source of the animal-adapted bacteria (Hamidou Soumana et al., 2017). Not surprisingly, the environmental *Bordetellae* species exhibit a higher genetic diversity. However, even some of the pathogenic animal-adapted species, such as *B. bronchiseptica* (Goodnow, 1980) and *B. hinzii* (Vandamme et al., 1995), are able to grow and proliferate in soil extracts at an even faster rate than the solely environmental bacterium *B. petrii* (Gross et al., 2008; Hamidou Soumana et al., 2017). Recent genomic analysis of 167 genomic sequences from different *Bordetella* species isolates, together with a set of 469 genomic sequences of *B. pertussis* isolates, revealed high rates of single nucleotide polymorphisms (SNPs). The *B. bronchiseptica* isolates can be divided into two main clades (Complex I and Complex IV), in which their representative isolates differ by about 35,000 SNPs between each clade. The isolates of *B. hinzii* and *Bordetella trematum* were found to differ by about 10,000 SNPs. In contrast, the isolates of *B. pertussis* (complex II), *B. parapertussis* (complex III), and *B. holmesii* are genetically quite monomorphic, differing by even less than 100 SNPs (Weigand et al., 2019).

5.2 *"Classical" Bordetellae*

The pathogenic *B. pertussis, B. parapertussis*, and *B. bronchiseptica* species adapted to human and/or animals, are for historical reasons called the "classical" *Bordetellae* and previously were considered by some to be subspecies within a single species (von Wintzingerode et al., 2002). The whole-genome sequencing analysis of their reference strains (Figure 2) revealed that *B. pertussis* and *B. parapertussis* evolved independently from different *B. bronchiseptica*-like ancestors and that this evolution was linked to a large-scale gene loss and gene inactivation by mutations or by gene disruption by insertion sequence (IS) elements (Parkhill et al., 2003; Preston et al., 2004). Only about half of the "pan-genome" was found to be conserved in the examined strains (Park et al., 2012). All three *Bordetella* species produce an array of virulence factors, comprising numerous toxins, adhesins or components of different secretion systems. However, only genes for the adhesins pertactin (PRN) and filamentous hemagglutinin (FHA) and for components of type 3 secretion system (T3SS) were found to be conserved in all examined strains of

the three human/animal-pathogenic species (Park et al., 2012; Parkhill et al., 2003). Genes encoding for the virulence factors often carry internal sequence variations or differ in their regulation. This can be best illustrated on the example of the pertussis toxin (PTX), which was found to be expressed only in *B. pertussis*, even if the operon containing the genes for its subunits and the genes for the secretory apparatus involved in PTX excretion is present also in the genomes of *B. parapertussis* and *B. bronchiseptica* (Aricò and Rappuoli, 1987; Parkhill et al., 2003). Analysis of the promoter regions revealed that the majority of changes in nucleotide sequences were acquired only by *B. pertussis*, with some of these acquired mutations enhancing either the promoter or BvgA-binding sites affinities for their respective binding proteins. (Boucher and Stibitz, 1995; Parkhill et al., 2003).

Table 1 General features of the genomes of *B. pertussis*, *B. parapertussis* and *B. bronchiseptica*

	B. pertussis	*B. parapertussis*	*B. bronchiseptica*
Size (bp)	4,086,186	4,773,551	5,338,400
G+C content (%)	67.72	68.10	68.07
Coding sequences	3,816	4,404	5,007
Pseudogenes	358 (9.4%)	220 (5.0%)	18 (0.4%)
Coding density (intact genes)	82.9%	86.6%	91.4%
Coding density (all genes)	91.6%	92.2%	92.0%
Average gene size (bp)	978	987	978
rRNA operons	3	3	3
tRNA	51	53	55
IS*481*	238	0	0
IS*1001*	0	22	0
IS*1002*	6	90	0
IS*1663*	17	0	0

Figure 2: General characteristics of the genomes of reference strains of *B. pertussis*, *B. parapertussis* and *B. bronchiseptica*. Reprinted from (Parkhill et al., 2003)

The genome composition largely reflects the extent of host-adaptation of the individual bacterial species. As far as we know, *B. pertussis* is a strictly human-adapted pathogen that is capable to cause a typical whooping cough disease also in hominids (Gustavsson et al., 1990) and in some of non-human primates, such as in the olive baboon *Papio anubis* (Merkel and Halperin, 2014). *B. parapertussis* was originally considered to be also a strictly human-adapted pathogen, until it was found in sheep (Cullinane et al., 1987). The ovine strains differ in the regulation of *in vitro* expression of several virulence factors and contain more genetic material, including a unique lipopolysaccharide (LPS) locus that differs from that of human *B. parapertussis* isolates (Brinig et al., 2006). In contrast, *B. bronchiseptica* has the ability to colonize a variety of animal hosts, either mammalian or avian (Register et al., 2015) and retained its ability to grow and proliferate in (sterilized) soil extract (Hamidou Soumana et al., 2017). Most interestingly, *B. bronchiseptica* not only survives and grows inside the amoeba *Dictyostelium discoideum*, but it can also hijack its complex life cycle for dissemination within the sori of the multicellular fruiting body of *D. discoideum*, with the amoebae possibly serving as an environmental reservoir of *B. bronchiseptica* (Taylor-Mulneix et al., 2017). In contrast, no extra-host environmental niche was found for *B. pertussis* and *B. parapertussis* (Hamidou Soumana et al., 2017).

5.3 *Bordetella pertussis*

Due to the limited genetic variability of its genome, *B. pertussis* is considered to be a monomorphic pathogen (Belcher and Preston, 2015; Mooi, 2010). The limited set of polymorphic genomic regions with the highest SNP densities comprises gene for pertussis toxin subunit A (*ptxA*), the *cysB* gene encoding transcriptional regulator involved in sulfur metabolism, or promoters of pertussis toxin and *bvgAS* operons (Bart et al., 2014). The largest number of polymorphisms is observed in the promoter region (ptxP) of the *ptx-ptl* operon and for the *prn* and *ptxA* alleles encoding the S1 subunit of pertussis toxin (PTX) and the adhesin pertactin (PRN), the two key protective antigens of current acellular pertussis vaccines (Bart et al., 2014). Consequently, with the introduction of acellular vaccines (ACVs), new strains lacking some of its components – especially PRN, but occasionally also filamentous hemagglutinin (FHA) or PTX have emerged (Bouchez et al., 2009; Hegerle and Guiso, 2014). The genome of *B. pertussis* exhibits an enormous

structural fluidity due to the promiscuous expansion of an IS481 mobile genetic element (Mclafferty et al., 1988). This is present often in more than 240 copies per genome of a *B. pertussis* isolate. Homologous recombination between IS481 elements yields chromosomal rearrangements (Figure 3) consisting mainly of large inversions centered on the replication origin or terminus of the IS481 (Weigand et al., 2017). It appears that it was the expansion of IS elements, together with the genome reduction, which accompanied - if not even enabled - the niche jump and *B. pertussis* adaptation to the human host (Belcher and Preston, 2015). Interestingly, similar scenario likely occurred also during the emergence of *B. parapertussis* (Parkhill et al., 2003) and *B. holmesii* (Belcher and Preston, 2015; Harvill et al., 2014), as their chromosome structures also vary between isolates (Weigand et al., 2019). *B. pertussis* seems to have adapted to the human host relatively recently and it is very likely still undergoing adaptive evolution (Belcher and Preston, 2015). This represents a unique opportunity to observe and analyze the evolution of a "balanced relationship" between *B. pertussis* and its human host.

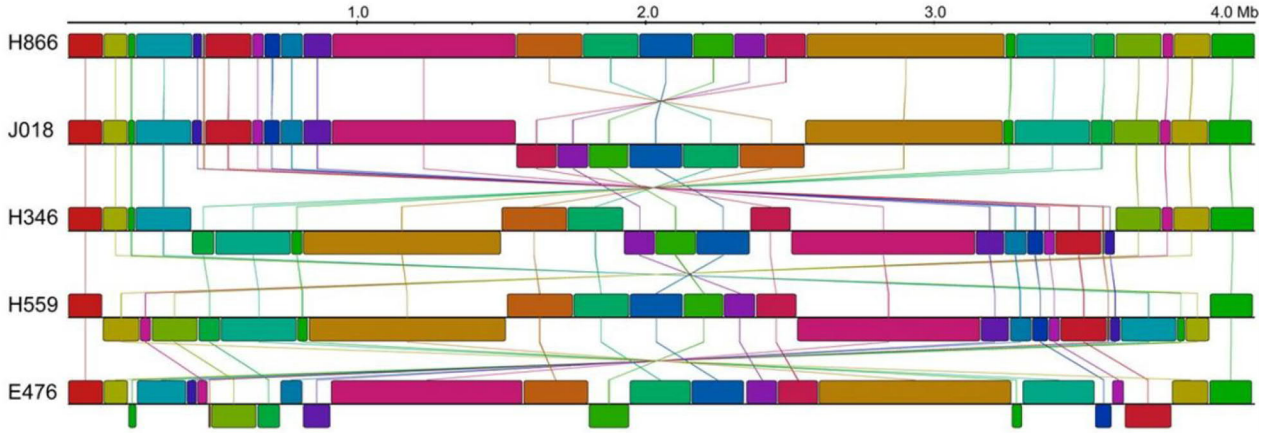

Figure 3: Schematic representation of structural variability among the genomes of different isolates of *B. pertussis*. Mainly large inversions are shaping the order and orientation of genome content in recent circulating isolates (e.g. H866, J018, H346, and H559), which then differs greatly from that of vaccine reference strains, such as Tohama I (E476). Reprinted from (Weigand et al., 2017).

5.4 Whooping cough disease

Pertussis or whooping cough disease is a serious and highly contagious acute respiratory infectious illness that used to be the first cause of infant mortality in developed

countries in the pre-vaccine era. The infection is transmitted *via* (bacteria-containing) aerosol droplets, produced by coughing and sneezing and the main causative agent of pertussis is the Gram-negative aerobic coccobacillus *Bordetella pertussis* (Melvin et al., 2014). Occasionally, the closely related bacterium *Bordetella parapertussis* is isolated as the etiological agent of less severe whooping cough disease with shorter-lasting symptoms (Mastrantonio et al., 1998). Due to absence of pertussis toxin production, *B. parapertussis* infections do not provoke the critical pertussis bronchopneumonia in infants. *Bordetella bronchiseptica* can also be transmitted from infected mammals to humans and can cause a respiratory disease in elderly or immunocompromised individuals (Mattoo and Cherry, 2005). Similarly, *Bordetella holmesii* was isolated from human patients with pertussis-like symptoms (Mattoo and Cherry, 2005).

Pertussis disease remains endemic in all countries and exhibits epidemic cycles with a periodicity of 3-4 years (WHO, 2015). Development of efficacious pertussis vaccines, formulated from whole killed bacterial cells (wP vaccines), enabled in the second half of the past century the introduction of world-wide vaccination programs that led to a steep decrease of global pertussis incidence. It was estimated that in 2014 an 86% global vaccination coverage with 3 doses of a pertussis-containing vaccine was reached (WHO, 2015). However, in the last decade of the past century the efficient but reactogenic wP vaccines were replaced in the wealthiest countries by the less reactogenic and also less efficacious subunit acellular pertussis (aP) vaccines, which resulted in the current pertussis resurgence observed in the most developed countries (Rocha et al., 2015; Sealey et al., 2016; Snyder and Fisher, 2012). This represents serious health threat especially for infants and a recent model estimated that 24.1 million cases of pertussis occurred globally in 2014, resulting in 160,700 deaths of children younger than 5 years of age (Yeung et al., 2017).

Interestingly, *B. pertussis* has not been reported to cause septicemia, by difference to the opportunistic pathogen species *B. trematum* (Majewski et al., 2016), *B. holmesii* (Shepard et al., 2004) or *B. bronchiseptica* (Sans et al., 1991). Pertussis infections remain restricted to the respiratory tract and the incubation period of pertussis can range from 5-21 days (but usually lasts for 7-10 days). Asymptomatic or only mildly symptomatic

infections are common in vaccinated populations or convalescent older people and only about 1 % of them gets diagnosed and reported (Chlibek et al., 2017).

Infants younger than 12 months are at the highest risk of complications and death from pertussis and even in the highly vaccinated populations, such as that of the United States, the average annual infant mortality rate due to the pertussis used to be 3.8 per 1,000,000 live births, while for children younger than 2 months, the mortality rate was found to increase to 13.1 per 1,000,000 live births (Haberling et al., 2009). Therefore, since 2012, maternal pertussis immunization with a Tdap (tetanus, diphtheria, pertussis) vaccine is offered to pregnant women in the third trimester of gestation, in order to elicit maternal antibodies that cross the placenta into fetus and protect the infant until vaccination (Baxter et al., 2017; Vygen-Bonnet et al., 2020).

The classical clinical manifestations of pertussis start with common cold-like symptoms of the catarrhal phase of the disease that is characterized by rhinorrhea, lacrimation and mild cough in the absence of elevated temperature of fever. Pertussis is the only major infectious disease that is not accompanied by fever. The cold-like symptoms are thus often underestimated and the disease is most of the time recognized too late to be effectively treated by antibiotics. In the smallest infants, below 3 month of age, that are typically too young to be vaccinated, the infection can rapidly reach lungs and provoke a sudden and life-threatening (critical) bronchopneumonia that is accompanied by hyperleukocytosis and pulmonary hypertension, eventually leading to heart failure. In this age group, ~40% of infected infants require hospitalization and about 1% of the hospitalized infants still dies, often due to complications caused by opportunistic secondary infections (CDC, 2019; Kline et al., 2013).

More typically, the catarrhal phase eventually progresses into the so-called paroxysmal stage, with its typical coughing fits consisting of five to ten uninterrupted coughs in a row followed by a “whoop” sound and often accompanied by post-tussive vomiting. Manifestations of the paroxysmal phase may vary largely, depending on the individual, and can be preceded by apnea and cyanosis in very young infants, while in immunized adolescents and adults only persistent coughing would typically be present (Kimberlin et al., 2015; Mattoo and Cherry, 2005; WHO, 2015). Paroxysms can be accompanied by cyanosis, salivation or lacrimation. Depending on the intensity of coughing fits, these might lead to variety of other symptoms, including pneumothorax, pneumomediastinum,

subcutaneous emphysema, superficial petechial hemorrhage, rib fracture, rectal prolapse or intracranial hemorrhage, with 0.4 % of hospitalized infants developing encephalopathy. As paroxysms interfere with sleep or food intake, they might lead to malnutrition and/or sleep deprivation (Snyder and Fisher, 2012). Other major complications of pertussis include pneumonia, seizures or acute pertussis encephalopathy (Snyder and Fisher, 2012; WHO, 2015). In the following convalescent phase, respiratory tract integrity is reestablished and symptoms are slowly vanishing. This phase can last from weeks to months. In the whole course of the disease, there is virtually no fever or just minimal and between the paroxysms, the patients look normal, without any obvious problems (Kimberlin et al., 2015; Mattoo and Cherry, 2005).

5.5 Regulation of virulence of *B. pertussis*

5.5.1 Master regulator BvgAS two-component system

The expression of virulence factors in *B. pertussis* is regulated by environmental cues, such as changes in the temperature or at high concentrations of specific ions in the process called antigenic modulation (Lacey, 1960). This is due to activity of two genes of the *bvgAS* locus (originally called *vir* and *mod*) the products of which regulate two sets of *Bordetella* genes – the *vir*-activated genes (*vag* loci) and *vir*-repressed genes (*vrg* loci) (Knapp and Mekalanos, 1988; Weiss et al., 1983, 1989). These two genes encode a bacterial Two Component System (TCS) that consists of the transmembrane sensory histidine kinase BvgS and the response regulator BvgA protein, which contains a C-terminal DNA-binding helix–turn–helix domain (Figure 4). When bacteria are grown under the standard laboratory conditions, at temperatures of the human body (33 to 37°C) on Bordet-Gengou blood agar plates, the BvgAS system is active by default and addition of negative modulators, such as >2mM concentrations of nicotinic acid or of >5mM sulfate ions is needed for a regulatory switch. Nicotinic acid binding, or ionogenic and electrostatic effects (e.g. of sulfate ions) trigger a structural alteration of the periplasmic moiety of the BvgS protein that harbors two atypical bi-lobed Venus flytrap domains (VFT1 and VFT2) with pairs of mobile jaws delimiting a binding cavity. By default, the VFT1 is open and VFT2 is closed, providing an activating signal transmitted mechanically through the transmembrane segment and the PAS domain to the cytoplasmic histidine kinase domain.

This is antagonized by nicotinic acid and opening of the VFT2 domain (Dupré et al., 2015; Herrou et al., 2010). Recently, it was shown that the domain called PAS also serves in the inactivation of BvgS in *B. bronchiseptica* in the absence of PlrS kinase activity *in vivo* (Sobran and Cotter, 2019).

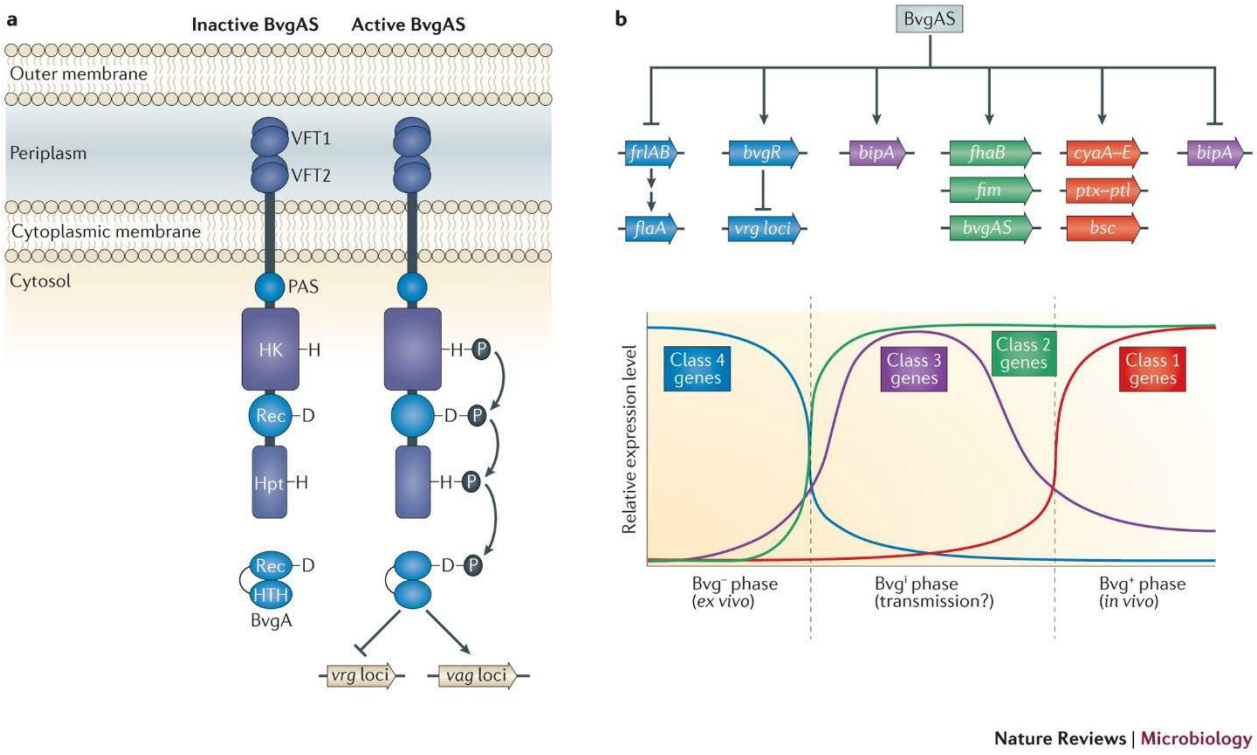

Figure 4: Scheme of the BvgAS two-component regulatory system. (A) Histidine sensor kinase BvgS contains two venus flytrap domains (VFT1 and VFT2), which are located in the periplasm, a transmembrane domain, a PAS domain, a histidine kinase domain (HK), a receiver domain (Rec) and a histidine phosphoryl transfer domain (Hpt). BvgS phosphorylates its response regulator BvgA that has an N-terminal Rec and a C-terminal helix–turn–helix domain (HTH). When active, BvgS becomes autophosphorylated at a conserved histidine and this phosphoryl group is then transferred in a phosphorelay on the other domains to the Rec domain of BvgA. Phosphorylated BvgA (BvgA-P) dimerizes and activates or represses the transcription of individual genes. **(B)** BvgAS controls four classes of genes and three distinct phenotypic phases - the Bvg^+ phase (maximal expression of genes that encode adhesins and toxins and minimal expression of class 3 and class 4 genes), Bvg^- phase (maximal expression of class 4 genes and minimal expression of class 1, class 2 and class 3 genes) and Bvg^i phase (maximal expression of class 2 and class 3 genes and minimal expression of class 1 and class 4 genes. Reprinted and adapted from (Melvin et al., 2014).

Under non-modulating conditions, a multistep phosphorylation cascade (a phosphorelay) is operating, yielding phosphorylation of the BvgA response regulator. The activated BvgA~P then acts as a transcriptional regulator (Decker et al., 2012). Both phosphorylated and non-phosphorylated forms of BvgA are able to dimerize and form stable complexes with the RNA polymerase holoenzyme (RNAP) on the target promoters and the phosphorylation state of BvgA regulates the conformation and binding affinities of BvgA dimers, rather than the stability of its complexes with RNAP. While the BvgA~P dimers promote formation of typical transcription initiation complexes, the complexes of non-phosphorylated BvgA dimers with RNAP produce higher amounts of very short abortive transcripts and are unable to generate full-length transcripts. This regulatory mechanism allows the bacteria to quickly respond to actual environmental cues (Boulanger et al., 2015). The *bvgR* gene immediately adjacent to *bvgS* is transcribed in the opposite direction to *bvgAS* genes and encodes the BvgR protein involved in regulation of the so-called *bvg*-repressed (*vrg*) genes (Merkel et al., 1998a). This mode of regulation, originally described as antigenic modulation by Lacey (Lacey, 1960) allows for a continuum of regulatory states with the three prominent Bvg^+, Bvg^- and Bvg^i phases (Figure 4). The Bvg^+ phase is both necessary and sufficient for respiratory infection in the mouse intranasal challenge model (Martinez de Tejada et al., 1998) and occurs under non-modulating conditions, at the temperature of the human respiratory tract. BvgS is fully active in this phase and most of the virulence-related adhesins and toxins (class 1 genes – e.g. *cyaA* or *ptxA* and class 2 genes – e.g. *fhaB*, *fim2/3* or *bvgAS*) are expressed. Bvg^i (intermediate) phase represents a transition phase, when the BvgAS phosphorelay is semi-active. In this phase, some of the Bvg-activated factors are still expressed (class 2 genes), while others are repressed (class 1 genes and class 4 genes – e.g. vrgs) (Cotter and Miller, 1994; Decker et al., 2012; Moon et al., 2017). During the Bvg^i phase, a maximal expression of the gene subset called class 3 genes (e.g. *bipA*) occurs (Stockbauer et al., 2001). Interestingly, a dual regulatory role of BvgA was described for the class 3 gene *bipA*. BvgA~P binds with high affinity the *bipA* promoter upstream from the RNAP binding site and activates its transcription. This is followed by a secondary low-affinity binding of BvgA~P to sequences immediately downstream from RNAP binding site. Such secondary BvgA~P binding then inhibits initiation and/or elongation of the *bipA* transcript (Williams et al., 2005). The exact biological role of Bvg^i phase is not clear, although it is

hypothesized that this phase might be important for aerosol transmission between hosts (Cotter and Miller, 1997; Martinez de Tejada et al., 1998; Stockbauer et al., 2001; Vergara-Irigaray et al., 2005). Under the modulating conditions, i.e. in response to the presence of 50 mM $MgSO_4$ or at temperatures below 25°C, the bacteria enter the Bvg^- phase, which is characterized by repression of virulence-related genes (classes 1-3) and maximal expression of class 4 genes (*vrgs*) (Lacey, 1960; Melvin et al., 2014; Moon et al., 2017; Scarlato and Rappuoli, 1991). The variation between Bvg^+ and Bvg^- phases also occurs spontaneously at a rather high frequency (~10^{-6} per generation per cell) due to chromosome replication errors that cause a frameshifting expansion or retraction of a C-rich homopolymeric tract in the bvgS open reading frame (Gogol et al., 2007; Stibitz et al., 1989). Enhanced survival of Bvg^- *B. bronchiseptica* in the nutrient-poor environment indicated that the Bvg^- phase might be important for adaptation of bordetellae to a specific niche inside their hosts or in their environmental reservoirs (Cotter and Miller, 1994). Indeed, recently a key role of the Bvg^- phase in *B. bronchiseptica* survival and dissemination during its infectious life cycle on the amoeba *Dictyostelium discoideum* was demonstrated (Taylor-Mulneix et al., 2017). However, no such example of a particular host-niche, or of specific environment in which the Bvg^- phase would play a role in the infectious cycle of *B. pertussis*, has been demonstrated yet and its biological relevance (if any) remains to be clarified. The conservation of phase variation is largely considered to be an evolutionary remnant in *B. pertussis*. However, long-term follow-up of experimentally infected non-human primates revealed accumulation of Bvg^- phase-locked *B. pertussis* bacteria in the upper respiratory tract over several months post infection, suggesting a selective pressure for loss of virulence factor production in establishment of persistent asymptomatic infection (Karataev et al., 2016). The recent analysis of the BvgAS regulon further supported a possible role of the Bvg^- phase in bacterial survival, transmission, and/or persistence (Moon et al., 2017).

5.5.2 RisA/RisK

Originally described in *B. bronchiseptica*, the BvgAS-independent *risAS* locus was found to play a role in bacterial oxidative stress resistance, in *in vivo* persistence in mice and in the intracellular survival inside macrophages (Jungnitz et al., 1998; Zimna et al., 2001). This locus encodes for the response regulator RisA of another two-component

system, which is an ortholog of the EnvZ/OmpR system found in other Gram-negative bacteria, including *E. coli*, *Xenorhabdus nematophilus* or *Salmonella typhimurium* (Forst and Roberts, 1994; Stenson et al., 2005). Surprisingly, the *risS* gene for the presumed cognate kinase RisS is a pseudogene in *B. pertussis*, in line with the observation that deletion of *risS* did not affect the expression of *risA*-dependent genes (Stenson et al., 2005). A decade later, the *BP3223* gene was described to encode a histidine kinase that phosphorylates RisA and was named as RisK (for cognate histidine kinase of RisA) (Chen et al., 2017; Coutte et al., 2016). The transcriptomic analysis of the RisA regulon showed that RisA activity is necessary for expression of almost all *vrgs* and that it also regulates the expression of several *vags* and other genes, including members of chemotaxis and flagellar operons or of iron-regulated genes (Coutte et al., 2016).

5.5.3 PlrSR

Recently, a new two-component regulatory system PlrSR (for persistence in the lower respiratory tract (LRT) sensor kinase/response regulator) has been characterized in *B. bronchiseptica*. This TCS was shown to regulate BvgAS activity in murine lungs, but not in the nasal cavity. The sequence of *plrSR* locus is almost identical (≥ 99%) in all classical *Bordetella* species and in line with this observation, the *plrS* gene was found to be necessary for survival and persistence in LRT also for *B. pertussis* (Bone et al., 2017).

5.6 Metabolic regulatory systems

5.6.1 Glutamate-limitation and stringent response

Despite high glutamate concentration in the standard Stainer-Scholte medium used for liquid cultures of *B. pertussis* (Stainer and Scholte, 1970), glutamate sources are scarce for bacteria *in vivo*. Such conditions then trigger bacterial stringent response to nutritional starvation, during which alarmons, the small second messengers guanosine tetra/pentaphosphates ((p)ppGpp), are produced (Dalebroux and Swanson, 2012). In *B. pertussis*, (p)ppGpp production is controlled by RelA and SpoT proteins and was shown to affect bacterial resistance to oxidative stress. Production of (p)ppGpp is also involved in the regulation of biofilm formation and autoaggregation (Hanawa et al., 2016; Sugisaki et al., 2013). There are several mechanisms of ppGpp action, which include its direct

interaction with RNAP in cooperation with DksA, or indirect regulation of transcription in the process called σ-factor competition (Dalebroux and Swanson, 2012). Lack of (p)ppGpp in *B. pertussis* led to decreased expression of *fim3* and *bsp22* genes, but did not affect expression of other virulence-related genes *cyaA* and *ptxA* (Sugisaki et al., 2013). Glutamate-limitation was shown to stimulate expression of T3SS genes in *B. pertussis* via the activation of the BvgAS system and (p)ppGpp was found to be essential for full expression of T3SS gene expression in *B. pertussis* (Hanawa et al., 2016).

5.6.2 Iron

Iron-deprivation represents another strong environmental cue that triggers bacterial response and regulates bacterial virulence. *B. pertussis* has several iron-acquisition systems, which differentially respond to iron availability. The ferric uptake regulator encoded by the *fur* gene is one of the major regulators of iron metabolism and virulence in Gram-negative bacteria and serves as a global regulator of iron starvation stress response also in *B. pertussis* (Beall and Sanden, 1995; Brickman and Armstrong, 1995; Brickman et al., 2007). One of the bacterial iron acquisition mechanisms is mediated by the heme iron acquisition system via the action of *bhu* (for *Bordetella* heme utilization) gene products. This system is encoded by *hurIR bhuRSTUV* genes and for its full expression, the Fur-mediated repression must first be relieved in the presence of heme (Vanderpool and Armstrong, 2001, 2004). Deregulation of this system reduced bacterial capacity to colonize trachea and lungs of mice seven days after the infection, indicating that this system is involved in the later stages of infection (Brickman et al., 2006). Iron limitation has a plethora of different phenotypic outcomes in bacteria, including enhanced bacterial binding of mucin, better attachment to the respiratory epithelial cells, or stimulation of pertussis toxin production (Passerini de Rossi et al., 2003; Perez Vidakovics et al., 2007; Thalen et al., 2006).

5.7 Virulence factors of *B. pertussis*

In the Bvg^+ phase *B. pertussis* expresses a whole array of various virulence factors, such as complement resistance factors, immunomodulatory protein toxins and adhesins that mediate bacterial adherence to the ciliated epithelial cells of human airways.

5.7.1 Toxins

5.7.1.1 Adenylate cyclase toxin (ACT)

As a result of immunosuppressive actions of *B. pertussis* virulence factors, infections caused by this bacteria are often complicated by secondary infections (Cherry, 2016; Confer and Eaton, 1982; Melvin et al., 2014). A major role in the subversion of several key host immune defense mechanisms can be attributed to the adenylate cyclase toxin–hemolysin (known as CyaA, ACT or AC-Hly), which is a 1706 amino acids-long polypeptide (Fedele et al., 2017; Novak et al., 2017; Vojtova et al., 2006). The *cyaA* gene for the toxin is located at the beginning of the operon (Figure 5) containing also other the genes *cyaB*, *cyaD* and *cyaE* that encode proteins involved in CyaA toxin secretion through the Type 1 Secretion system apparatus (Glaser et al., 1988). The *cyaC* gene, encoding a protein toxin acyltransferase activating the proCyaA by covalent attachment of 16-carbon fatty acyl chains, is located upstream of the *cyaA* operon and is transcribed from an independent promoter in the opposite direction (Barry et al., 1991; Sebo et al., 1991).

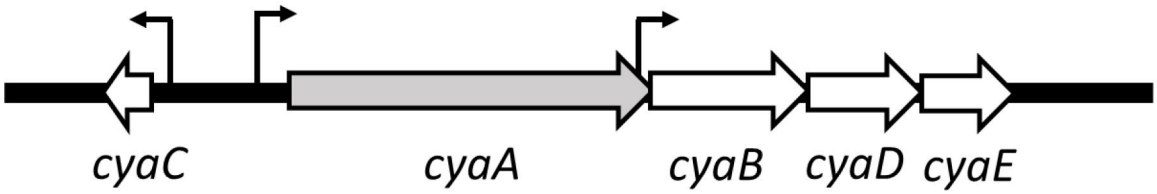

Figure 5: Schematic representation of the *cya* locus. *cyaA*, *cyaB*, *cyaD*, and *cyaE* genes are transcribed in the same direction. Gene *cyaC* encoding a protein toxin acyltransferase is transcribed from an independent promoter in the opposite direction to other genes of the locus.

CyaA consists of two structurally and functionally different domains (Figure 6) - ~400 residue-long N-terminal adenylate cyclase (AC) domain, which is linked to ~1306 residue-long C-terminal hemolysin (Hly) moiety of Repeats-in-toxin (RTX) family (Novak et al., 2017).

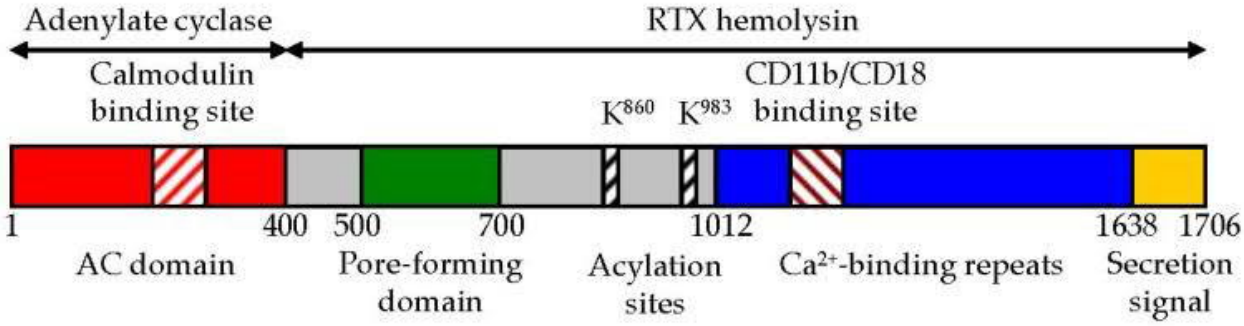

Figure 6: Schematic representation of CyaA. N-terminal AC enzyme domain and a C-terminal Hly moiety are linked together with a ~100 residues-long segment (residues 400 to 500). The Hly moiety harbors several functional subdomains: (i) a hydrophobic pore-forming domain (residues 500 to 700); (ii) an activation domain (residues 800 and 1000) with two lysine residues (K860 and K983), which are posttranslationally acylated; (iii) a typical calcium-binding RTX domain with the nonapeptide repeats binding calcium ions and with the CD11b/CD18-binding segment (residues 1166–1287); and (iv) a C-terminal secretion signal. Reprinted and adapted from (Novak et al., 2017)

Toxins of the RTX family are exoproteins of Gram-negative bacteria, structurally characterized by the presence of nonapeptides of glycine- and aspartate-rich repeats with a consensus sequence X-(L/I/F)-X-G-G-X-G-(N/D)-D that bind calcium ions (Linhartová et al., 2010; Welch, 1991). These proteins are secreted via the Type I secretion system (T1SS). Calcium ions drive folding of the capping structure on the C-terminus and the folding of β-rolls then accelerates the translocation of the protein through the channel-tunel duct of T1SS by the "push-ratchet" mechanism (Bumba et al., 2016). Secreted ACT then binds to the alpha(M)beta(2) integrin (CD11b/CD18) on the surface of host cells. CD11/CD18 is the complement receptor 3 (CR3) and is produced and presented on the surface of myeloid cells involved in innate immune response, including neutrophils, monocytes/macrophages, some B cell subpopulations, dendritic and natural killer cells (Guermonprez et al., 2001). CyaA preferentially binds the CD11b subunit of the non-activated form of the CR3 receptor, binding to the site in the thigh region outside of its I-domain of CD11b without triggering the downstream signaling of CR3 (Osicka et al., 2015). CyaA inserts into the plasma membrane of cells, permabilizes it for influx of extracellular calcium ions, relocates with CR3 into cholesterol-enriched membrane lipid microdomains (Figure 7) and delivers its catalytic AC enzyme domain directly into the cytosol of cells by

a mechanism that is entirely accomplished by RTX domain (Bumba et al., 2010; Holubova et al., 2012).

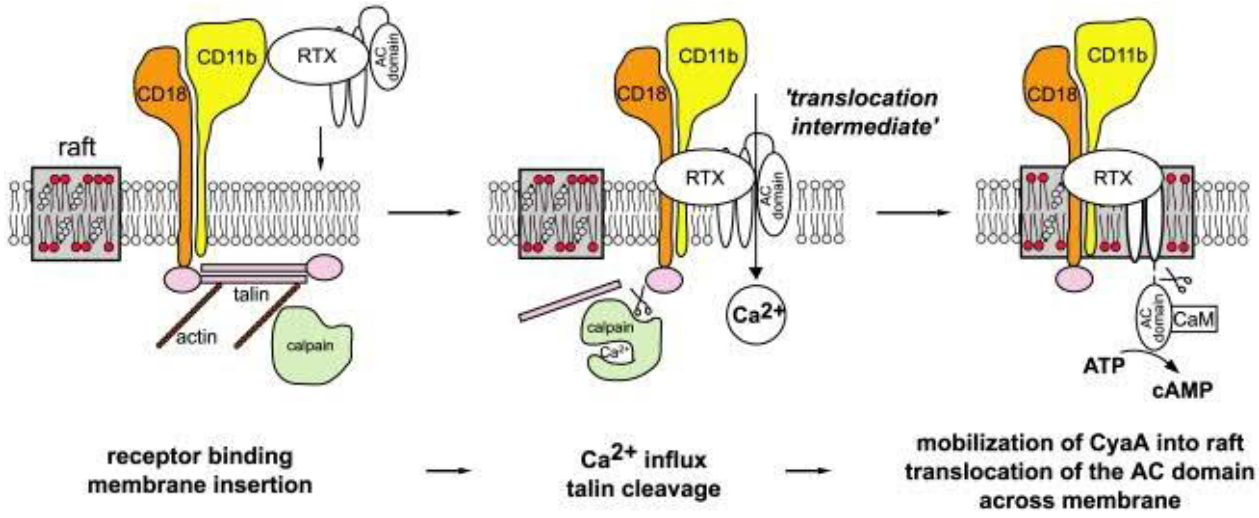

Figure 7: Model of CyaA translocation across target cell membrane. CyaA binds the CD11b/CD18 integrin receptor dispersed in the bulk of the membrane phase outside of lipid rafts, having the cytoplasmic tail of the CD18 subunit tethered to actin cytoskeleton via the linker protein talin. Upon receptor engagement, a 'translocation intermediate' of CyaA inserts into the lipid bilayer of cell membrane with the AC domain partially penetrating into cell membrane together with the pore-forming segments of the toxin and participating in formation of a transiently opened Ca2+-conducting path across cell membrane. Influx of external calcium ions into cells induces activation of the Ca2+-dependent protease calpain, yielding talin cleavage and liberation of the CyaA-CD11b/CD18 complex from binding to actin cytoskeleton. Consequently, CyaA is recruited with CD11b/CD18 into cholesterol-enriched lipid rafts, where the liquid-ordered packing of lipids and the specific presence of cholesterol enable completion of AC domain translocation across cytoplasmic membrane. Upon exposure at the cytosolic side of cell membrane, the AC domain is cleaved-off from the RTX cytolysin moiety of CyaA by a protease residing inside the cell. Binding of cytosolic calmodulin (CaM) then activates the AC enzyme and unregulated conversion of ATP to cAMP is catalyzed. Reprinted and adapted from (Bumba et al., 2010).

Inside the cytosol, the AC domain is bound and activated by calmodulin and catalyzes unregulated conversion of cytosolic adenosine triphosphate (ATP) into the key second messenger signaling molecule 3′,5′-cyclic adenosine monophosphate (cAMP), driving the local intracellular concentration of cAMP into supraphysiological levels and activation of protein kinase A (PKA) and of the Exchange protein activated by cAMP (Epac), thereby provoking deregulation of major cellular signaling pathways. This leads to the suppression

of a whole plethora of bactericidal mechanisms of phagocytes (Ahmad et al., 2016, 2019; Cerny et al., 2015, 2017; Confer and Eaton, 1982; Novák et al., 2017; Wolff et al., 1980).

The Hly moiety of CyaA itself can form cation-selective pores that cause potassium efflux and colloid-osmotic (oncotic) cell lysis manifesting as hemolysis of erythrocytes (Bellalou et al., 1990; Ehrmann et al., 1991; Gray et al., 1998; Szabo et al., 1994; Vojtova-Vodolanova et al., 2009). In parallel, the translocation of AC domain is accompanied by calcium influx, which elevates cytosolic calcium concentrations (Fiser et al., 2007). The synergy of cAMP elevation, potassium efflux and calcium influx elicited by CyaA has detrimental impact on the phagocytes and near-instantly ablates their bactericidal capacities. As a result, the phagocytes undergo apoptosis, or even necrotic cell death, depending on the toxin dose they encountered (Ahmad et al., 2016; Basler et al., 2006; Hewlett et al., 2006; Khelef and Guiso, 1995). In contrast to macrophages, the cAMP-elevating action of CyaA prolonges the life span of neutrophils, inhibits their apoptosis and suppresses their oxidative burst capacity, ROS production and formation of neutrophil extracellular traps (NETs) (Cerny et al., 2017; Eby et al., 2014). Increased levels of cAMP produced by CyaA in macrophages also lead to the suppression of oxidative burst responses, reduced production of bactericidal NO and inhibition of complement-mediated phagocytosis by inducing unproductive membrane ruffling (Cerny et al., 2015; Kamanova et al., 2008; Pearson et al., 1987). Importantly, very low concentrations (22 pM) of CyaA can - through cAMP elevation - suppress the maturation of human monocytes into macrophages and also can trigger dedifferentiation of mature alveolar macrophages into monocyte-like cells (Ahmad et al., 2019). Due to the extreme AC enzyme activity of the toxin, even cells lacking the CR3 receptor become affected by CyaA toxin action, as CyaA with low efficacy but promiscuously penetrates also the membranes of all kind of non-myeloid cells that do not express CR3, such as epithelial cells of the airways ((Hasan et al., 2018)). CyaA-produced cAMP can then cause a drop in a transepithelial electrical resistance (TEER) of polarized epithelial cell layers, as their barrier functions become compromised. cAMP produced by CyaA further suppresses the expression of the pro-inflammatory cytokines tumor necrosis factor-alpha (TNF-α), interleukin-1β, and interleukin-8 (IL-8), while stimulating secretion of interleukin-6 (Hasan et al., 2018).

5.7.1.2 Dermonecrotic toxin (DNT)

Dermonecrotic toxin, originally described as the heat-labile toxin, was discovered in the beginning of 19th century by Bordet and Gengou (Bordet and Gengou, 1909). Itscurrent name reflects the dermonecrotic effects of its action observed in the skin of guinea-pigs (Iida and Okonogi, 1971). DNT is a 1,464 amino acid residue-long single chain polypeptide, which is encoded by the *BP3439/dnt* gene. The first 30 amino acids in the N-terminal part are responsible for DNT binding to cells (Fukui-Miyazaki et al., 2011). The last approx. 300 amino acids in the C-terminus form a catalytically active domain with homology to the cytotoxic necrotizing factors of *E. coli* or *Yersinia pseudotuberculosis* (Horiguchi, 2012). Recently, the T-type voltage-gated calcium channels $Ca_V3.1$ and $Ca_V3.2$ have been identified as the cell surface receptors of DNT (Teruya et al., 2020). This toxin exhibits features of a neurotropic virulence factor, as it affects neural cells *in vitro* and causes flaccid paralysis in mice, when applied intracerebrally (Teruya et al., 2020). DNT intoxication led to the spleen damage in mice, resulting in their atrophy and reduction (Iida and Okonogi, 1971; Sekiya et al., 1982). These effects are long-term, despite of the observed instability of the toxin (Sekiya et al., 1982). DNT produced by the closely related *B. bronchiseptica* bacteria was shown to inhibit osteoblastic differentiation in infected snouts of pigs, provoking turbinate atrophy and atrophic rhinitis (Horiguchi, 2012). DNT does not appear to be secreted and appears to be released only upon bacterial cell lysis, indicating that this is not a classical exotoxin and its role in physiopathology of *B. pertussis* infections remains unclear (Cowell et al., 1979). DNT was found to be associated with fibronectin-based extracellular networks in both DNT-sensitive and -insensitive cells with unclear biological effects of such interaction (Fukui-Miyazaki et al., 2010). On the molecular level, DNT deamidates the Gln63 residue of the RhoA GTPase (and of other members of the family of Rho GTPases), or modifies the Gln63 residue with polyamines, thereby markedly increasing RhoA activity and binding to the ROCK effector. The irreversibly modified Rho GTPase then becomes constitutively active and causes anomalous stress-fiber formation (Masuda et al., 2000).

5.7.1.3 Pertussis toxin (PT)

Pertussis toxin is a complex oligomeric bacterial protein toxin, member of the AB5 family, which includes other major bacterial toxins, like the cholera toxin from *Vibrio cholerae,* shiga toxin produced by some *Shigella* and enteropathogenic *E. coli* strains, or the heat-labile LT enterotoxin from *E. coli* (Haan and Hirst, 2004). The structural components of PT are encoded by genes forming a single *ptx-ptl* operon, present in the genomes of all three classical *Bordetella* species (Figure 8). However, the toxin is expressed and produced only by *B. pertussis*. Both *B. parapertussis* and *B. bronchiseptica* bear mutations in the *ptx* promoters that make the expression of the toxin very inefficient (Aricò and Rappuoli, 1987). The *ptl* locus encodes for the components of the type IV secretion system (T4SS) accomplishing excretion of PT from the periplasmic space of *B. pertussis* cells. It is located immediately downstream from the *ptx* locus within the same operon and transcribed from the *ptx* promoter (Kotob et al., 1995).

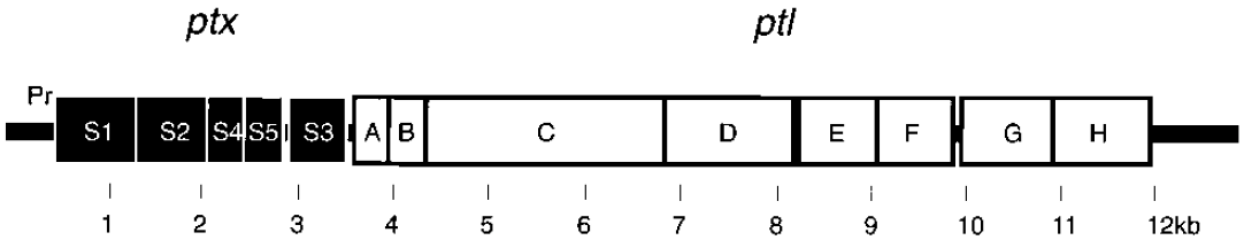

Figure 8: Schematic illustration of the *ptx-ptl* region. Pr indicates the location of the *ptx* promoter. Reprinted and adapted from (Kotob et al., 1995)

Pertussis toxin consists of a catalytic A-subunit (S1 subunit) associated with the cell-binding B-oligomer consisting of the S2 to S5 subunits, with two copies of S4 (Figure 9A). The A-subunit has a pyramid-shaped structure and harbors the ADP-ribosylating enzyme active site. Components of the B-oligomer then form a pentameric structure with a channel in its center, consisting of a ring of subunits containing antiparallel β-strands, into which the C-terminal α-helix of the S1 subunit is partly inserted. The S2 and S3 domains contain two unique amino-terminal extensions/peripheral domains of the B-oligomer, which are similar to lectin domains of the calcium-dependent eukaryotic lectins (Stein et al., 1994a). The initial reports of specific proteinaceous PT receptors on host cells do not hold anymore and it appears that PT rather promiscuously binds the

sialoglycoconjugate structures on numerous glycoproteins and glycolipids present on a broad variety of cell types, which then enables intoxication of wide range of cell and tissue types (Teter, 2019).

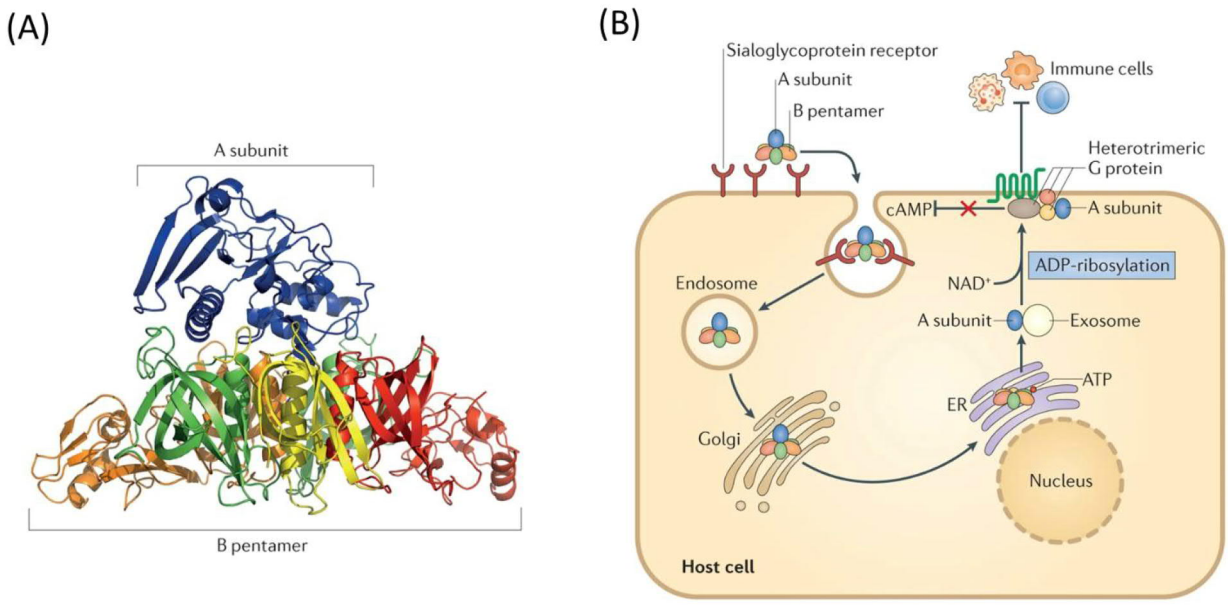

Figure 9: Pertussis toxin. (A) Schematic picture of the protein structure shows one catalytic subunit (the A subunit) and five membrane-binding or transport subunits (the B pentamer). (B) Following binding to a host cell, PT is endocytosed and trafficked through the Golgi apparatus to the endoplasmic reticulum (ER). There, the B pentamer binds to ATP and dissociates from the A subunit. The A subunit is then transported into the cytoplasm and traffics on exosomes to the cytoplasmic membrane, where it ADP-ribosylates the α-subunit of heterotrimeric G proteins. This modification alters the ability of G proteins to regulate multiple enzymes and pathways, including their ability to inhibit cAMP formation. Reprinted and adapted from (Melvin et al., 2014).

PT enters into the host cell via receptor-mediated endocytosis (Figure 9B), after which retrograde transport through the Golgi network follows (el Bayâ et al., 1997, 1999). The S1 subunit exits from the endoplasmic reticulum into cell cytosol and cleaves the nicotinamide adenine dinucleotide (NAD) to ADP-ribosylate the α-subunits of a range of inhibitory $G\alpha_{i/o}$ subunits of the trimeric G proteins that by transmitting signals from a wide variety of G protein-coupled receptors (GPCRs) regulate a plethora of cellular processes (Bokoch et al., 1983; Carbonetti, 2015; Katada, 2012; Katada and Ui, 1982; Stein et al., 1994b). The ADP-ribosylated isoforms of the $G\alpha_i$ subunits are then locked in the inactive state and the negative regulation of their targets, such as of the endogenous

membrane-bound adenylyl cyclase, is relieved. For example, the abolishment of inhibition of GPCR-activated adenylyl cyclase leads to increased intracellular concentrations of the key second messenger molecule 3′,5′-cyclic adenosine monophosphate (cAMP), which deregulates a wide range of cellular processes (Locht et al., 2011). In accordance with the described mode of action, in the neonatal mouse infection model of critical pertussis, intoxication by PT exhibited a wide range of systemic effects, including stimulation of bacterial colonization, leukocytosis, phenotypic changes of T-cells and host death (Carbonetti, 2015, 2016). Systemic effects of PT intoxication are also nicely illustrated by historic appellations of this toxin, as it was originally called as an islets-activating protein, casuing hyperinsulinemia (IAP) (Yajima et al., 1978), or as leukocytosis- and lymphocytosis-promoting factor (LPF). Among the toxic effects of PT initially described were granulocytosis, histamine sensitization, hypoglycemia or unresponsiveness to the hyperglycemic effects of epinephrine in mice (Morse and Morse, 1976). Later, PT was shown to inhibit lung inflammatory pathology in neonates, indicating that the systemic effects rather than lung pathology might be the real cause of mortality in critical pertussis (Scanlon et al., 2017). But in contrast to neonates, PT in adult mice promotes and exacerbates the airway inflammation (Connelly et al., 2012). With regard to its importance in pertussis pathology, toxoids of PT became a component of all current vaccines against pertussis, which was quickly reflected by adaptation of circulating strains (Locht et al., 2011; Mooi, 2010). Two globally predominant alleles of PT promoter are called as *ptxP1* and *ptxP3*. Based on the available data, *ptxP1* is still the predominant allele in Asia and only *ptxP1* strains were found also in Africa. In contrast to that, in Europe and both Americas, this allele has been recently replaced by the newly emerged *ptxP3* allele. Bacterial strains carrying this allele contain a single-nucleotide substitution in the promoter that most probably affects binding of BvgA regulator and thus leads to slightly increased (around 1.6 x) production of PT and a lower production of pertactin. Even though other factors might be involved as well, the emergence of *ptxP3* strains was accompanied by higher incidence of hospitalizations and increased lethality (Mooi et al., 2009). It was hypothesized that selection of more virulent strains might be, at least in part, driven by the need of the bacteria to produce higher PT levels during infection of the respiratory mucosa in order to overcome the anti-PT serum antibody levels in the vaccinated populations (Mooi, 2010). Surprisingly then, strains deficient in PT production

are occasionally isolated from infants with classical whooping cough manifestations, challenging the essential role of PT in *B. pertussis* virulence (Bouchez et al., 2009; Williams et al., 2016). While *B. parapertussis* causes whooping cough disease without producing PT, *B. pertussis* mutants not producing PT are extremely rarely isolated, which indicates that PT plays a rather important role in *B. pertussis* infections (Gregg and Merkel, 2019).

5.7.1.4 Type 3 secretion system (T3SS)

The Type 3 secretion system (T3SS) is a multicomponent assembly that forms the injectisome structure across bacterial cell envelope, mediating both selection of bacterial effectors from bacterial cytosol and their transfer through a channel/needle-like structure into the cytosol of host cells (Figure 10).

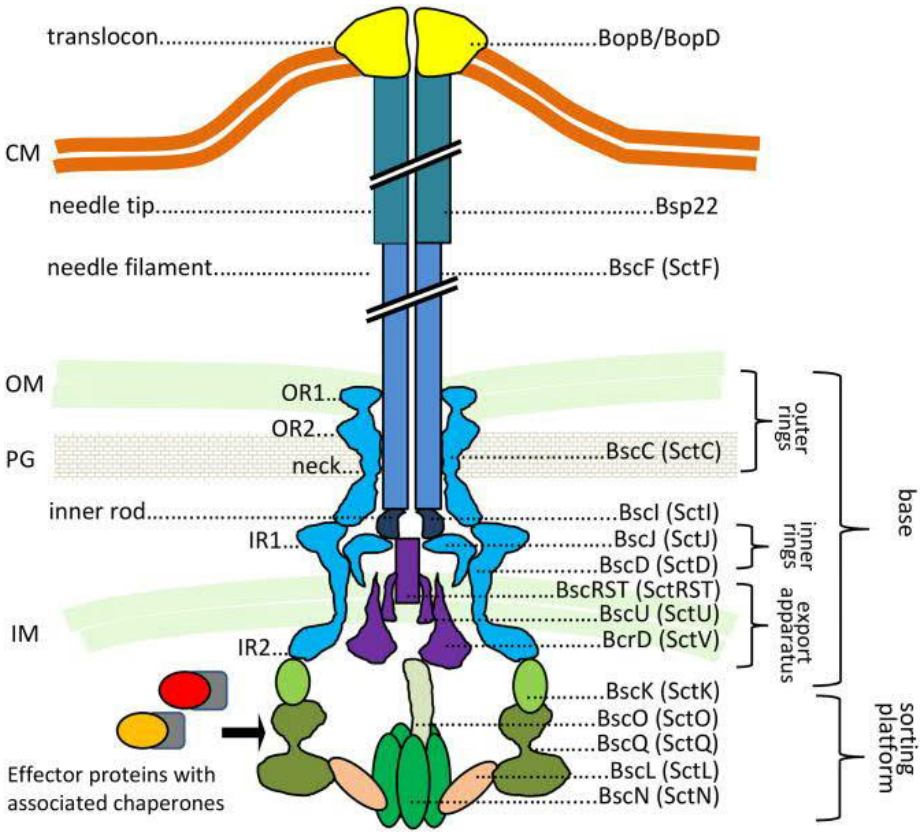

Figure 10: Predicted structure of *Bordetella* T3SS injectisome. Known or predicted functions and locations of *Bordetella* proteins are indicated. CM, cytoplasmic membrane; OM, outer membrane; PG, peptidoglycan; IM, inner membrane. Reprinted and adapted from (Kamanova, 2020).

T3SS assemblies are expressed by a wide range of both pathogenic and symbiotic Gram-negative bacteria, including *Salmonella enterica*, *Shigella* spp., *Yersinia pestis, Vibrio cholera*, *Pseudomonas aeruginosa* or *Bordetella pertussis* (Galán and Waksman, 2018). Nevertheless, the exact role of T3SS in *Bordetella* virulence remains to be elucidated. In *B. bronchispetica*, the T3SS and its single known injected effector BteA/BopC is required for maximal bacterial persistence in porcine lower respiratory tract, where it contributes to the severity of the disease, but not to the transmission of the pathogen (Nicholson et al., 2014). Similarly, T3SS activity appears to mediate persistent tracheal colonization in rodents via targeting of mechanisms of adaptive immunity and by downregulation of the humoral immune response (Yuk et al., 1998, 2000). *B. bronchiseptica* T3SS activity modulates the maturation of dendritic cells (DCs) in the airways and drives their migration into the secondary lymphoid tissues, where they act as immunosuppressive agents (Skinner et al., 2005). Furthermore, the activity of the T3SS effector(s) was shown to enhance production of anti-inflammatory cytokine IL-10, while it suppressed production of pro-inflammatory cytokine IFN-γ (Nicholson et al., 2014; Skinner et al., 2005) and thus favored bacterial persistence. In *B. pertussis*, T3SS was initially considered to be inactive, but later studies revealed that it becomes expressed during *in vivo* infection. T3SS expression is detected in all low-passage clinical isolates and if it is not produced, its expression can be reactivated upon bacterial passage through mice (Fennelly et al., 2008; Gaillard et al., 2011; Hegerle et al., 2013). So far, two T3SS effector proteins, BteA/BopC and BopN, were identified and described in *Bordetella* (Panina et al., 2005). In course of *B. bronchiseptica* infections the BopN effector was shown to inhibit proinflammatory NF-κB activation in host cells and increase production of the immunosuppressive IL-10 cytokine (Nagamatsu et al., 2009). The BteA effector is a highly potent cytotoxic protein that is both necessary and sufficient for induction of cytotoxicity in tissue cultures, but the mechanism of its mechanism of action remains unknown (Bayram et al., 2020; French et al., 2009; Panina et al., 2005). Despite its high conservation across *Bordetella bronchiseptica* between *Bordetella pertussis*, its cytotoxicity differs significantly in these species. A drastic reduction of specific cytotoxic activity of BteA from *B. pertussis*, as compared to the specific cytotoxic activity of BteA

from *B. bronchiseptica*, has recently been attributed to a single alanine insertion at position 503 in the *B. pertussis* BteA. Curiously, the A503 insertion causes strong attenuation of the cytotoxic potency of BteA and of its immunosuppressive activity, which results in increased lung inflammatory pathology from infections with wild type *B. pertussis* when compared to infection by a *B. pertussis* mutant secreting the much more cytotoxic BteAΔA503. Such modification might thus represent an evolutionary adaptation by fine-tuning virulence of *B. pertussis* (Bayram et al., 2020).

5.7.1.5 Tracheal cytotoxin (TCT)

TCT is a low molecular weight muramic acid-containing glycopeptide, a peptidoglycan fragment, which was shown to be responsible for the respiratory cytopathology during pertussis, including ciliostasis and extrusion of ciliated cells (Kessie et al., 2021). Due to absence of a functional AmpG permease in *B. pertussis,* the released TCT is imported by the SLC46A2 co-transporter into epithelial cells (Paik et al., 2017), where TCT activates the NOD1 sensor that, by activation of NF-κB, triggers inducible NO synthase (iNOS) expression and cytotoxic levels of NO production (Flak and Goldman, 1996, 1999; Flak et al., 2000). TCT action inhibited DNA synthesis in hamster tracheal epithelial cells (Cookson et al., 1989; Goldman et al., 1982) and TCT also affects *in vitro* migration of human neutrophils towards the chemotactic factor N-formyl-L-methionyl-L-leucyl-L-phenylalanine (FMLP) and was found to be toxic to these cells at higher concentrations, thereby promoting bacterial survival in the airways (Cundell et al., 1994). It is plausible to assume that compromising of the epithelial barrier integrity due to TCT release and cytotoxic activity enables *B. pertussis* to access nutrients from the syncytial fluid of lamina propria and promotes penetration of pertussis toxin through the draining lymphatic vessels and thoracic vein into blood stream, where it provokes the systemic manifestations of pertussis, such as hyperleukocytosis, hyperinsulinemia and histamine sensitization.

5.7.2 Adhesins and other surface structures

5.7.2.1 Tracheal colonization factor (Tcf)

Tracheal colonization factor, encoded by the *tcfA* gene, is an autotransporter uniquely produced only by *B. pertussis*, but not by other classical *Bordetellae* species. Tcf is a

proline-rich protein with an N-terminal RGD-motif and a C-terminal region resembling the C-terminal region of pertactin (Finn and Stevens, 1995). Mutants lacking the *tcfA* gene exhibited decreased ability to colonize trachea, but how TcfA promotes tracheal colonization remains unclear (Finn and Stevens, 1995; Henderson and Nataro, 2001). High level of *tcfA* gene polymorphism in comparison to other *B. pertussis* surface proteins indicates that this protein might be an important target of the immune system and thus under strong selective pressure for accumulation of mutations (van Loo et al., 2002). In line with this hypothesis, the loss or inactivation of *tcfA* gene was observed in several clinical isolates of *B. pertussis* (van Gent et al., 2007).

5.7.2.2 Filamentous haemagglutinin (FHA)

Mature released FHA protein is the product of processing of the FhaB precursor protein encoded by the *fhaB* gene, which belongs to the class 2 genes expressed during the Bvg^i and Bvg^+ phases (Jones et al., 2005). FhaB with its outer membrane transporter FhaC (Figure 11) represent a prototypical two-partner secretion (TPS) system, which allows to export large proteins across the outer membrane of Gram-negative bacteria via a channel-forming β-barrel protein (Mazar and Cotter, 2007). FHA is initially synthesized as the large (approx. 370 kDa) preproprotein FhaB, which contains i) 71 amino acids-long N-terminal secretion signal that is removed during Sec-mediated translocation across inner membrane and ii) a large C-terminal 'prodomain' that is required for establishing of proper conformation of the mature C-terminal domain, cleaved-off by the SphB1 protease and retained in bacterial periplasm, or degraded intracellularly (Coutte et al., 2001; Lambert-Buisine et al., 1998; Mazar and Cotter, 2007; Noël et al., 2012).

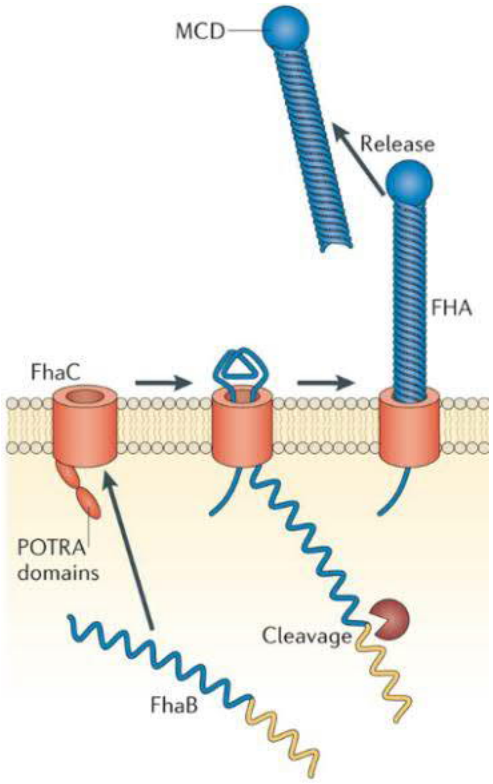

Figure 11: Presentation of FHA on the *Bordetella* cell surface. FHA is an exoprotein that is translocated across the outer membrane through its cognate pore protein FhaC. Processing during translocation removes the C-terminal 'prodomain' (yellow) from the full-length FhaB protein to produce the mature ~250kDa FHA protein. MCD, C-terminal domain of mature FHA. Reprinted and adapted from (Melvin et al., 2014).

Although the "mature" form of FHA used to be considered as the main biologically active form of the protein involved in adherence to respiratory epithelium, it appears that the unprocessed and bacterial cell-attached FhaB protein is the virulence factor of *Bordetella*, as the mutant *B. bronchiseptica* bacteria, with deletions in the C-terminal 'prodomain' were unable to persist in the lower respiratory tract of rats *in vivo* (Melvin et al., 2015). Processed FHA still mediates bacterial adherence to different cell types including the non-ciliated epithelium-like cells (Urisu et al., 1986), or ciliated cells, to which it also promotes binding of other pathogens when added exogenously (Locht et al., 1993; Tuomanen, 1986), or to macrophages (Locht et al., 1993). The interaction of FHA with macrophages occurs on two levels – first is via binding to the galactose-containing glycoconjugates and heparan sulfates on cell surface and it was also claimed to bind the β2 integrin CD11b/CD18 (Relman et al., 1990). FHA is required though not sufficient for

tracheal colonization in the rat model of respiratory infection (Cotter et al., 1998). In line with its role in adhesion, the deletion of *fhaB* gene severely affected bacterial adherence to host cells including rat lung epithelial L2 cells or mouse macrophage-like MH-S cells (Inatsuka et al., 2010). For several years, FHA was considered to act as an immunomodulatory effector. Nevertheless, results published along this topic yielded contradictory and conflicting results and the proper immunomodulatory capacity of FHA (if any) is not clear (Villarino Romero et al., 2014). As shown in our laboratory, the induction of cytokine secretion from human monocyte-derived dendritic cells (MDDCs), originally attributed to FHA activity, was in reality caused by contaminating endotoxin and associated lipidated components (Villarino Romero et al., 2016).

5.7.2.3 Fimbriae

Fimbriae are polymeric filamentous protein structures with a helical axial repeat of five repeating protein subunits in two complete turns that are interacting with the fimbrial backbone that has no axial channel. Originally called as agglutinogen 2 and agglutinogen 3, two major fimbrial subunits Fim2 and Fim3 were found to be two serologically distinct proteins with the molecular weights of 22,500 and 22,000, respectively. Mice immunization with either Fim2 or Fim3 led to serotype-specific protection (Ashworth et al., 1988). Sequences of the *fim2* and *fim3* genes, encoding the major subunits of the serotype 2 and serotype 3/6 fimbriae, respectively, exhibit approximately 60% homology and despite different properties their supramolecular structures are basically the same (Ashworth et al., 1982; Heck et al., 1996; Steven et al., 1986). Different bacterial strains differ in the size and numbers of expressed fimbriae and the bacteria can carry either only Fim2 or Fim3 fimbriae, or produce both Fim2 and Fim3 at the same time (Ashworth et al., 1982; Gorringe and Vaughan, 2014). Most *Bordetella* strains express also other alternative major fimbrial subunits, which are encoded by genes *fimA*, *fimN* and *fimX*, but in *B. pertussis*, only *fimX* was found to be produced (Boschwitz et al., 1997; Kania et al., 2000; Pedroni et al., 1988; Riboli et al., 1991; Scheller and Cotter, 2015). Phylogenetic analysis indicates that the *fimA* pseudogene, located upstream of the *fimB* gene, could represent the primordial gene, from which the gene duplication events gave rise to the major fimbrial subunit genes *fim2*, *fim3* and *fimX* (Willems et al., 1992). Besides the control by the master regulator BvgAS system, the transcription of fimbrial subunits is

controlled on several levels. The expression of *fim* genes undergoes the so-called phase-variation, which represents one of the bacterial mechanisms of immune evasion. Due to errors arising during replication of the bacterial chromosome, the homopolymeric C stretch in the *fim* gene promoter region is target of small deletions or insertions that affect the transcription of *fim* genes, possibly by alterations of the distance between -10 region and *cis*-regulatory elements (Willems et al., 1990). The *fimBCD* operon, located downstream from the *fhaB* gene, encodes for proteins that are involved in the biosynthesis of fimbriae (Figure 12).

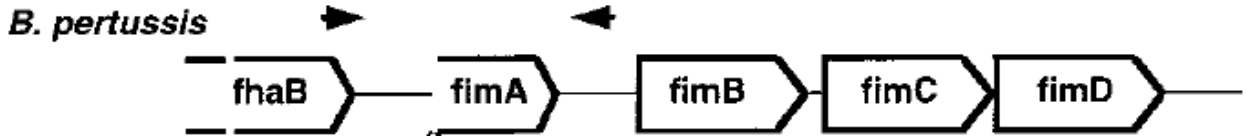

Figure 12: Schematic diagram of genomic structure at the *fimA* region of *B. pertussis*. Directional boxes indicate open reading frames. Reprinted and adapted from (Boschwitz et al., 1997)

Among these genes, *fimB* encodes for the putative chaperone protein, the product of *fimC* is presumably involved in the transport and anchorage of fimbrial subunits (so-called usher protein). The *fimD*-encoded protein, located on the tip of the fimbriae, is a glycan-binding lectin protein that plays an important role in colonization of the mouse respiratory tract and was found to interact with monocytic very late antigen-5 (VLA-5) (Geuijen et al., 1997; Hazenbos et al., 1995; Willems et al., 1992). According to the proposed model of fimbrial biogenesis, individual structural subunits are translocated across the cytoplasmic membrane via the Sec system, together with the chaperone and usher proteins. In bacterial periplasm, the Fim proteins interact first with the chaperone (FimB) that eventually delivers them to the usher protein (FimC) and Fim translocation across the outer membrane follows (Scheller and Cotter, 2015).

5.7.2.4 Lipooligosaccharide (LoS)

Lipopolysaccharide (LPS) forms the outer leaflet of the outer membrane of Gram-negative bacteria that serves as an important permeability barrier. LPS is recognized by host Toll-like receptor 4 (TLR4) (Arenas et al., 2019; Raetz and Whitfield, 2002). LPS consists of three main components – the anchoring lipid A moiety, the nonrepeating core oligosaccharide and long polysaccharide also known as the O-antigen. The LPS of *B.*

pertussis has a penta-acylated lipid A moiety and in contrast to both *B. bronchiseptica* and *B. parapertussis,* it lacks the O-antigen due to the presence of the insertion sequence in the locus responsible for O-antigen biosynthesis. Therefore, it is referred to as lipooligosaccharide (LOS) (Caroff et al., 1994; Preston et al., 1999). The lipid A of *B. pertussis* also exhibits unusual structural asymmetry due to the different length of the acyl chains, which are attached by the acyltransferase LpxA and further are modified by pyrophosphohydrolase LpxH (Arenas et al., 2019). Another reported lipid A modification includes substitution of both lipid A phosphate groups of the diglucosamine backbone by glucosamines, which is accomplished by the BvgAS-activated glycosyl transferase orthologue ArnT (*lgmB*) and this modification accounts for the strong pro-inflammatory signaling capacity of *B. pertussis* LOS through the TLR4 receptor of human macrophages (Marr et al., 2008, 2010).

5.7.2.5 Pertactin (PRN)

Pertactin is synthesized as 90-kDa precursor processed to a 69-kDa released protein. It forms monomers folded as a single domain formed by a three-stranded β-helix with several protruding loops. One of these loops contains the Arg-Gly-Asp tripeptide (RGD) motif followed by a proline-rich region (PRR), both typical properties of adhesive proteins. In addition to adhesion mediated by the RGD motif, the long linear form of pertactin promotes binding also via many nonspecific interactions (Emsley et al., 1996). The RGD sequence is a common key player in adhesion to cells through surface integrins and it was shown to mediate attachment of pertactin to Chinese hamster ovary cells (Hynes, 1987; Leininger et al., 1991), but the RGD motif-containing sequences do not seem to be involved in the observed biological activities of pertactin (Inatsuka et al., 2010). In the murine respiratory model of *B. pertussis* infection, the deletion of *prn* gene did not compromise the capacity of the bacterium to induce bronchopneumonia, alveolitis, or the influx of leukocytes into bronchoalveolar lavage fluids. However, it impacted bacterial persistence in this model (Khelef et al., 1994). Similar observation was done also for *B. bronchiseptica*, in which the deletion of *prn* gene resulted in more efficient bacterial clearance from the mouse lungs, although the adherence of bacteria to the epithelial cells and macrophage-like cells *in vitro* or the ability of this mutant to colonize the respiratory tract of rats was not affected. PRN enabled *B. bronchiseptica* to either grow and/or resist to inflammation-

mediated clearance in the lungs and was required for the bacterial protection from neutrophils (Inatsuka et al., 2010). Clearly, the function of PRN in bacterial infections is redundant with some other adhesion proteins, as fully virulent PRN-deficient *B. pertussis* strains arose under the selective pressure of acellular pertussis vaccine use in humans and replaced the originally circulating PRN-producing strains (Hegerle et al., 2014; Martin et al., 2015; Pawloski et al., 2014).

5.7.2.6 Virulence associated gene 8 (Vag8)

Vag8 autotransporter of *B. pertussis* is BvgAS-activated virulence factor, which was discovered and partially characterized as a 95-kDa protein (Finn and Amsbaugh, 1998). Vag8 binds the C1 esterase inhibitor, which regulates complement response, and thus interferes with its binding to C1s, C1r and MASP-2 complement components. As a result, the active proteases, which would otherwise cleave C2 and C4, are released away from the bacterial surface and by this mechanism, Vag8 promotes bacterial resistance against complement-mediated killing and activates the contact system (Hovingh et al., 2017, 2018; Marr et al., 2011).

5.8 The intracellular life of *B. pertussis*

The intracellular survival of *B. pertussis* has never been a central topic of *Bordetella*-related research, as compared to *bona fide* intracellular bacterial pathogens (e.g. *Listeria, Salamonella*, or *Shigella*) only low numbers of *B. pertussis* bacteria have been observed internalized in human cells. Nevertheless, starting in late 1950s, the intracellular presence of bacteria *B. pertussis* was analyzed and observed in tissue cultures treated with antibiotics, which indicated that the epithelial cells might provide a niche protecting the bacteria from bactericidal action of antibodies and complement (Crawford and Fishel, 1959). A few years later, Grey and Cheers described the similarities between murine pulmonary tuberculosis and pertussis, as in both infections the initial bacterial growth is largely stopped during the bactericidal phase and is eventually followed by more or less constant steady state, called by these authors as "complaisant" phase (Gray and Cheers, 1967). One week after the infection, *B. pertussis* bacteria were detected in alveolar macrophages of sub-lethally infected mice, in which their counts were still growing up until the drop occurred approximately two weeks after the infection. The following complaisant phase eventually progressed into the recovery phase, when no or only low amounts of bacteria were detected (Cheers and Gray, 1969). In the rat model of lung *B. pertussis* infection, wild-type bacteria were able to establish an infection that seemed to be completely cleared one week after infection, where no bacteria were recovered from the lungs of infected rats on days 10 and 14. Surprisingly, small amounts of bacteria were later recovered on day 21 after infection, suggesting the existence of an intracellular niche *in vivo*, most probably inside alveolar macrophages (Woods et al., 1989). Further studies revealed that the *B. pertussis* bacteria are in fact able to survive inside the body´s "first-line defenders", the polymorphonuclear leukocytes (PMNLs), in which they inhibited phagosome-lysosome fusions (Steed et al., 1991). In PMNLs, *B. pertussis* bacteria were not able to inhibit the respiratory burst and production of superoxide, but inhibited its release (Steed et al., 1992). During early 1990s, the analyses of bronchoalveolar lavages (BALs) from HIV-infected children revealed the presence of *B. pertussis* inside the pulmonary alveolar macrophages and these bacteria appeared to be non-culturable (Bromberg et al., 1991). Later, Friedman and colleagues observed that "long-term" residing intracellular *B. pertussis* bacteria from human macrophages were viable and

culturable (Friedman et al., 1992). At the same time, short-term intracellular survival in human macrophages was described by another group, which formulated the hypothesis that bacterial uptake was mediated via the CR3 receptor and that such internalization led to persisting bacteria rather than to their killing. These authors also suggested that the intracellular environment might promote the avirulent phenotype in *B. pertussis* (Saukkonen et al., 1991). This hypothesis was later supported by the observed downregulation of adenylate cyclase toxin production upon entry into human macrophages, after which even the reduced CyaA activity conferred protection against macrophage killing (Masure, 1992, 1993). Trends towards reduced expression of virulence factors have recently been described also by high-throughput transcriptomics analysis of *B. pertussis* bacteria internalized into human macrophage-like THP-1 cells (Petráčková et al., 2020). It might sound counterintuitive, but such modulation does not necessarily reduce bacterial ability to survive intracellularly, at least not in the long-term perspective. *B. pertussis* mutants having the RGD motif of FHA mutagenized to RAD and the *ptx* genes deleted, survived inside cells recovered in BALs from infected murine lungs longer than wild-type bacteria, with viable bacterial cells of the FHA-RAD Ptx mutant being present in cells even 19 days after the infection, establishing a 'persistent' infection (Hellwig et al., 1999). In the last decade, "long-term" intracellular survival (for days) of *B. pertussis* was further studied by the Argentinian group of M.E. Rodriguez, which also described the events following internalization of non-opsonized bacteria into human macrophages. A small portion of bacterial cells was found to evade killing in the phagolysosome and persist in the non-acidic cellular compartments, which resemble early endosomes, having access to essential nutrients and even being able to replicate (Lamberti et al., 2010).

5.9 Regulation by post-translational modifications

5.9.1 Protein phosphorylation

Regulatory networks of living organisms are not limited to transcriptional regulation, but rather comprise multiple layers of regulation that coexist and support fine-tuning of the response to the environmental conditions. Phosphorylation underlies the mechanism of function of the two-component system of *B. pertussis*, a prototypic bacterial regulatory system based on post-translational protein modification. In two-component systems like the BvgAS phosphorelay, the extracellular signals are sensed by a sensor kinase, which phosphorylates its response regulator (Boulanger et al., 2013; Forst and Roberts, 1994; Groisman, 2016). In *B. pertussis* this role of phosphorylation/dephosphorylation of the response regulator BvgA is very well described, but the overall phosphoproteome of this pathogen has not yet been described.

5.9.2 N-ε-lysine acetylation in bacterial virulence

Lysine is classified as a basic amino acid, which is charged at physiological pH. Acylation of the lysyl chain leads to the neutralization of its positive charge and it might also alter the conformation and/or increase hydrophobicity of the protein. Such modification can alter properties of the protein, such as its affinity for DNA or protein partners, enzymatic activities, cellular localization or stability (Allfrey et al., 1964; Choudhary et al., 2009; Liang et al., 2011; Yang and Seto, 2008a). Acylation represents an efficient mechanism for sensing of the actual metabolic state and coordination of its regulation, which is often linked to virulence (Figure 13). The most studied type of lysine acylation is lysine acetylation (further referred only as acetylation) (Christensen et al., 2019a; Ren et al., 2017). Acetylation can occur either non-enzymatically, when the protein reacts with reactive metabolic compounds, such as acetylphosphate (AcP), acetyl-CoA or acetyladenylate (Ramponi et al., 1975; Wagner and Payne, 2013), or it can be reversibly and enzymatically regulated by activities of lysine acetyltransferases (KATs) and lysine deacetylases (KDACs). In signal transduction, not only the “direct” effects of acetylation play a role, comprising regulation of protein-protein interactions or protein stability. Equally important can be the crosstalk of acetylation with other PTMs of a protein, e.g.

phosphorylation, methylation, ubiquitination or sumoylation (Christensen et al., 2019a; Ren et al., 2017; Walsh et al., 2005; Yang and Seto, 2008a).

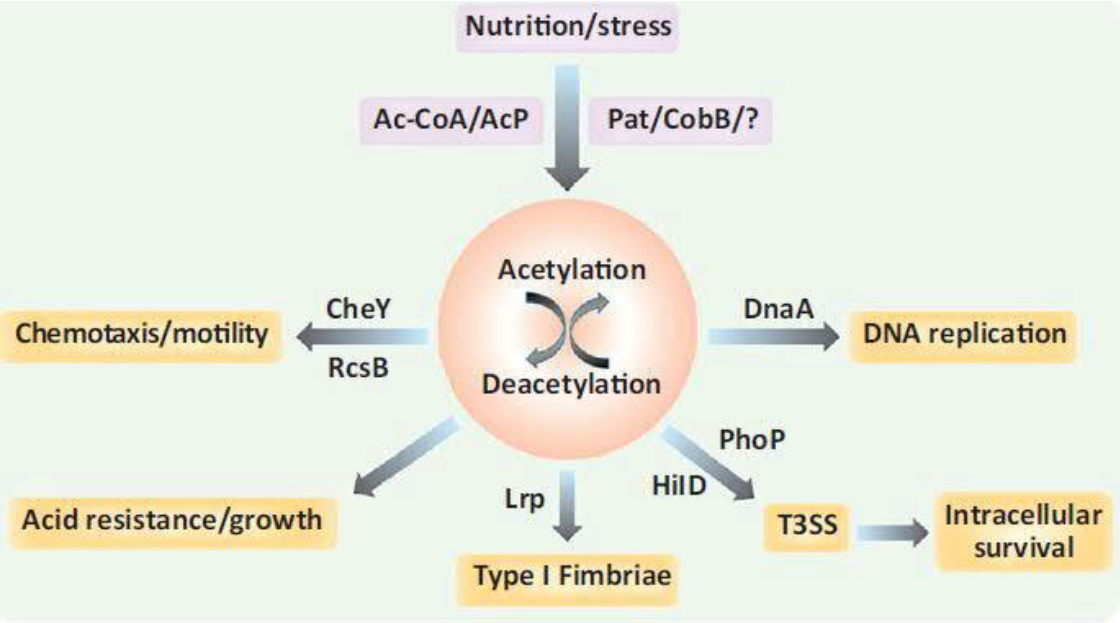

Figure 13: Acetylation can play various roles in bacterial pathogenesis. Acetylation occurs either enzymatically or non-enzymatically. Proteins Pat and CobB are protein acetyltransferase or lysine deacetylase, respectively. AcP (acetyl phosphate) and Ac- CoA (acetyl-coenzyme A) are both able to acetylate proteins non-enzymatically. The level of protein acetylation then affects a wide range of bacterial physical processes, including chemotaxis, motility, acid resistance, intracellular survival, and DNA replication. Reprinted and adapted from (Ren et al., 2017)

Acetylation was shown to be involved in various processes linked to bacterial virulence (Figure 13). For the PhoP protein of the prototypic two-component system PhoP-PhoQ of *Salmonella* Typhimurium, it was shown that the level of acetylation of lysine 201 in the C-terminal DNA-binding domain of PhoP alters its DNA-binding capacity, and this modification results in modulation of the inflammation caused by systemic *Salmonella* infection *in vivo* (Ren et al., 2016). Similarly, non-enzymatic acetylation of lysine 88 by AcP was shown to inhibit PhoP and thus regulate timing of its activity (Li et al., 2020). In *E. coli* the chemotaxis was found to be regulated by acetylation of the CheY protein, the response regulator of the chemotaxis system (Barak and Eisenbach, 2001). Acetylation of the lysine residue located in the helix–turn–helix motif of HliD, the key transcriptional regulator of *Salmonella* Pathogenicity Island 1, was then shown to increase its stability

and decrease DNA-binding ability (Sang et al., 2017). Furthermore, several proteins involved in the biosynthesis of exopolysaccharide amylovoran, or of proteins from the hypersensitive response and pathogenicity (hrp)-type III secretion system of plant-pathogen *Erwinia amylovora,* were shown to be acetylated, though the effects of these acetylation remain unclear (Wu et al., 2013). These examples point to the importance of lysine acetylation as a regulatory PTM. Despite the recent expansion of acetylome studies in different bacterial species, however, the extent and role of lysine acetylation has not yet been described in *Bordetellae* (Christensen et al., 2019b).

5.9.3 Bacterial lysine acetyltransferases (KATs)

In contrast to eukaryotes, only two bacterial KAT superfamilies have been identified so far, including Gcn5-related N-acetyltransferases (GNATs) and YopJ effector proteins (Christensen et al., 2019b). The GNAT superfamily represents one of the largest enzyme superfamilies and several GNAT-domain-containing proteins can be found also in *B. pertussis* (according to InterPro database (Mitchell et al., 2019)). However, none of them has been characterized in more detail. The general acid/base catalytic mechanism is shared by all KATs, but its implementation differs in each family. Catalytic glutamate is typically used to deprotonate the amino group of the substrate and tyrosine to reprotonate the coenzyme A (Christensen et al., 2019b). Upon binding of acyl-CoA as a donor of acetyl group, changes in the conserved GNAT fold are induced, which eventually leads to the generation of structural elements that recognize and bind the specific substrates. Acyl-CoA and the substrate to be acetylated then form a ternary complex, in which nucleophilic attack by the amine occurs and the thiol of CoA is eliminated (Vetting et al., 2005). Based on their size, GNATs in prokaryotes can be divided into three main groups. First identified and functionally described bacterial KAT (GNAT) was the protein acetyltransferase (Pat) from *Salmonella enterica* serovar Typhimurium (called YfiQ in *E. coli*), which was shown to regulate the activity of the acetyl-coenzyme A synthetase in concerted action with NAD^+-dependent lysine deacetylase CobB (Starai and Escalante-Semerena, 2004). Homologs of conserved acetyltransferase YfiQ can be found in many bacterial species (Christensen et al., 2019b).

The YopJ family of effectors, originally described in *Yersinia*, supposedly remain inactive inside bacterial cells, but become activated by a conformational change inside eukaryotic host cells. The proposed two-step "ping-pong" model of catalytic action of YopJ-like effectors presumes that the catalytic histidine residue deprotonates a neighboring cysteine, which then performs the nucleophilic attack of the carbonyl group of AcCoA, forming an acetyl-enzyme intermediate and CoA. The acetyl-enzyme intermediate then attacks the target protein and transfers its acetyl group onto a specific ε-amino group of a lysine residue. Members of the YopJ family of effectors produced by animal pathogens were shown to target MAPK and NF-κB signaling in order to suppress the inflammatory response (Ma and Ma, 2016).

5.9.4 Bacterial lysine deacetylases (KDACs)

Although the acetylation can occur both enzymatically and non-enzymatically, the reversed process, deacetylation, occurs only enzymatically by the action of KDACs. These enzymes, historically called histone deacetylases (HDACs), can be divided into four classes. "Classical" zinc-dependent deacetylases of the Rpd3/Hda1 family encompass classes I, II and IV. Class I (yRdp3-like) lysine deacetylases have an N-terminal deacetylase domain and often form multiprotein nuclear complexes involved in epigenetic regulation (e.g. HDAC1-3). Class II (yHda1-like) lysine deacetylases usually have a C-terminal deacetylase domain and shuttle between nucleus and cytoplasm, thus acting either as cytoplasmic regulators, or transduce signals between nucleus and cytoplasm (e.g. HDAC4-8). The only known member of class IV lysine deacetylases is HDAC11 (Gao et al., 2002; Marmorstein, 2001; Yang and Seto, 2008b). Class III KDACs are NAD^+-dependent deacetylases of the Sir2 family (Blander and Guarente, 2004) and are also called as sirtuins. Bacterial homologs of all of these lysine deacetylases have been found also in bacteria and are called either as acetylpolyamine amidohydrolases (APAHs), acetoin utilization proteins or as HDAC-like amidohydrolases/proteins, respectively (Hildmann et al., 2007). Bacterial APAHs are supposed to play a role in the metabolism of polyamines (Sakurada et al., 1996), the still rather enigmatic polycations that can regulate bacterial growth and protein synthesis, bind nucleic acids, form polyamine-based siderophores or affect biofilm formation (Igarashi and Kashiwagi, 2018; Michael, 2018). By their deacetylation, APAHs might be able to reactivate the "stored" and inert acetylpolyamines,

but this activity and its biological relevance remains obscure (Hildmann et al., 2007). Even more puzzling is then the function of acetoin utilization proteins of the AcuC type. Despite the observed effect of AcuC on the acetoin utilization in *Bacillus subtilis*, it seems likely that this effect is rather indirect (Grundy et al., 1993; Leipe and Landsman, 1997). From the numerous predicted putative bacterial lysine deacetylases only few were characterized to be true KDACs. One of them is the sirtuin CobB, likely the predominant deacetylase in *E. coli*, which deacetylates targets regardless of their mechanism of acetylation (enzymatic or non-enzymatic) and which forms several different isoforms in *Salmonella enterica* and *Erwinia amylovora* (AbouElfetouh et al., 2015; Tucker and Escalante-Semerena, 2010). Well described is the kinetics and substrate specificity of the histone-like amidohydrolase (HDAH) from *Bordetella/Alcaligenes* strain FB188, which was shown to share similar substrate affinity and inhibitor sensitivity as human HDAC6 (Hildmann et al., 2004; Moreth et al., 2007; Nielsen et al., 2005, 2007). In the proposed deacetylation mechanism of class I, II and IV deacetylases, the zinc ion in the active site of the enzyme binds the carbonyl oxygen to polarize the carbonyl group and thus increases the electrophilicity of the carbon. Zinc also binds the oxygen from the water molecule and increases its nucleophilicity. A water molecule carries out the nucleophilic attack on the carbonyl carbon, leading to the formation of a tetrahedral oxyanion transition state. The ε-nitrogen of the target lysine residue is then protonated by the "outer" histidine residue, releasing the acetate (Hildmann et al., 2007). Catalytic mechanism of sirtuins is different and each deacetylation reaction is accompanied by the cleavage of NAD+ molecule, during which nicotinamide and O-acetyl-ADP-ribose are produced (Blander and Guarente, 2004).

6. Research aims

The original aims of the hereby presented projects were:

1. To explore the impact of cAMP-dependent signaling triggered by CyaA action in primary murine bone marrow-derived dendritic cells by quantitative shotgun phosphoproteomic analysis.

2. To analyze the role of lysine acetylation in biology of *B. pertussis*, identify and characterize putative bacterial lysine deacetylase(s).

3. To analyze the long-term intracellular survival of *B. pertussis* inside primary human macrophages and to determine if virulence factor downregulation is involved in this process.

4. Elucidate the mechanism behind the pleiotropic phenotype of a single base transversion in the 5`-UTR of the *rplN-rpsD* operon of *Bordetella pertussis*.

7. Discussion

Infectious diseases represent significant burden for public health and the lower respiratory tract infections are among the leading causes of death due to respiratory disease worldwide (Gibson et al., 2013). Studies of molecular mechanisms of bacterial pathogenesis of the strictly human pathogens suffer significantly from the absence of appropriate animal models. This is also the case of the Gram-negative coccobacillus *Bordetella pertussis*, for which an appropriate animal model has long been missing, as infections of mice, rabbits or piglets do not adequately reproduce the course of the human pertussis disease (Elahi et al., 2007). The use of non-human primates as close human relatives, in which the course of infection is more truly reproduced, remains largely restricted due to the ethical concerns, low numbers of available animals, high cost, inter-species differences in innate immune functions and/or the influence of stress hormones on the course of the disease (Brinkworth et al., 2012; Elenkov and Chrousos, 1999). Three dimensional (3D) cell culture tissue systems, when grown under appropriate conditions, tend to successfully mimic the physiological performance of original tissues observed *in vivo* (Wrzesinski and Fey, 2018). Such systems represent valuable, albeit also costly models for this type of research. One of the projects described in this thesis, which focused on the analysis of epigenetic changes in epithelial cells caused by infection with *B. pertussis*, was originally aiming to implement a 3D culture test system of the airway mucosa developed by a collaborating research team from the University in Wuerzburg, Germany. This system uses human tracheobronchial epithelial cells (hTECs) and fibroblasts, which are seeded on a collagen scaffold, mimicking physiological microenvironment and thus representing a biologically highly relevant model for studying the behavior of obligate human pathogens, such as *B. pertussis* (Steinke et al., 2014). Unfortunately, the initially promising collaboration failed due to the lack of sufficient amounts of primary epithelial cells needed for seeding, which is a main drawback of this approach. In this situation, the conventional two dimensional (2D) cell cultures were the next choice, as they are most commonly used in preclinical studies. With their use, researchers have to only make the choice between established immortalized cell lines and primary cells. Although the cell lines represent almost inexhaustible and thus cheap source of "standardized" material, their biological relevance and resemblance to primary

cells often remains controversial (Drexler et al., 2003). Primary cells then usually introduce a wide donor-to-donor variation into the experiment, their supply is usually limited and their responses to various stimuli might significantly differ depending on which protocol was used for their cultivation (Lacey et al., 2012). Despite these drawbacks, primary cells certainly represent a more biologically relevant model and provide more accurate results e.g. in drug development studies, than immortalized cultured cells (Cree et al., 2010).

7.1 Phosphoproteomics of cAMP signaling of *Bordetella* adenylate cyclase toxin in mouse dendritic cells

In the first project, we explored the effects of CyaA-triggered cAMP-dependent signaling in primary murine dendritic cells. Adenylate cyclase toxin, the prominent immunosuppressive tool of *B. pertussis*, acts primarily via the unregulated conversion of intracellular ATP into supraphysiological levels of the key signaling molecule cAMP (Novak et al., 2017). cAMP then acts primarily by activating protein kinase A (PKA), but also partially by activation of Exchange Protein directly Activated (Epac) and thus shapes the response and behavior of intoxicated immune cells (Adkins et al., 2014; Ahmad et al., 2019; Cerny et al., 2015, 2017; Fedele et al., 2017). In order to study the molecular events resulting from CyaA intoxication, we performed an exploratory analysis in collaboration with the members of Department of Molecular Pathology and Biology from University of Defence in Hradec Kralove, using their proteomics facility. To obtain a maximum of quantitative information, we have used SILAC, the stable isotope labelling by amino acids in cell culture (Mann, 2006), for unbiased high-throughput phosphoproteomic analysis of primary mouse bone marrow derived dendritic cells (BMDC) intoxicated with CyaA. The advantages of these cells are that they can be easily obtained and could be labelled by SILAC, while still keeping reasonable biological relevance (Fabrik et al., 2014). To clearly differentiate the effects of cAMP elevation from the effects of other toxin actions, wild-type toxin was compared to non-enzymatic CyaA-AC$^-$ toxoid, which is unable to produce cAMP but still has the ability to bind the surface receptor CR3, permeabilize the host-cell membrane and eventually elicit Ca^{2+} influx into and K^+ efflux from the cells, respectively (Fiser et al., 2012; Ladant et al., 1992). This phosphoproteomic analysis was purely exploratory in its design as we did not intend to test any specific hypothesis. Nevertheless,

we were expecting to get at least some hints or answers to the questions raised by the results of other ongoing projects at that time, including the missing link between activation of Src homology domain 2 containing protein tyrosine phosphatase (SHP) 1 and cAMP-dependent PKA activation (Cerny et al., 2015). Unfortunately, we failed to obtain any conclusive data on the matter. Nevertheless, we obtained large amounts of data, corroborated by confirmatory immunoblotting analyses, which allowed us to describe at least some of the molecular events following cell intoxication by CyaA. One of the outcomes of this experiment was that it brought up the idea of epigenetic changes triggered during the infection of cells with *B. pertussis*, which was then followed in the next project discussed below. Using phosphoproteomic analysis, we described the molecular events involved in translation inhibition (dephosphorylation of 4E-BP1), phagocytosis (phosphorylation of VASP), maturation of dendritic cells, in the inhibition of pro-survival and induction of pro-apoptotic signaling (activation of tuberin leading to the inhibition of mTOR signaling), or promotion of tolerogenic immune response and production of IL-10 via the inhibitory phosphorylation of the SIK family of kinases, which promotes nuclear localization of the transcriptional co-activator CRTC3 (Novák et al., 2017). We observed dephosphorylation of the nuclear-localization signal of the class II histone deacetylase HDAC5. However, it was not possible to clearly confirm the nuclear translocation of HDAC5 in CyaA-treated cells due to the low signal detected by immunoblotting. In general, although this work represents a rather important source of data for analysis of cAMP-related signaling in dendritic cells intoxicated by CyaA, its limitation was that the effects of CyaA-elicited cAMP were not tested in the presence/absence of other stimuli, especially LPS, or of other bacterial components. Such stimuli are present in the real world context of a bacterial infection. The exploratory design of the study did not allow us to make any more specific conclusions, even though it yielded important information that promotes understanding of CyaA-triggered effects on target cells. To me personally, this project introduced me to the world of omics approaches, bioinformatics and data analysis.

7.1.1 My contribution in the "Phosphoproteomics of cAMP signaling of *Bordetella* adenylate cyclase toxin in mouse dendritic cells" project.

In this project, I helped with the intoxication of murine BMDCs, performed the bioinformatics analyses of the obtained data, did the Western blots and wrote the first version of the manuscript.

7.2 *Bordetella pertussis* acetylome is shaped by the lysine deacetylase Bkd1

The main driver of this project was the observed long persistence of clinical manifestations of pertussis infection, e.g. prolonged coughing in the absence of culturable bacteria months after the infection and the generally prolonged course of the disease, which can last for up to 12 weeks, or more (Mattoo and Cherry, 2005; Melvin et al., 2014). These observations indicated that viable but non-culturable (VBNC) bacteria may be persisting in the infected tissue (Li et al., 2014), or that long-lasting epigenetic changes may have resulted from the infection in host cells, or both. Long-lasting changes of host cells might be (at least in part) caused and maintained by epigenetic changes triggered during the infection and several hints exist that such changes might persist even when the pathogen has been cleared from the organism (Bierne et al., 2012; Fischer, 2020). Our preliminary data, obtained by global phosphoproteomic analysis of CyaA action on mouse dendritic cells, revealed post-translational modification of HDAC5, indicating that *B. pertussis* might possess a mechanisms that would deregulate the host cell signaling on epigenetic level (Novák et al., 2017), albeit upon CyaA intoxication such effects would be rather indirect. Potential impact of such modifications induced by CyaA intoxication (or by other bacterial factor) during *Bordetella* infection could only be hypothesized based on the work done with other bacterial pathogens, such as *Mycobacterium*, *Shigella*, *Listeria* or *Helicobacter* (Hamon and Cossart, 2008). Infection with *Helicobacter pylori* is a known risk factor for gastric cancer and the observed aberrant DNA methylation and other epigenetic changes might be the cause (Ushijima and Hattori, 2012; Wroblewski et al., 2010). This brought me to the question whether a highly prevalent pathogenic bacterium, such as *B. pertussis*, that is equipped with vast repertoire of different types of toxins and virulence factors, might potentially provoke heritable epigenetic changes in host cells and thus eventually sensitize its host to secondary bacterial or viral infections? Therefore, the initial hypotheses to be tested were that (i) the infection with *B. pertussis* triggers chromatin remodeling and thus deregulates gene expression in host cells and that (ii) it produces and eventually secretes bacterial effector(s) directly involved in host cell chromatin remodeling.

7.2.1 Development of the *in vitro* model used for infection experiments

Originally, chromatin remodeling was intended to be tested by analyzing the changes in several histone marks by immunofluorescent microscopy and by immunoblotting. As a model, 3D tissue model of human airway mucosa with hTECs and fibroblasts seeded on a collagen scaffold (Steinke et al., 2014) was planned to be used. Nevertheless, as mentioned above, this was not accomplished. Therefore, I started looking for another suitable model based on primary human cells, which then turned out to be an approximately a one year-long project of reading, testing and fine-tuning. With respect to their role in the first-line of innate immune response (Higgs et al., 2012) phagocytes - especially dendritic cells and macrophages – were the first choice. On both of these cell types, pertussis-related research was previously done, although cell lines were rather used (Adkins et al., 2014; Bromberg et al., 1991; Fedele et al., 2005, 2010; Friedman et al., 1992; Masure, 1992; Novák et al., 2017; Skopova et al., 2017). As I was also interested in the idea of intracellular survival of *B. pertussis*, I decided to further explore the interaction between this pathogen and macrophages. The most biologically relevant model for this purpose would be primary human alveolar macrophages, but the overall benefit of this approach is largely diminished by the limiting availability of such clinical material obtained by bronchoalveolar lavages (BALs) of patient lungs. Such approach is thus reasonable and justified for confirmatory analyses (Ahmad et al., 2019), but it would be unethical in a preliminary exploratory analysis. In this situation, I decided to work with peripheral blood monocyte-derived macrophages. There were several methods described for the isolation of these cells, which rely either on adhesion to the plastic surface, or on cell-sorting, usually employing anti-CD14 antibodies (Ahmad et al., 2019; Friedman et al., 1992; Graziani-Bowering et al., 1997; Menck et al., 2014; Miltenyi et al., 1990). The latter approach allows to obtain monocytes of high purity, but it may also negatively affect their further capacity to appropriately respond to LPS, become activated or proliferate (Bhattacharjee et al., 2018; Nielsen et al., 2020). Finally yet importantly, this approach is more expensive and time-consuming as special reagents and devices are necessary. However, convincing results were previously achieved also with the use of centrifugation and/or adhesion methods (Menck et al., 2014). I thus decided to follow and adapt these methods in our laboratory. For the isolation of monocytes and their differentiation into

macrophages, I used the protocol of Menck and her colleagues, in which they used the double gradient centrifugation method, with the first centrifugation onto a Ficoll cushion and a second one on a Percoll-based gradient. After that the purified cells were cultured in fluorinated ethylene propylene (FEP) Teflon-coated cell culture bags in the presence of M-CSF, the macrophage colony-stimulating factor (Menck et al., 2014). As manipulation with these bags often led to their rupture, contamination and low macrophage yields, I decided to try to use non-treated Petri dishes. As the result of this modification, I was able to obtain high macrophage yields with the cells being in a good shape. Properly done washing steps then allowed to minimize the presence of other cell types. In contrast to tissue-culture treated plates, macrophages cultured on the non-treated plastic surface could be detached from these plates without the need of enzymatic treatment by trypsin, by using only PBS or PBS with EDTA for cell liberation from the plastic. This feature was quite valuable, as the cellular surface structures remained largely intact and besides the macrophage´s well-being, their direct characterization by FACS could be performed without unnecessary artifacts introduced by enzymatic digestion of surface proteins. For the differentiation step, Menck and colleagues were using medium supplemented with both M-CSF and 2% human AB serum. Following the harvest, M-CSF was removed from the cultivating medium and human serum was used to replace 10% FCS. In contrast to their protocol, I used higher concentrations of M-CSF and 5% human serum during the differentiation step, which resulted in higher macrophage yields and increased viability. Following the harvest, I changed the medium from phosphate-buffered RPMI to the HEPES-buffered DMEM medium to permit a proper action of the calcium-dependent adenylate cyclase toxin (Basler et al., 2006). Third, I kept the cells in 5% human serum over the entire period of cultivation. Originally, I also tried to cultivate the cells in a serum-free medium, but such cultivation was not economically sustainable and did not bring any clear benefit. Instead, I kept the cells in the medium supplemented with human serum for the over the time of cultivation. Using human serum has important consequences, as bovine transferrin was shown to bind human cells with much less affinity, resulting in 8.6-fold lower rate of iron delivery, compared to human transferrin (Young and Garner, 1990). Cultivation of human cells with bovine serum/transferrin may thus lead to cellular iron deprivation with serious consequences (Soares and Hamza, 2016; Yauger et al., 2019). The widespread use of bovine serum may lead to artefactual observations and misleading

conclusions (Young and Garner, 1990). With this experimental set-up, I was able to keep the macrophages in culture for about 15 weeks, which was a quite surprising and unexpected result for primary cells, until I later learned about the successful cultivation of human peripheral blood mononuclear cells (PBMCs), for 46 days either in the medium containing normal human serum, or in a serum-free medium (Helinski et al., 1988). Several experiments including Western blots for analysis of changes in some of the histone marks were performed during the *in vitro* model development and fine-tuning, but I was not able to get any conclusive data, partially due to the immaturity of the model, technical issues and due to the high donor-to-donor variability of cell properties.

7.2.2 Discovery and characterization of a novel bacterial lysine deacetylase Bkd1

In order to identify possible bacterial chromatin remodeling effector(s), I performed *in silico* analysis of *B. pertussis* proteome, searching for a putative bacterial methyltransferases (MET) and lysine deacetylases (KDAC). The genome of *B. pertussis* encodes many proteins that might be classified as putative chromatin remodelers including putative KATs. However, in the light of limited sources I narrowed down the selection to only the putative METs and KDACs. One putative methyltransferases appeared to be encoded by the *BP0470* gene and was predicted to bear both SET and post-SET domains that were previously shown to act as chromatin regulators (Jenuwein, 2001; Jenuwein et al., 1998). From the lysine deacetylase hints, three putative proteins were predicted in *B. pertussis*, which might belong to the family of "histone deacetylase superfamily" according to the InterPro database (Mitchell et al., 2019). These were a predicted "histone deacetylase family protein" encoded by gene *BP0960*, a "putative acetylpolyamine aminohydrolase" encoded by gene *BP2300* and a "putative aminohydrolase" encoded by gene *BP3063*. All these genes were cloned, expressed in *E. coli* as FLAG-fusion proteins and purified. In parallel, mutant bacterial strains lacking these genes due to chromosomal deletions were constructed. As more evidence regarding the expression of some of these genes became available from different high-throughput proteomics and transcriptomics analyses (data from Ana Dienstbier and David Jurnecka, (Gouw et al., 2014; Williamson et al., 2015), I further narrowed down the selection to the proteins encoded by the *BP0960* and *BP3063* genes. For these proteins we had some

preliminary data supporting the idea that these proteins were produced by *B. pertussis* and might, eventually, be even secreted, albeit this needed validation. In order to do so, these two products of these genes were FLAG-tagged on their N- or C-termini by insertion of corresponding oligonucleotide sequences into the respective open reading frames of the genes in the bacterial genome, the bacteria were grown under standard conditions, lysed and processed in order to separate cytosolic and secreted proteins. The lysates were analyzed by Western blots, using immunostaining with an anti-FLAG antibody. The results suggested that BP0960 tagged on its N-terminus and BP3063 tagged on its C-terminus might by present also in the secreted protein fraction. Nevertheless, when we fused these proteins with the adenylate cyclase domain from CyaA (Sory and Cornelis, 1994) in the Δ*cyaA* mutant strain, no adenylate cyclase enzyme activity in supernatants was detected, indicating that these proteins were either not secreted or were not properly folded. Therefore, we could not conclusively confirm that these are secreted proteins.

For the structural analysis of the purified BP0960 (Bkd1) and BP3063 proteins, we used circular dichroism (CD) spectroscopy to confirm that both proteins were folded. We then tried to characterize their structure by the Small angle X-ray scattering (SAXS) measurements that can be used for liquid samples and allows to determine low resolution molecular envelope of the protein species. Calculations predicted envelopes formed by multimeric complexes, which was in striking contrast with the monomers observed by liquid chromatography. As we were the first, whose samples were measured by the newly installed SAXS instrument, we kept these data in mind, but were rather cautious with their interpretation. We also attempted to crystallize both proteins, but the purified Bkd1 protein tended to precipitate at higher concentrations needed for crystallization. BP3063 protein, in contrast, crystallized readily and rapidly, but formed small crystals, which could not be measured.

Purified proteins were tested for lysine deacetylase activity *in vitro* by the luminescence assay suitable for both class I and II lysine (or histone) deacetylases as it uses an HDAC I/II-optimized consensus substrate sequence derived from histone 4. When luminogenic substrate becomes deacetylated by the tested enzyme, the deacetylation activity can be measured by the combination of protease treatment, which cleaves the link between the peptide and aminoluciferin, then used as substrate by the

luciferase enzyme, generating a stable emission of light. As a positive control, we used recombinant human HDAC6 (kind gift from Cyril Barinka), which is a large multi-domain enzyme containing tandem catalytic domains (Hai and Christianson, 2016). In this context, we were surprised by the extent of substrate deacetylation by Bkd1, which is a small monomeric bacterial enzyme. In contrast, the BP3063 protein did not exhibit any detectable activity towards the tested lysine deacetylase substrate (Novak et al., 2020). These results then nicely correlated with the observed changes in the compositions of the total acetylomes of the *Δbkd1* and *Δbp3063* mutant bacterial biomass. Whereas the total numbers of the quantified acetyl-lysine (AcK) sites in both wild-type and *Δbp3063* mutant bacteria were similar, almost twice as many AcK sites were identified in *Δbkd1* mutant bacteria. Based on bioinformatics analysis of the measured data, we concluded that Bkd1 acted as a regulator of the overall bacterial metabolism, rather than a regulator of bacterial virulence through deacetylation of some key regulatory proteins. This was further supported by the shorter doubling time of the *Δbkd1* mutant bacteria in the exponential phase of growth in carbon source-limited liquid media. Despite and overall similar intracellular survival capacity inside primary human macrophages of the wild-type and *Δbkd1* mutant bacteria, a reduced virulence of the Δ*bkd1* mutant *in vivo* in the model of mouse lung infection did not come as a surprise. The bacterial strain with deregulated growth under nutrient-limiting conditions would certainly exhibit a reduced fitness in the more complex and regulation highly-demanding *in vivo* environment. A possible explanation of the similar survival capacities of the wild-type and *Δbkd1* mutant bacteria in the quite hostile environment inside primary human macrophages was then suggested by the results of the subsequent project.

7.2.3 My contribution in the "*Bordetella pertussis* Acetylome is Shaped by Lysine Deacetylase Bkd1" project.

In this project, I designed the study, established the *in vitro* infection model with primary human macrophages, cooperated in purification of the proteins, cooperated in the preparation of mutant strains, did the bioinformatics analysis of the obtained data, phenotypically characterized the *Δbkd1* mutant (growth curves and intracellular survival), analyzed BvgA and BvgA~P protein levels and wrote the first version of the manuscript.

7.3 A mutation upstream of the *rplN-rpsD* ribosomal operon downregulates *Bordetella pertussis* virulence factor production without compromising bacterial survival within human macrophages

Production of virulence factors by *B. pertussis* is controlled by the main regulatory BvgAS two component system (TCS), with input from several other sensory systems involved in fine-tuning of the bacterial response to specific environmental conditions. The Bvg^+ phase is both necessary and sufficient for successful respiratory infection in mice (Bone et al., 2017; Coutte et al., 2016; Martinez de Tejada et al., 1998; Moon et al., 2017; Uhl and Miller, 1994; Yuk et al., 1998) (see Introduction). In this context, mutations affecting the BvgAS function would be expected to severely impair bacterial survival, with mutations in individual virulence factors having detrimental effects on bacterial interactions with host cells, e.g. mutations or deletions of CyaA (Cerny et al., 2015) or Vag8 (Marr et al., 2011). Therefore, it was surprising, if not shocking, to observe an enhanced intracellular survival capacity of *B. pertussis* bacteria that had altered CyaA activity or production, when compared to the wild-type bacteria producing normal levels of CyaA. Initially, we thought that the bacterial strain, which formed both hemolytic and non-hemolytic colonies following the lysis of infected macrophages was a mutant strain only lacking *BP3063* gene. This would have indicated that this protein might have a regulatory role in virulence. However, we later found that these initial observations were obtained with a mixture of two clones, since both hemolytic and non-hemolytic clones had the *BP3063* gene deleted and the stability of the observed phenotypes was confirmed by serial platings of cultures prepared form isolated single clone colonies. We observed that with the non-hemolytic mutant the hemolysis halos were not fully absent, but rather their appearance was significantly delayed. Independent construction of a new *Δbp3063* mutant strain with normal hemolytic phenotype showed that instead of a bacterial strain with a bi-stable phenotype, we were using a mix of two bacterial clones that were both lacking *BP3063*. This meant that the non-hemolytic clone carried an additional mutation accounting for the non-hemolytic phenotype. To identify this mutation, I first performed PCR-based sequencing of the *cya* operon and of the *bvgAS* locus, but did not detect any additional mutation in these loci. Several Western blots for additional virulence factor detection were performed to check if production any other virulence factor might have

also been affected. Whereas the production of pertactin was not importantly different between the hemolytic and non-hemolytic *Δbp3063* mutants, lower amounts of FHA or of the pertussis toxin S1 subunit were produced by the non-hemolytic strain. Analysis of the intracellular survival capacity inside primary human macrophages revealed an enhanced intracellular survival capacity of the non-hemolytic strain. To identify the additional mutation present in the non-hemolytic strain, we thus decided to sequence the entire genomic DNA of this mutant by using the Illumina technology. The outcome of the sequence analysis was, indeed, rather unexpected. On top of the deletion of the *BP3063* open reading frame we identified a single G to T base transversion located in the 5´-UTR of the *BP3626/rplN* gene at 18 bases upstream from the start codon of the *rplN* ORF that is the first gene of the operon encoding for ribosomal proteins. Thus instead of a clear explanation of the observed phenotype, we found rather a confusing mutation of unclear importance in the non-coding region far away from any virulence-related gene loci. To confirm that the observed non-hemolytic phenotype was due to the detected SNP, we introduced this mutation into the chromosome of the wild-type *B. pertussis* strain and obtained a non-hemolytic mutant that was then called JN1. When we removed this mutation by allelic exchange on bacterial chromosome, the strain became hemolytic again, showing unequivocally that the SNP accounted for the non-hemolytic phenotype. Detailed characterization of the JN1 mutant strain phenotype was thus performed by high-throughput unbiased transcriptomic (RNA-seq) and proteomic analyses. In the proteomic analysis, both total proteome and secretome were analyzed. In line with the phenotypic data, downregulation of many virulence factors was confirmed, including CyaA, PT or FHA and even pertactin production levels were found to be downregulated, although to a lesser extent than for other virulence factors. The observed differences in the extent of down-regulation were largely reflecting the differential sensitivity to BvgA-dependent gene expression regulation of the individual virulence factor genes (Kinnear et al., 2001). The same trend as for the virulence factors was observed also for the components of the four bacterial secretion systems expressed in *B. pertussis*. This in turn further enhanced the effects of gene down-regulation and even the proteins that accumulated at similar to wild-type levels in the cytosol of the JN1 mutant bacteria were still significantly reduced in amounts secreted into culture supernatant. This was particularly striking for pertussis toxin secretion.

The steady-state abundance of transcripts originating from the *rplN-rpsD* operon was higher in the JN1 mutant strain, but this was not reflected on the produced protein level. One of the exceptions, in which the increase in steady-state transcript abundance translated into increased protein level, was the alpha subunit of the DNA-dependent RNA polymerase (RpoA). Interestingly, the *rpoA* ORF is located about 7.5 kb downstream from the detected G to T transversion SNP and it is not fully clear, if *rpoA* is part of the upstream ribosomal protein operon, even if it is more than likely that it is part of it (Amman et al., 2018). Analysis of the RNA-seq data did not reveal any small RNA, the level of which would be affected by the G to T transversion SNP. Nevertheless, several other groups have previously observed that deregulation of expression of the *rpoA* gene due to the mutations in the region immediately upstream of the *rpoA* ORF translated into reduced BvgA-activated virulence factor production ((Carbonetti et al., 1994, 2000) and personal communication with Camille Locht and Loic Coutte). Unfortunately, based on our data, we were not able to elucidate how the increased RpoA protein level could account for the overall deregulation of virulence factors. We hypothesized that such upregulation might cause partial sequestration of the phosphorylated BvgA (BvgA~P) protein into non-productive complexes with overproduced RpoA, yielding in the first place a reduced transcription of the BvgA positively regulated *bvgAS* locus itself (Uhl and Miller, 1994; Williams and Cotter, 2007). Indeed, we detected a reduced concentration of the BvgA~P protein in the lysates of the JN1 mutant strain, compared to lysates of wild type bacteria.

7.3.1 Long-term survival of *B. pertussis* inside human macrophages

By using the infection model of primary human macrophages, I monitored long-term intracellular survival of *B. pertussis* bacteria in these cells. Up to now, three days after the infection has been the latest time point used in monitoring of *B. pertussis* infection of monocytes/macrophages (Cerny et al., 2015; Friedman et al., 1992; Lamberti et al., 2016; Masure, 1993). This was due to the fact that it no culturable bacteria were obtained from macrophage lysates beyond this time point. To overcome this problem, I utilized the currently developed qPCR-based assay to determine the numbers of live and dead bacteria inside macrophages over prolonged culture periods (Ramkissoon et al., 2020). By using fluorescence microscopy we were also able to follow the presence of internalized bacteria producing red fluorescent protein mScarlet (Bindels et al., 2017) for about four weeks after

macrophage infection. These bacteria were non-culturable, same as the bacteria from the pulmonary alveolar macrophages from BALs of HIV-infected children (Bromberg et al., 1991). This suggested that macrophages might represent a niche from which the bacteria could be released under as yet undefined conditions, as suggested by early results of rat respiratory infection with *B. pertussis* (Woods et al., 1989). Long-term persistence of *in vitro* non-culturable *B. pertussis* bacteria within primary alveolar macrophages in infected airways might, indeed, provide an explanation for at least some of the long-lasting clinical manifestations of pertussis in humans (Mattoo and Cherry, 2005; Melvin et al., 2014).

7.3.2 The "hidden orchestra" of virulence factors inside macrophages

With the JN1 mutant strain, we serendipitously obtained an excellent tool for further analysis of the intracellular survival of *B. pertussis* in macrophages and other cells. Despite the initial expectations based on the existing evidence (Cerny et al., 2015), we did not observe an immediate clearance of the defected bacteria by host immune cells. Although the bacterial cells of the JN1 mutant strain were extremely sensitive to complement-mediated killing, due to the reduced production of the BrkA and Vag8 complement resistance proteins (Barnes and Weiss, 2001; Marr et al., 2011), the JN1 bacteria were surviving inside primary human macrophages for several weeks at similar, or even higher rates, as the wild-type bacteria. When we analyzed the cells infected either by wild-type or JN1 mutant strain by FACS, we found out that the expression of the phenotypic markers CD11b, CD36 or HLA-DR was not really different in these cells. Some statistically significant differences were observed only for the CD14 marker. Furthermore, the expression of several inflammatory/anti-inflammatory cytokines, such as TNFα, IFNγ, IL-10 and TGFβ was analyzed for these cells by using qPCR and yielded similar expression patterns. These data, complemented by the recent observation of down-regulation of virulence factor expression by internalized *B. pertussis* bacteria during short-term intracellular survival (Petráčková et al., 2020), indicate that *B. pertussis* tends to adapt to the intracellular niche by down-regulation of virulence factor production to the levels allowing the bacteria to evade the cellular defense mechanisms. We also observed *in vivo* that the JN1 mutant bacteria were able to persist longer inside infected mouse lungs than wild-type bacteria, despite (or rather because of) lower initial proliferation.

These data are in line with the observed long-term accumulation of Bvg$^-$ phase-locked mutants of *B. pertussis* in the airways of primates (Karataev et al., 2016; Medkova et al., 2013). These results thus indicate that the so far unclear roles of the Bvg^i or Bvg$^-$ phases (Merkel et al., 1998b) might relate to the intracellular stage of airway infection by *B. pertussis*, warranting further research in this direction.

7.3.3 My contribution in "A Mutation Upstream of the *rplN-rpsD* Ribosomal Operon Downregulates *Bordetella pertussis* Virulence Factor Production without Compromising Bacterial Survival within Human Macrophages" project.

In this project, I designed the study, constructed the JN1 mutant strain, isolated, differentiated and cultivated the primary human macrophages, performed the infection experiments and analyzed the intracellular bacterial survival, performed live/dead quantitative real-time PCR, prepared the samples for FACS analysis, analyzed the BvgA and BvgA~P protein levels, prepared the samples for RNA-seq and proteomic analysis, analyzed the generated omics data, performed the autoaggregation assay and wrote the first version of the manuscript.

8. Conclusions

Bordetella pertussis is a bacterial pathogen that has quite recently adapted to its human host and that is equipped with a wide variety of virulence factors that support its various immune evasion strategies. Despite the high relevance for human health, the biology underlying *B. pertussis* infections remains poorly explored in several important aspects. The main intent of the work described in this thesis was to analyze the host-pathogen interaction between *B. pertussis* and phagocytes, which are on the frontline of body´s defense to infection. The main conclusions drawn from the presented work are as follows:

1) We found that the cAMP-dependent signaling triggered by CyaA intoxication of murine dendritic cells:
   a) leads to repression of mTOR signaling via the activation of mTORC1 inhibitors TSC2 and PRAS40
   b) triggers inhibitory phosphorylation of SIK family kinases and thus provokes dephosphorylation of the transcriptional coactivator CRTC3, which might promote its nuclear translocation and eventually induce production of the anti-inflammatory cytokine IL-10
   c) alters the phosphorylation status of multiple regulators of actin cytoskeleton homeostasis

2) Even though I failed in the originally intended analysis of epigenetic changes accompanying infection by *B. pertussis,* in this project we:
   a) identified, cloned and purified one of the few described bacterial lysine deacetylases, which we called Bkd1
   b) found that Bkd1 enzyme efficiently deacetylated a substrate having an HDAC I/II-optimized consensus sequence derived from histone 4 HDAC substrate and that expression of Bkd1 in *B. pertussis* extensively shaped the bacterial acetylome
   c) established model of *B. pertussis* long-term infection of primary human macrophages

3) Using a virulence factor expression impaired JN1 mutant and the model of *in vitro* infection of primary human macrophages, we found that:
   a) *B. pertussis* bacteria survived inside primary human macrophages for several weeks after infection
   b) the downregulation of virulence factors may represent the adaptation of *B. pertussis* to intracellular environment enabling bacterial survival inside primary human macrophages
   c) downregulation of virulence factors in the JN1 mutant allowed establishment of persistent infection *in vivo* in the mouse model of *B. pertussis* respiratory infection
   d) RpoA overproduction due to a single G to T transverion SNP in the 5`-UTR region of the *rplN-rpsD* operon for ribosomal proteins enhances expression of the RpoA subunit of the DNA-dependent RNA polymerase. By an as yet undefined mechanism this SNP causes important deregulation of *B. pertussis* genome expression, downregulating particularly the expression of virulence factors genes

9. References

AbouElfetouh, A., Kuhn, M.L., Hu, L.I., Scholle, M.D., Sorensen, D.J., Sahu, A.K., Becher, D., Antelmann, H., Mrksich, M., Anderson, W.F., et al. (2015). The *E. coli* sirtuin CobB shows no preference for enzymatic and nonenzymatic lysine acetylation substrate sites. MicrobiologyOpen *4*, 66–83.

Adkins, I., Kamanova, J., Kocourkova, A., Svedova, M., Tomala, J., Janova, H., Masin, J., Chladkova, B., Bumba, L., Kovar, M., et al. (2014). Bordetella adenylate cyclase toxin differentially modulates toll-like receptor-stimulated activation, migration and T cell stimulatory capacity of dendritic cells. PLoS ONE *9*, e104064.

Ahmad, J.N., Cerny, O., Linhartova, I., Masin, J., Osicka, R., and Sebo, P. (2016). cAMP signalling of *Bordetella* adenylate cyclase toxin through the SHP-1 phosphatase activates the BimEL-Bax pro-apoptotic cascade in phagocytes. Cellular Microbiology *18*, 384–398.

Ahmad, J.N., Holubova, J., Benada, O., Kofronova, O., Stehlik, L., Vasakova, M., and Sebo, P. (2019). Bordetella Adenylate Cyclase Toxin Inhibits Monocyte-to-Macrophage Transition and Dedifferentiates Human Alveolar Macrophages into Monocyte-like Cells. MBio *10*.

Allfrey, V.G., Faulkner, R., and Mirsky, A.E. (1964). ACETYLATION AND METHYLATION OF HISTONES AND THEIR POSSIBLE ROLE IN THE REGULATION OF RNA SYNTHESIS. Proceedings of the National Academy of Sciences *51*, 786–794.

Amman, F., D'Halluin, A., Antoine, R., Huot, L., Bibova, I., Keidel, K., Slupek, S., Bouquet, P., Coutte, L., Caboche, S., et al. (2018). Primary transcriptome analysis reveals importance of IS elements for the shaping of the transcriptional landscape of Bordetella pertussis. RNA Biol *15*, 967–975.

Arenas, J., Pupo, E., de Jonge, E., Pérez-Ortega, J., Schaarschmidt, J., van der Ley, P., and Tommassen, J. (2019). Substrate specificity of the pyrophosphohydrolase LpxH determines the asymmetry of *Bordetella pertussis* lipid A. J. Biol. Chem. *294*, 7982–7989.

Aricò, B., and Rappuoli, R. (1987). Bordetella parapertussis and Bordetella bronchiseptica contain transcriptionally silent pertussis toxin genes. Journal of Bacteriology *169*, 2847–2853.

Ashworth, L.A., Irons, L.I., and Dowsett, A.B. (1982). Antigenic relationship between serotype-specific agglutinogen and fimbriae of Bordetella pertussis. Infect. Immun. *37*, 1278–1281.

Ashworth, L.A., Robinson, A., Funnell, S., Gorringe, A.R., Irons, L.I., and Seabrook, R.N. (1988). Agglutinogens and fimbriae of Bordetella pertussis. Tokai J. Exp. Clin. Med. *13 Suppl*, 203–210.

Barak, R., and Eisenbach, M. (2001). Acetylation of the response regulator, CheY, is involved in bacterial chemotaxis: CheY acetylation is involved in chemotaxis. Molecular Microbiology *40*, 731–743.

Barnes, M.G., and Weiss, A.A. (2001). BrkA protein of Bordetella pertussis inhibits the classical pathway of complement after C1 deposition. Infect Immun *69*, 3067–3072.

Barry, E.M., Weiss, A.A., Ehrmann, I.E., Gray, M.C., Hewlett, E.L., and Goodwin, M.S. (1991). Bordetella pertussis adenylate cyclase toxin and hemolytic activities require a second gene, cyaC, for activation. J. Bacteriol. *173*, 720–726.

Bart, M.J., Harris, S.R., Advani, A., Arakawa, Y., Bottero, D., Bouchez, V., Cassiday, P.K., Chiang, C.-S., Dalby, T., Fry, N.K., et al. (2014). Global Population Structure and Evolution of Bordetella pertussis and Their Relationship with Vaccination. MBio *5*, e01074-14.

Basler, M., Masin, J., Osicka, R., and Sebo, P. (2006). Pore-forming and enzymatic activities of Bordetella pertussis adenylate cyclase toxin synergize in promoting lysis of monocytes. Infect. Immun. *74*, 2207–2214.

Baxter, R., Bartlett, J., Fireman, B., Lewis, E., and Klein, N.P. (2017). Effectiveness of Vaccination During Pregnancy to Prevent Infant Pertussis. Pediatrics *139*, e20164091.

el Bayâ, A., Linnemann, R., von Olleschik-Elbheim, L., Robenek, H., and Schmidt, M.A. (1997). Endocytosis and retrograde transport of pertussis toxin to the Golgi complex as a prerequisite for cellular intoxication. Eur. J. Cell Biol. *73*, 40–48.

el Bayâ, A., Brückener, K., and Schmidt, M.A. (1999). Nonrestricted differential intoxication of cells by pertussis toxin. Infect. Immun. *67*, 433–435.

Bayram, J., Malcova, I., Sinkovec, L., Holubova, J., Streparola, G., Jurnecka, D., Kucera, J., Sedlacek, R., Sebo, P., and Kamanova, J. (2020). Cytotoxicity of the effector protein BteA was attenuated in Bordetella pertussis by insertion of an alanine residue. PLoS Pathog. *16*, e1008512.

Beall, B.W., and Sanden, G.N. (1995). Cloning and initial characterization of the Bordetella pertussis fur gene. Current Microbiology *30*, 223–226.

Belcher, T., and Preston, A. (2015). *Bordetella pertussis* evolution in the (functional) genomics era. Pathogens and Disease *73*, ftv064.

Bellalou, J., Sakamoto, H., Ladant, D., Geoffroy, C., and Ullmann, A. (1990). Deletions affecting hemolytic and toxin activities of Bordetella pertussis adenylate cyclase. Infect Immun *58*, 3242–3247.

Bhattacharjee, J., Das, B., Mishra, A., Sahay, P., and Upadhyay, P. (2018). Monocytes isolated by positive and negative magnetic sorting techniques show different molecular characteristics and immunophenotypic behaviour. F1000Res *6*, 2045.

Bierne, H., Hamon, M., and Cossart, P. (2012). Epigenetics and bacterial infections. Cold Spring Harb Perspect Med *2*, a010272.

Bindels, D.S., Haarbosch, L., van Weeren, L., Postma, M., Wiese, K.E., Mastop, M., Aumonier, S., Gotthard, G., Royant, A., Hink, M.A., et al. (2017). mScarlet: a bright monomeric red fluorescent protein for cellular imaging. Nat. Methods *14*, 53–56.

Blander, G., and Guarente, L. (2004). The Sir2 Family of Protein Deacetylases. Annu. Rev. Biochem. *73*, 417–435.

Bokoch, G.M., Katada, T., Northup, J.K., Hewlett, E.L., and Gilman, A.G. (1983). Identification of the predominant substrate for ADP-ribosylation by islet activating protein. J. Biol. Chem. *258*, 2072–2075.

Bone, M.A., Wilk, A.J., Perault, A.I., Marlatt, S.A., Scheller, E.V., Anthouard, R., Chen, Q., Stibitz, S., Cotter, P.A., and Julio, S.M. (2017). *Bordetella* PlrSR regulatory system controls BvgAS activity and virulence in the lower respiratory tract. Proc Natl Acad Sci USA *114*, E1519–E1527.

Bordet, J., and Gengou, O. (1909). L'endotoxine coquelucheuse. Ann.Inst,Pasteur. 415–419.

Boschwitz, J.S., van der Heide, H.G., Mooi, F.R., and Relman, D.A. (1997). Bordetella bronchiseptica expresses the fimbrial structural subunit gene fimA. Journal of Bacteriology *179*, 7882–7885.

Boucher, P.E., and Stibitz, S. (1995). Synergistic binding of RNA polymerase and BvgA phosphate to the pertussis toxin promoter of Bordetella pertussis. Journal of Bacteriology *177*, 6486–6491.

Bouchez, V., Brun, D., Cantinelli, T., Dore, G., Njamkepo, E., and Guiso, N. (2009). First report and detailed characterization of B. pertussis isolates not expressing pertussis toxin or pertactin. Vaccine *27*, 6034–6041.

Boulanger, A., Chen, Q., Hinton, D.M., and Stibitz, S. (2013). *In vivo* phosphorylation dynamics of the *Bordetella pertussis* virulence-controlling response regulator BvgA: *In vivo* phosphorylation of BvgA. Molecular Microbiology *88*, 156–172.

Boulanger, A., Moon, K., Decker, K.B., Chen, Q., Knipling, L., Stibitz, S., and Hinton, D.M. (2015). *Bordetella pertussis fim3* gene regulation by BvgA: Phosphorylation controls the formation of inactive vs. active transcription complexes. Proc Natl Acad Sci USA *112*, E526–E535.

Brickman, T.J., and Armstrong, S.K. (1995). Bordetella pertussis fur gene restores iron repressibility of siderophore and protein expression to deregulated Bordetella bronchiseptica mutants. Journal of Bacteriology *177*, 268–270.

Brickman, T.J., Vanderpool, C.K., and Armstrong, S.K. (2006). Heme Transport Contributes to In Vivo Fitness of Bordetella pertussis during Primary Infection in Mice. IAI *74*, 1741–1744.

Brickman, T.J., Anderson, M.T., and Armstrong, S.K. (2007). Bordetella iron transport and virulence. Biometals *20*, 303–322.

Brinig, M.M., Register, K.B., Ackermann, M.R., and Relman, D.A. (2006). Genomic features of Bordetella parapertussis clades with distinct host species specificity. Genome Biol *7*, R81.

Brinkworth, J.F., Pechenkina, E.A., Silver, J., and Goyert, S.M. (2012). Innate immune responses to TLR2 and TLR4 agonists differ between baboons, chimpanzees and humans. J. Med. Primatol. *41*, 388–393.

Bromberg, K., Tannis, G., and Steiner, P. (1991). Detection of Bordetella pertussis associated with the alveolar macrophages of children with human immunodeficiency virus infection. Infect. Immun. *59*, 4715–4719.

Bumba, L., Masin, J., Fiser, R., and Sebo, P. (2010). Bordetella adenylate cyclase toxin mobilizes its beta2 integrin receptor into lipid rafts to accomplish translocation across target cell membrane in two steps. PLoS Pathog *6*, e1000901.

Bumba, L., Masin, J., Macek, P., Wald, T., Motlova, L., Bibova, I., Klimova, N., Bednarova, L., Veverka, V., Kachala, M., et al. (2016). Calcium-Driven Folding of RTX Domain β-Rolls Ratchets Translocation of RTX Proteins through Type I Secretion Ducts. Mol. Cell *62*, 47–62.

Carbonetti, N.H. (2015). Contribution of pertussis toxin to the pathogenesis of pertussis disease: Graphical Abstract Figure. Pathogens and Disease *73*, ftv073.

Carbonetti, N.H. (2016). Pertussis leukocytosis: mechanisms, clinical relevance and treatment. Pathogens and Disease *74*, ftw087.

Carbonetti, N.H., Fuchs, T.M., Patamawenu, A.A., Irish, T.J., Deppisch, H., and Gross, R. (1994). Effect of mutations causing overexpression of RNA polymerase alpha subunit on regulation of virulence factors in Bordetella pertussis. Journal of Bacteriology *176*, 7267–7273.

Carbonetti, N.H., Romashko, A., and Irish, T.J. (2000). Overexpression of the RNA Polymerase Alpha Subunit Reduces Transcription of Bvg-Activated Virulence Genes inBordetella pertussis. Journal of Bacteriology *182*, 529–531.

Caroff, M., Deprun, C., Richards, J.C., and Karibian, D. (1994). Structural characterization of the lipid A of Bordetella pertussis 1414 endotoxin. Journal of Bacteriology *176*, 5156–5159.

CDC (2019). Pertussis (Whooping Cough) - Clinical Complications.

Cerny, O., Kamanova, J., Masin, J., Bibova, I., Skopova, K., and Sebo, P. (2015). Bordetella pertussis Adenylate Cyclase Toxin Blocks Induction of Bactericidal Nitric Oxide in Macrophages through cAMP-Dependent Activation of the SHP-1 Phosphatase. J. Immunol. *194*, 4901–4913.

Cerny, O., Anderson, K.E., Stephens, L.R., Hawkins, P.T., and Sebo, P. (2017). cAMP Signaling of Adenylate Cyclase Toxin Blocks the Oxidative Burst of Neutrophils through Epac-Mediated Inhibition of Phospholipase C Activity. J. Immunol. *198*, 1285–1296.

Cheers, C., and Gray, D.F. (1969). Macrophage behaviour during the complaisant phase of murine pertussis. Immunology *17*, 875–887.

Chen, Q., Ng, V., Warfel, J.M., Merkel, T.J., and Stibitz, S. (2017). Activation of Bvg-Repressed Genes in Bordetella pertussis by RisA Requires Cross Talk from Noncooperonic Histidine Kinase RisK. J. Bacteriol. *199*, e00475-17, /jb/199/22/e00475-17.atom.

Cherry, J.D. (2016). Pertussis in Young Infants Throughout the World. Clin. Infect. Dis. *63*, S119–S122.

Chlibek, R., Smetana, J., Sosovickova, R., Fabianova, K., Zavadilova, J., Dite, P., Gal, P., Naplava, P., and Lzicarova, D. (2017). Seroepidemiology of whooping cough in the Czech Republic: estimates of incidence of infection in adults. Public Health *150*, 77–83.

Choudhary, C., Kumar, C., Gnad, F., Nielsen, M.L., Rehman, M., Walther, T.C., Olsen, J.V., and Mann, M. (2009). Lysine acetylation targets protein complexes and co-regulates major cellular functions. Science *325*, 834–840.

Christensen, D.G., Xie, X., Basisty, N., Byrnes, J., McSweeney, S., Schilling, B., and Wolfe, A.J. (2019a). Post-translational Protein Acetylation: An Elegant Mechanism for Bacteria to Dynamically Regulate Metabolic Functions. Front. Microbiol. *10*, 1604.

Christensen, D.G., Baumgartner, J.T., Xie, X., Jew, K.M., Basisty, N., Schilling, B., Kuhn, M.L., and Wolfe, A.J. (2019b). Mechanisms, Detection, and Relevance of Protein Acetylation in Prokaryotes. MBio *10*.

Confer, D.L., and Eaton, J.W. (1982). Phagocyte impotence caused by an invasive bacterial adenylate cyclase. Science *217*, 948–950.

Connelly, C.E., Sun, Y., and Carbonetti, N.H. (2012). Pertussis Toxin Exacerbates and Prolongs Airway Inflammatory Responses during Bordetella pertussis Infection. Infect. Immun. *80*, 4317–4332.

Cookson, B.T., Cho, H.L., Herwaldt, L.A., and Goldman, W.E. (1989). Biological activities and chemical composition of purified tracheal cytotoxin of Bordetella pertussis. Infect. Immun. *57*, 2223–2229.

Cotter, P.A., and Miller, J.F. (1994). BvgAS-mediated signal transduction: analysis of phase-locked regulatory mutants of Bordetella bronchiseptica in a rabbit model. Infect. Immun. *62*, 3381–3390.

Cotter, P.A., and Miller, J.F. (1997). A mutation in the *Bordetella bronchiseptica bvgS* gene results in reduced virulence and increased resistance to starvation, and identifies a new class of Bvg-regulated antigens. Molecular Microbiology *24*, 671–685.

Cotter, P.A., Yuk, M.H., Mattoo, S., Akerley, B.J., Boschwitz, J., Relman, D.A., and Miller, J.F. (1998). Filamentous hemagglutinin of Bordetella bronchiseptica is required for efficient establishment of tracheal colonization. Infect. Immun. *66*, 5921–5929.

Coutte, L., Antoine, R., Drobecq, H., Locht, C., and Jacob-Dubuisson, F. (2001). Subtilisin-like autotransporter serves as maturation protease in a bacterial secretion pathway. EMBO J. *20*, 5040–5048.

Coutte, L., Huot, L., Antoine, R., Slupek, S., Merkel, T.J., Chen, Q., Stibitz, S., Hot, D., and Locht, C. (2016). The multifaceted RisA regulon of Bordetella pertussis. Sci Rep *6*, 32774.

Cowell, J.L., Hewlett, E.L., and Manclark, C.R. (1979). Intracellular localization of the dermonecrotic toxin of Bordetella pertussis. Infect. Immun. *25*, 896–901.

Crawford, J.G., and Fishel, C.W. (1959). Growth of Bordetella pertussis in tissue culture. J. Bacteriol. *77*, 465–474.

Cree, I.A., Glaysher, S., and Harvey, A.L. (2010). Efficacy of anti-cancer agents in cell lines versus human primary tumour tissue. Curr Opin Pharmacol *10*, 375–379.

Cullinane, L.C., Alley, M.R., Marshall, R.B., and Manktelow, B.W. (1987). *Bordetella parapertussis* from lambs. New Zealand Veterinary Journal *35*, 175–175.

Cundell, D.R., Kanthakumar, K., Taylor, G.W., Goldman, W.E., Flak, T., Cole, P.J., and Wilson, R. (1994). Effect of tracheal cytotoxin from Bordetella pertussis on human neutrophil function in vitro. Infect. Immun. *62*, 639–643.

Dalebroux, Z.D., and Swanson, M.S. (2012). ppGpp: magic beyond RNA polymerase. Nat Rev Microbiol *10*, 203–212.

Decker, K.B., James, T.D., Stibitz, S., and Hinton, D.M. (2012). The Bordetella pertussis model of exquisite gene control by the global transcription factor BvgA. Microbiology *158*, 1665–1676.

Drexler, H.G., Dirks, W.G., Matsuo, Y., and MacLeod, R. a. F. (2003). False leukemia-lymphoma cell lines: an update on over 500 cell lines. Leukemia *17*, 416–426.

Dupré, E., Herrou, J., Lensink, M.F., Wintjens, R., Vagin, A., Lebedev, A., Crosson, S., Villeret, V., Locht, C., Antoine, R., et al. (2015). Virulence Regulation with Venus Flytrap Domains: Structure and Function of the Periplasmic Moiety of the Sensor-Kinase BvgS. PLoS Pathog *11*, e1004700.

Eby, J.C., Gray, M.C., and Hewlett, E.L. (2014). Cyclic AMP-mediated suppression of neutrophil extracellular trap formation and apoptosis by the Bordetella pertussis adenylate cyclase toxin. Infect. Immun. *82*, 5256–5269.

Ehrmann, I.E., Gray, M.C., Gordon, V.M., Gray, L.S., and Hewlett, E.L. (1991). Hemolytic activity of adenylate cyclase toxin from Bordetella pertussis. FEBS Lett. *278*, 79–83.

Elahi, S., Holmstrom, J., and Gerdts, V. (2007). The benefits of using diverse animal models for studying pertussis. Trends Microbiol. *15*, 462–468.

Elenkov, null, and Chrousos, null (1999). Stress Hormones, Th1/Th2 patterns, Pro/Anti-inflammatory Cytokines and Susceptibility to Disease. Trends Endocrinol. Metab. *10*, 359–368.

Emsley, P., Charles, I.G., Fairweather, N.F., and Isaacs, N.W. (1996). Structure of Bordetella pertussis virulence factor P.69 pertactin. Nature *381*, 90–92.

Fabrik, I., Link, M., Härtlova, A., Dankova, V., Rehulka, P., and Stulik, J. (2014). Application of SILAC labeling to primary bone marrow-derived dendritic cells reveals extensive GM-CSF-dependent arginine metabolism. J. Proteome Res. *13*, 752–762.

Fedele, G., Stefanelli, P., Spensieri, F., Fazio, C., Mastrantonio, P., and Ausiello, C.M. (2005). Bordetella pertussis-infected human monocyte-derived dendritic cells undergo maturation and induce Th1 polarization and interleukin-23 expression. Infection and Immunity *73*, 1590–1597.

Fedele, G., Spensieri, F., Palazzo, R., Nasso, M., Cheung, G.Y.C., Coote, J.G., and Ausiello, C.M. (2010). Bordetella pertussis commits human dendritic cells to promote a Th1/Th17 response through the activity of adenylate cyclase toxin and MAPK-pathways. PloS One *5*, e8734.

Fedele, G., Schiavoni, I., Adkins, I., Klimova, N., and Sebo, P. (2017). Invasion of Dendritic Cells, Macrophages and Neutrophils by the Bordetella Adenylate Cyclase Toxin: A Subversive Move to Fool Host Immunity. Toxins (Basel) *9*.

Fennelly, N.K., Sisti, F., Higgins, S.C., Ross, P.J., van der Heide, H., Mooi, F.R., Boyd, A., and Mills, K.H.G. (2008). Bordetella pertussis Expresses a Functional Type III Secretion System That Subverts Protective Innate and Adaptive Immune Responses. Infection and Immunity *76*, 1257–1266.

Finn, T.M., and Amsbaugh, D.F. (1998). Vag8, a Bordetella pertussis bvg-regulated protein. Infect. Immun. *66*, 3985–3989.

Finn, T.M., and Stevens, L.A. (1995). Tracheal colonization factor: a Bordetella pertussis secreted virulence determinant. Mol. Microbiol. *16*, 625–634.

Fischer, N. (2020). Infection-induced epigenetic changes and their impact on the pathogenesis of diseases. Semin Immunopathol *42*, 127–130.

Fiser, R., Masín, J., Basler, M., Krusek, J., Spuláková, V., Konopásek, I., and Sebo, P. (2007). Third activity of Bordetella adenylate cyclase (AC) toxin-hemolysin. Membrane translocation of AC domain polypeptide promotes calcium influx into CD11b+ monocytes independently of the catalytic and hemolytic activities. J. Biol. Chem. *282*, 2808–2820.

Fiser, R., Masin, J., Bumba, L., Pospisilova, E., Fayolle, C., Basler, M., Sadilkova, L., Adkins, I., Kamanova, J., Cerny, J., et al. (2012). Calcium influx rescues adenylate cyclase-hemolysin from rapid cell membrane removal and enables phagocyte permeabilization by toxin pores. PLoS Pathog. *8*, e1002580.

Flak, T.A., and Goldman, W.E. (1996). Autotoxicity of nitric oxide in airway disease. Am J Respir Crit Care Med *154*, S202-206.

Flak, T.A., and Goldman, W.E. (1999). Signalling and cellular specificity of airway nitric oxide production in pertussis. Cell Microbiol *1*, 51–60.

Flak, T.A., Heiss, L.N., Engle, J.T., and Goldman, W.E. (2000). Synergistic epithelial responses to endotoxin and a naturally occurring muramyl peptide. Infect Immun *68*, 1235–1242.

Forst, S.A., and Roberts, D.L. (1994). Signal transduction by the EnvZ-OmpR phosphotransfer system in bacteria. Research in Microbiology *145*, 363–373.

French, C.T., Panina, E.M., Yeh, S.H., Griffith, N., Arambula, D.G., and Miller, J.F. (2009). The *Bordetella* type III secretion system effector BteA contains a conserved N-terminal motif that guides bacterial virulence factors to lipid rafts. Cellular Microbiology *11*, 1735–1749.

Friedman, R.L., Nordensson, K., Wilson, L., Akporiaye, E.T., and Yocum, D.E. (1992). Uptake and intracellular survival of Bordetella pertussis in human macrophages. Infect. Immun. *60*, 4578–4585.

Fukui-Miyazaki, A., Kamitani, S., Miyake, M., and Horiguchi, Y. (2010). Association of Bordetella dermonecrotic toxin with the extracellular matrix. BMC Microbiol *10*, 247.

Fukui-Miyazaki, A., Ohnishi, S., Kamitani, S., Abe, H., and Horiguchi, Y. (2011). Bordetella dermonecrotic toxin binds to target cells via the N-terminal 30 amino acids: Cell-binding region of DNT. Microbiology and Immunology *55*, 154–159.

Gaillard, M.E., Bottero, D., Castuma, C.E., Basile, L.A., and Hozbor, D. (2011). Laboratory Adaptation of Bordetella pertussis Is Associated with the Loss of Type Three Secretion System Functionality. Infect. Immun. *79*, 3677–3682.

Galán, J.E., and Waksman, G. (2018). Protein-Injection Machines in Bacteria. Cell *172*, 1306–1318.

Gao, L., Cueto, M.A., Asselbergs, F., and Atadja, P. (2002). Cloning and Functional Characterization of HDAC11, a Novel Member of the Human Histone Deacetylase Family. J. Biol. Chem. *277*, 25748–25755.

van Gent, M., Pierard, D., Lauwers, S., van der Heide, H.G.J., King, A.J., and Mooi, F.R. (2007). Characterization of *Bordetella pertussis* clinical isolates that do not express the tracheal colonization factor. FEMS Immunology & Medical Microbiology *51*, 149–154.

Geuijen, C.A., Willems, R.J., Bongaerts, M., Top, J., Gielen, H., and Mooi, F.R. (1997). Role of the Bordetella pertussis minor fimbrial subunit, FimD, in colonization of the mouse respiratory tract. Infect. Immun. *65*, 4222–4228.

Gibson, G.J., Loddenkemper, R., Lundbäck, B., and Sibille, Y. (2013). Respiratory health and disease in Europe: the new European Lung White Book. European Respiratory Journal *42*, 559–563.

Glaser, P., Sakamoto, H., Bellalou, J., Ullmann, A., and Danchin, A. (1988). Secretion of cyclolysin, the calmodulin-sensitive adenylate cyclase-haemolysin bifunctional protein of Bordetella pertussis. EMBO J. *7*, 3997–4004.

Gogol, E.B., Cummings, C.A., Burns, R.C., and Relman, D.A. (2007). Phase variation and microevolution at homopolymeric tracts in Bordetella pertussis. BMC Genomics *8*, 122.

Goldman, W.E., Klapper, D.G., and Baseman, J.B. (1982). Detection, isolation, and analysis of a released Bordetella pertussis product toxic to cultured tracheal cells. Infect. Immun. *36*, 782–794.

Goodnow, R.A. (1980). Biology of Bordetella bronchiseptica. Microbiol. Rev. *44*, 722–738.

Gorringe, A.R., and Vaughan, T.E. (2014). *Bordetella pertussis* fimbriae (Fim): relevance for vaccines. Expert Review of Vaccines *13*, 1205–1214.

Gouw, D. de, Hermans, P.W.M., Bootsma, H.J., Zomer, A., Heuvelman, K., Diavatopoulos, D.A., and Mooi, F.R. (2014). Differentially Expressed Genes in Bordetella pertussis Strains Belonging to a Lineage Which Recently Spread Globally. PLoS ONE *9*, e84523.

Gray, D.F., and Cheers, C. (1967). The steady state in cellular immunity. II. Immunological complaisance in murine pertussis. Aust J Exp Biol Med Sci *45*, 417–426.

Gray, M., Szabo, G., Otero, A.S., Gray, L., and Hewlett, E. (1998). Distinct Mechanisms for K^+ Efflux, Intoxication, and Hemolysis by *Bordetella pertussis* AC Toxin. J. Biol. Chem. *273*, 18260–18267.

Graziani-Bowering, G.M., Graham, J.M., and Filion, L.G. (1997). A quick, easy and inexpensive method for the isolation of human peripheral blood monocytes. Journal of Immunological Methods *207*, 157–168.

Gregg, K.A., and Merkel, T.J. (2019). Pertussis Toxin: A Key Component in Pertussis Vaccines? Toxins *11*, 557.

Groisman, E.A. (2016). Feedback Control of Two-Component Regulatory Systems. Annu. Rev. Microbiol. *70*, 103–124.

Gross, R., Guzman, C.A., Sebaihia, M., Martins dos Santos, V.A., Pieper, D.H., Koebnik, R., Lechner, M., Bartels, D., Buhrmester, J., Choudhuri, J.V., et al. (2008). The missing link: Bordetella petrii is endowed

with both the metabolic versatility of environmental bacteria and virulence traits of pathogenic Bordetellae. BMC Genomics *9*, 449.

Grundy, F.J., Waters, D.A., Takova, T.Y., and Henkin, T.M. (1993). Identification of genes involved in utilization of acetate and acetoin in *Bacillus subtilis*. Molecular Microbiology *10*, 259–271.

Guermonprez, P., Khelef, N., Blouin, E., Rieu, P., Ricciardi-Castagnoli, P., Guiso, N., Ladant, D., and Leclerc, C. (2001). The adenylate cyclase toxin of Bordetella pertussis binds to target cells via the alpha(M)beta(2) integrin (CD11b/CD18). J. Exp. Med. *193*, 1035–1044.

Gustavsson, O.E.A., Röken, B.O., and Serrander, R. (1990). An Epizootic of Whooping Cough among Chimpanzees in a Zoo. Folia Primatol *55*, 45–50.

Haan, L. de, and Hirst, T.R. (2004). Cholera toxin: A paradigm for multi-functional engagement of cellular mechanisms (Review). Molecular Membrane Biology *21*, 77–92.

Haberling, D.L., Holman, R.C., Paddock, C.D., and Murphy, T.V. (2009). Infant and maternal risk factors for pertussis-related infant mortality in the United States, 1999 to 2004. Pediatr. Infect. Dis. J. *28*, 194–198.

Hai, Y., and Christianson, D.W. (2016). Histone deacetylase 6 structure and molecular basis of catalysis and inhibition. Nat. Chem. Biol. *12*, 741–747.

Hamidou Soumana, I., Linz, B., and Harvill, E.T. (2017). Environmental Origin of the Genus Bordetella. Front. Microbiol. *8*.

Hamon, M.A., and Cossart, P. (2008). Histone modifications and chromatin remodeling during bacterial infections. Cell Host Microbe *4*, 100–109.

Hanawa, T., Kamachi, K., Yonezawa, H., Fukutomi, T., Kawakami, H., and Kamiya, S. (2016). Glutamate Limitation, BvgAS Activation, and (p)ppGpp Regulate the Expression of the Bordetella pertussis Type 3 Secretion System. J. Bacteriol. *198*, 343–351.

Harvill, E.T., Goodfield, L.L., Ivanov, Y., Smallridge, W.E., Meyer, J.A., Cassiday, P.K., Tondella, M.L., Brinkac, L., Sanka, R., Kim, M., et al. (2014). Genome Sequences of Nine Bordetella holmesii Strains Isolated in the United States. Genome Announcements *2*, e00438-14, 2/3/e00438-14.

Hasan, S., Kulkarni, N.N., Asbjarnarson, A., Linhartova, I., Osicka, R., Sebo, P., and Gudmundsson, G.H. (2018). Bordetella pertussis Adenylate Cyclase Toxin Disrupts Functional Integrity of Bronchial Epithelial Layers. Infect. Immun. *86*.

Hazenbos, W.L., van den Berg, B.M., Geuijen, C.W., Mooi, F.R., and van Furth, R. (1995). Binding of FimD on Bordetella pertussis to very late antigen-5 on monocytes activates complement receptor type 3 via protein tyrosine kinases. J. Immunol. *155*, 3972–3978.

Heck, D.V., Trus, B.L., and Steven, A.C. (1996). Three-Dimensional Structure ofBordetella pertussisFimbriae. Journal of Structural Biology *116*, 264–269.

Hegerle, N., and Guiso, N. (2014). Bordetella pertussis and pertactin-deficient clinical isolates: lessons for pertussis vaccines. Expert Rev Vaccines *13*, 1135–1146.

Hegerle, N., Rayat, L., Dore, G., Zidane, N., Bedouelle, H., and Guiso, N. (2013). In-vitro and in-vivo analysis of the production of the Bordetella type three secretion system effector A in Bordetella pertussis, Bordetella parapertussis and Bordetella bronchiseptica. Microbes and Infection *15*, 399–408.

Hegerle, N., Dore, G., and Guiso, N. (2014). Pertactin deficient Bordetella pertussis present a better fitness in mice immunized with an acellular pertussis vaccine. Vaccine *32*, 6597–6600.

Helinski, E.H., Bielat, K.L., Ovak, G.M., and Pauly, J.L. (1988). Long-Term Cultivation of Functional Human Macrophages in Teflon Dishes With Serum-Free Media. J Leukoc Biol *44*, 111–121.

Hellwig, S.M., Hazenbos, W.L., van de Winkel, J.G., and Mooi, F.R. (1999). Evidence for an intracellular niche for Bordetella pertussis in broncho-alveolar lavage cells of mice. FEMS Immunol. Med. Microbiol. *26*, 203–207.

Henderson, I.R., and Nataro, J.P. (2001). Virulence Functions of Autotransporter Proteins. Infect. Immun. *69*, 1231–1243.

Herrou, J., Bompard, C., Wintjens, R., Dupre, E., Willery, E., Villeret, V., Locht, C., Antoine, R., and Jacob-Dubuisson, F. (2010). Periplasmic domain of the sensor-kinase BvgS reveals a new paradigm for the Venus flytrap mechanism. Proceedings of the National Academy of Sciences *107*, 17351–17355.

Hewlett, E.L., Donato, G.M., and Gray, M.C. (2006). Macrophage cytotoxicity produced by adenylate cyclase toxin from Bordetella pertussis: more than just making cyclic AMP! Mol. Microbiol. *59*, 447–459.

Higgs, R., Higgins, S.C., Ross, P.J., and Mills, K.H.G. (2012). Immunity to the respiratory pathogen Bordetella pertussis. Mucosal Immunol *5*, 485–500.

Hildmann, C., Ninkovic, M., Dietrich, R., Wegener, D., Riester, D., Zimmermann, T., Birch, O.M., Bernegger, C., Loidl, P., and Schwienhorst, A. (2004). A new amidohydrolase from Bordetella or Alcaligenes strain FB188 with similarities to histone deacetylases. J. Bacteriol. *186*, 2328–2339.

Hildmann, C., Riester, D., and Schwienhorst, A. (2007). Histone deacetylases--an important class of cellular regulators with a variety of functions. Appl. Microbiol. Biotechnol. *75*, 487–497.

Holubova, J., Kamanova, J., Jelinek, J., Tomala, J., Masin, J., Kosova, M., Stanek, O., Bumba, L., Michalek, J., Kovar, M., et al. (2012). Delivery of large heterologous polypeptides across the cytoplasmic membrane of antigen-presenting cells by the Bordetella RTX hemolysin moiety lacking the adenylyl cyclase domain. Infect. Immun. *80*, 1181–1192.

Horiguchi, Y. (2012). Swine Atrophic Rhinitis Caused by Pasteurella multocida Toxin and Bordetella Dermonecrotic Toxin. In Pasteurella Multocida, K. Aktories, J.H.C. Orth, and B. Adler, eds. (Berlin, Heidelberg: Springer Berlin Heidelberg), pp. 113–129.

Hovingh, E.S., van den Broek, B., Kuipers, B., Pinelli, E., Rooijakkers, S.H.M., and Jongerius, I. (2017). Acquisition of C1 inhibitor by Bordetella pertussis virulence associated gene 8 results in C2 and C4 consumption away from the bacterial surface. PLoS Pathog *13*, e1006531.

Hovingh, E.S., de Maat, S., Cloherty, A.P.M., Johnson, S., Pinelli, E., Maas, C., and Jongerius, I. (2018). Virulence Associated Gene 8 of Bordetella pertussis Enhances Contact System Activity by Inhibiting the Regulatory Function of Complement Regulator C1 Inhibitor. Front. Immunol. *9*, 1172.

Hynes, R.O. (1987). Integrins: a family of cell surface receptors. Cell *48*, 549–554.

Igarashi, K., and Kashiwagi, K. (2018). Effects of polyamines on protein synthesis and growth of *Escherichia coli*. J. Biol. Chem. *293*, 18702–18709.

Iida, T., and Okonogi, T. (1971). Lienotoxicity Of Bordetella Pertussis In Mice. Journal of Medical Microbiology *4*, 51–61.

Inatsuka, C.S., Xu, Q., Vujkovic-Cvijin, I., Wong, S., Stibitz, S., Miller, J.F., and Cotter, P.A. (2010). Pertactin Is Required for Bordetella Species To Resist Neutrophil-Mediated Clearance. IAI *78*, 2901–2909.

Jenuwein, T. (2001). Re-SET-ting heterochromatin by histone methyltransferases. Trends Cell Biol. *11*, 266–273.

Jenuwein, T., Laible, G., Dorn, R., and Reuter, G. (1998). SET domain proteins modulate chromatin domains in eu- and heterochromatin. Cell. Mol. Life Sci. *54*, 80–93.

Jones, A.M., Boucher, P.E., Williams, C.L., Stibitz, S., and Cotter, P.A. (2005). Role of BvgA phosphorylation and DNA binding affinity in control of Bvg-mediated phenotypic phase transition in *Bordetella pertussis*: BvgA phosphorylation and DNA binding mutants. Molecular Microbiology *58*, 700–713.

Jungnitz, H., West, N.P., Walker, M.J., Chhatwal, G.S., and Guzmán, C.A. (1998). A second two-component regulatory system of Bordetella bronchiseptica required for bacterial resistance to oxidative stress, production of acid phosphatase, and in vivo persistence. Infect. Immun. *66*, 4640–4650.

Kamanova, J. (2020). Bordetella Type III Secretion Injectosome and Effector Proteins. Front Cell Infect Microbiol *10*, 466.

Kamanova, J., Kofronova, O., Masin, J., Genth, H., Vojtova, J., Linhartova, I., Benada, O., Just, I., and Sebo, P. (2008). Adenylate cyclase toxin subverts phagocyte function by RhoA inhibition and unproductive ruffling. J. Immunol. *181*, 5587–5597.

Kania, S.A., Rajeev, S., Burns, E.H., Odom, T.F., Holloway, S.M., and Bemis, D.A. (2000). Characterization of fimN, a new Bordetella bronchiseptica major fimbrial subunit gene. Gene *256*, 149–155.

Karataev, G.I., Sinyashina, L.N., Medkova, A.Yu., Semin, E.G., Shevtsova, Z.V., Matua, A.Z., Kondzariya, I.G., Amichba, A.A., Kubrava, D.T., and Mikvabia, Z.Ya. (2016). Insertional inactivation of virulence operon in population of persistent Bordetella pertussis bacteria. Russ J Genet *52*, 370–377.

Katada, T. (2012). The Inhibitory G Protein Gi Identified as Pertussis Toxin-Catalyzed ADP-Ribosylation. Biological ^|^ Pharmaceutical Bulletin *35*, 2103–2111.

Katada, T., and Ui, M. (1982). ADP ribosylation of the specific membrane protein of C6 cells by islet-activating protein associated with modification of adenylate cyclase activity. J. Biol. Chem. *257*, 7210–7216.

Kessie, D.K., Lodes, N., Oberwinkler, H., Goldman, W.E., Walles, T., Steinke, M., and Gross, R. (2021). Activity of Tracheal Cytotoxin of Bordetella pertussis in a Human Tracheobronchial 3D Tissue Model. Front. Cell. Infect. Microbiol. *10*, 614994.

Khelef, N., and Guiso, N. (1995). Induction of macrophage apoptosis by *Bordetella pertussis* adenylate cyclase-hemolysin. FEMS Microbiology Letters *134*, 27–32.

Khelef, N., Bachelet, C.M., Vargaftig, B.B., and Guiso, N. (1994). Characterization of murine lung inflammation after infection with parental Bordetella pertussis and mutants deficient in adhesins or toxins. Infect. Immun. *62*, 2893–2900.

Kimberlin, D.W., Brady, M.T., Jackson, M.A., and Long, S.S. (2015). Pertussis (Whooping Cough). In Red Book: 2015 Report of the Committee on Infectious Diseases. 30th Ed., (Elk Grove Village, IL: American Academy of Pediatrics), pp. 608–621.

Kinnear, S.M., Marques, R.R., and Carbonetti, N.H. (2001). Differential regulation of Bvg-activated virulence factors plays a role in Bordetella pertussis pathogenicity. Infection and Immunity *69*, 1983–1993.

Kline, J.M., Lewis, W.D., Smith, E.A., Tracy, L.R., and Moerschel, S.K. (2013). Pertussis: a reemerging infection. Am Fam Physician *88*, 507–514.

Knapp, S., and Mekalanos, J.J. (1988). Two trans-acting regulatory genes (vir and mod) control antigenic modulation in Bordetella pertussis. Journal of Bacteriology *170*, 5059–5066.

Kotob, S.I., Hausman, S.Z., and Burns, D.L. (1995). Localization of the promoter for the ptl genes of Bordetella pertussis, which encode proteins essential for secretion of pertussis toxin. Infect. Immun. *63*, 3227–3230.

Lacey, B.W. (1960). Antigenic modulation of *Bordetella pertussis*. J. Hyg. *58*, 57–93.

Lacey, D.C., Achuthan, A., Fleetwood, A.J., Dinh, H., Roiniotis, J., Scholz, G.M., Chang, M.W., Beckman, S.K., Cook, A.D., and Hamilton, J.A. (2012). Defining GM-CSF- and Macrophage-CSF-Dependent Macrophage Responses by In Vitro Models. The Journal of Immunology *188*, 5752–5765.

Ladant, D., Glaser, P., and Ullmann, A. (1992). Insertional mutagenesis of Bordetella pertussis adenylate cyclase. J. Biol. Chem. *267*, 2244–2250.

Lambert-Buisine, C., Willery, E., Locht, C., and Jacob-Dubuisson, F. (1998). N-terminal characterization of the Bordetella pertussis filamentous haemagglutinin. Mol. Microbiol. *28*, 1283–1293.

Lamberti, Y., Cafiero, J.H., Surmann, K., Valdez, H., Holubova, J., Večerek, B., Sebo, P., Schmidt, F., Völker, U., and Rodriguez, M.E. (2016). Proteome analysis of Bordetella pertussis isolated from human macrophages. J Proteomics *136*, 55–67.

Lamberti, Y.A., Hayes, J.A., Perez Vidakovics, M.L., Harvill, E.T., and Rodriguez, M.E. (2010). Intracellular trafficking of Bordetella pertussis in human macrophages. Infect. Immun. *78*, 907–913.

Leininger, E., Roberts, M., Kenimer, J.G., Charles, I.G., Fairweather, N., Novotny, P., and Brennan, M.J. (1991). Pertactin, an Arg-Gly-Asp-containing Bordetella pertussis surface protein that promotes adherence of mammalian cells. Proc. Natl. Acad. Sci. U.S.A. *88*, 345–349.

Leipe, D.D., and Landsman, D. (1997). Histone deacetylases, acetoin utilization proteins and acetylpolyamine amidohydrolases are members of an ancient protein superfamily. Nucleic Acids Research *25*, 3693–3697.

Li, J., Liu, S., Su, Y., Ren, J., Sang, Y., Ni, J., Lu, J., and Yao, Y.-F. (2020). Acetylation of PhoP K88 Is Involved in Regulating *Salmonella* Virulence. Infect Immun *89*, e00588-20, /iai/89/3/IAI.00588-20.atom.

Li, L., Mendis, N., Trigui, H., Oliver, J.D., and Faucher, S.P. (2014). The importance of the viable but non-culturable state in human bacterial pathogens. Front. Microbiol. *5*.

Liang, W., Malhotra, A., and Deutscher, M.P. (2011). Acetylation regulates the stability of a bacterial protein: growth stage-dependent modification of RNase R. Mol. Cell *44*, 160–166.

Linhartová, I., Bumba, L., Mašín, J., Basler, M., Osička, R., Kamanová, J., Procházková, K., Adkins, I., Hejnová-Holubová, J., Sadílková, L., et al. (2010). RTX proteins: a highly diverse family secreted by a common mechanism. FEMS Microbiol. Rev. *34*, 1076–1112.

Locht, C., Bertin, P., Menozzi, F.D., and Renauld, G. (1993). The filamentous haemagglutinin, a multifaceted adhesion produced by virulent Bordetella spp. Mol. Microbiol. *9*, 653–660.

Locht, C., Coutte, L., and Mielcarek, N. (2011). The ins and outs of pertussis toxin: Pertussis toxin. FEBS Journal *278*, 4668–4682.

van Loo, I.H.M., Heuvelman, K.J., King, A.J., and Mooi, F.R. (2002). Multilocus Sequence Typing of Bordetella pertussis Based on Surface Protein Genes. Journal of Clinical Microbiology *40*, 1994–2001.

Ma, K.-W., and Ma, W. (2016). YopJ Family Effectors Promote Bacterial Infection through a Unique Acetyltransferase Activity. Microbiol. Mol. Biol. Rev. *80*, 1011–1027.

Majewski, L.L., Nogi, M., Bankowski, M.J., and Chung, H.H. (2016). Bordetella trematum sepsis with shock in a diabetic patient with rapidly developing soft tissue infection. Diagnostic Microbiology and Infectious Disease *86*, 112–114.

Mann, M. (2006). Functional and quantitative proteomics using SILAC. Nat Rev Mol Cell Biol *7*, 952–958.

Marmorstein, R. (2001). Structure of Histone Deacetylases. Structure *9*, 1127–1133.

Marr, N., Tirsoaga, A., Blanot, D., Fernandez, R., and Caroff, M. (2008). Glucosamine Found as a Substituent of Both Phosphate Groups in Bordetella Lipid A Backbones: Role of a BvgAS-Activated ArnT Ortholog. JB *190*, 4281–4290.

Marr, N., Hajjar, A.M., Shah, N.R., Novikov, A., Yam, C.S., Caroff, M., and Fernandez, R.C. (2010). Substitution of the Bordetella pertussis Lipid A Phosphate Groups with Glucosamine Is Required for

Robust NF-κB Activation and Release of Proinflammatory Cytokines in Cells Expressing Human but Not Murine Toll-Like Receptor 4-MD-2-CD14. IAI *78*, 2060–2069.

Marr, N., Shah, N.R., Lee, R., Kim, E.J., and Fernandez, R.C. (2011). Bordetella pertussis Autotransporter Vag8 Binds Human C1 Esterase Inhibitor and Confers Serum Resistance. PLoS ONE *6*, e20585.

Martin, S.W., Pawloski, L., Williams, M., Weening, K., DeBolt, C., Qin, X., Reynolds, L., Kenyon, C., Giambrone, G., Kudish, K., et al. (2015). Pertactin-negative Bordetella pertussis strains: evidence for a possible selective advantage. Clin Infect Dis *60*, 223–227.

Martinez de Tejada, G., Cotter, P.A., Heininger, U., Camilli, A., Akerley, B.J., Mekalanos, J.J., and Miller, J.F. (1998). Neither the Bvg- phase nor the vrg6 locus of Bordetella pertussis is required for respiratory infection in mice. Infect. Immun. *66*, 2762–2768.

Mastrantonio, P., Stefanelli, P., Giuliano, M., Herrera Rojas, Y., Ciofi degli Atti, M., Anemona, A., and Tozzi, A.E. (1998). Bordetella parapertussis infection in children: epidemiology, clinical symptoms, and molecular characteristics of isolates. J. Clin. Microbiol. *36*, 999–1002.

Masuda, M., Betancourt, L., Matsuzawa, T., Kashimoto, T., Takao, T., Shimonishi, Y., and Horiguchi, Y. (2000). Activation of Rho through a cross-link with polyamines catalyzed by Bordetella dermonecrotizing toxin. EMBO J *19*, 521–530.

Masure, H.R. (1992). Modulation of adenylate cyclase toxin production as Bordetella pertussis enters human macrophages. Proc. Natl. Acad. Sci. U.S.A. *89*, 6521–6525.

Masure, H.R. (1993). The adenylate cyclase toxin contributes to the survival of Bordetella pertussis within human macrophages. Microb. Pathog. *14*, 253–260.

Mattoo, S., and Cherry, J.D. (2005). Molecular pathogenesis, epidemiology, and clinical manifestations of respiratory infections due to Bordetella pertussis and other Bordetella subspecies. Clin. Microbiol. Rev. *18*, 326–382.

Mazar, J., and Cotter, P.A. (2007). New insight into the molecular mechanisms of two-partner secretion. Trends Microbiol. *15*, 508–515.

Mclafferty, M.A., Harcus, D.R., and Hewlett, E.L. (1988). Nucleotide Sequence and Characterization of a Repetitive DNA Element from the Genome of Bordetella pertussis with Characteristics of an Insertion Sequence. Microbiology *134*, 2297–2306.

Medkova, A.I., Siniashina, L.N., Rumiantseva, I.P., Voronina, O.L., Kunda, M.S., and Karataev, G.I. (2013). [Accumulation of the bvg- Bordetella pertussis a virulent mutants in the process of experimental whooping cough in mice]. Mol. Gen. Mikrobiol. Virusol. 22–26.

Melvin, J.A., Scheller, E.V., Miller, J.F., and Cotter, P.A. (2014). Bordetella pertussis pathogenesis: current and future challenges. Nat. Rev. Microbiol. *12*, 274–288.

Melvin, J.A., Scheller, E.V., Noël, C.R., and Cotter, P.A. (2015). New Insight into Filamentous Hemagglutinin Secretion Reveals a Role for Full-Length FhaB in Bordetella Virulence. MBio *6*, e01189-15.

Menck, K., Behme, D., Pantke, M., Reiling, N., Binder, C., Pukrop, T., and Klemm, F. (2014). Isolation of Human Monocytes by Double Gradient Centrifugation and Their Differentiation to Macrophages in Teflon-coated Cell Culture Bags. JoVE 51554.

Merkel, T.J., and Halperin, S.A. (2014). Nonhuman Primate and Human Challenge Models of Pertussis. Journal of Infectious Diseases *209*, S20–S23.

Merkel, T.J., Barros, C., and Stibitz, S. (1998a). Characterization of the bvgR locus of Bordetella pertussis. J. Bacteriol. *180*, 1682–1690.

Merkel, T.J., Stibitz, S., Keith, J.M., Leef, M., and Shahin, R. (1998b). Contribution of regulation by the bvg locus to respiratory infection of mice by Bordetella pertussis. Infect. Immun. *66*, 4367–4373.

Michael, A.J. (2018). Polyamine function in archaea and bacteria. J. Biol. Chem. *293*, 18693–18701.

Miltenyi, S., Müller, W., Weichel, W., and Radbruch, A. (1990). High gradient magnetic cell separation with MACS. Cytometry *11*, 231–238.

Mitchell, A.L., Attwood, T.K., Babbitt, P.C., Blum, M., Bork, P., Bridge, A., Brown, S.D., Chang, H.-Y., El-Gebali, S., Fraser, M.I., et al. (2019). InterPro in 2019: improving coverage, classification and access to protein sequence annotations. Nucleic Acids Research *47*, D351–D360.

Mooi, F.R. (2010). Bordetella pertussis and vaccination: The persistence of a genetically monomorphic pathogen. Infection, Genetics and Evolution *10*, 36–49.

Mooi, F.R., van Loo, I.H.M., van Gent, M., He, Q., Bart, M.J., Heuvelman, K.J., de Greeff, S.C., Diavatopoulos, D., Teunis, P., Nagelkerke, N., et al. (2009). Bordetella pertussis strains with increased toxin production associated with pertussis resurgence. Emerging Infect. Dis. *15*, 1206–1213.

Moon, K., Bonocora, R.P., Kim, D.D., Chen, Q., Wade, J.T., Stibitz, S., and Hinton, D.M. (2017). The BvgAS Regulon of *Bordetella pertussis*. MBio *8*, e01526-17, /mbio/8/5/e01526-17.atom.

Moreth, K., Riester, D., Hildmann, C., Hempel, R., Wegener, D., Schober, A., and Schwienhorst, A. (2007). An active site tyrosine residue is essential for amidohydrolase but not for esterase activity of a class 2 histone deacetylase-like bacterial enzyme. Biochem. J. *401*, 659–665.

Morse, S.I., and Morse, J.H. (1976). Isolation and properties of the leukocytosis- and lymphocytosis-promoting factor of Bordetella pertussis. The Journal of Experimental Medicine *143*, 1483–1502.

Nagamatsu, K., Kuwae, A., Konaka, T., Nagai, S., Yoshida, S., Eguchi, M., Watanabe, M., Mimuro, H., Koyasu, S., and Abe, A. (2009). Bordetella evades the host immune system by inducing IL-10 through a type III effector, BopN. Journal of Experimental Medicine *206*, 3073–3088.

Nicholson, T.L., Brockmeier, S.L., Loving, C.L., Register, K.B., Kehrli, M.E., and Shore, S.M. (2014). The Bordetella bronchiseptica Type III Secretion System Is Required for Persistence and Disease Severity but Not Transmission in Swine. Infect. Immun. *82*, 1092–1103.

Nielsen, M.C., Andersen, M.N., and Møller, H.J. (2020). Monocyte isolation techniques significantly impact the phenotype of both isolated monocytes and derived macrophages *in vitro*. Immunology *159*, 63–74.

Nielsen, T.K., Hildmann, C., Dickmanns, A., Schwienhorst, A., and Ficner, R. (2005). Crystal structure of a bacterial class 2 histone deacetylase homologue. J. Mol. Biol. *354*, 107–120.

Nielsen, T.K., Hildmann, C., Riester, D., Wegener, D., Schwienhorst, A., and Ficner, R. (2007). Complex structure of a bacterial class 2 histone deacetylase homologue with a trifluoromethylketone inhibitor. Acta Crystallogr. Sect. F Struct. Biol. Cryst. Commun. *63*, 270–273.

Noël, C.R., Mazar, J., Melvin, J.A., Sexton, J.A., and Cotter, P.A. (2012). The prodomain of the *Bordetella* two-partner secretion pathway protein FhaB remains intracellular yet affects the conformation of the mature C-terminal domain: Transmembrane intramolecular chaperone. Molecular Microbiology *86*, 988–1006.

Novak, J., Cerny, O., Osickova, A., Linhartova, I., Masin, J., Bumba, L., Sebo, P., and Osicka, R. (2017). Structure–Function Relationships Underlying the Capacity of Bordetella Adenylate Cyclase Toxin to Disarm Host Phagocytes. Toxins *9*, 300.

Novák, J., Fabrik, I., Linhartová, I., Link, M., Černý, O., Stulík, J., and Šebo, P. (2017). Phosphoproteomics of cAMP signaling of Bordetella adenylate cyclase toxin in mouse dendritic cells. Sci Rep *7*, 16298.

Novak, J., Fabrik, I., Jurnecka, D., Holubova, J., Stanek, O., and Sebo, P. (2020). *Bordetella pertussis* Acetylome is Shaped by Lysine Deacetylase Bkd1. J. Proteome Res. *19*, 3680–3696.

Osicka, R., Osickova, A., Hasan, S., Bumba, L., Cerny, J., and Sebo, P. (2015). Bordetella adenylate cyclase toxin is a unique ligand of the integrin complement receptor 3. Elife *4*, e10766.

Paik, D., Monahan, A., Caffrey, D.R., Elling, R., Goldman, W.E., and Silverman, N. (2017). SLC46 Family Transporters Facilitate Cytosolic Innate Immune Recognition of Monomeric Peptidoglycans. J.I. *199*, 263–270.

Panina, E.M., Mattoo, S., Griffith, N., Kozak, N.A., Yuk, M.H., and Miller, J.F. (2005). A genome-wide screen identifies a Bordetella type III secretion effector and candidate effectors in other species: Bordetella type III effector. Molecular Microbiology *58*, 267–279.

Park, J., Zhang, Y., Buboltz, A.M., Zhang, X., Schuster, S.C., Ahuja, U., Liu, M., Miller, J.F., Sebaihia, M., Bentley, S.D., et al. (2012). Comparative genomics of the classical Bordetella subspecies: the evolution and exchange of virulence-associated diversity amongst closely related pathogens. BMC Genomics *13*, 545.

Parkhill, J., Sebaihia, M., Preston, A., Murphy, L.D., Thomson, N., Harris, D.E., Holden, M.T.G., Churcher, C.M., Bentley, S.D., Mungall, K.L., et al. (2003). Comparative analysis of the genome sequences of Bordetella pertussis, Bordetella parapertussis and Bordetella bronchiseptica. Nat Genet *35*, 32–40.

Passerini de Rossi, B.N., Friedman, L.E., Belzoni, C.B., Savino, S., Aricò, B., Rappuoli, R., Masignani, V., and Franco, M.A. (2003). vir90, a virulence-activated gene coding for a Bordetella pertussis iron-regulated outer membrane protein. Research in Microbiology *154*, 443–450.

Pawloski, L.C., Queenan, A.M., Cassiday, P.K., Lynch, A.S., Harrison, M.J., Shang, W., Williams, M.M., Bowden, K.E., Burgos-Rivera, B., Qin, X., et al. (2014). Prevalence and Molecular Characterization of Pertactin-Deficient Bordetella pertussis in the United States. Clin. Vaccine Immunol. *21*, 119–125.

Pearson, R.D., Symes, P., Conboy, M., Weiss, A.A., and Hewlett, E.L. (1987). Inhibition of monocyte oxidative responses by Bordetella pertussis adenylate cyclase toxin. J. Immunol. *139*, 2749–2754.

Pedroni, P., Riboli, B., Ferra, F., Grandi, G., Toma, S., Aricò, B., and Rappuoli, R. (1988). Cloning of a novel pilin-like gene from Bordetella pertussis: homology to the fim2 gene. Mol Microbiol *2*, 539–543.

Perez Vidakovics, M.L.A., Lamberti, Y., Serra, D., Berbers, G.A.M., van der Pol, W.-L., and Rodriguez, M.E. (2007). Iron stress increases *Bordetella pertussis* mucin-binding capacity and attachment to respiratory epithelial cells. FEMS Immunology & Medical Microbiology *51*, 414–421.

Petráčková, D., Farman, M.R., Amman, F., Linhartová, I., Dienstbier, A., Kumar, D., Držmíšek, J., Hofacker, I., Rodriguez, M.E., and Večerek, B. (2020). Transcriptional profiling of human macrophages during infection with Bordetella pertussis. RNA Biol 1–12.

Preston, A., Allen, A.G., Cadisch, J., Thomas, R., Stevens, K., Churcher, C.M., Badcock, K.L., Parkhill, J., Barrell, B., and Maskell, D.J. (1999). Genetic basis for lipopolysaccharide O-antigen biosynthesis in bordetellae. Infect. Immun. *67*, 3763–3767.

Preston, A., Parkhill, J., and Maskell, D.J. (2004). The Bordetellae: lessons from genomics. Nat Rev Microbiol *2*, 379–390.

Raetz, C.R.H., and Whitfield, C. (2002). Lipopolysaccharide Endotoxins. Annu. Rev. Biochem. *71*, 635–700.

Ramkissoon, S., MacArthur, I., Ibrahim, M., de Graaf, H., Read, R.C., and Preston, A. (2020). A qPCR assay for Bordetella pertussis cells that enumerates both live and dead bacteria. PLoS ONE *15*, e0232334.

Ramponi, G., Manao, G., and Camici, G. (1975). Nonenzymic acetylation of histones with acetyl phosphate and acetyl adenylate. Biochemistry *14*, 2681–2685.

Register, K.B., Ivanov, Y.V., Jacobs, N., Meyer, J.A., Goodfield, L.L., Muse, S.J., Smallridge, W.E., Brinkac, L., Kim, M., Sanka, R., et al. (2015). Draft Genome Sequences of 53 Genetically Distinct Isolates of *Bordetella bronchiseptica* Representing 11 Terrestrial and Aquatic Hosts: TABLE 1. Genome Announc. *3*, e00152-15, /ga/3/2/e00152-15.atom.

Relman, D., Tuomanen, E., Falkow, S., Golenbock, D.T., Saukkonen, K., and Wright, S.D. (1990). Recognition of a bacterial adhesion by an integrin: macrophage CR3 (alpha M beta 2, CD11b/CD18) binds filamentous hemagglutinin of Bordetella pertussis. Cell *61*, 1375–1382.

Ren, J., Sang, Y., Tan, Y., Tao, J., Ni, J., Liu, S., Fan, X., Zhao, W., Lu, J., Wu, W., et al. (2016). Acetylation of Lysine 201 Inhibits the DNA-Binding Ability of PhoP to Regulate Salmonella Virulence. PLoS Pathog. *12*, e1005458.

Ren, J., Sang, Y., Lu, J., and Yao, Y.-F. (2017). Protein Acetylation and Its Role in Bacterial Virulence. Trends in Microbiology *25*, 768–779.

Riboli, B., Pedroni, P., Cuzzoni, A., Grandi, G., and de Ferra, F. (1991). Expression of Bordetella pertussis fimbrial (fim) genes in Bordetella bronchiseptica: fimX is expressed at a low level and vir-regulated. Microbial Pathogenesis *10*, 393–403.

Rocha, G., Soares, P., Soares, H., Pissarra, S., and Guimarães, H. (2015). Pertussis in the newborn: certainties and uncertainties in 2014. Paediatr Respir Rev *16*, 112–118.

Sakurada, K., Ohta, T., Fujishiro, K., Hasegawa, M., and Aisaka, K. (1996). Acetylpolyamine amidohydrolase from Mycoplana ramosa: gene cloning and characterization of the metal-substituted enzyme. Journal of Bacteriology *178*, 5781–5786.

Sang, Y., Ren, J., Qin, R., Liu, S., Cui, Z., Cheng, S., Liu, X., Lu, J., Tao, J., and Yao, Y.-F. (2017). Acetylation Regulating Protein Stability and DNA-Binding Ability of HilD, thus Modulating Salmonella Typhimurium Virulence. The Journal of Infectious Diseases *216*, 1018–1026.

Sans, B., Bonal, J., Bonet, J., Arnal, J., Roca, F., and Caralps, A. (1991). Bordetella Bronchiseptica Septicemia in a Hemodialysis Patient. Nephron *59*, 676–676.

Saukkonen, K., Cabellos, C., Burroughs, M., Prasad, S., and Tuomanen, E. (1991). Integrin-mediated localization of Bordetella pertussis within macrophages: role in pulmonary colonization. J. Exp. Med. *173*, 1143–1149.

Scanlon, K.M., Snyder, Y.G., Skerry, C., and Carbonetti, N.H. (2017). Fatal Pertussis in the Neonatal Mouse Model Is Associated with Pertussis Toxin-Mediated Pathology beyond the Airways. Infect Immun *85*, e00355-17, e00355-17.

Scarlato, V., and Rappuoli, R. (1991). Differential response of the bvg virulence regulon of Bordetella pertussis to MgSO4 modulation. Journal of Bacteriology *173*, 7401–7404.

Scheller, E.V., and Cotter, P.A. (2015). *Bordetella* filamentous hemagglutinin and fimbriae: critical adhesins with unrealized vaccine potential. Pathogens and Disease *73*, ftv079.

Sealey, K.L., Belcher, T., and Preston, A. (2016). Bordetella pertussis epidemiology and evolution in the light of pertussis resurgence. Infect. Genet. Evol. *40*, 136–143.

Sebo, P., Glaser, P., Sakamoto, H., and Ullmann, A. (1991). High-level synthesis of active adenylate cyclase toxin of Bordetella pertussis in a reconstructed Escherichia coli system. Gene *104*, 19–24.

Sekiya, K., Munoz, J.J., and Nakase, Y. (1982). Effect of Dermonecrotic Toxin of *Bordetella pertussis* on the Spleen of CFW and C57BL/10ScN Mice. Microbiology and Immunology *26*, 971–977.

Shepard, C.W., Daneshvar, M.I., Kaiser, R.M., Ashford, D.A., Lonsway, D., Patel, J.B., Morey, R.E., Jordan, J.G., Weyant, R.S., and Fischer, M. (2004). *Bordetella holmesii* Bacteremia: A Newly Recognized Clinical Entity among Asplenic Patients. CLIN INFECT DIS *38*, 799–804.

Skinner, J.A., Pilione, M.R., Shen, H., Harvill, E.T., and Yuk, M.H. (2005). *Bordetella* Type III Secretion Modulates Dendritic Cell Migration Resulting in Immunosuppression and Bacterial Persistence. J Immunol *175*, 4647–4652.

Skopova, K., Tomalova, B., Kanchev, I., Rossmann, P., Svedova, M., Adkins, I., Bibova, I., Tomala, J., Masin, J., Guiso, N., et al. (2017). Cyclic AMP-Elevating Capacity of Adenylate Cyclase Toxin-Hemolysin Is Sufficient for Lung Infection but Not for Full Virulence of Bordetella pertussis. Infect. Immun. *85*.

Snyder, J., and Fisher, D. (2012). Pertussis in Childhood. Pediatrics in Review *33*, 412–421.

Soares, M.P., and Hamza, I. (2016). Macrophages and Iron Metabolism. Immunity *44*, 492–504.

Sobran, M.A., and Cotter, P.A. (2019). The BvgS PAS Domain, an Independent Sensory Perception Module in the *Bordetella bronchiseptica* BvgAS Phosphorelay. J Bacteriol *201*, e00286-19, /jb/201/17/JB.00286-19.atom.

Sory, M.P., and Cornelis, G.R. (1994). Translocation of a hybrid YopE-adenylate cyclase from Yersinia enterocolitica into HeLa cells. Mol. Microbiol. *14*, 583–594.

Stainer, D.W., and Scholte, M.J. (1970). A simple chemically defined medium for the production of phase I Bordetella pertussis. J. Gen. Microbiol. *63*, 211–220.

Starai, V.J., and Escalante-Semerena, J.C. (2004). Identification of the Protein Acetyltransferase (Pat) Enzyme that Acetylates Acetyl-CoA Synthetase in Salmonella enterica. Journal of Molecular Biology *340*, 1005–1012.

Steed, L.L., Setareh, M., and Friedman, R.L. (1991). Intracellular survival of virulent Bordetella pertussis in human polymorphonuclear leukocytes. J. Leukoc. Biol. *50*, 321–330.

Steed, L.L., Akporiaye, E.T., and Friedman, R.L. (1992). Bordetella pertussis induces respiratory burst activity in human polymorphonuclear leukocytes. Infect. Immun. *60*, 2101–2105.

Stein, P.E., Boodhoo, A., Armstrong, G.D., Cockle, S.A., Klein, M.H., and Read, R.J. (1994a). The crystal structure of pertussis toxin. Structure *2*, 45–57.

Stein, P.E., Boodhoo, A., Armstrong, G.D., Heerze, L.D., Cockle, S.A., Klein, M.H., and Read, R.J. (1994b). Structure of a pertussis toxin–sugar complex as a model for receptor binding. Nat Struct Mol Biol *1*, 591–596.

Steinke, M., Gross, R., Walles, H., Gangnus, R., Schütze, K., and Walles, T. (2014). An engineered 3D human airway mucosa model based on an SIS scaffold. Biomaterials *35*, 7355–7362.

Stenson, T.H., Allen, A.G., al-Meer, J.A., Maskell, D., and Peppler, M.S. (2005). Bordetella pertussis risA, but Not risS, Is Required for Maximal Expression of Bvg-Repressed Genes. Infection and Immunity *73*, 5995–6004.

Steven, A.C., Bisher, M.E., Trus, B.L., Thomas, D., Zhang, J.M., and Cowell, J.L. (1986). Helical structure of Bordetella pertussis fimbriae. J. Bacteriol. *167*, 968–974.

Stibitz, S., Aaronson, W., Monack, D., and Falkow, S. (1989). Phase variation in Bordetella pertussis by frameshift mutation in a gene for a novel two-component system. Nature *338*, 266–269.

Stockbauer, K.E., Fuchslocher, B., Miller, J.F., and Cotter, P.A. (2001). Identification and characterization of BipA, a Bordetella Bvg-intermediate phase protein. Mol. Microbiol. *39*, 65–78.

Sugisaki, K., Hanawa, T., Yonezawa, H., Osaki, T., Fukutomi, T., Kawakami, H., Yamamoto, T., and Kamiya, S. (2013). Role of (p)ppGpp in biofilm formation and expression of filamentous structures in Bordetella pertussis. Microbiology *159*, 1379–1389.

Szabo, G., Gray, M.C., and Hewlett, E.L. (1994). Adenylate cyclase toxin from Bordetella pertussis produces ion conductance across artificial lipid bilayers in a calcium- and polarity-dependent manner. J. Biol. Chem. *269*, 22496–22499.

Taylor-Mulneix, D.L., Bendor, L., Linz, B., Rivera, I., Ryman, V.E., Dewan, K.K., Wagner, S.M., Wilson, E.F., Hilburger, L.J., Cuff, L.E., et al. (2017). Bordetella bronchiseptica exploits the complex life cycle of Dictyostelium discoideum as an amplifying transmission vector. PLoS Biol *15*, e2000420.

Teruya, S., Hiramatsu, Y., Nakamura, K., Fukui-Miyazaki, A., Tsukamoto, K., Shinoda, N., Motooka, D., Nakamura, S., Ishigaki, K., Shinzawa, N., et al. (2020). *Bordetella* Dermonecrotic Toxin Is a Neurotropic Virulence Factor That Uses $Ca_V3.1$ as the Cell Surface Receptor. MBio *11*, e03146-19, /mbio/11/2/mBio.03146-19.atom.

Teter, K. (2019). Intracellular Trafficking and Translocation of Pertussis Toxin. Toxins *11*, 437.

Thalen, M., Venema, M., van den IJssel, J., Berwald, L., Beuvery, C., Martens, D., and Tramper, J. (2006). Effect of relevant culture parameters on Pertussis Toxin expression by Bordetella pertussis. Biologicals *34*, 213–220.

Tucker, A.C., and Escalante-Semerena, J.C. (2010). Biologically Active Isoforms of CobB Sirtuin Deacetylase in Salmonella enterica and Erwinia amylovora. JB *192*, 6200–6208.

Tuomanen, E. (1986). Piracy of adhesins: attachment of superinfecting pathogens to respiratory cilia by secreted adhesins of Bordetella pertussis. Infect. Immun. *54*, 905–908.

Uhl, M.A., and Miller, J.F. (1994). Autophosphorylation and phosphotransfer in the Bordetella pertussis BvgAS signal transduction cascade. Proc. Natl. Acad. Sci. U.S.A. *91*, 1163–1167.

Urisu, A., Cowell, J.L., and Manclark, C.R. (1986). Filamentous hemagglutinin has a major role in mediating adherence of Bordetella pertussis to human WiDr cells. Infect. Immun. *52*, 695–701.

Ushijima, T., and Hattori, N. (2012). Molecular pathways: involvement of Helicobacter pylori-triggered inflammation in the formation of an epigenetic field defect, and its usefulness as cancer risk and exposure markers. Clin. Cancer Res. *18*, 923–929.

Vandamme, P., Hommez, J., Vancanneyt, M., Monsieurs, M., Hoste, B., Cookson, B., Wirsing Von Konig, C.H., Kersters, K., and Blackall, P.J. (1995). Bordetella hinzii sp. nov., Isolated from Poultry and Humans. International Journal of Systematic Bacteriology *45*, 37–45.

Vanderpool, C.K., and Armstrong, S.K. (2001). The Bordetella bhu Locus Is Required for Heme Iron Utilization. J. Bacteriol. *183*, 4278–4287.

Vanderpool, C.K., and Armstrong, S.K. (2004). Integration of Environmental Signals Controls Expression of Bordetella Heme Utilization Genes. JB *186*, 938–948.

Vergara-Irigaray, N., Chavarri-Martinez, A., Rodriguez-Cuesta, J., Miller, J.F., Cotter, P.A., and Martinez de Tejada, G. (2005). Evaluation of the Role of the Bvg Intermediate Phase in Bordetella pertussis during Experimental Respiratory Infection. Infection and Immunity *73*, 748–760.

Vetting, M.W., S. de Carvalho, L.P., Yu, M., Hegde, S.S., Magnet, S., Roderick, S.L., and Blanchard, J.S. (2005). Structure and functions of the GNAT superfamily of acetyltransferases. Archives of Biochemistry and Biophysics *433*, 212–226.

Villarino Romero, R., Osicka, R., and Sebo, P. (2014). Filamentous hemagglutinin of Bordetella pertussis: a key adhesin with immunomodulatory properties? Future Microbiol *9*, 1339–1360.

Villarino Romero, R., Hasan, S., Faé, K., Holubova, J., Geurtsen, J., Schwarzer, M., Wiertsema, S., Osicka, R., Poolman, J., and Sebo, P. (2016). Bordetella pertussis filamentous hemagglutinin itself does not trigger anti-inflammatory interleukin-10 production by human dendritic cells. International Journal of Medical Microbiology *306*, 38–47.

Vojtova, J., Kamanova, J., and Sebo, P. (2006). Bordetella adenylate cyclase toxin: a swift saboteur of host defense. Curr. Opin. Microbiol. *9*, 69–75.

Vojtova-Vodolanova, J., Basler, M., Osicka, R., Knapp, O., Maier, E., Cerny, J., Benada, O., Benz, R., and Sebo, P. (2009). Oligomerization is involved in pore formation by *Bordetella* adenylate cyclase toxin. FASEB j. *23*, 2831–2843.

Vygen-Bonnet, S., Hellenbrand, W., Garbe, E., von Kries, R., Bogdan, C., Heininger, U., Röbl-Mathieu, M., and Harder, T. (2020). Safety and effectiveness of acellular pertussis vaccination during pregnancy: a systematic review. BMC Infect Dis *20*, 136.

Wagner, G.R., and Payne, R.M. (2013). Widespread and Enzyme-independent N^{ϵ}-Acetylation and N^{ϵ}-Succinylation of Proteins in the Chemical Conditions of the Mitochondrial Matrix. J. Biol. Chem. *288*, 29036–29045.

Walsh, C.T., Garneau-Tsodikova, S., and Gatto, G.J. (2005). Protein posttranslational modifications: the chemistry of proteome diversifications. Angew. Chem. Int. Ed. Engl. *44*, 7342–7372.

Weigand, M.R., Peng, Y., Loparev, V., Batra, D., Bowden, K.E., Burroughs, M., Cassiday, P.K., Davis, J.K., Johnson, T., Juieng, P., et al. (2017). The History of Bordetella pertussis Genome Evolution Includes Structural Rearrangement. J. Bacteriol. *199*, e00806-16, /jb/199/8/e00806-16.atom.

Weigand, M.R., Peng, Y., Batra, D., Burroughs, M., Davis, J.K., Knipe, K., Loparev, V.N., Johnson, T., Juieng, P., Rowe, L.A., et al. (2019). Conserved Patterns of Symmetric Inversion in the Genome Evolution of *Bordetella* Respiratory Pathogens. MSystems *4*, e00702-19, /msystems/4/6/msys.00702-19.atom.

Weiss, A.A., Hewlett, E.L., Myers, G.A., and Falkow, S. (1983). Tn5-induced mutations affecting virulence factors of Bordetella pertussis. Infect. Immun. *42*, 33–41.

Weiss, A.A., Melton, A.R., Walker, K.E., Andraos-Selim, C., and Meidl, J.J. (1989). Use of the promoter fusion transposon Tn5 lac to identify mutations in Bordetella pertussis vir-regulated genes. Infect. Immun. *57*, 2674–2682.

Welch, R.A. (1991). Pore-forming cytolysins of gram-negative bacteria. Mol. Microbiol. *5*, 521–528.

WHO (2015). Pertussis vaccines: WHO position paper - September 2015. Wkly. Epidemiol. Rec. *90*, 433–458.

Willems, R., Paul, A., van der Heide, H.G., ter Avest, A.R., and Mooi, F.R. (1990). Fimbrial phase variation in Bordetella pertussis: a novel mechanism for transcriptional regulation. EMBO J. *9*, 2803–2809.

Willems, R.J.L., Heide, H.G.J., and Mooi, F.R. (1992). Characterization of a Bordetella pertussis fimbrial gene cluster which is located directly downstream of the filamentous haemagglutinin gene. Mol Microbiol *6*, 2661–2671.

Williams, C.L., and Cotter, P.A. (2007). Autoregulation is essential for precise temporal and steady-state regulation by the Bordetella BvgAS phosphorelay. J Bacteriol *189*, 1974–1982.

Williams, C.L., Boucher, P.E., Stibitz, S., and Cotter, P.A. (2005). BvgA functions as both an activator and a repressor to control Bvgi phase expression of bipA in Bordetella pertussis: bipA transcription in B. pertussis. Molecular Microbiology *56*, 175–188.

Williams, M.M., Sen, K., Weigand, M.R., Skoff, T.H., Cunningham, V.A., Halse, T.A., Tondella, M.L., and CDC Pertussis Working Group (2016). *Bordetella pertussis* Strain Lacking Pertactin and Pertussis Toxin. Emerg. Infect. Dis. *22*, 319–322.

Williamson, Y.M., Moura, H., Whitmon, J., Woolfitt, A.R., Schieltz, D.M., Rees, J.C., Guo, S., Kirkham, H., Bouck, D., Ades, E.W., et al. (2015). A Proteomic Characterization of Bordetella pertussis Clinical Isolates Associated with a California State Pertussis Outbreak. Int J Proteomics *2015*, 536537.

von Wintzingerode, F., Gerlach, G., Schneider, B., and Gross, R. (2002). Phylogenetic Relationships and Virulence Evolution in the Genus Bordetella. In Pathogenicity Islands and the Evolution of Pathogenic Microbes, J. Hacker, and J.B. Kaper, eds. (Berlin, Heidelberg: Springer Berlin Heidelberg), pp. 177–199.

Wolff, J., Cook, G.H., Goldhammer, A.R., and Berkowitz, S.A. (1980). Calmodulin activates prokaryotic adenylate cyclase. Proc. Natl. Acad. Sci. U.S.A. *77*, 3841–3844.

Woods, D.E., Franklin, R., Cryz, S.J., Ganss, M., Peppler, M., and Ewanowich, C. (1989). Development of a rat model for respiratory infection with Bordetella pertussis. Infect. Immun. *57*, 1018–1024.

Wroblewski, L.E., Peek, R.M., and Wilson, K.T. (2010). Helicobacter pylori and gastric cancer: factors that modulate disease risk. Clin. Microbiol. Rev. *23*, 713–739.

Wrzesinski, K., and Fey, S.J. (2018). Metabolic Reprogramming and the Recovery of Physiological Functionality in 3D Cultures in Micro-Bioreactors. Bioengineering (Basel) *5*.

Wu, X., Vellaichamy, A., Wang, D., Zamdborg, L., Kelleher, N.L., Huber, S.C., and Zhao, Y. (2013). Differential lysine acetylation profiles of Erwinia amylovora strains revealed by proteomics. Journal of Proteomics *79*, 60–71.

Yajima, M., Hosoda, K., Kanbayashi, Y., Nakamura, T., Nogimori, K., Mizushima, Y., Nakase, Y., and Ui, M. (1978). Islets-activating protein (IAP) in Bordetella pertussis that potentiates insulin secretory responses of rats. Purification and characterization. J. Biochem. *83*, 295–303.

Yang, X.-J., and Seto, E. (2008a). Lysine Acetylation: Codified Crosstalk with Other Posttranslational Modifications. Molecular Cell *31*, 449–461.

Yang, X.-J., and Seto, E. (2008b). The Rpd3/Hda1 family of lysine deacetylases: from bacteria and yeast to mice and men. Nat. Rev. Mol. Cell Biol. *9*, 206–218.

Yauger, Y.J., Bermudez, S., Moritz, K.E., Glaser, E., Stoica, B., and Byrnes, K.R. (2019). Iron accentuated reactive oxygen species release by NADPH oxidase in activated microglia contributes to oxidative stress in vitro. J Neuroinflammation *16*, 41.

Yeung, K.H.T., Duclos, P., Nelson, E.A.S., and Hutubessy, R.C.W. (2017). An update of the global burden of pertussis in children younger than 5 years: a modelling study. Lancet Infect Dis *17*, 974–980.

Young, S.P., and Garner, C. (1990). Delivery of iron to human cells by bovine transferrin. Implications for the growth of human cells in vitro. The Biochemical Journal *265*, 587–591.

Yuk, M.H., Harvill, E.T., and Miller, J.F. (1998). The BvgAS virulence control system regulates type III secretion in Bordetella bronchiseptica. Mol. Microbiol. *28*, 945–959.

Yuk, M.H., Harvill, E.T., Cotter, P.A., and Miller, J.F. (2000). Modulation of host immune responses, induction of apoptosis and inhibition of NF-kappaB activation by the Bordetella type III secretion system. Mol Microbiol *35*, 991–1004.

Zimna, K., Medina, E., Jungnitz, H., and GuzmÃ¡n, C.A. (2001). Role played by the response regulator Ris in Bordetella bronchiseptica resistance to macrophage killing. FEMS Microbiology Letters *201*, 177–180.

APPENDIX I

Phosphoproteomics of cAMP signaling of *Bordetella* adenylate cyclase toxin in mouse dendritic cells

Novák J, Fabrik I, Linhartová I, Link M, Černý O, Stulík J, Šebo P.

Sci Rep. 2017 Nov 24;7(1):16298. doi: 10.1038/s41598-017-14501-x.

SCIENTIFIC REPORTS

OPEN

Received: 20 June 2017
Accepted: 11 October 2017
Published online: 24 November 2017

Phosphoproteomics of cAMP signaling of *Bordetella* adenylate cyclase toxin in mouse dendritic cells

Jakub Novák[1], Ivo Fabrik[2], Irena Linhartová[1], Marek Link[2], Ondřej Černý[1], Jiří Stulík[2] & Peter Šebo[1]

The adenylate cyclase toxin (CyaA) of the whooping cough agent *Bordetella pertussis* subverts immune functions of host myeloid cells expressing the $\alpha_M\beta_2$ integrin (CD11b/CD18, CR3 or Mac-1). CyaA delivers into cytosol of cells an extremely catalytically active adenylyl cyclase enzyme, which disrupts the innate and adaptive immune functions of phagocytes through unregulated production of the key signaling molecule cAMP. We have used phosphoproteomics to analyze cAMP signaling of CyaA in murine bone marrow-derived dendritic cells. CyaA action resulted in alterations of phosphorylation state of a number of proteins that regulate actin cytoskeleton homeostasis, including Mena, Talin-1 and VASP. CyaA action repressed mTOR signaling through activation of mTORC1 inhibitors TSC2 and PRAS40 and altered phosphorylation of multiple chromatin remodelers, including the class II histone deacetylase HDAC5. CyaA toxin action further elicited inhibitory phosphorylation of SIK family kinases involved in modulation of immune response and provoked dephosphorylation of the transcriptional coactivator CRTC3, indicating that CyaA-promoted nuclear translocation of CRTC3 may account for CyaA-induced IL-10 production. These findings document the complexity of subversive physiological manipulation of myeloid phagocytes by the CyaA toxin, serving in immune evasion of the pertussis agent.

The Gram-negative coccobacillus *Bordetella pertussis* excels in sophistication of its immunomodulatory action. The bacterium causes the respiratory infectious disease called whooping cough, or pertussis, which can be lethal to unvaccinated infants[1] and still accounts for an estimated 15 to 50 million cases and ~150,000–300,000 deaths annually world-wide[2]. Among the first cells of the immune system that respond to *B. pertussis* infection are the myeloid phagocytic cells that bear the complement receptor 3 (CR3, the $\alpha_M\beta_2$ integrin CD11b/CD18 or Mac-1). This includes macrophages, neutrophils and dendritic cells (DCs)[3]. *B. pertussis* employs several mechanisms to subvert their functions. A prominent role in paralysis of these sentinel cells is played by the CR3-binding adenylate cyclase (AC) toxin-hemolysin (CyaA, ACT, or AC-Hly). CyaA is a member of the Repeat In ToXin (RTX) family of leukotoxins[4] and consists of a cell-invasive adenylyl cyclase (AC) enzyme fused to a pore-forming RTX cytolysin (Hly) moiety[5]. Upon binding to CR3 on cell surface, the toxin translocates its AC domain directly across the plasma membrane into cytosol of phagocytes. There, the AC enzyme is activated by calmodulin and catalyzes unregulated production of a key signaling molecule, the 3′,5′-cyclic adenosine monophosphate (cAMP). Supraphysiological concentrations of cAMP then signal through protein kinase A (PKA) and Exchange Protein directly Activated by cAMP (Epac) pathways[6] and rapidly annihilate the bactericidal capacities of phagocytes. Signaling of CyaA-produced cAMP provokes massive but unproductive cell ruffling, inhibits opsonophagocytic uptake of bacteria, blocks induction of nitric oxide (NO) production, inhibits NADPH assembly and oxidative burst and induces macrophage apoptosis[6–9]. The molecular details of how CyaA-triggered cAMP signaling interferes with phagocyte functions remain, however, poorly defined. The high specific activity of the CyaA-delivered adenylyl cyclase (AC) enzyme represents, hence, a unique tool for analysis of the impact of cAMP signaling on myeloid cell function in general.

[1]Institute of Microbiology of the Czech Academy of Sciences, v.v.i., Prague, Czech Republic. [2]Department of Molecular Pathology and Biology, Faculty of Military Health Sciences, University of Defence, Hradec Kralove, Czech Republic. Correspondence and requests for materials should be addressed to P.Š. (email: sebo@biomed.cas.cz)

We have used stable isotope labelling by amino acids in cell culture (SILAC)[10] for quantitative shotgun phosphoproteomic analysis of cAMP signaling resulting from CyaA toxin action on primary mouse bone marrow derived dendritic cells (BMDC). The results reveal that CyaA action causes alteration of phosphorylation of a number of proteins involved in regulation of actin cytoskeleton homeostasis, phagocytosis, translation, chromatin remodeling, IL-10 secretion and tolerogenic DC shaping.

Materials and Methods

CyaA toxin preparation. CyaA toxin and its enzymatically inactive CyaA-AC$^-$ toxoid were produced in *Escherichia coli* XL-1 Blue cells and purified as previously described[11], including 60% isopropanol washes of the chromatography resin with bound CyaA, which reduced the endotoxin content of eluted CyaA below 300 IU/mg protein (QCL-1000 Limulus amebocyte lysate assay, Cambrex, East Rutherford, NJ).

Preparation and SILAC labelling of bone marrow-derived DCs (BMDCs). The handling of animals was approved by the ethical committees of the Faculty of Military Health Sciences of the University of Defence and of the Institute of Microbiology of the Czech Academy of Sciences. Handling of animals and all experiments were performed in accordance with relevant guidelines and regulations, according to Guidelines for the Care and Use of Laboratory Animals, the Act of the Czech National Assembly, Collection of Laws No. 149/2004, inclusive of the amendments, on the Protection of Animals against Cruelty, and Public Notice of the Ministry of Agriculture of the Czech Republic, Collection of Laws No. 207/2004, on care and use of experimental animals.

The generation and SILAC labelling of C57BL/6 murine BMDCs was carried out as previously described[12] and outlined in detail in the Supplementary methods section. BMDCs were generated from bone marrow progenitors isolated from femurs and tibias of 6- to 8-week-old female C57BL/6 mice. GM-CSF induces catabolism of $^{13}C/^{15}N$-labelled arginine, yielding heavy arginine-derived proline and ^{15}N isotope incorporation, thus skewing estimation of SILAC ratios. Therefore an optimized SILAC-labeling medium was used to suppress these effects, as described earlier[12].

Toxin treatment. SILAC-labelled BMDCs were first incubated in D-MEM (1.9 mM Ca^{2+}) for 2 hours at 37 °C. 'Light' isotope-labelled cells (^{12}C6-arginine/^{12}C6-lysine) were next treated for 10 or 30 minutes at 37 °C with 100 ng/ml of either CyaA toxin or CyaA-AC$^-$ toxoid dissolved in TUC buffer (50 mM Tris-HCl, 8 M urea, 2 mM $CaCl_2$, pH 8). Corresponding 'heavy' isotope-labelled cells (^{13}C6-arginine/^{13}C6-lysine) were treated by TUC buffer alone and served as controls for both CyaA and CyaA-AC$^-$-treated BMDCs (Supplementary Fig. S1). The whole experiment was performed in biological triplicate and SILAC groups were swapped in one replicate. Cells were next washed in ice-cold PBS and lysed in Lysis buffer (50 mM NH_4HCO_3, 1% (w/v) sodium deoxycholate (SDC)) containing a cocktail of phosphatase inhibitors (cocktail set II; Merck). Lysis was accomplished by placing the cell suspension into a boiling water bath for 5 min[13]. After cooling of the lysed suspension to room temperature, the samples were subjected to benzonase treatment (Sigma) for 1 h and cell debris was removed by centrifugation (14,000 *g*, 10 min and 4 °C). Protein concentrations in supernatants were measured using the Micro BCA kit (Thermo Pierce) and the corresponding 'light' and 'heavy' isotope-labelled lysates were mixed at a 1:1 ratio based on their protein content.

Phosphoproteomic analysis. Details of sample preparation and data processing are provided in the Supplementary methods. Briefly, proteins in SILAC-labelled BMDC lysates were digested with trypsin and the peptides were fractionated by hydrophilic interaction liquid chromatography (HILIC)[14]. The phosphopeptides were enriched on TiO_2 resin (GL Sciences), separated by reversed-phase nano-scale LC and analyzed by mass spectrometry on a Q-Exactive MS instrument (Thermo Scientific) operating in data-dependent acquisition (DDA) mode. Data processing, identification and quantitation was performed with MaxQuant software[15,16] and the MS data were deposited via the PRIDE partner repository[17] in the ProteomeXchange Consortium database (http://proteomecentral.proteomexchange.org) under the dataset identifier PXD004733. Both WT CyaA and CyaA-AC$^-$treated samples were first compared to buffer-treated controls in order to determine the changes in phosphorylation status of each phosphosite. The resulting ratios for individual phosphosites were derived from normalized ratios of the least modified phosphopeptides in a given replicate. Ratio values > 1 then represent dephosphorylation and values < 1 represent increase in phosphorylation. The statistical significance of differences in the phosphorylation status at individual sites was determined by the Global Mean Rank Test[18]. Significantly enriched phosphorylation motifs were assembled using the web-based motif-x algorithm[19]. Assignment to known kinase motifs was performed by Motif Matcher, a web-based online tool from the PHOSIDA posttranslational modification database[20,21]. Alternatively, Fisher's exact test analysis of kinase motif enrichment was performed for significantly regulated phosphosites by using the Perseus software[22] with built-in Human Protein Reference Database[23] as the source of kinase motifs. Functional association between significantly regulated phosphoproteins was visualized using the online-based STRING database (v10; http://string-db.org/; confidence values 0.900 and 0.400, respectively)[24]. Gene Ontology (GO)[25] enrichment analysis was performed in Cytoscape[26] using the plugin ClueGO[27].

Results

CyaA triggers PKA and CaMK2-dependent phosphorylation of regulatory proteins. CR3-expressing intraepithelial DCs of myeloid origin (CD11b$^+$) are a likely cellular target of the CyaA toxin in the course of *B. pertussis* infection of host airways. We thus assessed the impact of the subversive signaling of CyaA-produced cAMP in DCs by a quantitative phosphoproteomic analysis. Since human monocyte-derived dendritic cells exhibit high inter-donor variation, BMDCs from inbred C57BL/6 mice were used. The cells were labelled *ex vivo* with stable isotopes (SILAC)[12] and advantage was taken of the use of a non-enzymatic CyaA-AC$^-$ toxoid as negative control. CyaA-AC$^-$ is unable to elevate cAMP in cells[28,29] but retains the full capacity to bind the cell

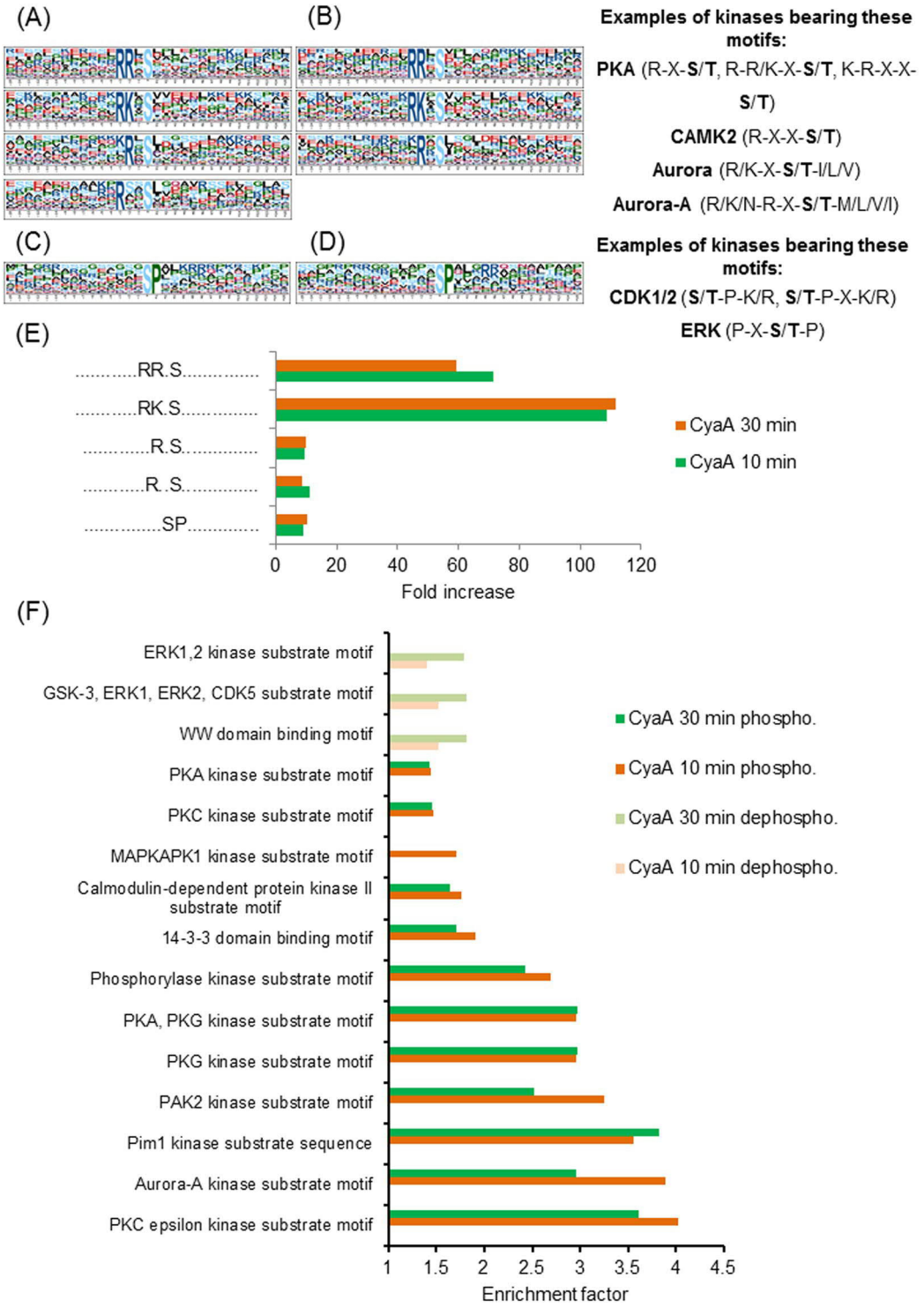

Figure 1. Kinase enrichment analysis of significantly regulated phosphosites. Significantly regulated phosphosites in all replicates for the given experimental condition were identified by Global Mean Rank Test as described in Supplementary Methods. The kinase motifs were next extracted with the web-based motif-x (http://motif-x.med.harvard.edu/) application (Chou & Schwartz, Curr Protoc Bioinformatics. 2011) and assigned to characterized kinases using the PHOSIDA database (http://141.61.102.18/phosida/home.aspx) with the IPI mouse proteome data background (ftp://ftp.ebi.ac.uk/pub/databases/IPI), using a significance threshold of 0.000001 and a minimal occurrence value of the motif set to 20. (**A**) Overrepresented phosphosite motifs extracted as upregulated (phosphorylated) phosphosites by motif-x for samples incubated with CyaA for 10 or (**B**) 30 minutes. Occurrence value of the "..R..S.." motif was 19, hence, just below the set threshold of 20. (**C**) Overrepresented motifs extracted as downregulated (dephosphorylated) phosphosites by motif-x for samples incubated with CyaA for 10 or (**D**) 30 minutes. The "..SP…R.." motif found in the samples treated with

CyaA for 30 min exhibited an occurrence number of 19, hence, below the threshold of 20. (**E**) Fold increase of extracted motifs shown in (**A**) and (**B**). Fold increase was calculated as the ratio (foreground matches divided by foreground size) divided by (background matches divided by background size), where the background is the predefined organism background from IPI Mouse Proteome. (**F**) Prediction of kinase-specific phosphorylation sites found among the significantly differentially regulated (both phosphorylated and dephosphorylated) phosphosites in samples treated with CyaA (with localization probability >0.75 in all replicates in 10 and 30 min samples), compared to buffer-treated controls, by Fisher exact test (Benjamini-Hochberg FDR with the threshold value 0.05). Results are expressed as enrichment factors that are counted using the following formula: (number of hits for particular kinase divided by the number of significantly regulated phosphosites) divided by (number of hits of the particular kinase in the whole given cluster divided by the total size of the dataset). Only kinase enrichment factors >1 are depicted. Perseus software package for shotgun proteomics data analyzes, version 1.5.1.6, was used for the analysis, employing the Human Protein Reference Database (Release 9).

surface receptor CR3, to permeabilize cellular membrane and to elicit Ca^{2+} influx into cells and K^+ efflux from cells, like intact CyaA. This control thus enabled exclusion of phosphorylation changes that were unrelated to cAMP signaling elicited by the CyaA toxin and were due to cell handling and/or cell permeabilization by the pore-forming activity of CyaA. To capture the early cAMP-triggered signaling events and to mimic the physiological concentrations of CyaA encountered by the phagocytes on *B. pertussis*-infected airway mucosa[30,31], the SILAC-labelled BMDCs (10^6/ml) were exposed to 100 ng/ml of CyaA or of CyaA-AC$^-$ for 10 or 30 minutes.

SILAC-based phosphoproteomic analysis of tryptic digests of 1:1 mixtures of lyzates form 'heavy' and 'light' isotope-labelled cells was then accomplished as schematically outlined in Supplementary Fig. S1, using biological triplicates and including one label swap condition. This yielded a total of 19,310 identified phosphosites that could be confirmed by MS/MS analysis, including two phosphosites on CyaA itself. From all identified phosphosites, 14,389 were found to be class I sites having a localization probability of >0.75[32]. The observed global phosphorylation pattern of 12,562 serine (87.3%), 1,700 threonine (11.81%) and 127 tyrosine (0.9%) phosphosites (Supplementary Fig. S2B) resembled well the classical radioisotope-based estimates of phosphosite distribution in cells[33]. In total, 6,931 phosphosites were quantified for all three replicates in at least one experimental condition, including the serine residue 393 of CyaA. Compared to buffer control, the treatment of cells with CyaA for 10 or 30 min yielded a significant alteration of the phosphorylation state of the proteome for a total of 313 and 275 sites, respectively. In contrast, upon treatment with CyaA-AC$^-$ for 10 min, the alteration of phosphorylation state of only 3 sites passed the significance test. However, phosphorylation status of 56 sites was significantly modulated when BMDCs were exposed to the cell-permeabilizing CyaA-AC$^-$ toxoid for 30 min (Supplementary Fig. S2B-C, Supplementary Fig. S3 and Supplementary Table S1).

PKA isoforms are the central cAMP-regulated protein kinases that are likely to mediate most of the immunomodulatory effects of CyaA toxin action[6,7,34,35]. We therefore searched the phosphoproteome data specifically for cAMP-dependent alterations of the phosphorylation state of proteins (Supplementary Table S1) and the overrepresented phosphorylation patterns were extracted using motif-x[19,36]. As expected, the cAMP-activated PKA and Ca^{2+}/calmodulin-dependent protein kinase II (CaMK2) were found to be the major kinases mediating cAMP signaling elicited by CyaA (Fig. 1A,B and E). Indeed, the involvement of CaMK2 goes well with the intrinsic capacity of CyaA to bind calmodulin and mediate influx of extracellular Ca^{2+} ions across the plasma membrane of cells[37,38]. Moreover, activation of CaMK2 by the other cAMP effector Epac was previously reported[39], which suggested a potential indirect role of Epac in phosphoproteome alterations in CyaA-treated cells. The obtained dataset revealed a significant modulation of phosphorylation at sites recognized by the Aurora A kinase[40] (Fig. 1A,B and E), in line with the previously reported inhibitory impact of CyaA toxin action on mitotic progression and G1/S transition of macrophage cells[41,42]. As further highlighted in Fig. 1C and D, action of CyaA led to the inhibition of cyclin-dependent (CDKs) and extracellular-signal-regulated (ERKs) kinases, yielding an overrepresentation of dephosphorylated proline-directed sites in the dataset.

To corroborate this analysis by an alternative approach, individual phosphosites were annotated for potential kinase motifs according to Human Protein Reference Database[23] and the enrichment level for regulated sites was next evaluated by Fisher's exact test using the Perseus software. Following CyaA treatment for 10 or 30 minutes, the PKA, CAMK2 and Aurora A kinase motifs were found to be overrepresented among the increasingly phosphorylated sites, while the Erk1/2 kinase motifs were overrepresented among significantly dephosphorylated sites (Fig. 1C–E). However, BMDC exposure to CyaA for 30 minutes had no effect on the phosphorylation status of the threonine 203 and tyrosine 205 residues in the activation loop of Erk kinases (Supplementary Fig. S4A and B). This indicates that CyaA-produced cAMP signaling activated some phosphatase(s) dephosphorylating the Erk1/2 target motifs.

CyaA is itself phosphorylated upon translocation into target cells. The 384 N-terminal amino residues of the AC enzyme domain of CyaA are fused to the 'AC to Hly-linking segment' (residues 385–485)[43] that plays an essential role in AC domain translocation across the plasma membrane of cells[44]. The phosphoproteomic analysis revealed a phosphorylation signal of the serine 393 residue of CyaA (Supplementary Table S1, for processed MS/MS spectrum see Supplementary Fig. S5), showing that the N-proximal end of the 'AC to Hly-linking segment' penetrates into cell cytosol.

Adenylyl cyclase enzyme and pore-forming activities of CyaA exert counteracting effects on PI3K-Akt pathway. The impact of toxin and toxoid treatments on the phosphoproteome of BMDCs is summarized in Supplementary Fig. S3A-D. Only a small number of significantly regulated phosphosites was observed upon treatment of cells with the CyaA-AC$^-$ toxoid for 10 minutes. Therefore, only samples from the 30 minutes

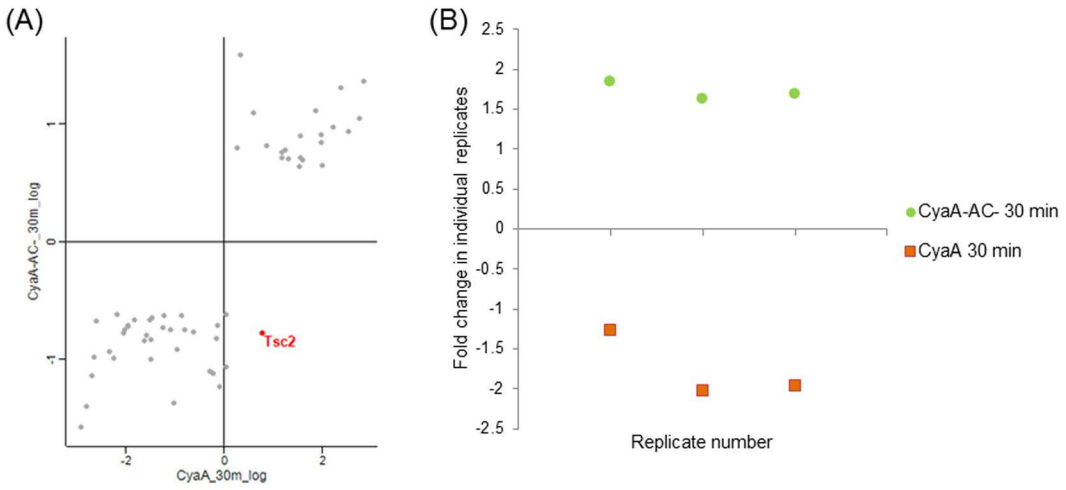

Figure 2. Phosphorylation of tuberin (Tsc2) is oppositely manipulated by the cAMP signaling and pore-forming activities of CyaA. (**A**) Scatter plot of all significantly regulated phosphosites (based on signal ratios of toxin or toxoid-treated samples to buffer-treated samples). Values for the samples treated by CyaA-AC$^-$ toxoid for 30 minutes are plotted against the corresponding values for the samples treated by WT CyaA for 30 minutes. Tsc2, showing an inverse correlation between the two conditions, is highlighted. (**B**) Fold change of phosphorylation status (toxin- or toxoid-treated sample *versus* buffer-treated control) of the threonine residue 1465 of Tsc2 for three individual replicates (values >0 represent phosphorylation, values <0 represent dephosphorylation).

time point for the toxoid were analyzed in more detail. When the significantly regulated phosphosites of the toxoid-treated sample were plotted against the matching phosphosites from the CyaA-treated condition, a prominent alteration of the phosphorylation state of the threonine residue 1465 (1462 in man) of tuberin (product of the Tsc2 gene) was observed (Fig. 2). Tuberin, a well described mTOR-signaling suppressor[45], was dephosphorylated in CyaA-treated cells and was phosphorylated in toxoid-treated cells (Fig. 2A and B). cAMP signaling of CyaA thus inhibited the activity of the PI3K-Akt pathway accounting for tuberin phosphorylation[46], while the permeabilization of cells by the toxoid activated this pathway. Besides, Western blot analysis revealed that phosphorylation of the PRAS40 protein, yet another mTOR signaling inhibitor[47], was deregulated. PRAS40 exhibited diminished phosphorylation of the threonine residue 247[48] in CyaA-treated cells (Fig. 3A,B, Supplementary Figs S6A and S7A-C). For mTOR itself, only a mild decrease in phosphorylation of serine residue 2448 was observed after 30 min of CyaA action on cells (Fig. 3B, Supplementary Figs S6B and S7D-E). To test if these changes affected the downstream targets of mTOR, the phosphorylation status of serine residue 64 of 4E-BP1 was probed by a specific antibody. Dephosphorylation at this site was detected both by SILAC phosphoproteomics and Western blotting (Fig. 3, Supplementary Figs S6C and D7F-H and Supplementary Table S1).

CyaA-elicited phosphoproteome alterations modulate small GTPase signaling and actin cytoskeleton homeostasis. When Gene Ontology (GO)[25] terms enrichment analysis was applied to the phosphoproteome dataset, the action of CyaA on BMDCs resulted in the over-representation of terms related to GTPase signaling pathways and regulation of actin cytoskeleton (Fig. 4). This was further corroborated by construction of protein-protein interaction networks, using the STRING v10 database software[24] to decode the signaling processes triggered by toxin action in BMDCs (Fig. 5A–C). The network capturing of CyaA action in the first 10 minutes consisted of 43 nodes of phosphoproteins (Fig. 5A), with the most highly interconnected nodes comprising Mena (Enah), Talin-1 (Tln1), VASP (Fig. 3C, Supplementary Fig. S7I-J) or Abl2 proteins, which are all involved in the regulation of cytoskeleton homeostasis[49–52]. This goes well with the previous observation that CyaA-elicited cAMP signaling provokes transient inhibition of RhoA and triggers massive actin cytoskeleton rearrangements and membrane ruffling[9]. CyaA-triggered signaling remained similar at 30 min of BMDC treatment with CyaA, yielding a network of 57 nodes (Fig. 5B). The interconnected cluster of the largest subnetwork then again contained components of the small GTPase signaling pathways, such as the small GTPase-activators Gmip[53] and Arhgap11a[54], which are involved in cytoskeleton homeostasis regulation. Altogether, these results show that the early effects of CyaA-elicited cAMP signaling largely affect small GTPases that regulate actin remodeling and cytoskeletal rearrangements.

For the sample treated with CyaA-AC$^-$ (Fig. 5C), the STRING-based interaction network of affected phosphoproteins at the 30 min time point could only be constructed upon lowering of the stringency conditions (medium confidence 0.400). The resulting network then comprised, among others, the Heterochromatin protein 1 homolog alpha (CBX5), the E3 ubiquitin-protein ligase MDM2, the Rho guanine nucleotide exchange factor 7 (Arhgef7), PML and the SAFB-like transcription modulator (SLTM). Alterations of phosphorylation of these proteins might thus reflect the cell-permeabilizing activity of the CyaA-AC$^-$ toxoid.

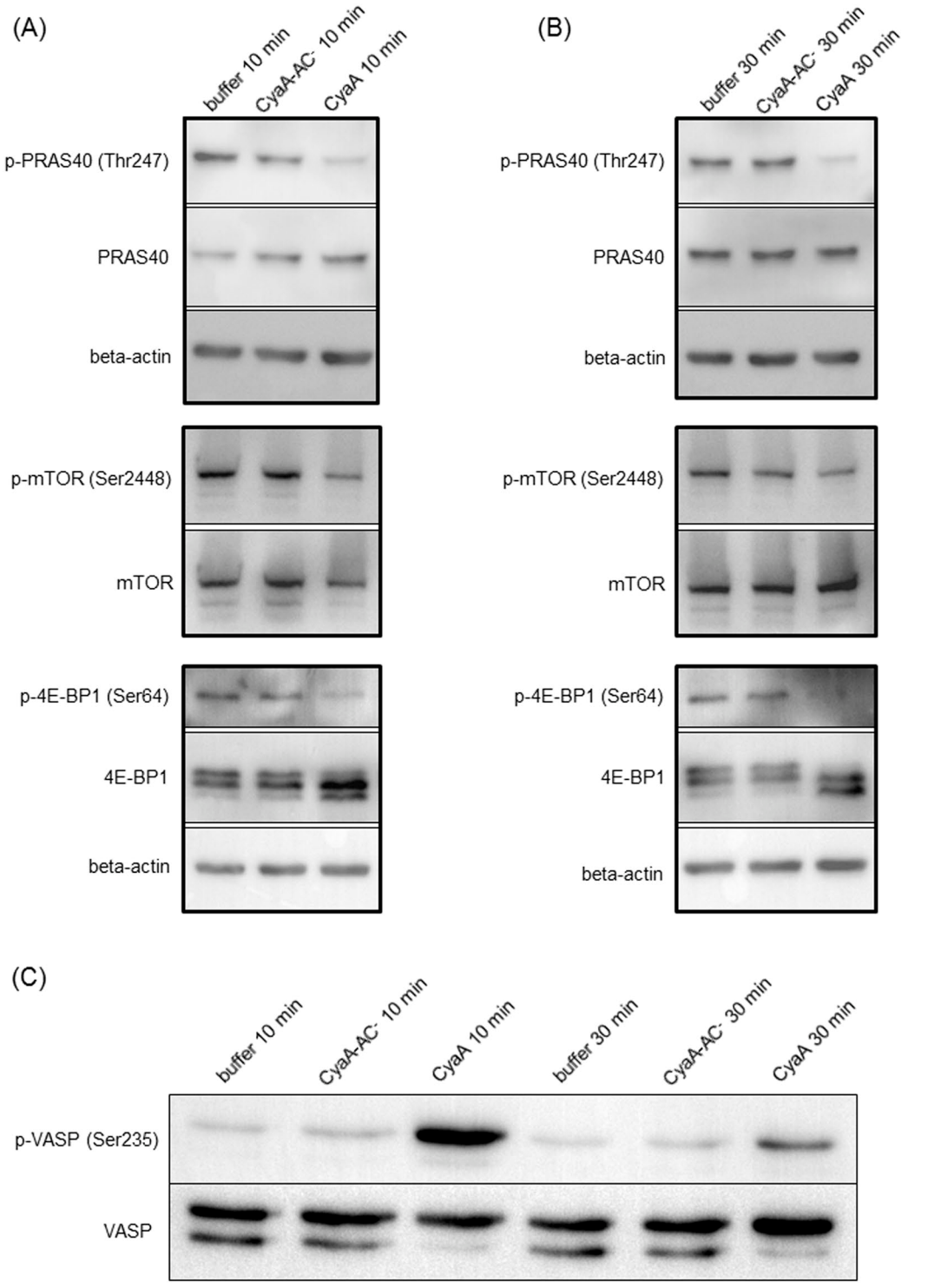

Figure 3. Changes in phosphorylation status of selected phosphoproteins. Members of mTOR signaling pathway after the toxin/toxoid treatment for (**A**) 10 minutes or (**B**) 30 minutes. (**C**) Phosphorylation status of serine 235 residue of cytoskeletal regulator VASP. In general, 10^6 BMDCs in 1 mL were exposed for 10 or 30 minutes to 100 ng of CyaA or of the CyaA-AC$^-$ toxoid, cellular lyzates were separated by SDS-PAGE and phosphorylation of indicated proteins was probed by Western blotting with specific antibodies. Images representative of at least three biological replicates are shown and quantifications of the Western blots of mTOR signaling pathway members are shown in Supplementary Fig. S6. Cropped images are shown and full-length blots are presented in Supplementary Fig. S7. "Buffer" stands for TUC-treated cells (TUC buffer −50 mM Tris-HCl, 8 M urea, 2 mM $CaCl_2$, pH 8; used for toxin/toxoid dilution).

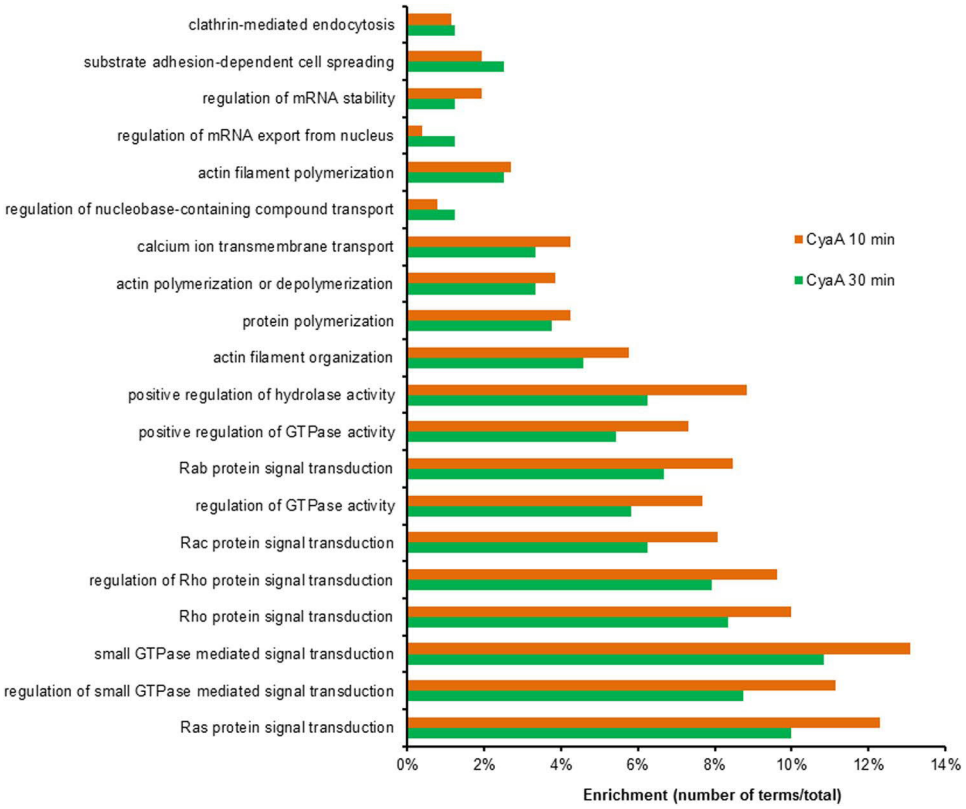

Figure 4. Functional analysis of CyaA-induced phosphoproteome changes. Analysis was performed using Gene Ontology Term enrichment and the top 20 terms ($p \leq 0.05$) enriched in „Biological process" library were ranked according to their p-values (corrected with Benjamini-Hochberg).The enrichment was counted as a number of genes belonging to each GO term divided by the total number of genes in each input gene set.

CyaA-elicited cAMP signaling impacts on phosphorylation status of SIK kinases involved in immune response. Based on their annotation[25,55,56] (selected GO terms are listed in Supplementary Table S2) we identified 32 kinases that contain at least one phosphosite having a significantly altered phosphorylation state upon BMDCs treatment with CyaA (Supplementary Table S3). Among them, the phosphorylation of regulatory serine residues of several salt-inducible kinases (SIK), known for their involvement in modulation of immune responses[57–60], was importantly altered (Fig. 6).

Discussion

We report here the first phosphoproteome-wide analysis of the signaling impact of the cAMP-elevating activity of *B. pertussis* adenylate cyclase toxin in primary myeloid cells. The AC domain of the CyaA toxin binds calmodulin in the cytosol of cells and acquires an extremely high specific enzymatic activity of about 2,000 molecules of ATP converted to cAMP per second per AC enzyme molecule[61]. This yields a steep and uncontrolled elevation of intracellular cAMP concentration in cells. The data reported here thus provides important insight into the pleiotropic effects of cAMP signaling in myeloid cells and point to two main areas of CyaA toxin interference within normal DC physiology. These comprise cAMP signaling towards inhibition of mTOR activity, signaling promoting cytoskeletal rearrangements and signaling regulating cytokine production by dendritic cells, as discussed below. Pro-survival signaling of mTOR is negatively regulated by the protein tuberin, the activity of which is inhibited by phosphorylation of the threonine residue 1465 by Akt[45,46]. Tuberin is also known to be inhibited by Erk[62]. In contrast to previous reports using mouse or human macrophage or neutrophil cells[7,63], we observed here that the Thr203 and Tyr205 residues in the activation loop of Erk1/2 were not dephosphorylated and the Erk kinases likely remained active even after 30 minutes of BMDC incubation with both the active CyaA toxin and its CyaA-AC$^-$ toxoid (*c.f.* Supplementary Fig. S4). Nevertheless, we found by phosphoproteomics that in CyaA-treated cells the threonine 1465 residue of tuberin was dephosphorylated. However, we were unable to detect tuberin by immunoblotting with antibodies from various suppliers, which may suggest that only very low levels of tuberin are produced in BMDCs. Alternatively, these cells may express an isoform of tuberin that is not detected by the commercially available antibodies. Nevertheless, the dephosphorylation of threonine 1465 of tuberin, as detected by SILAC phosphoproteomics, would yield activated tuberin[46] capable of inhibiting mTOR and its pro-survival signaling. In line with this, WT CyaA action caused inhibition of Akt, as observed by dephosphorylation of serine 475 and threonine 308 residues[64] (see Supplementary Fig. S8 and the work of Ahmad *et al.*[7]). Deactivation of Akt kinase also yielded dephosphorylation of the threonine 247 residue of PRAS40, promoting mTOR inhibition[47]

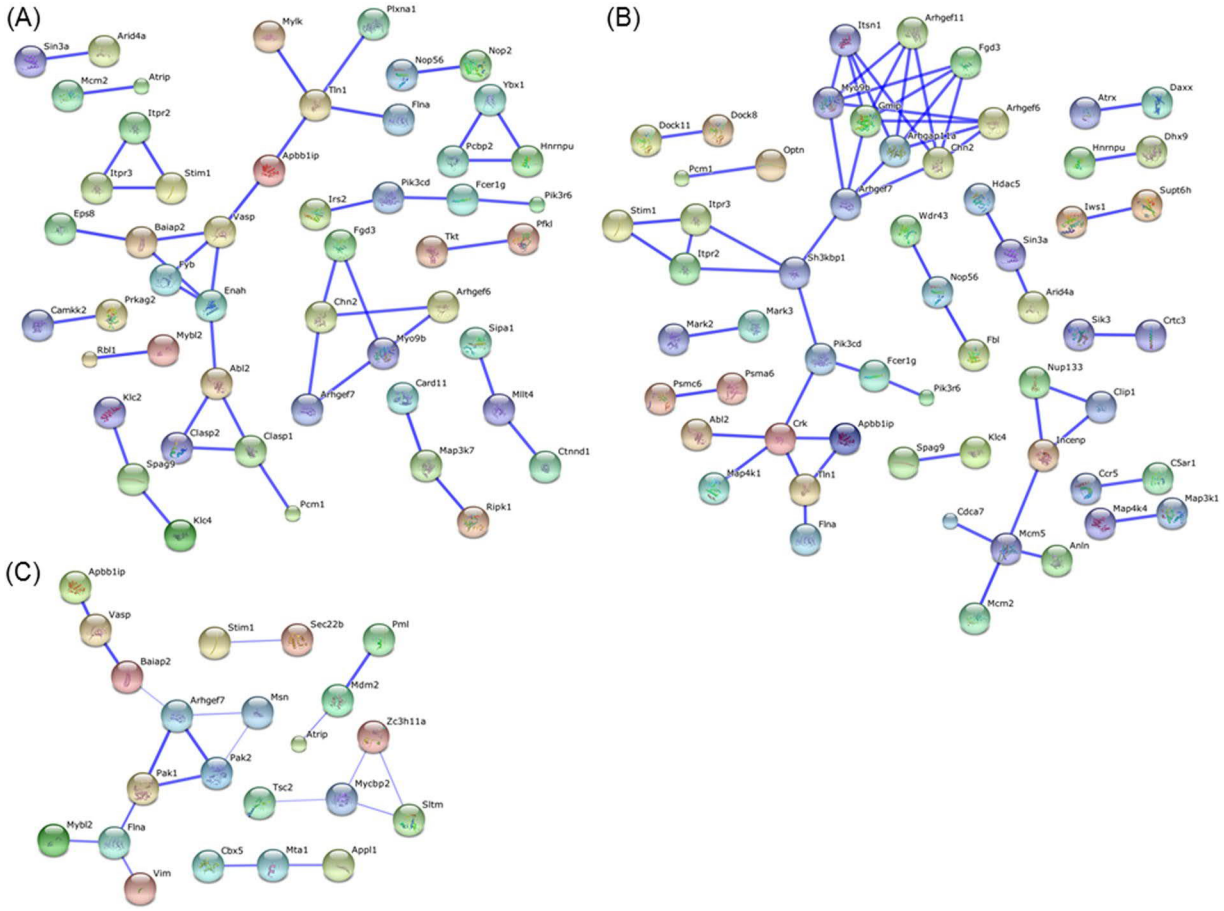

Figure 5. Functional association between significantly regulated phosphoproteins. Visualization of functional association of significantly regulated phosphoproteins was performed using STRING database v10 at the highest confidence level of 0.900 for (**A**) the sample treated with 100 ng/ml of WT CyaA for 10 min and (**B**) for 30 min. (**C**) Association at medium confidence 0.400 for significantly regulated phosphoproteins in the sample treated with 100 ng/ml CyaA-AC$^-$ toxoid. C). The software-assigned coloring of nodes has no particular meaning and many of the indicated proteins are involved in several signaling pathways in parallel. Confidence view with stronger associations is represented by thicker lines.

(Figs 3 and 7). As a result, the downstream effectors of mTOR involved in the synthesis of cellular proteins, such as 4E-BP1 (serine 64)[65] (c.f. Fig. 3 and Supplementary Fig. S7F-H) and p70S6K (serine 427)[66], were found to be dephosphorylated in CyaA-treated cells (Supplementary Table S1), where hypophosphorylated 4E-BP1 strongly binds to eukaryotic translation initiation factor and prevents translation[67]. The proposed model of mTOR signaling regulation by CyaA in BMDCs is then shown in Fig. 7. mTOR acts as an important regulator of the antibacterial inflammatory response in monocytes, macrophages and primary dendritic cells[68,69]. Inhibition of mTOR also leads to the activation and nuclear translocation of NF-κB and CyaA-provoked inhibition of mTOR would go well with our previous observation that NF-κB is activated upon CyaA-produced elevation of cAMP in macrophages[6,68]. The CyaA-provoked inhibition of mTOR is likely to have rather pleiotropic effects and these would vary in different DC subtypes[70,71]. For example, inhibition of mTOR was reported to result in the inhibition of IL-4-dependent maturation of BMDCs and in lowering of their T cell stimulatory capacity[72,73]. This would go well with our observations that CyaA treatment skews TLR-induced maturation of dendritic cells, inhibits their capacity to present antigens to both $CD4^+$ and $CD8^+$ T cells and enables the toxin-treated DCs to expand regulatory T cells *in vitro*[74].

CyaA action elicited phosphorylation of the hub-like Crk adaptor protein on the conserved serine 125 residue that is located between the SH2 and SH3 domains (c.f. Supplementary Table S1). This is likely to be of relevance during *Bordetella* infections, as hijacking of Crk appears to be implicated in bacterial pathogenesis through diverse mechanisms, including subversion of cellular ruffle formation (reviewed in Martinez-Quiles *et al.*[75]). The Crk-associated proteins retained in the interaction network (c.f. Fig. 5B) then comprised Talin-1, Filamin-A and the APBB1-interacting protein 1/RIAM, which are involved in cellular actin remodeling and phagocytosis. It is of note that CyaA action was previously reported to manipulate RhoA signaling and induce unproductive membrane ruffling[9]. Phosphorylation of the vasodilator-stimulated phosphoprotein (VASP) by the cAMP-activated PKA was then shown to play an important role in membrane ruffle formation, causing a significant reduction of the retraction of membrane ruffles[76]. In line with that, increased phosphorylation of the known PKA/PKG target

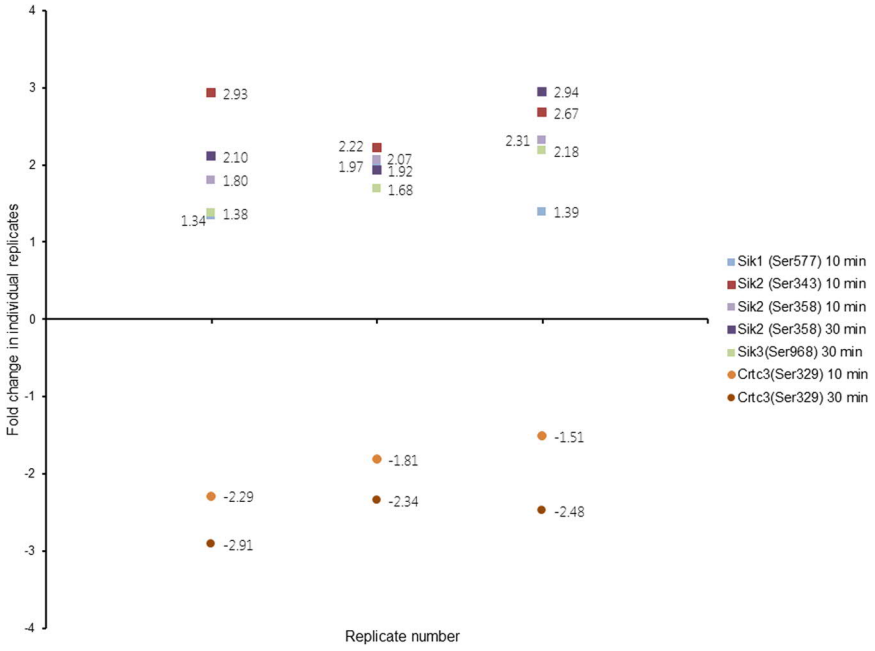

Figure 6. Changes in phosphorylation status of SIK family kinases and CRTC3/TORC3. Changes in the phosphorylation status of selected phosphosites are depicted here as fold change, representing the ratios of signals from toxin- or toxoid-treated samples to the corresponding buffer-treated control samples. Each data point represents one ratio value for one of the three replicates. The values > 0 represent phosphorylation, values < 0 represent dephosphorylation.

VASP on serine residue 235 was observed in WT CyaA-treated BMDCs samples (c.f. Fig. 3C and Supplementary Table S1). This VASP site lies within the EVH2 domain that has been reported to account for VASP oligomerization and F-actin binding[77]. Phosphorylation of VASP then prevents actin polymerization by inhibiting the formation of profilin-actin complexes in myogenic cells[50]. This modification may thus complement the impact exerted on cytoskeleton rearrangements by CyaA-provoked RhoA inhibition. However, what causes this particular RhoA inhibition remains unknown.

Indeed, three possible mechanisms of small GTPase inhibition due to cAMP signaling can plausibly be invoked. The activities of small GTPases like RhoA, Cdc42 or Rac1 involve cycling between GDP-bound (inactive) and GTP-bound (active) states and are regulated by the interplay of activating GEFs (activating guanine nucleotide exchange factor) and inhibitory GAPs (GTPase-activating proteins)[78]. Besides, RhoA, as other small GTPases, can also be kept in an inactive state by guanine nucleotide dissociation inhibitors (GDIs)[79]. We observed that the action of CyaA provoked alterations of the phosphorylation state of several members of the GEF protein family, some of which were previously shown to directly promote RhoA activity[80]. For example, the protein known as Solo (or ARHGEF40) was shown to specifically induce RhoA activity in vascular endothelial cells[81]. Here, the treatment of BMDCs with CyaA resulted in dephosphorylation of the serine residue located in the region closest to the GEF domain of Solo. Another RhoA activator that is regulated by CyaA action is PDZRhoGEF (PRG; also known as ARHGEF11). This protein was found to be phosphorylated on the serine residue (c.f. Supplementary Table S1) that is localized in the center of the proposed key autoinhibitory element[82], which may affect the conformation of the surrounding regions and may eventually lead to changes in PRG and affect its affinity for RhoA.

Among the GAPs known to be involved in RhoA regulation, three were found to be phosphorylated upon CyaA action on BMDCs (c.f. Supplementary Table S1), including the unconventional myosin-IXb (*Myo9b*), whose depletion was shown to impair the migratory capacity of dendritic cells and alter their interaction with T cells[83]. The other GAPs found to be regulated upon CyaA action was the ARHGAP18 protein, which is required for cellular polarization involved in cell migration[84] and the ARHGAP11A protein, a key regulator of RhoA during cell division (also called MP-GAP or M Phase GAP)[85].

The prolonged course of the whooping cough disease, often lasting for up to 12 weeks or longer, raises the hypothesis that *B. pertussis* infection may exert long-lasting effects on the cells of host mucosa and these would persist long after the bacteria have been cleared from the airway[86,87]. Although this effect is presumably due to the changes in epithelial cells, we hypothesize, that also airway intraepithelial DC might be affected similarly. Therefore, we examined the phosphorylation state of epigenetic effectors and chromatin remodeling proteins[88] in CyaA-treated DC. Indeed, the class II histone deacetylase, HDAC5, was found to be dephosphorylated on serine 270 (serine 279 in human orthologue) in the nuclear localization signal. This would go well with the report of Taniguchi *et al.*[89] that cAMP-stimulated nuclear import of HDAC5 requires dephosphorylation of Ser 270 by protein phosphatase 2 A (PP2A). Furthermore, CyaA action on DC provoked alterations of phosphorylation state of additional proteins that are involved in chromatin remodeling and epigenetic regulation. Among them, the

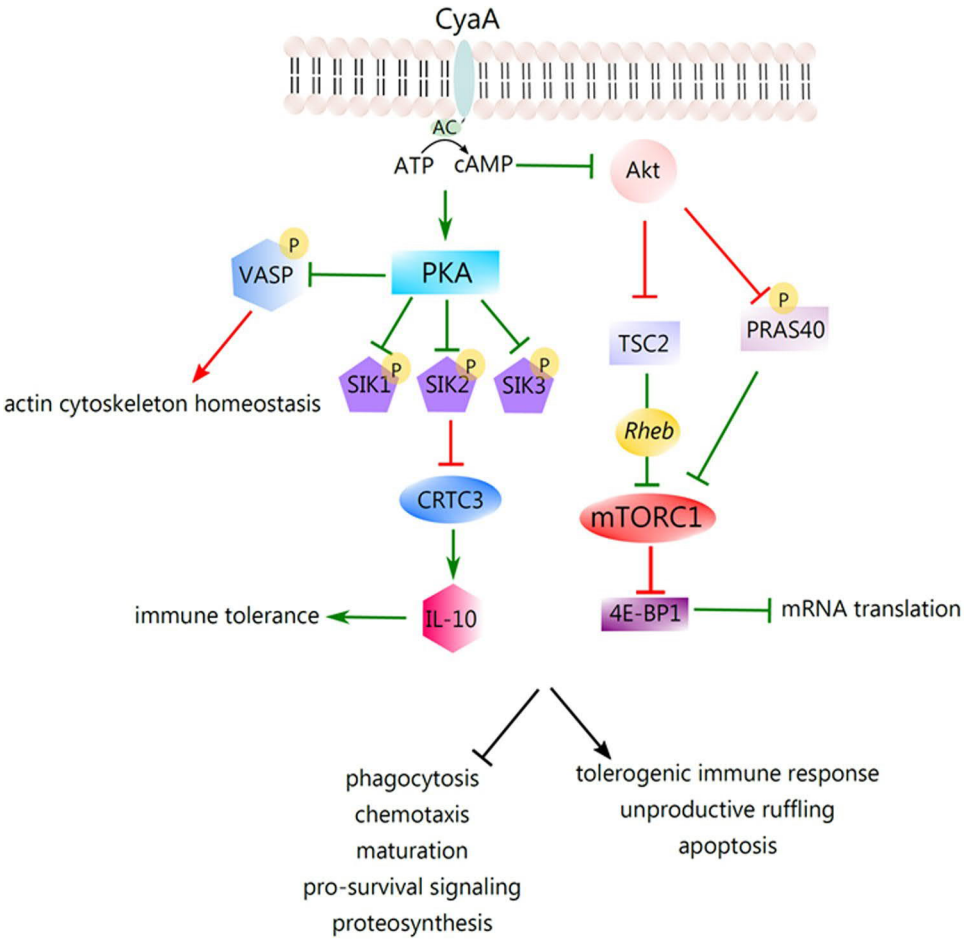

Figure 7. Schematic depiction of CyaA-induced signaling that would lead to induction of IL-10 production, inhibition of protein translation and deregulation of actin cytoskeleton homeostasis. Elevation of intracellular cAMP concentration due to the catalytic action of internalized AC domain of CyaA provokes activation of the protein kinase A, which performs an inhibitory phosphorylation of the SIK family proteins. This would promote nuclear localization of the transcriptional co-activator CRTC3. In parallel, PKA phosphorylates CREB and the phospho-CREB-CRTC3 complex would activate expression of the IL-10 gene. cAMP-dependent phosphorylation of VASP, presumably by PKA, affects actin cytoskeleton homeostasis. CyaA action further yields inhibition of Akt signaling, thus provoking inhibition of mTOR signaling. Pointed arrowheads indicate an activating effect and flat arrowheads indicate an inhibitory effect under normal physiological conditions. The red color of the arrowhead indicates an inhibitory effect, or interference, resulting from cAMP signaling elicited by the CyaA toxin and the green color indicates an enhancing effect of CyaA/cAMP signaling action. For the broader context of these signaling processes the reader is referred to dedicated reviews on immunity to *B. pertussis* infections and on CyaA toxin action[3,97].

Cbx5 gene-encoded HP1α protein, involved in propagation and maintenance of pericentric heterochromatin[90], was found to be phosphorylated on serine 93. Another Chromo domain-containing protein that was significantly phosphorylated (on serine 305) upon CyaA treatment of BMDC was the transcriptional repressor CBX8, also known as PC3[91]. In addition, significant phosphorylation of the replication-dependent histone H1.4 (*Hist1h1e*) on threonine 35 and serine 36 was observed. This goes well with the observation that H1.4 can be phosphorylated by PKA during mitosis and when it dissociates from mitotic chromatin[92]. CyaA-triggered changes in chromatin state and histone modifications could then also result in alteration of pre-mRNA splicing[93] and numerous other effects on gene expression and cell cycle progression.

An important effect of CyaA toxin action, with relevance for host defense capacities, was observed for the phosphorylation state of the regulatory serine residues of the salt-inducible kinases (SIK). These are known for their involvement in modulation of immune responses[57–60]. Indeed, inhibition of SIKs by cAMP-activated and PKA-mediated phosphorylation was shown to suppress secretion of the pro-inflammatory cytokines IL-6, IL-12, and TNF-α by macrophages and appears to promote formation of regulatory (M2b) macrophages[59]. One of the SIK targets is the CREB-regulated transcription co-activator 3 (CRTC3) that can be phosphorylated at several serine residues. SIK-mediated phosphorylation was then shown to promote sequestering of CRTC3 into cytosolic complexes with the 14-3-3 protein, inhibiting CRTC3-assisted transcription of CREB-dependent genes, such as the anti-inflammatory cytokine IL-10[59]. In turn, phosphorylation of CRTC3 is inhibited by the cAMP-activated

PKA and this enables translocation of the non-phosphorylated CRTC3 into the nucleus, where interaction of CRTC3 with CREB, activated by CyaA-produced cAMP[94], may upregulate IL-10 gene transcription. In line with that we observed significant dephosphorylation of the serine 329 residue of CRTC3 and increased phosphorylation of the upstream regulatory kinases SIK1 (SIK), SIK2 (QIK) and SIK3 (QSK) in CyaA-treated BMDCs (*c.f.* Fig. 6). There was also enhanced phosphorylation of SIK1 on serine 577, which would promote the export of SIK1 from cell nucleus into the cytoplasm[95], rescuing CRTC3-dependent transcription. Similarly, in CyaA-treated cells an increased phosphorylation of serine 343 at the critical regulatory site of SIK2/QIK was observed, where this modification was shown to inhibit the ability of SIK2/QIK to phosphorylate CRTC3[60]. Moreover, we also observed the enhanced phosphorylation of serine 358 of SIK2. This modification is known to promote cytoplasmic localization of SIK2 into complexes that contain the 14-3-3 proteins[96]. Last but not least, SIK3 phosphorylation was also observed. All of these results are thus in line with previous reports that TLR-activated DCs exposed to CyaA secrete increased amounts of the IL-10 cytokine and promote IL-10 secretion by regulatory T cells[74]. The sum of the data then allows proposing a model of immunosubversive signaling activated by CyaA in myeloid cells, as depicted in Fig. 7. It predicts that activation of PKA isoforms by the CyaA-produced cAMP yields inhibitory phosphorylation of the SIK family kinases and CRTC3-activated transcription of the CREB-dependent IL-10 gene. Altogether these results document the pleiotropic immunosubversive effects of the massive cAMP signaling that is elicited in primary myeloid cells by the AC enzyme action of the CyaA toxin.

References

1. Rocha, G., Soares, P., Soares, H., Pissarra, S. & Guimarães, H. Pertussis in the newborn: certainties and uncertainties in 2014. *Paediatr Respir Rev* **16**, 112–118, https://doi.org/10.1016/j.prrv.2014.01.004 (2015).
2. Snyder, J. & Fisher, D. Pertussis in childhood. *Pediatr Rev* **33**, 412-420; quiz 420-411, https://doi.org/10.1542/pir.33-9-412 (2012).
3. Higgs, R., Higgins, S. C., Ross, P. J. & Mills, K. H. Immunity to the respiratory pathogen Bordetella pertussis. *Mucosal Immunol* **5**, 485–500, https://doi.org/10.1038/mi.2012.54 (2012).
4. Linhartová, I. *et al.* RTX proteins: a highly diverse family secreted by a common mechanism. *FEMS Microbiol Rev* **34**, 1076–1112, https://doi.org/10.1111/j.1574-6976.2010.00231.x (2010).
5. Ladant, D. & Ullmann, A. *Bordetella pertussis* adenylate cyclase: a toxin with multiple talents. *Trends Microbiol* **7**, 172–176 (1999).
6. Cerny, O. *et al. Bordetella pertussis* Adenylate Cyclase Toxin Blocks Induction of Bactericidal Nitric Oxide in Macrophages through cAMP-Dependent Activation of the SHP-1 Phosphatase. *J Immunol* **194**, 4901–4913, https://doi.org/10.4049/jimmunol.1402941 (2015).
7. Ahmad, J. N. *et al.* cAMP signalling of *Bordetella* adenylate cyclase toxin through the SHP-1 phosphatase activates the BimEL-Bax pro-apoptotic cascade in phagocytes. *Cell Microbiol*, https://doi.org/10.1111/cmi.12519 (2015).
8. Eby, J. C., Gray, M. C. & Hewlett, E. L. Cyclic AMP-mediated suppression of neutrophil extracellular trap formation and apoptosis by the *Bordetella pertussis* adenylate cyclase toxin. *Infect Immun* **82**, 5256–5269, https://doi.org/10.1128/IAI.02487-14 (2014).
9. Kamanova, J. *et al.* Adenylate cyclase toxin subverts phagocyte function by RhoA inhibition and unproductive ruffling. *J Immunol* **181**, 5587–5597, https://doi.org/10.4049/jimmunol.181.8.5587 (2008).
10. Mann, M. Functional and quantitative proteomics using SILAC. *Nat Rev Mol Cell Biol* **7**, 952–958, https://doi.org/10.1038/nrm2067 (2006).
11. Karimova, G. *et al.* Charge-dependent translocation of *Bordetella pertussis* adenylate cyclase toxin into eukaryotic cells: implication for the *in vivo* delivery of CD8(+) T cell epitopes into antigen-presenting cells. *Proc Natl Acad Sci USA* **95**, 12532–12537 (1998).
12. Fabrik, I. *et al.* Application of SILAC labeling to primary bone marrow-derived dendritic cells reveals extensive GM-CSF-dependent arginine metabolism. *J Proteome Res* **13**, 752–762, https://doi.org/10.1021/pr4007798 (2014).
13. Rogers, L. D., Fang, Y. & Foster, L. J. An integrated global strategy for cell lysis, fractionation, enrichment and mass spectrometric analysis of phosphorylated peptides. *Mol Biosyst* **6**, 822–829, https://doi.org/10.1039/b915986j (2010).
14. McNulty, D. E. & Annan, R. S. Hydrophilic interaction chromatography reduces the complexity of the phosphoproteome and improves global phosphopeptide isolation and detection. *Mol Cell Proteomics* **7**, 971–980, https://doi.org/10.1074/mcp.M700543-MCP200 (2008).
15. Cox, J. & Mann, M. MaxQuant enables high peptide identification rates, individualized p.p.b.-range mass accuracies and proteome-wide protein quantification. *Nat Biotechnol* **26**, 1367–1372, https://doi.org/10.1038/nbt.1511 (2008).
16. Cox, J. *et al.* Andromeda: a peptide search engine integrated into the MaxQuant environment. *J Proteome Res* **10**, 1794–1805, https://doi.org/10.1021/pr101065j (2011).
17. Vizcaíno, J. A. *et al.* The PRoteomics IDEntifications (PRIDE) database and associated tools: status in 2013. *Nucleic Acids Res* **41**, D1063–1069, https://doi.org/10.1093/nar/gks1262 (2013).
18. Klammer, M., Dybowski, J. N., Hoffmann, D. & Schaab, C. Identification of significant features by the Global Mean Rank test. *PLoS One* **9**, e104504, https://doi.org/10.1371/journal.pone.0104504 (2014).
19. Chou, M. F. & Schwartz, D. Biological sequence motif discovery using motif-x. *Curr Protoc Bioinformatics* Chapter 13, Unit13.15–24, https://doi.org/10.1002/0471250953.bi1315s35 (2011).
20. Gnad, F. *et al.* PHOSIDA (phosphorylation site database): management, structural and evolutionary investigation, and prediction of phosphosites. *Genome Biol* **8**, R250, https://doi.org/10.1186/gb-2007-8-11-r250 (2007).
21. Gnad, F., Gunawardena, J. & Mann, M. PHOSIDA 2011: the posttranslational modification database. *Nucleic Acids Res* **39**, D253–260, https://doi.org/10.1093/nar/gkq1159 (2011).
22. Tyanova, S. *et al.* The Perseus computational platform for comprehensive analysis of (prote)omics data. *Nat Methods*, https://doi.org/10.1038/nmeth.3901 (2016).
23. Keshava Prasad, T. S. *et al.* Human Protein Reference Database–2009 update. *Nucleic Acids Res* **37**, D767–772, https://doi.org/10.1093/nar/gkn892 (2009).
24. Szklarczyk, D. *et al.* STRINGv10: protein-protein interaction networks, integrated over the tree of life. *Nucleic Acids Res* **43**, D447–452, https://doi.org/10.1093/nar/gku1003 (2015).
25. Ashburner, M. *et al.* Gene ontology: tool for the unification of biology. The Gene Ontology Consortium. *Nat Genet* **25**, 25–29, https://doi.org/10.1038/75556 (2000).
26. Shannon, P. *et al.* Cytoscape: a software environment for integrated models of biomolecular interaction networks. *Genome Res* **13**, 2498–2504, https://doi.org/10.1101/gr.1239303 (2003).
27. Bindea, G. *et al.* ClueGO: a Cytoscape plug-in to decipher functionally grouped gene ontology and pathway annotation networks. *Bioinformatics* **25**, 1091–1093, https://doi.org/10.1093/bioinformatics/btp101 (2009).
28. Ladant, D., Glaser, P. & Ullmann, A. Insertional mutagenesis of *Bordetella pertussis* adenylate cyclase. *J Biol Chem* **267**, 2244–2250 (1992).
29. Fiser, R. *et al.* Calcium influx rescues adenylate cyclase-hemolysin from rapid cell membrane removal and enables phagocyte permeabilization by toxin pores. *PLoS Pathog* **8**, e1002580, https://doi.org/10.1371/journal.ppat.1002580 (2012).

30. Gonyar, L. A., Gray, M. C., Christianson, G. J., Mehrad, B. & Hewlett, E. L. Albumin, in the Presence of Calcium, Elicits a Massive Increase in Extracellular *Bordetella* Adenylate Cyclase Toxin. *Infect Immun* **85**, https://doi.org/10.1128/IAI.00198-17 (2017).
31. Eby, J. C. *et al*. Quantification of the adenylate cyclase toxin of *Bordetella* pertussis *in vitro* and during respiratory infection. *Infect Immun* **81**, 1390–1398, https://doi.org/10.1128/IAI.00110-13 (2013).
32. Olsen, J. V. *et al*. Global, *in vivo*, and site-specific phosphorylation dynamics in signaling networks. *Cell* **127**, 635**–**648, https://doi.org/10.1016/j.cell.2006.09.026 (2006).
33. Hunter, T. & Sefton, B. M. Transforming gene product of Rous sarcoma virus phosphorylates tyrosine. *Proc Natl Acad Sci USA* **77**, 1311**–**1315 (1980).
34. Serezani, C. H., Ballinger, M. N., Aronoff, D. M. & Peters-Golden, M. Cyclic AMP: master regulator of innate immune cell function. *Am J Respir Cell Mol Biol* **39**, 127**–**132, https://doi.org/10.1165/rcmb.2008-0091TR (2008).
35. Aronoff, D. M., Canetti, C., Serezani, C. H., Luo, M. & Peters-Golden, M. Cutting edge: macrophage inhibition by cyclic AMP (cAMP): differential roles of protein kinase A and exchange protein directly activated by cAMP-1. *J Immunol* **174**, 595**–**599, https://doi.org/10.4049/jimmunol.174.2.595 (2005).
36. Schwartz, D. & Gygi, S. P. An iterative statistical approach to the identification of protein phosphorylation motifs from large-scale data sets. *Nat Biotechnol* **23**, 1391–1398, https://doi.org/10.1038/nbt1146 (2005).
37. Wolff, J., Cook, G. H., Goldhammer, A. R. & Berkowitz, S. A. Calmodulin activates prokaryotic adenylate cyclase. *Proc Natl Acad Sci USA* **77**, 3841–3844 (1980).
38. Fiser, R. *et al*. Third activity of *Bordetella* adenylate cyclase (AC) toxin-hemolysin. Membrane translocation of AC domain polypeptide promotes calcium influx into CD11b + monocytes independently of the catalytic and hemolytic activities. *J Biol Chem* **282**, 2808**–**2820, https://doi.org/10.1074/jbc.M609979200 (2007).
39. Pereira, L. *et al*. The cAMP binding protein Epac modulates Ca2 + sparks by a Ca2 + /calmodulin kinase signalling pathway in rat cardiac myocytes. *J Physiol* **583**, 685**–**694, https://doi.org/10.1113/jphysiol.2007.133066 (2007).
40. Marumoto, T., Zhang, D. & Saya, H. Aurora-A - a guardian of poles. *Nat Rev Cancer* **5**, 42–50, https://doi.org/10.1038/nrc1526 (2005).
41. Jantscher, F., Pirker, C., Mayer, C. E., Berger, W. & Sutterluety, H. Overexpression of Aurora-A in primary cells interferes with S-phase entry by diminishing Cyclin D1 dependent activities. *Mol Cancer* **10**, 28, https://doi.org/10.1186/1476-4598-10-28 (2011).
42. Gray, M. C. & Hewlett, E. L. Cell cycle arrest induced by the bacterial adenylate cyclase toxins from *Bacillus anthracis* and *Bordetella pertussis*. *Cell Microbiol* **13**, 123–134, https://doi.org/10.1111/j.1462-5822.2010.01525.x (2011).
43. Masin, J. *et al*. Negatively charged residues of the segment linking the enzyme and cytolysin moieties restrict the membrane-permeabilizing capacity of adenylate cyclase toxin. *Sci Rep* **6**, 29137, https://doi.org/10.1038/srep29137 (2016).
44. Karst, J. C. *et al*. Identification of a region that assists membrane insertion and translocation of the catalytic domain of *Bordetella pertussis* CyaA toxin. *J Biol Chem* **287**, 9200–9212, https://doi.org/10.1074/jbc.M111.316166 (2012).
45. Inoki, K., Li, Y., Zhu, T., Wu, J. & Guan, K. L. TSC2 is phosphorylated and inhibited by Akt and suppresses mTOR signalling. *Nat Cell Biol* **4**, 648–657, https://doi.org/10.1038/ncb839 (2002).
46. Manning, B. D., Tee, A. R., Logsdon, M. N., Blenis, J. & Cantley, L. C. Identification of the tuberous sclerosis complex-2 tumor suppressor gene product tuberin as a target of the phosphoinositide 3-kinase/akt pathway. *Mol Cell* **10**, 151–162 (2002).
47. Sancak, Y. *et al*. PRAS40 is an insulin-regulated inhibitor of the mTORC1 protein kinase. *Mol Cell* **25**, 903**–**915, https://doi.org/10.1016/j.molcel.2007.03.003 (2007).
48. Kovacina, K. S. *et al*. Identification of a proline-rich Akt substrate as a 14-3-3 binding partner. *J Biol Chem* **278**, 10189**–**10194, https://doi.org/10.1074/jbc.M210837200 (2003).
49. Courtemanche, N., Gifford, S. M., Simpson, M. A., Pollard, T. D. & Koleske, A. J. Abl2/Abl-related gene stabilizes actin filaments, stimulates actin branching by actin-related protein 2/3 complex, and promotes actin filament severing by cofilin. *J Biol Chem* **290**, 4038**–**4046, https://doi.org/10.1074/jbc.M114.608117 (2015).
50. Harbeck, B., Hüttelmaier, S., Schluter, K., Jockusch, B. M. & Illenberger, S. Phosphorylation of the vasodilator-stimulated phosphoprotein regulates its interaction with actin. *J Biol Chem* **275**, 30817–30825, https://doi.org/10.1074/jbc.M005066200 (2000).
51. Haining, A. W., Lieberthal, T. J. & Del Río Hernández, A. Talin: a mechanosensitive molecule in health and disease. *FASEB J* **30**, 2073–2085, https://doi.org/10.1096/fj.201500080R (2016).
52. Vasioukhin, V., Bauer, C., Yin, M. & Fuchs, E. Directed actin polymerization is the driving force for epithelial cell-cell adhesion. *Cell* **100**, 209–219 (2000).
53. Aresta, S., de Tand-Heim, M. F., Béranger, F. & de Gunzburg, J. A novel Rho GTPase-activating-protein interacts with Gem, a member of the Ras superfamily of GTPases. *Biochem J* **367**, 57–65, https://doi.org/10.1042/BJ20020829 (2002).
54. Kagawa, Y. *et al*. Cell cycle-dependent Rho GTPase activity dynamically regulates cancer cell motility and invasion *in vivo*. *PLoS One* **8**, e83629, https://doi.org/10.1371/journal.pone.0083629 (2013).
55. Consortium, G. O. Gene Ontology Consortium: going forward. *Nucleic Acids Res* **43**, D1049**–**1056, https://doi.org/10.1093/nar/gku1179 (2015).
56. Huntley, R. P. *et al*. The GOA database: gene Ontology annotation updates for 2015. *Nucleic Acids Res* **43**, D1057**–**1063, https://doi.org/10.1093/nar/gku1113 (2015).
57. Yong Kim, S. *et al*. Salt-inducible kinases 1 and 3 negatively regulate Toll-like receptor 4-mediated signal. *Mol Endocrinol* **27**, 1958–1968, https://doi.org/10.1210/me.2013-1240 (2013).
58. Sundberg, T. B. *et al*. Small-molecule screening identifies inhibition of salt-inducible kinases as a therapeutic strategy to enhance immunoregulatory functions of dendritic cells. *Proc Natl Acad Sci USA* **111**, 12468–12473, https://doi.org/10.1073/pnas.1412308111 (2014).
59. Clark, K. *et al*. Phosphorylation of CRTC3 by the salt-inducible kinases controls the interconversion of classically activated and regulatory macrophages. *Proc Natl Acad Sci USA* **109**, 16986–16991, https://doi.org/10.1073/pnas.1215450109 (2012).
60. MacKenzie, K. F. *et al*. PGE(2) induces macrophage IL-10 production and a regulatory-like phenotype via a protein kinase A-SIK-CRTC3 pathway. *J Immunol* **190**, 565–577, https://doi.org/10.4049/jimmunol.1202462 (2013).
61. Shen, Y. *et al*. Physiological calcium concentrations regulate calmodulin binding and catalysis of adenylyl cyclase exotoxins. *EMBO J* **21**, 6721–6732 (2002).
62. Ma, L., Chen, Z., Erdjument-Bromage, H., Tempst, P. & Pandolfi, P. P. Phosphorylation and functional inactivation of TSC2 by Erk implications for tuberous sclerosis and cancer pathogenesis. *Cell* **121**, 179–193, https://doi.org/10.1016/j.cell.2005.02.031 (2005).
63. Cerny, O., Anderson, K. E., Stephens, L. R., Hawkins, P. T. & Sebo, P. cAMP Signaling of Adenylate Cyclase Toxin Blocks the Oxidative Burst of Neutrophils through Epac-Mediated Inhibition of Phospholipase C Activity. *J Immunol* **198**, 1285–1296, https://doi.org/10.4049/jimmunol.1601309 (2017).
64. Alessi, D. R. *et al*. Mechanism of activation of protein kinase B by insulin and IGF-1. *EMBO J* **15**, 6541–6551 (1996).
65. Tee, A. R. *et al*. Tuberous sclerosis complex-1 and -2 gene products function together to inhibit mammalian target of rapamycin (mTOR)-mediated downstream signaling. *Proc Natl Acad Sci USA* **99**, 13571–13576, https://doi.org/10.1073/pnas.202476899 (2002).
66. Han, J. W., Pearson, R. B., Dennis, P. B. & Thomas, G. Rapamycin, wortmannin, and the methylxanthine SQ20006 inactivate p70s6k by inducing dephosphorylation of the same subset of sites. *J Biol Chem* **270**, 21396**–**21403 (1995).
67. Gingras, A. C. *et al*. Regulation of 4E-BP1 phosphorylation: a novel two-step mechanism. *Genes Dev* **13**, 1422**–**1437 (1999).

68. Weichhart, T. *et al*. The TSC-mTOR signaling pathway regulates the innate inflammatory response. *Immunity* **29**, 565–577, https://doi.org/10.1016/j.immuni.2008.08.012 (2008).
69. Schmitz, F. *et al*. Mammalian target of rapamycin (mTOR) orchestrates the defense program of innate immune cells. *Eur J Immunol* **38**, 2981–2992, https://doi.org/10.1002/eji.200838761 (2008).
70. Thomson, A. W., Turnquist, H. R. & Raimondi, G. Immunoregulatory functions of mTOR inhibition. *Nat Rev Immunol* **9**, 324–337, https://doi.org/10.1038/nri2546 (2009).
71. Haidinger, M. *et al*. A versatile role of mammalian target of rapamycin in human dendritic cell function and differentiation. *J Immunol* **185**, 3919–3931, https://doi.org/10.4049/jimmunol.1000296 (2010).
72. Hackstein, H. *et al*. Rapamycin inhibits IL-4–induced dendritic cell maturation *in vitro* and dendritic cell mobilization and function *in vivo*. *Blood* **101**, 4457–4463, https://doi.org/10.1182/blood-2002-11-3370 (2003).
73. Taner, T., Hackstein, H., Wang, Z., Morelli, A. E. & Thomson, A. W. Rapamycin-treated, alloantigen-pulsed host dendritic cells induce ag-specific T cell regulation and prolong graft survival. *Am J Transplant* **5**, 228–236, https://doi.org/10.1046/j.1600-6143.2004.00673.x (2005).
74. Adkins, I. *et al*. *Bordetella* adenylate cyclase toxin differentially modulates toll-like receptor-stimulated activation, migration and T cell stimulatory capacity of dendritic cells. *PLoS One* **9**, e104064, https://doi.org/10.1371/journal.pone.0104064 (2014).
75. Martinez-Quiles, N., Feuerbacher, L. A., Benito-León, M. & Hardwidge, P. R. Contribution of Crk adaptor proteins to host cell and bacteria interactions. *Biomed Res Int* **2014**, 372901, https://doi.org/10.1155/2014/372901 (2014).
76. Lee, S. & Chung, C. Y. Role of VASP phosphorylation for the regulation of microglia chemotaxis via the regulation of focal adhesion formation/maturation. *Mol Cell Neurosci* **42**, 382–390, https://doi.org/10.1016/j.mcn.2009.08.010 (2009).
77. Bachmann, C., Fischer, L., Walter, U. & Reinhard, M. The EVH2 domain of the vasodilator-stimulated phosphoprotein mediates tetramerization, F-actin binding, and actin bundle formation. *J Biol Chem* **274**, 23549–23557 (1999).
78. Bos, J. L., Rehmann, H. & Wittinghofer, A. GEFs and GAPs: critical elements in the control of small G proteins. *Cell* **129**, 865–877, https://doi.org/10.1016/j.cell.2007.05.018 (2007).
79. Cherfils, J. & Zeghouf, M. Regulation of small GTPases by GEFs, GAPs, and GDIs. *Physiol Rev* **93**, 269–309, https://doi.org/10.1152/physrev.00003.2012 (2013).
80. Patel, M. & Karginov, A. V. Phosphorylation-mediated regulation of GEFs for RhoA. *Cell Adh Migr* **8**, 11–18, https://doi.org/10.4161/cam.28058 (2014).
81. Abiko, H. *et al*. Rho guanine nucleotide exchange factors involved in cyclic-stretch-induced reorientation of vascular endothelial cells. *J Cell Sci* **128**, 1683–1695, https://doi.org/10.1242/jcs.157503 (2015).
82. Bielnicki, J. A. *et al*. Insights into the molecular activation mechanism of the RhoA-specific guanine nucleotide exchange factor, PDZRhoGEF. *J Biol Chem* **286**, 35163–35175, https://doi.org/10.1074/jbc.M111.270918 (2011).
83. Xu, Y. *et al*. Dendritic cell motility and T cell activation requires regulation of Rho-cofilin signaling by the Rho-GTPase activating protein myosin IXb. *J Immunol* **192**, 3559–3568, https://doi.org/10.4049/jimmunol.1300695 (2014).
84. Maeda, M. *et al*. ARHGAP18, a GTPase-activating protein for RhoA, controls cell shape, spreading, and motility. *Mol Biol Cell* **22**, 3840–3852, https://doi.org/10.1091/mbc.E11-04-0364 (2011).
85. Zanin, E. *et al*. A conserved RhoGAP limits M phase contractility and coordinates with microtubule asters to confine RhoA during cytokinesis. *Dev Cell* **26**, 496–510, https://doi.org/10.1016/j.devcel.2013.08.005 (2013).
86. Melvin, J. A., Scheller, E. V., Miller, J. F. & Cotter, P. A. *Bordetella pertussis* pathogenesis: current and future challenges. *Nat Rev Microbiol* **12**, 274–288, https://doi.org/10.1038/nrmicro3235 (2014).
87. Mattoo, S. & Cherry, J. D. Molecular pathogenesis, epidemiology, and clinical manifestations of respiratory infections due to *Bordetella pertussis* and other *Bordetella* subspecies. *Clin Microbiol Rev* **18**, 326–382, https://doi.org/10.1128/CMR.18.2.326-382.2005 (2005).
88. Suárez-Álvarez, B., Baragaño Raneros, A., Ortega, F. & López-Larrea, C. Epigenetic modulation of the immune function: a potential target for tolerance. *Epigenetics* **8**, 694–702, https://doi.org/10.4161/epi.25201 (2013).
89. Taniguchi, M. *et al*. Histone deacetylase 5 limits cocaine reward through cAMP-induced nuclear import. *Neuron* **73**, 108–120, https://doi.org/10.1016/j.neuron.2011.10.032 (2012).
90. Maison, C. & Almouzni, G. HP1 and the dynamics of heterochromatin maintenance. *Nat Rev Mol Cell Biol* **5**, 296–304, https://doi.org/10.1038/nrm1355 (2004).
91. Bárdos, J. I., Saurin, A. J., Tissot, C., Duprez, E. & Freemont, P. S. HPC3 is a new human polycomb orthologue that interacts and associates with RING1 and Bmi1 and has transcriptional repression properties. *J Biol Chem* **275**, 28785–28792, https://doi.org/10.1074/jbc.M001835200 (2000).
92. Chu, C. S. *et al*. Protein kinase A-mediated serine 35 phosphorylation dissociates histone H1.4 from mitotic chromosome. *J Biol Chem* **286**, 35843–35851, https://doi.org/10.1074/jbc.M111.228064 (2011).
93. Luco, R. F., Allo, M., Schor, I. E., Kornblihtt, A. R. & Misteli, T. Epigenetics in alternative pre-mRNA splicing. *Cell* **144**, 16–26, https://doi.org/10.1016/j.cell.2010.11.056 (2011).
94. Perkins, D. J., Gray, M. C., Hewlett, E. L. & Vogel, S. N. *Bordetella pertussis* adenylate cyclase toxin (ACT) induces cyclooxygenase-2 (COX-2) in murine macrophages and is facilitated by ACT interaction with CD11b/CD18 (Mac-1). *Mol Microbiol* **66**, 1003–1015, https://doi.org/10.1111/j.1365-2958.2007.05972.x (2007).
95. Katoh, Y. *et al*. Salt-inducible kinase-1 represses cAMP response element-binding protein activity both in the nucleus and in the cytoplasm. *Eur J Biochem* **271**, 4307–4319, https://doi.org/10.1111/j.1432-1033.2004.04372.x (2004).
96. Henriksson, E. *et al*. The AMPK-related kinase SIK2 is regulated by cAMP via phosphorylation at Ser358 in adipocytes. *Biochem J* **444**, 503–514, https://doi.org/10.1042/BJ20111932 (2012).
97. Sebo, P., Osicka, R. & Masin, J. Adenylate cyclase toxin-hemolysin relevance for pertussis vaccines. *Expert Rev Vaccines* **13**, 1215–1227, https://doi.org/10.1586/14760584.2014.944900 (2014).

Acknowledgements

This work was supported by the grants NV16-28126A, GA13-145475 (P.S.), the GAUK grant No. 228216 (J.N.), the EATRIS-CZ project CZ.02.1.01/0.0/0.0/16_013/0001818 funded by the Operational Programme Research, Development and Education, and The long-term organization development plan 'Medical Aspects of Weapons of Mass Destruction' of the Faculty of Military Health Sciences, University of Defence of the Czech Ministry of Defence. J.N. is PhD student of the Charles University, Faculty of Science, Czech Republic. I.F. is a PhD student of the University of Defence in Brno. We thank Jasper E. Manning from Institute of Molecular Genetics of the CAS, v. v. i. for careful reading of the manuscript and editorial assistance.

Author Contributions

J.N. performed research, analyzed the data and wrote the paper; I.F. performed research, prepared, collected and processed the samples and wrote the paper; I.L. contributed to study design and performed research; M.L. measured the samples; O.Č. prepared samples and analyzed data; J.S. contributed to the study design and P.Š. contributed study design, data interpretation and wrote the paper.

Additional Information

Supplementary information accompanies this paper at https://doi.org/10.1038/s41598-017-14501-x.

Competing Interests: P.Š. is co-inventor on patents protecting use of CyaA as pertussis vaccine antigen and is a founder and shareholder of Revabiotech SE, which develops a next generation of whole cell pertussis vaccines.

Publisher's note: Springer Nature remains neutral with regard to jurisdictional claims in published maps and institutional affiliations.

APPENDIX II

Bordetella pertussis Acetylome is Shaped by Lysine Deacetylase Bkd1

Novak J, Fabrik I, Jurnecka D, Holubova J, Stanek O, Sebo P.

J Proteome Res. 2020 Sep 4;19(9):3680-3696. doi: 10.1021/acs.jproteome.0c00178. Epub 2020 Jul 31.

Journal of proteome research

pubs.acs.org/jpr

Article

Bordetella pertussis Acetylome is Shaped by Lysine Deacetylase Bkd1

Jakub Novak, Ivo Fabrik, David Jurnecka, Jana Holubova, Ondrej Stanek, and Peter Sebo*

Cite This: *J. Proteome Res.* 2020, 19, 3680–3696

Read Online

ACCESS | Metrics & More | Article Recommendations | Supporting Information

ABSTRACT: Post-translational modifications of proteins enable swift physiological adaptation of cells to altered growth conditions and stress. Aside from protein phosphorylation, acetylation on ε-amino groups of lysine residues (*N*-ε-lysine acetylation) represents another important post-translational modification of proteins. For many bacterial pathogens, including the whooping cough agent *Bordetella pertussis*, the role and extent of protein acetylation remain to be defined. We expressed in *Escherichia coli* the BP0960 and BP3063 genes encoding two putative deacetylases of *B. pertussis* and show that BP0960 encodes a lysine deacetylase enzyme, named Bkd1, that regulates acetylation of a range of *B. pertussis* proteins. Comparison of the proteome and acetylome of a Δ*bkd1* mutant with the proteome and acetylome of wild-type *B. pertussis* (PRIDE ID. PXD016384) revealed that acetylation on lysine residues may modulate activities or stabilities of proteins involved in bacterial metabolism and histone-like proteins. However, increased acetylation of the BvgA response regulator protein of the *B. pertussis* master virulence-regulating BvgAS two-component system affected neither the total levels of produced BvgA nor its phosphorylation status. Indeed, the Δ*bkd1* mutant was not impaired in the production of key virulence factors and its survival within human macrophages *in vitro* was not affected. The Δ*bkd1* mutant exhibited an increased growth rate under carbon source-limiting conditions and its virulence in the *in vivo* mouse lung infection model was somewhat affected. These results indicate that the lysine deacetylase Bkd1 and *N*-ε-lysine acetylation primarily modulate the general metabolism rather than the virulence of *B. pertussis*.

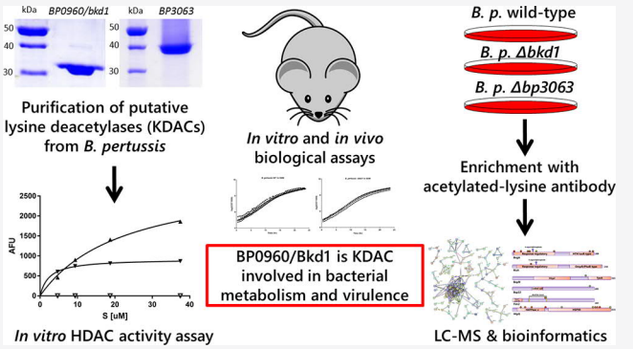

KEYWORDS: *Bordetella pertussis, acetylome, KDAC, deacetylation, Bkd1, post-translational modification*

INTRODUCTION

The human respiratory pathogen *Bordetella pertussis* is known for its ability to subvert host immunity.[1,2] To colonize the host and transmit, the bacterium has to deal with a diversity of environmental and metabolic conditions that require rapid and multilayered regulation of metabolic functions and virulence factor expression. Such cellular adaptation usually involves various types of post-translational modifications (PTMs),[3] which fine tune the stability and function of cellular proteins.[4] Recently, protein acetylation on ε-amino groups of lysine residues (*N*-ε-lysine acetylation, further referred as acetylation) has been gaining increasing attention as an important type of PTM involved in epigenetic regulation of gene expression and cell metabolism. Acetylation of lysine residues can result from a direct chemical reaction with the metabolites acetyl-phosphate and acetyl-CoA or from the catalytic action of a lysine acetyltransferase enzyme (KAT). The level of protein acetylation is then subject to crosstalk with other PTMs, such as protein phosphorylation, and can be regulated by the action of protein deacetylases (KDACs), described initially as histone deacetylases (HDACs).[5−7]

Two families of KAT enzymes were described in bacteria, one consisting of Gcn5-related *N*-acetyltransferases (GNATs) and the other having as a prototype the Yersinia YopJ effector of the Type III secretion system. Both bacterial KAT enzyme families use acetyl coenzyme A (AcCoA) as the acetyl group donor in the acetylation reaction. Deacetylation of proteins can then occur through the action of two respective classes of KDAC enzymes,[6] the NAD^+-dependent sirtuins and the Zn^{2+}-dependent deacetylases, both having homologues in bacteria.[8] Acetylation is often found in proteins forming large macromolecular complexes and in contrast to phosphorylation, it is often located within regions of an ordered secondary structure.[9] Acetylation of a variety of virulence factors across different bacterial species has been reported and was proposed to be involved in the regulation of virulence of bacterial

Received: March 18, 2020
Published: July 17, 2020

(A)

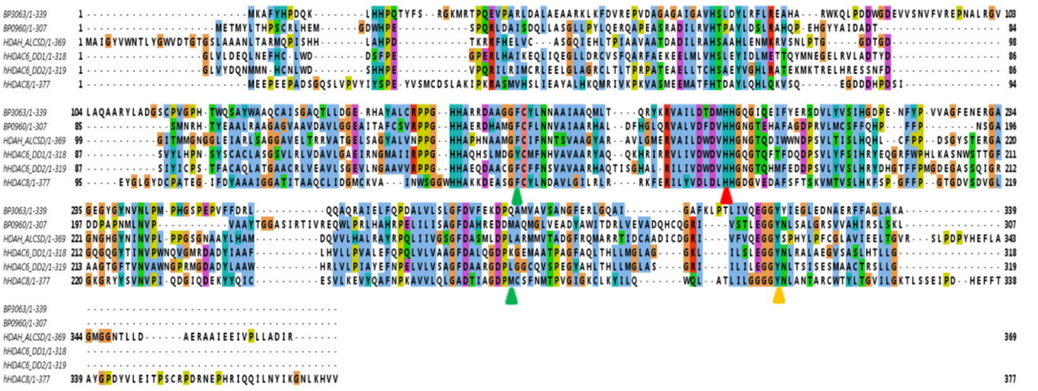

(B)

	hHDAC8	BP3063	HDAH_ALCSD	BP0960	hHDAC6_DD1	hHDAC6_DD2
hHDAC8	100	26.94	21.86	24.03	22.22	25.5
BP3063	26.94	100	29.14	27.05	27.21	26.8
HDAH_ALCSD	21.86	29.14	100	33.77	31.7	33.99
BP0960	24.03	27.05	33.77	100	34.22	36.88
hHDAC6_DD1	22.22	27.21	31.7	34.22	100	49.3
hHDAC6_DD2	25.5	26.8	33.99	36.88	49.37	100

(C)

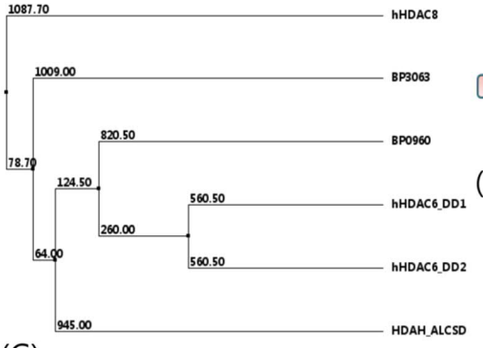

(D)

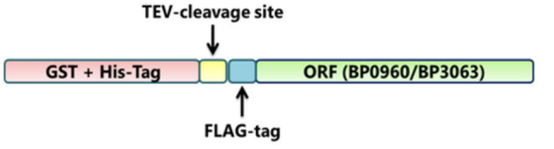

(E)

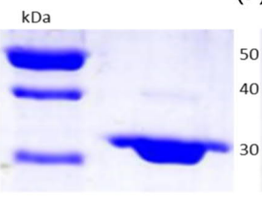

(F)

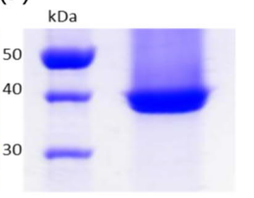

(G)

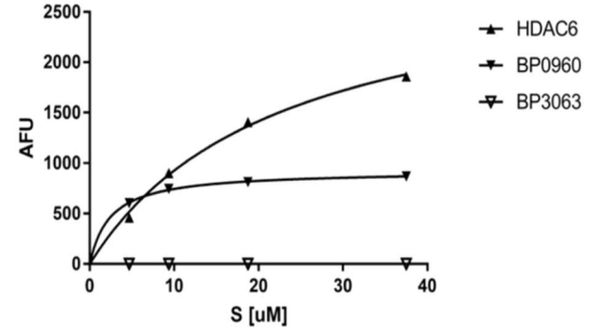

Figure 1. Sequence comparison of bacterial and human histone/lysine deacetylases. (A) Sequence alignment generated in MafftWS of two putative bacterial lysine deacetylases from *B. pertussis* BP0960 and BP3063, histone deacetylase-like amidohydrolase HdaH from bacterium *Alcaligenes* sp. (strain DSM 11172) individual catalytic domains from human HDAC6 (DD—deacetylating domain; DD1—first catalytic domain, and DD2—second catalytic domain) and the full length human HDAC8. Catalytic residues, orange triangle; Zn^{2+} ligands binding residues, red triangle; and active site residues, green triangles [based on data from Hai and Christianson (*Nat Chem Biol.* **2016** Sep; 12(9):741−7. Doi: 10.1038/nchembio.2134)]. (B) Percent identity matrix calculation created by Clustal2.1, highest similarities are shown in red and lowest in blue. (C) Phylogenetic tree calculated by Blosum 62 in Jalview, an average distance-based tree is shown. (D) Scheme of the BP0960 and BP3063 fusion protein constructs containing the N-terminal glutathione S-transferase (GST) purification tag followed by a TEV protease recognition site and FLAG octapeptide. (E) SDS-PAGE of purified N-FLAG-Bkd1 and (F) N-FLAG-BP3063 proteins. (G) HDAC *in vitro* activity as a function of Ac-GAK substrate concentration at 1 μg/mL of BP0960, BP3063, and human HDAC6 protein.

https://dx.doi.org/10.1021/acs.jproteome.0c00178
J. Proteome Res. 2020, 19, 3680−3696

pathogens (reviewed in Ren *et al.*[4]), such as the acetylation of the *Salmonella* Typhimurium cytoplasmic regulator PhoP[10] or of the leucine-responsive regulatory protein (Lrp) that regulates fimbriae production.[11] Protein acetylation in *Bordetellae* remains unexplored, and the role of PTMs has only been investigated in detail for the phosphorylation of the *Bordetella* virulence-regulating two-component system proteins (*e.g.*, BvgAS or RisA/RisK).[12,13] Therefore, we explored the activities of two putative lysine deacetylases of *B. pertussis* encoded by the BP3063 and BP0960 genes. We report that the BP0960-encoded protein, named Bkd1, exhibits lysine deacetylase activity *in vitro*. Analysis of the Δ*bkd1* mutant proteome and acetylome combined with phenotypic characterization *in vitro* and *in vivo* revealed that Bkd1 rather plays a role in physiological regulation than in virulence of *B. pertussis*.

EXPERIMENTAL PROCEDURES

Bacterial Strains and Culture

The Tohama I strain of *B. pertussis* CIP 81.32[14] and derived Δ*bkd1* and Δ*bp3063* mutants were cultured at 37 °C on Bordet-Gengou agar (Difco, USA) supplemented with 10% glycerol and 15% defibrinated sheep blood (BG) in a humidified atmosphere containing 5% CO_2. Liquid culture inocula were grown for 24 h at 37 °C in 5 mL of modified Stainer−Scholte medium (SSM)[15] supplemented with 5 g/L Casamino acids (Difco, USA) and 1 g/L cyclodextrin and diluted 1/10 into 45 mL of fresh SSM. The cultures for acetylome analysis were then grown overnight until an OD_{600} of 1.5.

For determination of bacterial growth rates, three different media were used—(1) SSM, (2) SSM without added iron, and (3) SSM without added Casamino acids and with five-fold reduced glutamate concentration (2.14 g/L). Liquid cultures of the wild-type and Δ*bkd1* strains were inoculated from BG plates, grown for several hours, and diluted to an OD_{600} of about 0.1. These cultures were grown overnight and then diluted again to OD_{600} ∼0.1 into 2 mL of media in untreated 12-well plates, in which bacterial growth at 37 °C with shaking was continually monitored using an Epoch 2 microplate spectrophotometer (BioTek) for 24 h. The doubling time in the exponential phase ($1/k$) was calculated from the growth curves by least square regression of the trendline equation $y = k{\cdot}x + q$, where y means Log_2OD_{600}, x means culture time in hours, and q represents the obtained constant.

Mutagenesis of *bkd1* and BP3063 Genes on the Chromosome of *B. pertussis*

The primers used for mutagenesis are listed in Table S4. The mutant *B. pertussis* strains were constructed by allelic exchange using the pSS4245 vector kindly provided by Dr. Scott Stibitz.[16,17] Fragments with ∼500 bp length of the upstream and downstream sequences of the open reading frames (ORFs) to be deleted were PCR-amplified and inserted into the BamHI site of pSS4245. The entire reading frames of the BP0960 and BP3063 genes were then deleted by marker-less allelic exchange. To construct the genes for FLAG-tagged Bkd1 or BP3063 proteins, appropriate oligonucleotides encoding either N-terminal or C-terminal 3xFLAG tags were inserted into the respective PCR-amplified chromosomal fragments on pSS4245 and introduced into the chromosome of *B. pertussis* by allelic exchange.[17] The resulting mutant strains were named *BP0960_3N Flag*, *BP0960_3C Flag*, *BP3063_3N Flag*, and *BP3063_3C Flag*. The presence of the desired deletions or insertions was verified by restriction analysis and sequencing of the PCR-amplified fragments of the respective portions of the bacterial chromosome.

Protein Purification

The Bkd1 and BP3063 proteins were expressed in *Escherichia coli* as fusions containing an N-terminal glutathione S-transferase (GST) purification tag, followed by a TEV protease recognition site (Glu-Asn-Leu-Tyr-Phe-Gln-Gly) and a FLAG octapeptide (Asp-Tyr-Lys-Asp-Asp-Asp-Asp-Lys) sequence, as schematically depicted in Figure 1D (see the Supporting Information Table S4 for the used primers). The GST-fusion proteins were expressed in *E. coli* BL21(DE3) from the pET42b vector in exponential *E. coli* cultures (1 L) grown in the LB medium supplemented with kanamycin (60 μg/mL) at 30 °C. Production of the fusion proteins was induced at an OD_{600} of 0.6 by addition of 1 mM IPTG for 4 h. Harvested and washed bacterial cells were suspended in PBSE buffer (PBS complemented with 1 mM EDTA and 1 mM DTT, pH 7.4) and disrupted by sonication at 4 °C and cell lysates were cleared by centrifugation at 20,000*g* for 20 min at 4 °C. Cell extracts were loaded onto glutathione-Sepharose bead columns equilibrated with PBSE buffer. The columns were extensively washed and the fusion proteins were eluted with reduced glutathione (3 mg/mL) in PBSE. TEV protease was added at a protease/target ratio of 1:20 (w/w), and the cleavage of the GST purification tags was allowed to proceed overnight during dialysis of the samples against PBSN buffer (PBS containing 0.287 M NaCl) at 4 °C. The processed proteins were loaded onto Ni-NTA agarose columns equilibrated with PBSN, and the FLAG-tagged Bkd1 and BP3063 proteins were eluted with 25 mM or 10 mM imidazole, respectively. Protein fractions were dialyzed overnight against PBSN and checked for purity by SDS-PAGE. The Bkd1 and BP3063 proteins were next concentrated by ultrafiltration on Amicon filters with 10 kDa cut-off (Millipore, Ireland) and purified close to homogeneity by size exclusion chromatography on a Superdex HR 200 (GE Healthcare) column in PBSN buffer.

Western Blots

Bacterial cells were grown overnight in 5 mL of SSM to OD_{600} 1−1.3, and cell pellets were lysed in 2 mL of 8 M urea in 50 mM ammonium bicarbonate. The extracted proteins were separated by 10% SDS-PAGE, transferred to the PVDF membrane, probed at 1:1000 dilution by the anti-FLAG M2 mAb (F3165, Sigma), followed by a peroxidase-labelled secondary antibody, and detected using enhanced chemiluminescence (ECL) with a SuperSignal West Femto maximum sensitivity substrate (Thermo Scientific).

HDAC *In Vitro* Functional Analysis

The fluorogenic histone deacetylase assay based on the measurement of 7-amino-4-methylcoumarin (AMC) release was adapted from the work of Wegener and colleagues.[18] The substrate Ac-Gly-Ala-Lys(Ac)-AMC (Bachem) and the calibration standard Ac-Gly-Ala-Lys-AMC (Bachem) were dissolved in DMSO to 30 mM stock and next diluted in HDP buffer (15 mM Tris-HCl, pH 8.1, 250 μM EDTA, 250 mM NaCl, 0.1% PEG8000) to a 300 μM solution containing 1.0% DMSO. A total of 40 μL of HDP buffer was then mixed with 10 μL of diluted enzyme solution (10 μg/mL) at 30 °C and the HDAC reaction was started by addition of 50 μL of the substrate solution in HDP, followed by incubation at 30 °C for 30 min. The reactions were stopped by addition of 67 μL of

https://dx.doi.org/10.1021/acs.jproteome.0c00178
J. Proteome Res. 2020, 19, 3680−3696

trypsin/trichostatin A (TSA) stop solution (0.01 mg/mL trypsin in 50 mM Tris-HCl, pH 8.0, 100 mM NaCl, 2 μM TSA, 30% (v/v) isopropanol). After 20 min of incubation at 30 °C, the release of AMC was monitored as fluorescence at 460 nm (λ_{ex} = 390 nm). Fluorescence intensity was calibrated using free AMC and the background fluorescence of the negative control (HDP buffer with substrate) was subtracted. Alternatively, HDAC-Glo I/II Assay and screening system (G6420, Promega) was used according to manufacturer's instructions. Human recombinant enzymes used in these assays were HDAC6 (kind gift from Cyril Barinka, IBT CAS) and HDAC8 (19380, Cayman Chemical).

Intracellular Survival Assay

Human peripheral blood mononuclear cells (PBMCs) were purified from buffy coats from anonymous healthy donors purchased at Thomayer Hospital in Prague, Czech Republic. Isolation of monocytes was performed by double-gradient centrifugation as described by Menck and colleagues,[19] with the exception that the fetal calf serum was replaced by the human AB serum obtained from fresh frozen plasma (also purchased at Thomayer Hospital in Prague, Czech Republic). Monocyte differentiation was performed in Petri dishes for bacterial cultures for six to seven days with the medium supplemented with 50 ng/mL rhM-CSF (ImmunoTools) and half of the medium was changed after four days. The day before infection, cells were transferred into a 12-well plate with DMEM (5% human serum, without antibiotics).

Bacterial liquid subcultures were grown as described above, until an OD_{600} of 1, which corresponds to about ~2×10^9 cfu/mL. Cells were infected at MOI 10:1 and the plates were centrifuged at 640*g* for 5 min to facilitate bacterial attachment to monocytes, followed by coincubation for 1 h at 37 °C in a humidified 5% CO_2 atmosphere. Unattached bacteria were washed away with prewarmed PBS, and a medium containing 100 μg/mL kanamycin was added for 1 h to kill extracellular bacteria. Plates were washed, and kanamycin concentration in the fresh culture medium was next decreased to 50 μg/mL for another 24 or 48 h of incubation, to eliminate any noninternalized or released bacteria, before the cells were washed with warm PBS and lysed in sterile water. Lysates were serially diluted in PBS and plated on BGA for determination of *B. pertussis* colony forming units (CFUs) after 5 days of growth.

Sample Preparation and Acetylome Analysis

Liquid cultures grown as described above were harvested (35 mL) and centrifuged (35,000*g* for 20 min, at 4 °C). Cell pellets were first washed with 5 mL of cold PBS, centrifuged (35,000*g* for 10 min, at 4 °C), and dissolved in 5 mL of 8 M urea in 50 mM ammonium bicarbonate on a rotator for 3 h at room temperature. The lysates were cleared (35,000*g* for 20 min, RT), and the supernatants were stored frozen.

Bacterial Lysis, Protein Digestion, and Immunoaffinity Purification

Bacterial lysates prepared in biological triplicates, each containing 6 mg of protein, were reduced with 10 mM dithiotreitol (DTT) at 37 °C for 60 min and alkylated with 20 mM iodoacetamide (IAA) in the dark at room temperature for 30 min. The residual of IAA was quenched by another addition of DTT and left to react for 15 min. Samples were then diluted with 25 mM NH_4HCO_3 to reach 2 M urea and digested with trypsin (Sigma) added at 1:40 ratio (trypsin/proteins) and incubated overnight at 37 °C. Digested samples were acidified with trifluoroacetic acid (TFA) to reach pH ~2 and desalted on Discovery C18 SPE cartridges (500 mg, Sigma). Peptides were eluted with 6 mL of 60% acetonitrile (ACN)/0.1% TFA and volumes corresponding to approximately 50 μg of the peptide material were transferred into new tubes and dried in a Speed-Vac for proteome analysis. The rests of eluates were frozen at −80 °C overnight and lyophilized for at least 2 days. Lyophilized digests were processed and enriched for AcK peptides using the PTMScan Acetyl-Lysine Motif [Ac-K] Kit (Cell Signaling) according to protocol supplied by the manufacturer. For a biological replicate consisting of three digests (one for each bacterial strain), one vial with immunoaffinity beads was split into three parts and the respective amounts were used for the immunoprecipitation (IP) of each digest. AcK peptides eluted from immunoaffinity beads were desalted employing 3M Empore C18 disks packed into pipette tips as described by Rappsilber and colleagues,[20] eluted with 60% ACN/0.1% TFA, and dried up in a Speed-Vac.

Liquid Chromatography–Mass Spectrometry

The UltiMate 3000 RSLCnano system connected through a Nanospray Flex ion source with a Q Exactive Plus mass spectrometer (both Thermo Scientific) was used for analysis. Acetylome samples were dissolved in 2% ACN/0.1% TFA and approximately two thirds of each sample was introduced onto trap column (PepMap100 C18, 3 μm, 100 Å, 75 μm × 20 mm) and separated using a linear gradient [2% ACN/0.1% formic acid (FA) as phase A; 80% ACN/0.1% FA as phase B] from 2 to 34.5% B in 45 min and from 34.5 to 45% B in 5 min at a flow rate of 250 nL/min on an analytical column (PepMap RSLC C18, 2 μm, 100 Å, 75 μm × 250 mm; both columns from Thermo). A full MS/Top10 setup was used for mass spectrum acquisition. Positive ion MS spectra in the 300 to 1700 m/z range were obtained in an Orbitrap at a resolution of 70,000. Multiply charged precursor ions with a minimal AGC target of 2.5×10^4, not fragmented during previous 20 s, were admitted for higher energy collisional dissociation (HCD) with 1.6 m/z isolation window. Tandem mass spectra were acquired at the following settings: resolution at 35,000, AGC target value at 1×10^6, 120 ms maximum ion injection time, and normalized collision energy set to 28. For analysis of bacterial proteomes, 2.5 μg of the peptide material was analyzed using the same instrumentation using a linear gradient from 2 to 9% B in 57 min, 9 to 34.5% B in 160 min, and 34.5 to 45% B in 23 min. The mass spectrometer operated in the Top12 setup and collected MS spectra were in the range of 350−1600 m/z. The minimal AGC target for triggering MS/MS was 1.2×10^4, the isolation window was 2.0 m/z, and the resulting spectra were acquired at resolution set to 17,500.

Identification and Label-free Quantitation

Acetylome and proteome datasets were processed using MaxQuant ver. 1.6.5.0.[21] Data were searched against the FASTA database of the reference proteome of *B. pertussis* (Tohama I strain/ATCC BAA-589/NCTC 13251; July 29, 2019; 3258 sequences) downloaded from Uniprot. The MaxQuant-implemented database was used for the identification of contaminants. AcK site identification was performed using the following MaxQuant parameters: mass tolerance for the first search 20 ppm and for the second search from recalibrated spectra 4.5 ppm (with individual mass error filtering enabled); maximum of three missed cleavages;

https://dx.doi.org/10.1021/acs.jproteome.0c00178
J. Proteome Res. 2020, 19, 3680−3696

maximal charge per peptide $z = 7$; minimal length of peptide 7 amino acids, maximal mass of peptide 4600 Da; carbamidomethylation (C) as fixed and acetylation (K and protein N-term) and oxidation (M) as variable modifications with the maximum number of variable modifications per peptide set to 5. Trypsin with no cleavage restriction was set as a protease. Mass tolerance for fragments in MS/MS was 20 ppm, taking the 12 most intensive peaks per 100 Da for search (with enabled possibility of cofragmented peptide identification). The minimal Andromeda score for modified peptides was 40, and the minimal delta score for modified peptides was 6. FDR filtering on the peptide spectrum match was 0.01 (with separate FDR filtering for each modification set to 0.01) using a target-decoy approach with reversed database as a decoy. MaxQuant parameters for processing of proteome data were identical except for only that oxidation (M) and acetylation (protein N-term) were allowed as variable modifications and the maximal number of missed cleavages was set to 2. All hits identified in searches as contaminants were filtered out. Proteins were quantified using the MaxLFQ function[22] with at least two peptide ratios required for pair-wise comparisons of protein abundance between samples.

Statistical Testing and Normalization

Proteins regulated differentially in wild-type and mutant strains were found by Student's *T*-test ($s_0 = 0.1$, permutation-based FDR $\leq$0.05) applied on log-transformed MaxLFQ values (performed in Perseus ver. 1.6.2.1[23]). Only those proteins quantified by MaxLFQ in all three biological replicates of both compared strains were tested. In addition, proteins quantified in all three replicates of one strain and lacking MaxLFQ intensities consistently across all three replicates of the other compared strain were considered significantly regulated. Prior to quantitation of acetylome changes, AcK site intensities were corrected for technical variation using unmodified peptides present in AcK-enriched samples (~38% of all identified peptides in IP samples). First, proteins with similar MaxLFQ intensities across all biological replicates of all bacterial strains were extracted from the proteome dataset (108 proteins; CV <8%) and unmodified peptides from the corresponding proteins were found in IP data (total of 108 unique peptides identified across all IP samples). Intensities of these peptides in IP samples were divided by their intensity in one IP sample selected for normalization purposes and the ratios were log-transformed. Sample-specific medians of ratio distributions were used for correction of AcK site intensities in the respective IP sample. The abundance of acetyl-lysine sites was corrected for changes in protein abundance in analyzed bacterial lyzates. Briefly, protein MaxLFQ intensities from each sample were divided by values from the sample selected for normalization purposes and abundances of acetylated sites of the respective protein in the given sample were modified by these ratios. AcK site intensities corrected for both technical variation and protein expression were directly compared between samples and significantly regulated sites were found as described for proteins (see above).

Bioinformatics Analysis

Multiple sequence alignments, their annotation, and analyzes were performed in Jalview 2.10.5.[24] Alignment was done using Mafft[25] with default settings, and the phylogenetic tree was calculated with Blosum62. Calculation of the percent identity matrix was done using Clustal2.1 in the Clustal Omega[26] web interface. Analysis of acetylation motifs was done using the software tool MoMo (http://meme-suite.org)[27] with a reimplemented motif-x algorithm.[28] Gene ontology (GO) enrichment analyzes were performed in Cytoscape[29] using the plugin ClueGO.[30]

Production of Recombinant BvgA

The recombinant BvgA protein carrying the N-terminal polyhistidine tag was produced in *E. coli* BL21(DE3) cells from the pET42b vector in the LB medium supplemented with kanamycin (60 μg/mL). Expression of the protein was induced at an OD_{600} of 0.6 by addition of 1 mM IPTG for 4 h at 37 °C. The cleared urea extract of washed inclusion bodies was loaded at room temperature on a Ni-NTA agarose column (GE Healthcare BioSciences, Pittsburgh, PA, USA) equilibrated with TU buffer (8 M urea, 50 mM Tris-HCl pH 8.0), and contaminants were washed out with TU buffer supplemented with 50 mM imidazole. The BvgA protein was eluted with 250 mM imidazole in the same buffer and its homogeneity was analyzed by SDS-PAGE.

Analysis of BvgA and BvgA~P Protein Levels

Wild-type and Δ*bkd1 B. pertussis* bacteria were cultured in SSM without added Casamino acids and with five-fold-reduced glutamate concentration (2.14 g/L) to OD_{600} ~1 and whole bacterial cell lysates were prepared and analyzed as described in Chen at al 2013.[31] Proteins were separated on SuperSep Phos-tag gels (Wako) and BvgA isoforms were detected by western blotting using a rabbit polyclonal α-BvgA antibody.[32]

Data Availability

The mass spectrometry proteomics data have been deposited to the ProteomeXchange Consortium *via* the PRIDE partner repository with the dataset identifier PXD016384. MS/MS spectra can be viewed on MS-Viewer using the search key bw6zrsnsts (http://msviewer.ucsf.edu/prospector/cgi-bin/mssearch.cgi?report_title=MS-Viewer&search_key=bw6zrsnsts&search_name=msviewer).

Animal Infection Experiments

All animal experiments were approved by the Animal Welfare Committee of the Institute of Molecular Genetics of the Czech Academy of Sciences, v. v. i., in Prague, Czech Republic. Handling of animals was performed according to the *Guidelines for the Care and Use of Laboratory Animals*, the Act of the Czech National Assembly, Collection of Laws no. 246/1992. Permission no. 41/2019 was issued by the Animal Welfare Committee of the Institute of Molecular Genetics of the Czech Academy of Sciences in Prague.

Five week-old female Balb/cByJ mice (Charles River, France) were used in this study. The mice were anesthetized by intraperitoneal (i.p.) injection of ketamine (80 mg/kg) and xylazine (8 mg/kg), and the mice were intranasally infected with the indicated amounts of colony forming units (CFUs) of midexponential phase *B. pertussis* CIP 81.32 or its *B. pertussis* Δ*bkd1* bacteria suspended in 50 μL. To determine viable CFUs of the *B. pertussis* inoculum, aliquots of the inoculum were diluted in PBS and plated on BG agar plates. For survival curves (LD_{50}), groups of six Balb/cByJ mice were infected with serially diluted bacterial suspension and their survival was monitored over a 10 day period. The results are expressed as the percentage of surviving mice and are representative of two independent experiments. The LD_{50} values were calculated by the probit analysis method of Finney, as previously reported.[16]

https://dx.doi.org/10.1021/acs.jproteome.0c00178
J. Proteome Res. 2020, 19, 3680−3696

RESULTS

BP0960 Encodes a Lysine Deacetylase Enzyme Bkd1

Screening of the InterPro database[33] for *B. pertussis* proteins harboring a histone deacetylase superfamily domain (IPR000286) revealed three ORFs. For two of them, BP0960 and BP3063, the protein products were previously detected in proteomic studies.[34,35] Subsequent sequence alignments (Figure 1A) with the human histone deacetylases HDAC6 (class IIb HDAC) and HDAC8 (class I), or the deacetylase-like amidohydrolase *hdaH* of *Alcaligenes* sp. (strain DSM 11172), revealed the presence of highly conserved catalytic and Zn^{2+}-binding residue motifs in the deduced protein sequences of BP0960 and BP3063. Percent identity matrix calculation (Figure 1B) and phylogenetic tree analysis (Figure 1C) showed that the BP0960-encoded protein exhibited higher homology to the deacetylating domains of HDAC6 than to any other tested protein sequence. In contrast, the BP3063-encoded polypeptide exhibited 68.73% sequence identity with the acetylpolyamine amidohydrolase *aphA* from *Burkholderia pseudomallei* (strain 1710b) and ∼40% sequence identity with the acetylpolyamine aminohydrolase (APAH) from *Mycoplana ramosa*[36] (Figure S1A−C).

To examine the production of the BP0960- and BP3063-encoded proteins, FLAG tag-encoding sequences were inserted in frame at the 5′- or 3′- ends of the BP0960 or BP3063 ORFs on the *B. pertussis* chromosome. Immunoblotting of bacterial lysates using an anti-FLAG antibody revealed that both FLAG-tagged proteins were produced and the C-terminally tagged BP0960-encoded protein formed SDS-resistant dimers (Figure S2A−D).

To examine if the BP0960 and BP3063 genes encode KDAC enzymes, their ORFs were expressed in *E. coli* (Figure 1D−F) and the KDAC activity of the purified recombinant proteins was assessed (Figure 1G).

Briefly, an N-terminal GST purification tag, followed by a TEV protease recognition site and a FLAG octapeptide tag was fused to the N-termini of the BP0960 and BP3063 polypeptides (Figure 1D). The fusion proteins were purified from cytosolic extracts of *E. coli* using glutathione-Sepharose beads and the GST tag was removed by TEV protease treatment. The 6xHis-GST tag and the 6xHis-TEV protease were next removed from the liberated BP0960 and BP3063 proteins on a Ni-NTA column (Figure S3A,B).

To test the KDAC activity of the putative lysine deacetylases, we first used the luminometric HDAC-Glo I/II assay and screening system that measures the KDAC activity on an acetylated luminogenic substrate peptide derived from the histone 4 consensus sequence and optimized for recognition with HDACI/II enzymes. As shown in Figure S3C, KDAC activity was measured for the BP0960 product but not for the BP3063-encoded protein. Therefore, the activity of the BP0960-encoded enzyme, further named Bkd1, was compared to that of the human HDAC6 enzyme using the fluorogenic Ac-GAK substrate of histone deacetylases.[18] This assay measures the fluorescent signal following the proteolytic release of 7-amino-4-methylcoumarin (AMC) from the deacetylated synthetic peptide Ac-Gly-Ala-Lys(Ac)-AMC. As shown in Figure 1G, both HDAC6 and Bkd1 enzymes deacetylated the Ac-GAK substrate, yielding a fluorescent product, while the BP3063-encoded protein did not. Hence, only Bkd1 possessed a bona fide KDAC activity under the used experimental conditions.

Bkd1 Deacetylates a Broad Range of *B. pertussis* Proteins

To determine if the Bkd1 and BP3063-encoded proteins exert KDAC activities in *B. pertussis* cells, the BP0960 and BP3063 ORFs were individually deleted from the *B. pertussis* chromosome and the total acetylomes of the Δ*bkd1* and Δ*bp3063* mutants were compared to the acetylome of wild-type *B. pertussis* cells. As documented in the Table S1 and summarized in Table 1, label-free high-throughput acetylome analysis of the three proteomes revealed up to 2,061 individual acetylation sites in *B. pertussis* proteins across all samples and replicates. A total of 761 unique proteins were found to be acetylated on at least one lysine residue in at least one replicate, thus comprising approximately one-quarter of the annotated *B. pertussis* proteome. Over half of these proteins was mono- or diacetylated (354 and 147 proteins, respectively). The GO enrichment analysis assigned the acetylated proteins as involved in a wide range of housekeeping and metabolic processes, including organonitrogen compound biosynthetic and metabolic pathways, gene transcription and mRNA translation, various transport processes, and so on (Figure 2A). The highest extent of acetylation was observed for the GroEL chaperonin acetylated at 31 sites, followed by the chaperones DnaK and ClpB (21 sites) and the elongation factor G (18 sites). In the wild-type bacteria, 568 acetylation sites were found to be acetylated in all three replicates. Similarly, the acetylome of the Δ*bp3063* mutant comprised 523 individual acetylation sites, further suggesting that BP3063 does not encode a KDAC enzyme under the tested conditions.

Table 1. Summary of the Acetylome and Total Proteome Analysis

total numbers of identified	
acetylated sites	2061
acetylated proteins	761
Proteins	1616
total number of quantified AcK sites in	
WT *B. pertussis*	568
Δ*bkd1 B. pertussis*	977
Δ*bp3063 B. pertussis*	523

To enable the comparison of the extent of protein acetylation between samples, the intensities of all quantified acetyl-lysine sites were normalized for changes in protein levels (see Experimental Procedures). As a result, only two proteins were found to have increased acetylation and four were found to have decreased acetylation in the Δ*bp3063* acetylome, as compared to the wild-type bacteria. In contrast, 977 individual acetylated sites were identified in the acetylome of the Δ*bkd1* mutant over three biological replicates (Tables 1 and S1). Moreover, 271 lysine residues of 198 unique proteins exhibited a significantly increased level of acetylation in the Δ*bkd1* acetylome, compared to the acetylome of wild-type *B. pertussis*, whereas 91 lysine residues of 73 unique proteins exhibited a reduced acetylation level.

To define the potential target sequence motifs recognized by the Bkd1 deacetylase, we performed enrichment analysis for sites exhibiting an increased level of acetylation (upregulated) in the Δ*bkd1* acetylome. Two most frequent lysine acetylation target motifs, "KL" and "EK", were identified (Figure 2B). The set of enriched acetylated proteins with a "KL" motif comprised proteins involved in cell morphogenesis, electron-transfer activity, carboxylic acid catabolism, and protein

https://dx.doi.org/10.1021/acs.jproteome.0c00178
J. Proteome Res. 2020, 19, 3680−3696

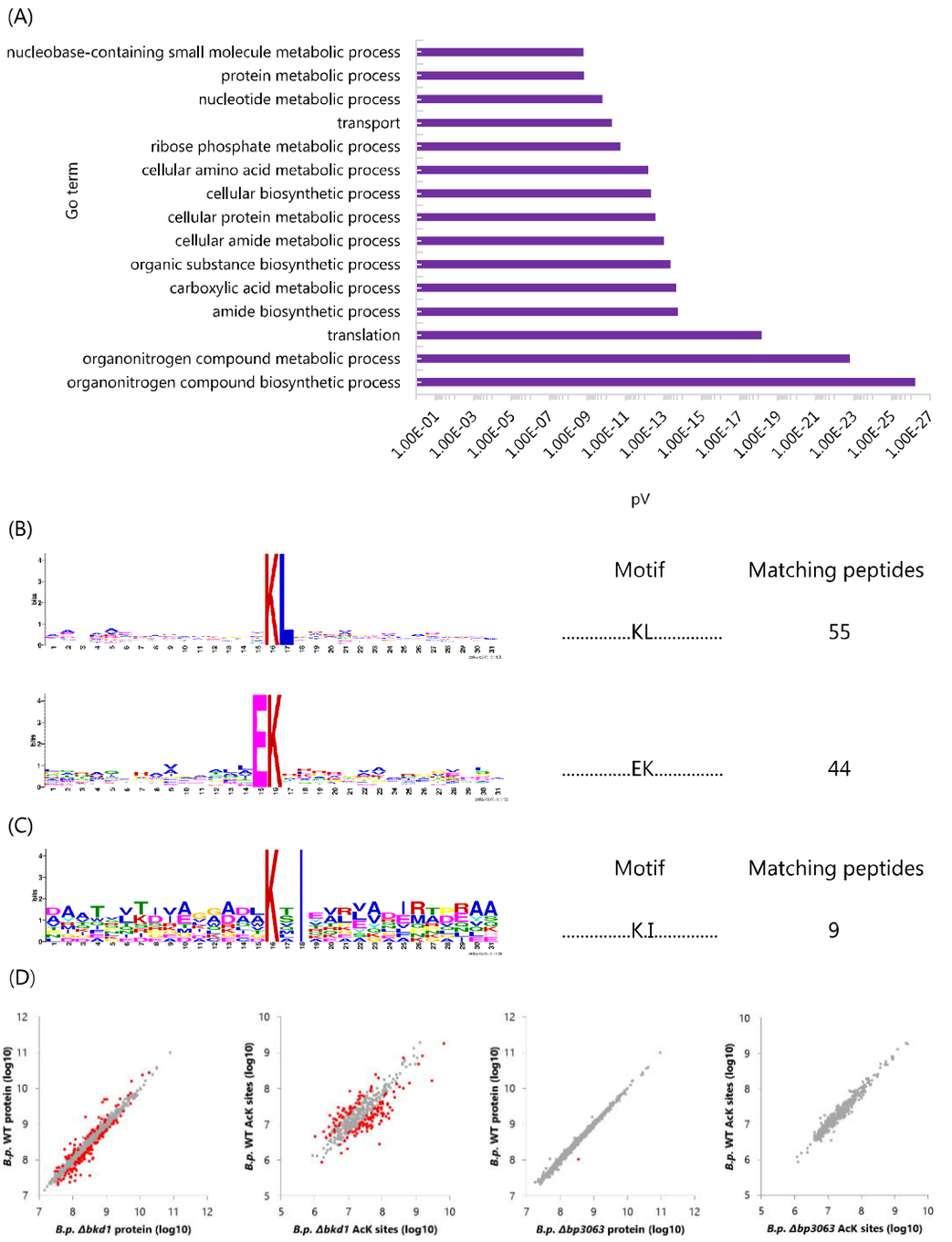

Figure 2. Bioinformatics analysis of the *B. pertussis* acetylome. (A) Top 15 most enriched GO terms based on functional analysis of the *B. pertussis* acetylome. ClueGO top terms ($p \leq 0.05$) enriched in "Biological process" library were ranked according to their *p*-values (corrected by the Benjamini−Hochberg test). Discovered sequence motifs in peptides were found to be significantly acetylated (B) or deacetylated (C) in the Δ*bkd1* strain compared to the wild type. (D) Comparison of individual proteins or acetyl-lysine sites between wild-type and Δ*bkd1*/Δ*bp3063* mutant strains based on their average normalized log values. Only values quantified in all three replicates were selected. Gray points indicate those proteins/sites, which did not pass the significance test and red points indicate significant proteins/sites based on the *t*-test.

translation. The set of acetylated proteins with a "EK" motif comprised proteins involved in purine ribonucleotide metabolism or cellular protein modification processes. Analysis of downregulated sites with lower levels of acetylation in the Δ*bkd1* acetylome revealed a significant enrichment of the "KxI" motif-containing proteins (Figure 2C). Deletion of the *bkd1* gene further yielded extensive changes in both acetylome and proteome composition (Tables S1 and S3). In contrast, deletion of the BP3063 gene did not impact acetylome or proteome composition, which resembled that of the wild-type bacteria (Figure 2D).

STRING database interaction analysis[37] of proteins harboring sites with increased levels of acetylation in the Δ*bkd1* acetylome revealed a crowded cluster of proteins

https://dx.doi.org/10.1021/acs.jproteome.0c00178
J. Proteome Res. 2020, 19, 3680−3696

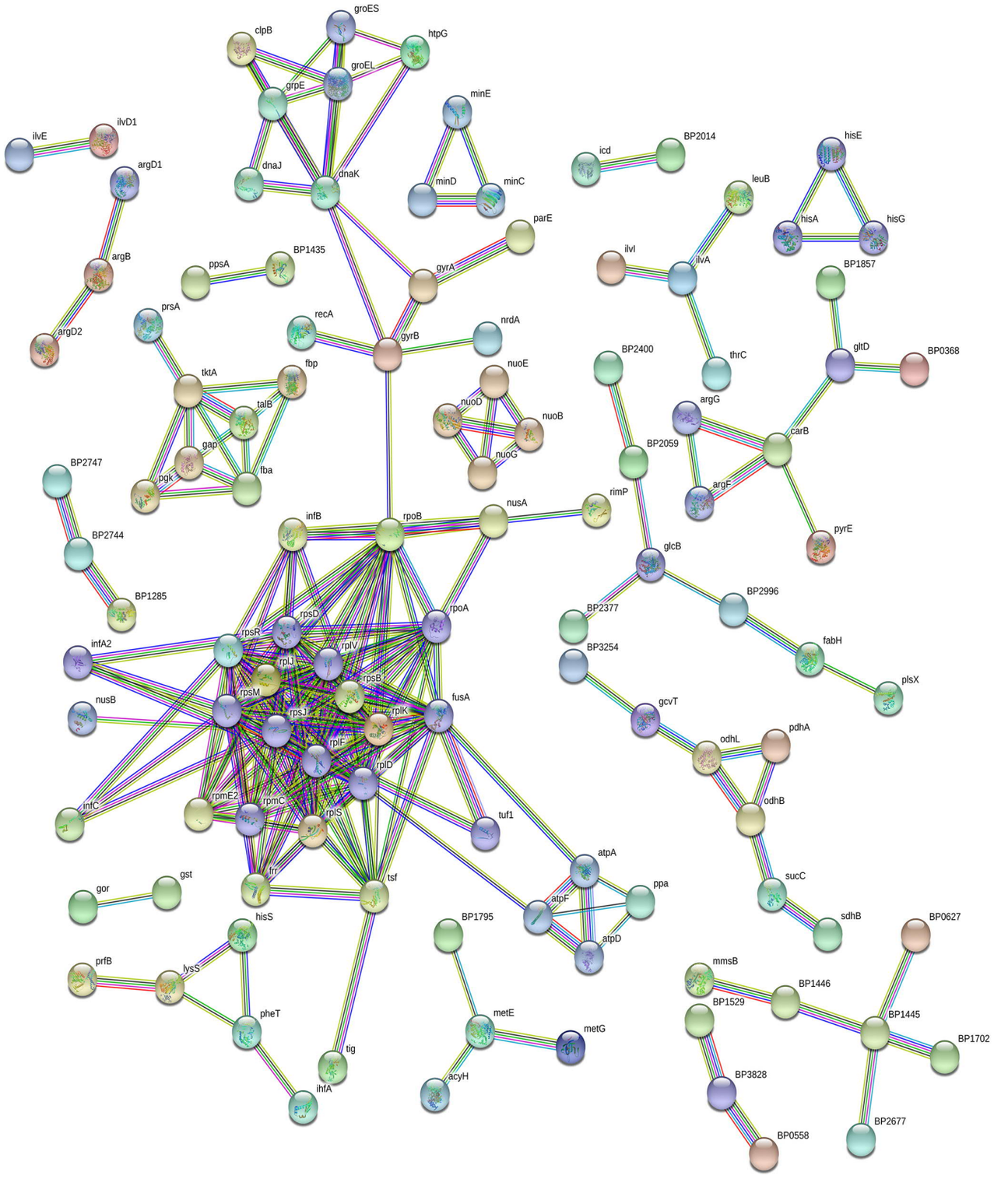

Figure 3. Protein−protein interaction network for proteins exhibiting significantly higher levels of acetylation of lysine residues in the Δ*bkd1* mutant proteome as compared to the wild-type *B. pertussis* proteome. The interaction network was built using the STRING database v11.0 (https://string-db.org/). Network edges are represented by lines. The colors indicate different types of interaction evidence. The minimum required interaction score was set to the highest confidence (0.900) and disconnected nodes in the network are hidden.

consisting of multiple ribosomal proteins and their interacting partners, including components of proteosynthetic and transcriptional machineries. Furthermore, clusters of acetylated proteins consisted of chaperone proteins and proteins involved in energy metabolism (Figure 3), indicating that lysine

https://dx.doi.org/10.1021/acs.jproteome.0c00178
J. Proteome Res. 2020, 19, 3680−3696

Table 2. Acetylation of Virulence-Related Proteins

			WT	Δ*bp3063*	Δ*bkd1*	
gene	protein	residue	AcK[a,b]	AcK[a,b]	AcK[a,b]	change[c]
fim2	fimbrial protein Fim2	81	−	−	+	
bvgA	response regulator BvgA	104	+	−	−	
		41	+	+	+	
		46	+	+	+	
		59	+	+	+	↑
		190	−	+	+	
		204	+	+	−	
		4	+	+	+	↓
		24	+	+	+	
fhaB	filamentous hemagglutinin FhaB	470	−	+	+	
		2219	−	−	+	
		1805	+	+	−	
		239	+	−	+	
prn	pertactin Prn	116	+	+	+	
fhaE	filamentous hemagglutinin FhaE	81	+	+	+	
brkA	*Bordetella* resistance to killing BrkA	366	+	+	+	↓
risA	response regulator RisA	47	+	+	+	
bopN	T3SS protein	270	+	+	+	↑
tcfA	tracheal colonization factor TcfA	65	−	+	+	
ftsY	SRP receptor FtsY	268	+	−	+	
secA	protein translocase SecA	482	+	−	+	↓
		246	−	−	+	
bsp22	T3SS tip filament Bsp22	191	−	−	+	↑
htpG	Hsp90 chaperone HtpG	198	+	−	−	↓
		119	+	+	+	
		51	+	+	+	
		509	+	+	+	
		510	+	+	+	↑
		308	+	+	+	↑
		535	+	+	+	↓
		520	+	+	−	
		634	−	−	+	↑
		77	+	+	+	

[a]+ Acetylation was quantified (found in all three replicates of the respective sample). [b]− Acetylation was not quantified (not found in all three replicates of the respective sample). [c]↑/↓ Lysine residue was significantly more/less acetylated in the Δ*bkd1* mutant strain.

acetylation may play a role in modulation of "housekeeping" functions of *B. pertussis*.

Acetylation of Virulence-Regulating and DNA-Packaging Proteins

We next assessed if Bkd1 deacetylates virulence-associated proteins and whether its activity may modulate gene expression through deacetylation of the DNA-packaging proteins. Proteins of these classes were filtered from the Δ*bkd1* acetylome using their GO annotation terms and manual selection. The individual acetylation sites were almost two times more likely (1.7×) to be scored as acetylated in the acetylome of the Δ*bkd1* mutant than in the acetylome of the wild-type bacteria. For the set of virulence-related proteins selected according to their GO annotation and/or literature search (Table 2), no difference was observed between the Δ*bkd1* and wild-type bacteria, indicating that this protein group is not a major target of Bkd1 activity (Figure 4A). There were 43 unique acetylated or deacetylated sites found in 13 virulence-related proteins (Figure 4B and Table 2). Most of these sites were found in the stress-induced Hsp90 chaperone protein HtpG (10 acetylated sites). Interestingly, eight acetylated sites were identified in the BvgA protein, the key DNA-binding regulator protein of the BvgAS two-component system that is the master regulator of virulence of all pathogenic *Bordetellae*.[38] Two significantly deregulated sites on BvgA were identified in the acetylome of the Δ*bkd1* mutant, with significantly increased acetylation of the lysine 59 (K59) residue and a decreased acetylation of lysine 4 (K4) of BvgA.

Because BvgS-catalyzed phosphorylation of the asparate residue 54 (D54) of BvgA to BvgA∼P determines the levels of expression of key *B. pertussis* virulence factor genes, we examined whether enhanced acetylation of BvgA affected the levels of BvgA∼P in the Δ*bkd1* mutant. Triplicate whole cell lysates of wild-type and Δ*bkd1* bacteria cells were separated on 12.5% SuperSep Phos-tag gels that allow resolving of BvgA from BvgA−P and the respective levels of BvgA and BvgA∼P proteins were detected in western blots with a rabbit polyclonal α-BvgA antibody.[32] As documented in Figure 5, deletion of the *bkd1* gene and the thus resulting increased level of BvgA acetylation affected neither the total amount of BvgA protein nor the level of its phosphorylation and the BvgA/Bvg−P ratio in the Δ*bkd1* cells was at least as high as that in wild-type bacteria. This result goes well with the comparable levels of key virulence proteins detected in the proteomes of wild-type and Δ*bkd1* *B. pertussis* cells (Table S3).

https://dx.doi.org/10.1021/acs.jproteome.0c00178
J. Proteome Res. 2020, 19, 3680−3696

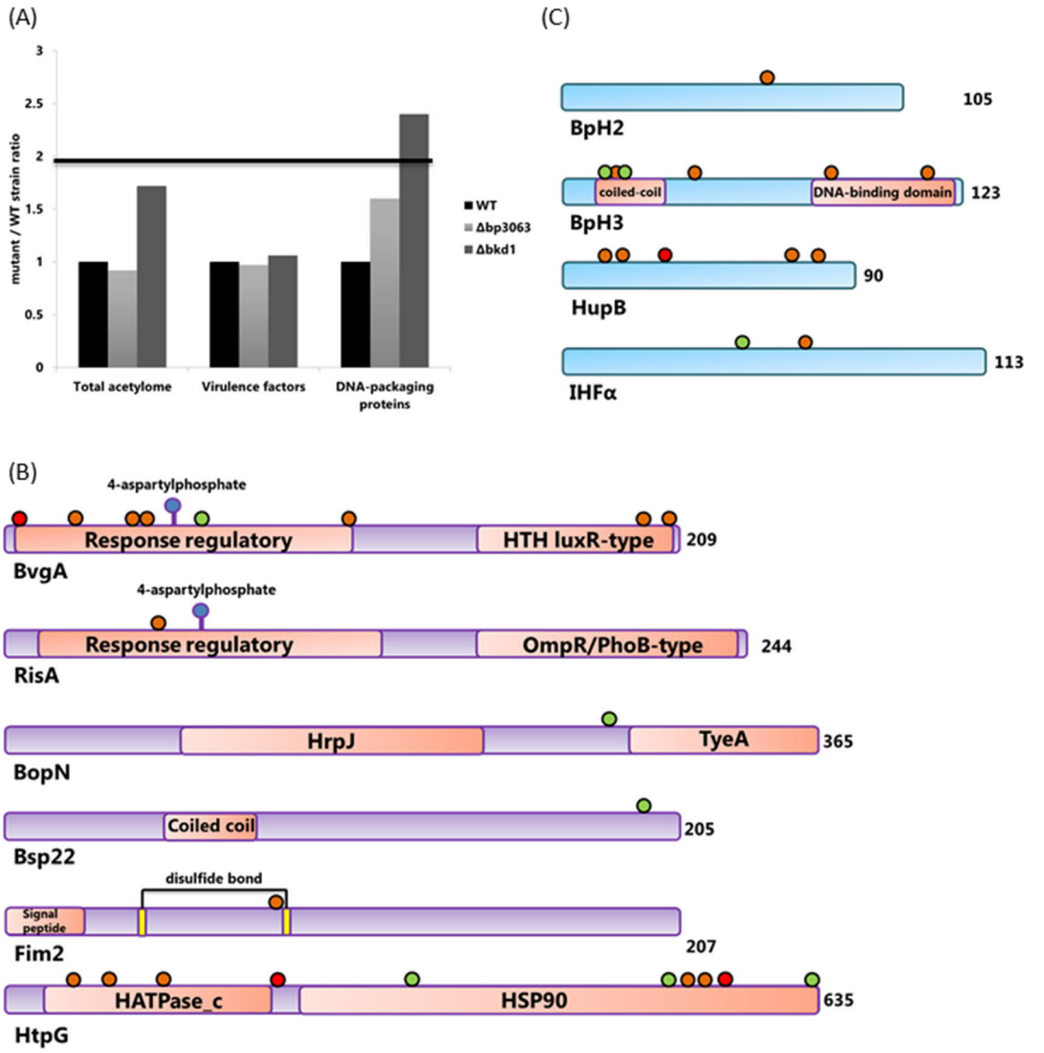

Figure 4. (A) Ratio of total counts of sites with acetylation present in all three replicates between wild-type, Δ*bp3063*, and Δ*bkd1* mutant strains, normalized to the wild-type bacteria proteome and shown for three datasets—the total acetylome and two subsets of proteins related to virulence and the histone-like proteins, respectively. The black line represents a two-fold cut-off. (B) Selected virulence-related proteins and (C) histone-like proteins with indicated acetyl-lysine sites. The green or red circles indicate sites where the acetylation was significantly increased or decreased, respectively, in the Δ*bkd1* mutant proteome, compared to the wild type. The orange circles indicate the presence of the acetyl-lysine site in at least one sample in all three replicates.

In contrast to BvgA, no significant difference in the acetylation status in wild-type and Δ*bkd1* bacteria was found for the lysine 47 residue of RisA, another transcriptional regulator protein of the RisA/RisK two-component system that regulates some genes that may or may not be regulated also by BvgAS.[39] Increased acetylation levels of BopN and Bsp22 protein components of the Type III secretion system of *Bordetella*[40] were also observed in the Δ*bkd1* acetylome.

Among the histone-like proteins, 16 unique acetylated or deacetylated sites were found across the wild-type and Δ*bkd1* acetylomes (Figure 4C and Table 3) and individual sites were 2.4 times more likely to be scored as acetylated in the acetylome of the Δ*bkd1* mutant than in the acetylome of wild-type bacteria (Figure 4A). The protein with highest number of acetylated lysines from this group in the Δ*bkd1* acetylome was the H-NS-like protein BpH3, acetylated on six residues (Figure 4C and Table 3). Hence, BpH3 clearly was a substrate of the Bkd1 deacetylase. Four of its lysine residues were found to be acetylated only in the Δ*bkd1* mutant, indicating that Bkd1 targeted this protein involved in DNA packaging. Similarly, the α-subunit of the IHF protein involved in condensation of the bacterial nucleoid[41,42] was found to be acetylated only in the Δ*bkd1* mutant, even though on protein level, its amount was significantly downregulated (Figure 4C and Table S3). However, acetylation of the five lysine residues of another histone-like protein, HupB, appears to be regulated by another deacetylase than Bkd1, or the protein is not deacetylated at all, because acetylation levels of HupB were similar in the wild-type and Δ*bkd1* acetylomes. In the Δ*bp3063* acetylome, the apparent increase in acetylation of DNA-packaging proteins (Figure 4A) in respect to the wild type was found only for three acetylation sites and may reflect technical variation or an unspecific effect of the BP3063 deletion.

https://dx.doi.org/10.1021/acs.jproteome.0c00178
J. Proteome Res. 2020, 19, 3680−3696

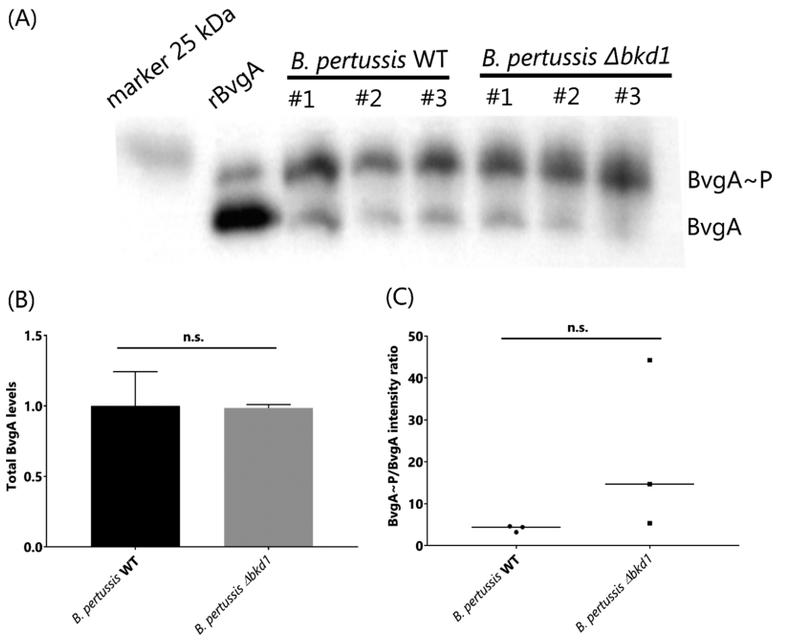

Figure 5. Comparison of total amounts of the BvgA protein and its phosphorylation status in wild-type *B. pertussis* and the Δ*bkd1* mutant. (A) Bacterial lyzates from three biological replicates of wild-type and Δ*bkd1* bacterial cells were separated on a 12.5% SuperSep Phos-tag gel and BvgA and Bvg–P proteins were detected by western blot using a polyclonal α-BvgA antibody. (B) Total BvgA (BvgA + BvgA~P) levels. The mean relative intensity for wild-type *B. pertussis* was set as 1. (C) Comparison of the relative levels of phosphorylated *vs* nonphosphorylated BvgA as determined by densitometry.

Table 3. Acetylation of Histone-like Proteins

			WT	Δ*bp3063*	Δ*bkd1*	
gene		residue	AcK[a,b]	AcK[a,b]	AcK[a,b]	change[c,d]
hupB	histone-like protein HupB	18	+	+	–	
hupB		78	–	+	+	
hupB		13	+	+	–	
hupB		33	+	+	+	↓
hupB		70	+	+	+	
bph3	H-NS-like protein BpH3	86	–	–	+	
bph3		12	–	–	+	↑
bph3		15	–	+	+	
bph3		19	–	–	+	↑
bph3		41	–	–	+	
bph3		115	+	+	+	
ihfA	α-subunit of IHF protein	54	–	–	+	↑
ihfA		75	–	–	+	
bph2	histone H1 homolog BpH2	63	–	+	+	

[a] + Acetylation was quantified (found in all three replicates of the respective sample). [b] – Acetylation was not quantified (not found in all three replicates of the respective sample). [c] ↑ The lysine residue was significantly more acetylated in the Δ*bkd1* mutant strain. [d] ↓ The lysine residue was significantly less acetylated in the Δ*bkd1* mutant strain.

Activity of the Bkd1 Enzyme Affects Proteome Composition and Bacterial Growth under Nutrient-Limiting Conditions *In Vitro*

Acetylation of eukaryotic histone proteins is known to decrease their affinity for DNA and thereby affect nucleosome formation and gene transcription. We thus examined if the altered acetylation status of DNA-packaging proteins translated into alterations of *B. pertussis* proteome composition. The proteome of the Δ*bp3063* mutant (Table S3) differed from that of the wild-type strain in only five significantly deregulated proteins (Figure 2D and Table S1), reflecting the very minor difference in acetylation of the histone-like proteins in the Δ*bp3063* mutant (Table 3). It can, hence, be concluded that the product of the BP3063 gene was not involved in the regulation of gene expression in *B. pertussis* under the tested conditions.

In contrast, the proteome composition of the Δ*bkd1* mutant (Table S3) differed from that of wild-type bacteria in 170 upregulated proteins, with 72 of them being detectable only in the Δ*bkd1* mutant biomass and nondetectable in the wild-type proteome (Table S3). A total of 59 proteins were down-regulated (low expression or undetectable) in the Δ*bkd1* mutant proteome. This strongly suggests that Bkd1 deacetylase modulates gene expression and/or steady-state protein stability and turnover in *B. pertussis*. The proteins differentially regulated by Bkd1 activity comprised, among others, the Bvg-intermediate phase protein BipA,[43] fimbrial protein Fim2, BatB autotransporter,[44] or the tracheal colonization factor[45] (Table S3). Some of the most importantly deregulated proteins are listed in Tables 4 and 5 and comprise among other enzymes involved in metabolic processes, several uncharacterized transcriptional regulators of various classes or proteins involved in membrane localization functions (*e.g.*, BamD and BamE in Table 5). Most notably, the acetyl-coenzyme A synthetase levels were strongly upregulated in the

https://dx.doi.org/10.1021/acs.jproteome.0c00178
J. Proteome Res. 2020, 19, 3680–3696

Table 4. Importantly Deregulated Proteins in the *B.p.* Δ*bkd1* Mutant[a]

gene name	protein name	Δ*bkd1 vs* WT	FC	Ac(K) site positions
acsA	acetyl-coenzyme A synthetase	↑	8.8	607
BP2397	putative ABC transporter ATP-binding subunit	↑	4.5	
rlmD	23S rRNA (uracil(1939)-C(5))-methyltransferase RlmD	↑	4.5	279
fim2	serotype 2 fimbrial subunit	↑	3.7	81
pheT	phenylalanine-tRNA ligase beta subunit	↑	3.7	104; 109; 351
BP3034	putative ABC transporter ATP-binding protein	↑	3.4	
topB	DNA topoisomerase iii	↑	3.4	10; 78; 414; 489; 555
plsX	phosphate acyltransferase	↑	3.0	93; 118; 321; 335
sdaA	L-serine dehydratase 1	↑	2.7	
fahA	fumarylacetoacetase	↑	2.6	
BP3744	cytochrome *c* oxidase subunit 2	↑	2.4	
BP1561	putative exported protein	↑	2.3	
gcvP	glycine dehydrogenase (decarboxylating)	↑	2.3	
BP0465	probable aldehyde dehydrogenase	↑	2.1	
bph2	DNA-binding protein Bph2	↑	2.1	45; 63
atpF	ATP synthase subunit b	↑	2.0	49; 137
dfp	coenzyme A biosynthesis bifunctional protein CoaBC	↑	2.0	289; 332; 340
BP3584	uncharacterized protein	↓	6.8	10; 58
etfB	electron transfer flavoprotein beta-subunit	↓	5.7	8; 16; 20; 32; 50; 52; 99; 102; 107; 193; 219; 241; 247
etfA	rlectron transfer flavoprotein alpha-subunit	↓	4.7	211; 219
BP0535	alkyl hydroperoxide reductase AhpD	↓	4.0	20; 27; 45
BP1738	UPF0337 protein BP1738	↓	3.5	9
BP3302	uncharacterized protein	↓	3.4	
BP3037	uncharacterized protein	↓	3.0	12; 19; 50; 60; 68; 85
BP1766	putative exported protein	↓	2.9	
groS	10 kDa chaperonin	↓	2.9	34; 47; 48; 53; 60; 64; 69; 76
BP2255	uncharacterized protein	↓	2.3	
BP2924	putative exported protein	↓	2.0	39; 66; 77; 92; 95

[a]Δ*bkd1 vs* WT-significant trend (p-value ≤ 0.05, FC ≥ 2.0) in protein expression observed in *B.p.* The Δ*bkd1* mutant compared to wild-type bacteria, as determined by the *t*-test; ↑/↓—increased/decreased protein levels in the Δ*bkd1* mutant compared to wild-type bacteria; FC—fold change difference between the Δ*bkd1* mutant and wild-type strains; and acetyl(K) site positions—localization of lysine acetylation site(s) of particular protein (if applied).

Δ*bkd1* mutant (Table 4), possibly compensating for an increased level of the potentially inhibitory acetylation of the lysine 607 residue of the essential enzyme.[46] This was accompanied by upregulated levels of the CoaBC protein involved in the biosynthesis of coenzyme A.[47]

Deletion of the *bkd1* gene also negatively affected the levels of the A and B subunits of the electron transfer flavoprotein (Table 4). However, this did not affect the capacity of the Δ*bkd1* mutant to grow in the common laboratory growth media or under iron-limiting conditions (Figure 6A). However, a metabolic deregulation was observable under carbon source-limiting conditions in the Stainer−Scholte medium without added Casamino acids and with five-fold-reduced glutamate level, where the Δ*bkd1* mutant exhibited a shorter doubling time in the exponential phase of growth (Figure 6A) and exited the exponential phase earlier than the wild-type strain (Figure S4).

Therefore, we next assessed the capacity of the Δ*bkd1* mutant strain to survive inside primary human monocyte-derived macrophages. As shown in Figure 6B, no significant difference to the wild-type bacteria in the uptake or survival of the Δ*bkd1* or Δ*bp3063* mutants inside primary human macrophages was observed. Similarly, the deletion of the *bkd1* gene did not influence bacterial autoaggregation or biofilm-forming capacities of the mutant (data not shown).

Absence of the Bkd1 Deacetylase Modulates *B. pertussis* Virulence

To examine whether the deregulated production of house-keeping proteins and the increased acetylation of the key master regulator protein BvgA affected the *in vivo* fitness of the Δ*bkd1* mutant, we compared its virulence to that of wild-type *B. pertussis* in the model of mouse lung infection. Intriguingly, the same calculated LD_{50} value of 5×10^7 CFUs was obtained for both strains in two mouse infection experiments. Nevertheless, at the $2 \times LD_{50}$ dose of 10^8 CFUs, the mice inoculated with the Δ*bkd1* mutant exhibited milder disease symptoms, without signs of lethargy or bristled fur, and were reproducibly succumbing to the infection later than the mice inoculated with an equal dose of wild-type *B. pertussis* bacteria (Figure 7).

DISCUSSION

We report that the *B. pertussis* gene BP0960 encodes a bona fide lysine deacetylase enzyme that we propose to name Bkd1. Its activity appears to control the acetylation status of a number of bacterial proteins and in particular the acetylation of some bacterial DNA-packaging proteins (Table 3). Deletion of the *bkd1* gene yielded an increase in the number of acetylated sites in the acetylome of *B. pertussis* (Table S1). Moreover, the absence of the Bkd1 enzyme translated into an alteration of the overall composition of the *B. pertussis* proteome (*c.f.* Table S3). This may reflect altered gene expression and differences in

https://dx.doi.org/10.1021/acs.jproteome.0c00178
J. Proteome Res. 2020, 19, 3680−3696

Table 5. Proteins Detected in All Replicates from One Strain and Undetectable in All Replicates of the Other Strain[a]

gene name	protein name	Δ*bkd1 vs* WT	median log 2 expression	Ac(K) site position(s)
lpxK	tetraacyldisaccharide 4-kinase	↑	27.37	
yajC	sec translocon accessory complex subunit YajC	↑	27.17	
omlA	outer membrane protein assembly factor BamE	↑	26.02	
BP3345	putative TolR-like translocation protein	↑	25.79	
BP3559	cell division protein ZipA	↑	25.73	
mnmE	tRNA modification GTPase MnmE	↑	25.56	
lep	signal peptidase I	↑	25.53	
thiL	thiamine-monophosphate kinase	↑	25.48	
BP1924	probable TetR-family transcriptional regulator	↑	25.47	
comL	outer membrane protein assembly factor BamD	↑	25.41	
BP1298	uncharacterized protein	↑	25.38	
BP2802	putative exported protein	↑	25.35	
BP1721	putative peptidase	↑	25.28	
murG	UDP-*N*-acetylglucosamine-*N*-acetylmuramyl-(pentapeptide) pyrophosphoryl-undecaprenol *N*-acetylglucosamine transferase	↑	25.25	42
BP3699	GntR family transcriptional regulator	↑	25.17	
BP3117	putative restriction endonuclease	↑	25.15	
BP3658	deoxyguanosinetriphosphate triphosphohydrolase-like protein	↑	25.15	169
BP3503	LysR-family transcriptional regulator	↑	25.14	
bfrG	putative TonB-dependent receptor	↑	25.13	
BP1864	putative exported protein	↑	25.11	
BP2547	two-component response regulatory protein	↑	25.01	
BP2757	putative cold-shock protein	↓	28.49	21
gloA	lactoylglutathione lyase	↓	27.60	120; 126
BP1736	putative exported protein	↓	26.95	
xseB	exodeoxyribonuclease 7 small subunit	↓	25.92	
BP2393	probable D-aminopeptidase	↓	25.08	

[a]Δ*bkd1 vs* WT trend in protein expression observed in *B.p.* The Δ*bkd1* mutant compared to wild-type bacteria; ↑—protein was found only in *B.p.* Δ*bkd1* mutant strain (log_2 of median intensity ≥25); ↓—protein was found only in *B.p.* The wild-type strain (log_2 of median intensity ≥25); median log_2 expression—log_2 value of median intensities of three replicates of the given sample, where the protein was present; and acetyl(K) site positions—localization of lysine acetylation site(s) of particular proteins (if applied).

stability (steady-state turnover rates) of the acetylated *versus* nonacetylated proteins, such as for the exoribonuclease RNase R from *E. coli*, the stability of which is regulated by acetylation.[48] The here-reported acetylome analysis, hence, reveals a yet unexplored layer of signaling and homeostasis regulation in *B. pertussis*.

The Bkd1 protein is a 307 residue-long polypeptide that exhibits lysine-deacetylating enzyme activity toward histone deacetylase substrates *in vitro* (Figures 1G and S3C). As documented by this acetylome study and by detection of the FLAG-tagged Bkd1 protein in bacterial lysates (Figure S2A,B), Bkd1 deacetylase is produced in lab-adapted *B. pertussis* Tohama I bacteria under standard laboratory growth conditions. According to the available transcriptomic data, expression of the *bkd1* gene is not regulated by the BvgAS master regulator of *Bordetella* virulence genes, as *bkd1* is expressed also under virulence-modulating conditions in the presence of high sulfate concentrations.[38,49] This distinguishes the *bkd1* gene from the BP3063 gene for the putative deacetylase, which tends to be negatively regulated by BvgA∼P, and is induced under modulatory conditions at high concentrations of $MgSO_4$.[38,49]

The completeness of the here-reported high-throughput acetylome analysis should be interpreted with caution when it comes to downregulated proteins yielding low-abundance acetylated peptide signals. The deletion of the *bkd1* gene not only leads to a significant increase in acetylation of many bacterial proteins but the absence of Bkd1 also affected the overall composition of the detected proteome (Figure 2D, Tables 4 and 5). For example, the α and β subunits of the electron-transfer flavoprotein (Etf) were much less abundant in the proteome of the Δ*bkd1* mutant than in the wild-type *B. pertussis* proteome (Tables 4 and S3). We did not examine if this was due to a polar effect of the *bkd1* gene deletion on the transcription of the downstream *etfB* and *etfA* genes, whether the acetylation of some of the DNA-binding protein(s) in the Δ*bkd1* mutant affected transcription of the *etfB* and *etfA* genes, or whether the deacetylase activity Bkd1 itself regulated the stability of the EtfBA complex and the turnover of its α and β subunits. Similar electron transfer flavoproteins can play essential or nonessential functions in various bacterial species[50] and we did not observe any growth defect related to downregulation of EtfBA with the Δ*bkd1* mutant under standard laboratory conditions in SSM, under limited iron supply conditions, or inside primary human macrophages, respectively (*c.f.* Figures 6 and S4A,B). Surprisingly, compared to the wild-type bacteria, the Δ*bkd1* mutant exhibited an even shorter doubling time during the exponential phase of growth under reduced carbon source availability conditions (Figures 6A and S4C). It will, hence, be of interest to determine whether this was solely due to upregulated expression of the acetyl-coenzyme A synthetase system in the Δ*bkd1* mutant (*c.f.* Table 4) or the deregulation and synergy of several enzymes of the energy metabolism of the bacterium was involved in this phenotype.

https://dx.doi.org/10.1021/acs.jproteome.0c00178
J. Proteome Res. 2020, 19, 3680−3696

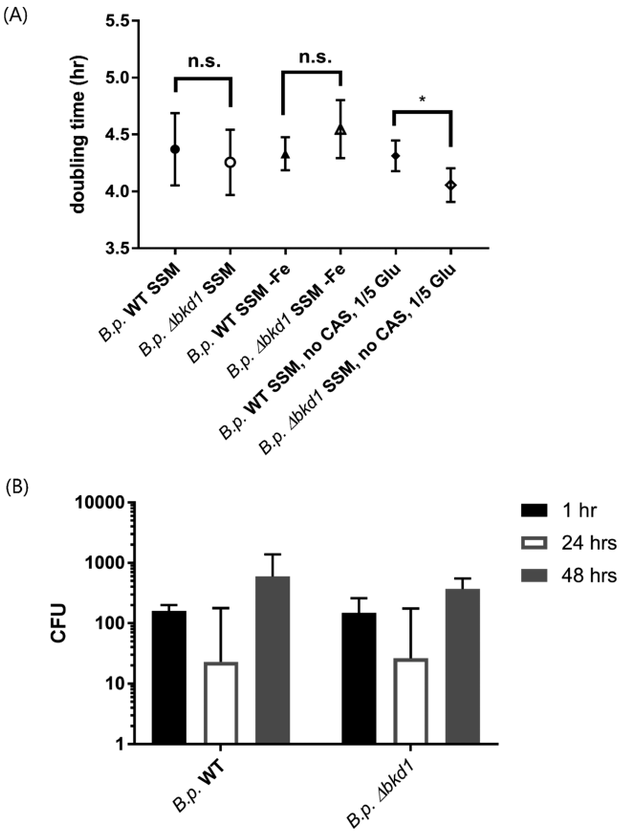

Figure 6. Phenotypic characterization of wild-type and Δ*bkd1* mutant strains of *B. pertussis*. (A) Comparison of median doubling time during the exponential phase under different growth conditions. (B) Survival of wild-type and Δ*bkd1* mutant strains of *B. pertussis* inside primary human macrophages. The infected cells were lysed after 1 h of infection or were incubated for additional 24 or 48 h prior to lysis and the CFUs of recovered bacteria were determined by plating on Bordet-Gengou agar. The values represent median values with error bars indicating the range of the values obtained with cells of six (1 and 24 h) or four (48 h) anonymous healthy donors.

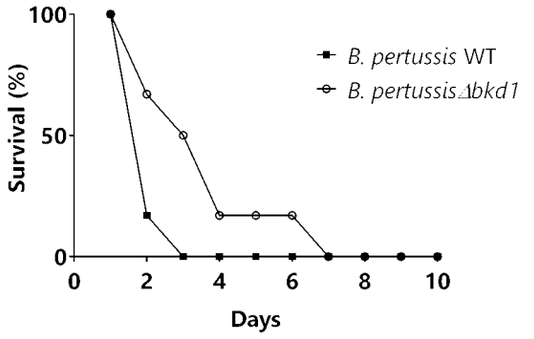

Figure 7. Δ*bkd1* mutant exhibits reduced virulence *in vivo*. Groups of five week-old 6 Balb/c mice were intranasally inoculated with 10^8 CFUs of wild-type or Δ*bkd1* mutant *B. pertussis* suspended in 50 μL of SSM and mice survival was monitored for 10 days. The shown result is representative of two performed infection experiments.

Indeed, protein acetylation has previously been linked to metabolic processes in living organisms.[46,51,52] Intriguingly, an extensive acetylation of the *Bordetella* virulence master regulator protein BvgA[38] was observed in the Δ*bkd1* mutant, raising the hypothesis that acetylation might modulate the activation of BvgA through phosphorylation of its Asp 54 residue by BvgS[12,53] as a function of the metabolic state of the bacteria. However, this was not observed when bacteria were grown *in vitro* in a standard (not shown) or reduced carbon source liquid medium (Figure 5), where unaltered amounts of total BvgA protein and its even higher relative level of phosphorylation was observed in the Δ*bkd1* mutant compared to wild-type bacteria. Moreover, in an *in vitro* virulence assay, no impact of the deletion of the *bkd1* gene on the intracellular survival of the Δ*bkd1* mutant inside primary human macrophages was observed (Figure 6B). However, a modest impact of the absence of the Bkd1 deacetylase on virulence of the bacteria was observed in the course of mouse lung infection *in vivo*. Intranasal inoculation by the Δ*bkd1* mutant provoked milder disease symptoms and a delayed death of the experimental animals than an equal dose of wild-type *B. pertussis* bacteria (*c.f.* Figure 7). Because no effect of the lack of Bkd1 enzyme on BvgA∼P levels or virulence factor production was observed under *in vitro* conditions, it is plausible to assume that the somewhat reduced virulence of the Δ*bkd1* mutant in mouse lungs was due to reduced fitness resulting from deregulation of its housekeeping functions.

The Δ*bkd1* mutant acetylome composition suggests a testable hypothesis that the enhanced acetylation of the DNA-packaging proteins BpH3 and IHFα (Figure 4C and Table 3) may have contributed to alteration of gene expression and thereby affected the alteration of composition of the Δ*bkd1* proteome. Indeed, such an effect of acetylation on the DNA-binding ability of bacterial histone-like proteins was described for the HU protein of *Mycobacterium tuberculosis* (MtHU).[54] Furthermore, the acetylation of the histone-like protein HBsu in *Bacillus subtilis* was also linked to regulation of nucleoid compaction.[55] We found that the two additional histone-like DNA-binding proteins of *Bordetella*, BpH1[56] and BpH2,[57] were present at increased levels in the proteome of the Δ*bkd1* mutant (Table S3) but their level of acetylation was not significantly increased (Figure 4C and Table 3). The increased acetylation of the BpH3 protein is likely to affect gene transcription, as BpH3 was shown to be functionally homologous to H-NS, the prototypic bacterial histone-like protein of *E. coli*,[58] designated as "factor H"[59] that binds double-stranded DNA with high affinity.[60] By analogy, the N-terminal domain of BpH3 would account for oligomerization and the C-terminal domain would account for DNA-binding capacity of BpH3. The extensive acetylation of BpH3 at six sites along the protein would possibly modulate both of these abilities. Increased acetylation was observed in the Δ*bkd1* mutant also for the carboxy-proximal lysine 78 residue of the DNA-binding protein HUβ (*c. f.* Figure 4C), which belongs to histone-like HU proteins that structure bacterial chromosomes.[61−63] However, the acetylation was located on a predicted β-strand that is not conserved in *E. coli* HUβ, and it thus remains open if this acetylation has any potential to affect the affinity of HUβ for DNA.[64] An altered amount and acetylation status were further found for the integration host factor subunit alpha (IHFα) that is known to modulate transcription of many target genes[41] and is most often found bound to transcriptionally silent portions of the bacterial chromosome.[65] Hence, a testable hypothesis would be that reduction of its total amount and the acetylation of lysine residues 54 and 75 of IHFα may have led to derepression of

https://dx.doi.org/10.1021/acs.jproteome.0c00178
J. Proteome Res. 2020, 19, 3680−3696

some genes and thereby may have contributed to altered composition of the Δ*bkd1* proteome.

In conclusion, we show that the BP0960/*bkd1* gene of *B. pertussis* encodes a lysine deacetylase enzyme that exhibits a histone deacetylase enzyme-like activity *in vitro* and acts as a regulator of the bacterial metabolism. In this study, we identified a whole plethora of Bkd1 substrates, as deletion of the gene for the deacetylase resulted in increased acetylation of many bacterial proteins, including the *Bordetella* virulence regulator protein BvgA, or the histone-like DNA-packaging proteins of *B. pertussis*.

■ ASSOCIATED CONTENT

Supporting Information

The Supporting Information is available free of charge at https://pubs.acs.org/doi/10.1021/acs.jproteome.0c00178.

Sequence comparison of BP3063 and bacterial acetylpolyamine aminohydrolases with the identity matrix and phylogenetic tree. Western blot analysis of mutant bacterial cultures with FLAG-tagged N- or C-termini on the genome. Preparation of recombinant proteins and their functional analysis. Growth rate comparison of *B. pertussis* WT and Δ*bkd1* strains in different media. Entire membrane of the western blot, which is presented in the Figure 5 (PDF)

All acetylated lysine sites found in wild-type, Δ*bkd1*, and Δ*bp3063* mutant bacteria (XLSX)

GO term enrichment analysis of the whole acetylome (XLSX)

Total proteome of wild-type, Δ*bkd1*, and Δ*bp3063* mutant bacteria (XLSX)

List of primers used in this study (XLSX)

Modification-specific peptides (XLSX)

■ AUTHOR INFORMATION

Corresponding Author

Peter Sebo − *Institute of Microbiology of the Czech Academy of Sciences, Prague 14220, Czech Republic;* orcid.org/0000-0002-9755-7715; Phone: (+420) 241062762; Email: sebo@biomed.cas.cz

Authors

Jakub Novak − *Institute of Microbiology of the Czech Academy of Sciences, Prague 14220, Czech Republic; Faculty of Science, Charles University, Prague 11636, Czech Republic*

Ivo Fabrik − *Biomedical Research Center, University Hospital Hradec Kralove, Hradec Kralove 50005, Czech Republic*

David Jurnecka − *Institute of Microbiology of the Czech Academy of Sciences, Prague 14220, Czech Republic; Faculty of Science, Charles University, Prague 11636, Czech Republic*

Jana Holubova − *Institute of Microbiology of the Czech Academy of Sciences, Prague 14220, Czech Republic*

Ondrej Stanek − *Institute of Microbiology of the Czech Academy of Sciences, Prague 14220, Czech Republic*

Complete contact information is available at: https://pubs.acs.org/10.1021/acs.jproteome.0c00178

Author Contributions

J.N. designed the study, performed research, analyzed the data, and wrote the paper; I.F. prepared, collected, and processed the samples for the acetylome analysis and performed quantification and statistics; D.J. performed research (cloning and purification, structural biology); J.H. constructed bacterial mutant strains with FLAG-tags and performed the *in vivo* mice experiments; O.S. performed the *in vivo* mice experiments; and P.S. contributed to study design and data interpretation and wrote the paper. The manuscript was written through contributions of all authors. All authors have given approval to the final version of the manuscript.

Funding

This work was supported by the grants 19-27630X (P.S.) and 18-20621S (P.S.) from the Czech Science Foundation, NV16-28126A (P.S.) of the Agency for Health Research and from the EATRIS infrastructure: LM2015064 (P.S.) from Ministry of Education, Youth and Sports of the Czech Republic, the grant MH CZ—DRO (UHHK, 00179906) from Ministry of Health, Czech Republic (I.F.) and by grant no. 228216 from the Grant Agency of the Charles University (J.N., D.J.). The funders had no role in study design, data collection, and interpretation or the decision to submit the work for publication.

Notes

The authors declare no competing financial interest.

■ ACKNOWLEDGMENTS

The help of Dr. Karolína Škopová with generation of the Δ*bkd1* and Δ*bp3063* mutants, the gift of HDAC6 by Dr. Cyril Bařinka and anti-BvgA serum by Dr. Branislav Večerek and the technical assistance of Hana Lukeová and Iva Maršíková are gratefully acknowledged.

■ REFERENCES

(1) Melvin, J. A.; Scheller, E. V.; Miller, J. F.; Cotter, P. A. Bordetella Pertussis Pathogenesis: Current and Future Challenges. *Nat. Rev. Microbiol.* **2014**, *12*, 274−288.

(2) Vojtova, J.; Kamanova, J.; Sebo, P. Bordetella Adenylate Cyclase Toxin: A Swift Saboteur of Host Defense. *Curr. Opin. Microbiol.* **2006**, *9*, 69−75.

(3) Walsh, C. T.; Garneau-Tsodikova, S.; Gatto, G. J. Protein Posttranslational Modifications: The Chemistry of Proteome Diversifications. *Angew. Chem., Int. Ed. Engl.* **2005**, *44*, 7342−7372.

(4) Ren, J.; Sang, Y.; Lu, J.; Yao, Y.-F. Protein Acetylation and Its Role in Bacterial Virulence. *Trends Microbiol.* **2017**, *25*, 768−779.

(5) Wagner, G. R.; Payne, R. M. Widespread and Enzyme-independentNε-Acetylation andNε-Succinylation of Proteins in the Chemical Conditions of the Mitochondrial Matrix. *J. Biol. Chem.* **2013**, *288*, 29036−29045.

(6) Christensen, D. G.; Baumgartner, J. T.; Xie, X.; Jew, K. M.; Basisty, N.; Schilling, B.; Kuhn, M. L.; Wolfe, A. J. Mechanisms, Detection, and Relevance of Protein Acetylation in Prokaryotes. *mBio* **2019**, *10*, No. e02708.

(7) Yang, X.-J.; Seto, E. Lysine Acetylation: Codified Crosstalk with Other Posttranslational Modifications. *Mol. Cell* **2008**, *31*, 449−461.

(8) Christensen, D. G.; Xie, X.; Basisty, N.; Byrnes, J.; McSweeney, S.; Schilling, B.; Wolfe, A. J. Post-Translational Protein Acetylation: An Elegant Mechanism for Bacteria to Dynamically Regulate Metabolic Functions. *Front. Microbiol.* **2019**, *10*, 1604.

(9) Choudhary, C.; Kumar, C.; Gnad, F.; Nielsen, M. L.; Rehman, M.; Walther, T. C.; Olsen, J. V.; Mann, M. Lysine Acetylation Targets Protein Complexes and Co-Regulates Major Cellular Functions. *Science* **2009**, *325*, 834−840.

(10) Ren, J.; Sang, Y.; Tan, Y.; Tao, J.; Ni, J.; Liu, S.; Fan, X.; Zhao, W.; Lu, J.; Wu, W.; Yao, Y.-F. Acetylation of Lysine 201 Inhibits the DNA-Binding Ability of PhoP to Regulate Salmonella Virulence. *PLoS Pathog.* **2016**, *12*, No. e1005458.

(11) Qin, R.; Sang, Y.; Ren, J.; Zhang, Q.; Li, S.; Cui, Z.; Yao, Y.-F. The Bacterial Two-Hybrid System Uncovers the Involvement of

Acetylation in Regulating of Lrp Activity in Salmonella Typhimurium. *Front. Microbiol.* **2016**, *7*, 1864.
(12) Boulanger, A.; Chen, Q.; Hinton, D. M.; Stibitz, S. In Vivo Phosphorylation Dynamics of the Bordetella Pertussis Virulence-Controlling Response Regulator BvgA: In Vivo Phosphorylation of BvgA. *Mol. Microbiol.* **2013**, *88*, 156−172.
(13) Chen, Q.; Ng, V.; Warfel, J. M.; Merkel, T. J.; Stibitz, S. Activation of Bvg-Repressed Genes in Bordetella Pertussis by RisA Requires Cross Talk from Noncooperonic Histidine Kinase RisK. *J. Bacteriol.* **2017**, *199*, No. e00475.
(14) Caro, V.; Hot, D.; Guigon, G.; Hubans, C.; Arrivé, M.; Soubigou, G.; Renauld-Mongénie, G.; Antoine, R.; Locht, C.; Lemoine, Y.; Guiso, N. Temporal Analysis of French Bordetella Pertussis Isolates by Comparative Whole-Genome Hybridization. *Microb. Infect.* **2006**, *8*, 2228−2235.
(15) Stainer, D. W.; Scholte, M. J. A Simple Chemically Defined Medium for the Production of Phase I Bordetella Pertussis. *J. Gen. Microbiol.* **1970**, *63*, 211−220.
(16) Skopova, K.; Tomalova, B.; Kanchev, I.; Rossmann, P.; Svedova, M.; Adkins, I.; Bibova, I.; Tomala, J.; Masin, J.; Guiso, N.; Osicka, R.; Sedlacek, R.; Kovar, M.; Sebo, P. Cyclic AMP-Elevating Capacity of Adenylate Cyclase Toxin-Hemolysin Is Sufficient for Lung Infection but Not for Full Virulence of Bordetella Pertussis. *Infect. Immun.* **2017**, *85*, No. e00937.
(17) Stibitz, S. [35] Use of conditionally counterselectable suicide vectors for allelic exchange. *Methods Enzymol.* **1994**, *235*, 458−465.
(18) Wegener, D.; Hildmann, C.; Riester, D.; Schwienhorst, A. Improved Fluorogenic Histone Deacetylase Assay for High-Throughput-Screening Applications. *Anal. Biochem.* **2003**, *321*, 202−208.
(19) Menck, K.; Behme, D.; Pantke, M.; Reiling, N.; Binder, C.; Pukrop, T.; Klemm, F. Isolation of Human Monocytes by Double Gradient Centrifugation and Their Differentiation to Macrophages in Teflon-Coated Cell Culture Bags. *J. Visualized Exp.* **2014**, *91*, 51554.
(20) Rappsilber, J.; Mann, M.; Ishihama, Y. Protocol for Micro-Purification, Enrichment, Pre-Fractionation and Storage of Peptides for Proteomics Using StageTips. *Nat. Protoc.* **2007**, *2*, 1896−1906.
(21) Cox, J.; Mann, M. MaxQuant Enables High Peptide Identification Rates, Individualized p.p.b.-Range Mass Accuracies and Proteome-Wide Protein Quantification. *Nat. Biotechnol.* **2008**, *26*, 1367−1372.
(22) Cox, J.; Hein, M. Y.; Luber, C. A.; Paron, I.; Nagaraj, N.; Mann, M. Accurate Proteome-Wide Label-Free Quantification by Delayed Normalization and Maximal Peptide Ratio Extraction, Termed MaxLFQ. *Mol. Cell. Proteomics* **2014**, *13*, 2513−2526.
(23) Tyanova, S.; Temu, T.; Sinitcyn, P.; Carlson, A.; Hein, M. Y.; Geiger, T.; Mann, M.; Cox, J. The Perseus Computational Platform for Comprehensive Analysis of (Prote)Omics Data. *Nat. Methods* **2016**, *13*, 731−740.
(24) Waterhouse, A. M.; Procter, J. B.; Martin, D. M. A.; Clamp, M.; Barton, G. J. Jalview Version 2−a Multiple Sequence Alignment Editor and Analysis Workbench. *Bioinformatics* **2009**, *25*, 1189−1191.
(25) Katoh, K.; Standley, D. M. MAFFT Multiple Sequence Alignment Software Version 7: Improvements in Performance and Usability. *Mol. Biol. Evol.* **2013**, *30*, 772−780.
(26) Sievers, F.; Wilm, A.; Dineen, D.; Gibson, T. J.; Karplus, K.; Li, W.; Lopez, R.; McWilliam, H.; Remmert, M.; Söding, J.; Thompson, J. D.; Higgins, D. G. Fast, Scalable Generation of High-Quality Protein Multiple Sequence Alignments Using Clustal Omega. *Mol. Syst. Biol.* **2011**, *7*, 539.
(27) Cheng, A.; Grant, C. E.; Noble, W. S.; Bailey, T. L. MoMo: Discovery of Statistically Significant Post-Translational Modification Motifs. *Bioinformatics* **2019**, *35*, 2774−2782.
(28) Chou, M. F.; Schwartz, D. Biological Sequence Motif Discovery Using Motif-x. In *Current Protocols in Bioinformatics*; Baxevanis, A. D., Petsko, G. A., Stein, L. D., Stormo, G. D., Eds.; John Wiley & Sons, Inc.: Hoboken, NJ, USA, 2011; p bi1315s35.
(29) Shannon, P. Cytoscape: A Software Environment for Integrated Models of Biomolecular Interaction Networks. *Genome Res.* **2003**, *13*, 2498−2504.
(30) Bindea, G.; Mlecnik, B.; Hackl, H.; Charoentong, P.; Tosolini, M.; Kirilovsky, A.; Fridman, W.-H.; Pagès, F.; Trajanoski, Z.; Galon, J. ClueGO: A Cytoscape Plug-in to Decipher Functionally Grouped Gene Ontology and Pathway Annotation Networks. *Bioinformatics* **2009**, *25*, 1091−1093.
(31) Chen, Q.; Boulanger, A.; Hinton, D. M.; Stibitz, S. Separation and Detection of Phosphorylated and Nonphosphorylated BvgA, a Bordetella Pertussis Response Regulator, in Vivo and in Vitro. *Bio-Protoc.* **2013**, *3*, No. e970.
(32) Keidel, K.; Amman, F.; Bibova, I.; Drzmisek, J.; Benes, V.; Hot, D.; Vecerek, B. Signal Transduction-Dependent Small Regulatory RNA Is Involved in Glutamate Metabolism of the Human Pathogen Bordetella Pertussis. *RNA* **2018**, *24*, 1530−1541.
(33) Mitchell, A. L.; Attwood, T. K.; Babbitt, P. C.; Blum, M.; Bork, P.; Bridge, A.; Brown, S. D.; Chang, H.-Y.; El-Gebali, S.; Fraser, M. I.; Gough, J.; Haft, D. R.; Huang, H.; Letunic, I.; Lopez, R.; Luciani, A.; Madeira, F.; Marchler-Bauer, A.; Mi, H.; Natale, D. A.; Necci, M.; Nuka, G.; Orengo, C.; Pandurangan, A. P.; Paysan-Lafosse, T.; Pesseat, S.; Potter, S. C.; Qureshi, M. A.; Rawlings, N. D.; Redaschi, N.; Richardson, L. J.; Rivoire, C.; Salazar, G. A.; Sangrador-Vegas, A.; Sigrist, C. J. A.; Sillitoe, I.; Sutton, G. G.; Thanki, N.; Thomas, P. D.; Tosatto, S. C. E.; Yong, S.-Y.; Finn, R. D. InterPro in 2019: Improving Coverage, Classification and Access to Protein Sequence Annotations. *Nucleic Acids Res.* **2019**, *47*, D351−D360.
(34) Williamson, Y. M.; Moura, H.; Whitmon, J.; Woolfitt, A. R.; Schieltz, D. M.; Rees, J. C.; Guo, S.; Kirkham, H.; Bouck, D.; Ades, E. W.; Tondella, M. L.; Carlone, G. M.; Sampson, J. S.; Barr, J. R. A Proteomic Characterization of Bordetella Pertussis Clinical Isolates Associated with a California State Pertussis Outbreak. *Int. J. Proteomics* **2015**, *2015*, 1.
(35) Alvarez Hayes, J.; Lamberti, Y.; Surmann, K.; Schmidt, F.; Völker, U.; Rodriguez, M. E. Shotgun Proteome Analysis of Bordetella Pertussis Reveals a Distinct Influence of Iron Availability on the Bacterial Metabolism, Virulence, and Defense Response. *Proteonomics* **2015**, *15*, 2258−2266.
(36) Lombardi, P. M.; Angell, H. D.; Whittington, D. A.; Flynn, E. F.; Rajashankar, K. R.; Christianson, D. W. Structure of Prokaryotic Polyamine Deacetylase Reveals Evolutionary Functional Relationships with Eukaryotic Histone Deacetylases. *Biochemistry* **2011**, *50*, 1808−1817.
(37) Szklarczyk, D.; Gable, A. L.; Lyon, D.; Junge, A.; Wyder, S.; Huerta-Cepas, J.; Simonovic, M.; Doncheva, N. T.; Morris, J. H.; Bork, P.; Jensen, L. J.; Mering, C. v. STRING V11: Protein-Protein Association Networks with Increased Coverage, Supporting Functional Discovery in Genome-Wide Experimental Datasets. *Nucleic Acids Res.* **2019**, *47*, D607−D613.
(38) Moon, K.; Bonocora, R. P.; Kim, D. D.; Chen, Q.; Wade, J. T.; Stibitz, S.; Hinton, D. M. The BvgAS Regulon of Bordetella Pertussis. *mBio* **2017**, *8*, No. e01526.
(39) Coutte, L.; Huot, L.; Antoine, R.; Slupek, S.; Merkel, T. J.; Chen, Q.; Stibitz, S.; Hot, D.; Locht, C. The Multifaceted RisA Regulon of Bordetella Pertussis. *Sci. Rep.* **2016**, *6*, 32774.
(40) Fennelly, N. K.; Sisti, F.; Higgins, S. C.; Ross, P. J.; van der Heide, H.; Mooi, F. R.; Boyd, A.; Mills, K. H. G. Bordetella Pertussis Expresses a Functional Type III Secretion System That Subverts Protective Innate and Adaptive Immune Responses. *Infect. Immun.* **2008**, *76*, 1257−1266.
(41) Arfin, S. M.; Long, A. D.; Ito, E. T.; Tolleri, L.; Riehle, M. M.; Paegle, E. S.; Hatfield, G. W. Global Gene Expression Profiling in Escherichia Coli K12: THE EFFECTS OF INTEGRATION HOST FACTOR. *J. Biol. Chem.* **2000**, *275*, 29672−29684.
(42) Oberto, J.; Drlica, K.; Rouvière-Yaniv, J. Histones, HMG, HU, IHF: Même combat. *Biochimie* **1994**, *76*, 901−908.
(43) Stockbauer, K. E.; Fuchslocher, B.; Miller, J. F.; Cotter, P. A. Identification and Characterization of BipA, a Bordetella Bvg-Intermediate Phase Protein. *Mol. Microbiol.* **2001**, *39*, 65−78.

https://dx.doi.org/10.1021/acs.jproteome.0c00178
J. Proteome Res. 2020, 19, 3680−3696

(44) Williams, C. L.; Haines, R.; Cotter, P. A. Serendipitous Discovery of an Immunoglobulin-Binding Autotransporter in Bordetella Species. *Infect. Immun.* **2008**, *76*, 2966−2977.
(45) Finn, T. M.; Stevens, L. A. Tracheal Colonization Factor: A Bordetella Pertussis Secreted Virulence Determinant. *Mol. Microbiol.* **1995**, *16*, 625−634.
(46) Castaño-Cerezo, S.; Bernal, V.; Post, H.; Fuhrer, T.; Cappadona, S.; Sánchez-Díaz, N. C.; Sauer, U.; Heck, A. J.; Altelaar, A. M.; Cánovas, M. Protein Acetylation Affects Acetate Metabolism, Motility and Acid Stress Response in Escherichia Coli. *Mol. Syst. Biol.* **2014**, *10*, 762.
(47) Evans, J. C.; Trujillo, C.; Wang, Z.; Eoh, H.; Ehrt, S.; Schnappinger, D.; Boshoff, H. I. M.; Rhee, K. Y.; Barry, C. E.; Mizrahi, V. Validation of CoaBC as a Bactericidal Target in the Coenzyme A Pathway of Mycobacterium Tuberculosis. *ACS Infect. Dis.* **2016**, *2*, 958−968.
(48) Liang, W.; Malhotra, A.; Deutscher, M. P. Acetylation Regulates the Stability of a Bacterial Protein: Growth Stage-Dependent Modification of RNase R. *J. Mol. Cell* **2011**, *44*, 160−166.
(49) Gouw, D. d.; Hermans, P. W. M.; Bootsma, H. J.; Zomer, A.; Heuvelman, K.; Diavatopoulos, D. A.; Mooi, F. R. Differentially Expressed Genes in Bordetella Pertussis Strains Belonging to a Lineage Which Recently Spread Globally. *PLoS One* **2014**, *9*, No. e84523.
(50) Bloodworth, R. A. M.; Zlitni, S.; Brown, E. D.; Cardona, S. T. An Electron Transfer Flavoprotein Is Essential for Viability and Its Depletion Causes a Rod-to-Sphere Change in Burkholderia Cenocepacia. *Microbiology* **2015**, *161*, 1909−1920.
(51) Wang, Q.; Zhang, Y.; Yang, C.; Xiong, H.; Lin, Y.; Yao, J.; Li, H.; Xie, L.; Zhao, W.; Yao, Y.; Ning, Z.-B.; Zeng, R.; Xiong, Y.; Guan, K.-L.; Zhao, S.; Zhao, G.-P. Acetylation of Metabolic Enzymes Coordinates Carbon Source Utilization and Metabolic Flux. *Science* **2010**, *327*, 1004−1007.
(52) Zhao, S.; Xu, W.; Jiang, W.; Yu, W.; Lin, Y.; Zhang, T.; Yao, J.; Zhou, L.; Zeng, Y.; Li, H.; Li, Y.; Shi, J.; An, W.; Hancock, S. M.; He, F.; Qin, L.; Chin, J.; Yang, P.; Chen, X.; Lei, Q.; Xiong, Y.; Guan, K.-L. Regulation of Cellular Metabolism by Protein Lysine Acetylation. *Science* **2010**, *327*, 1000−1004.
(53) Uhl, M. A.; Miller, J. F. Autophosphorylation and Phosphotransfer in the Bordetella Pertussis BvgAS Signal Transduction Cascade. *Proc. Natl. Acad. Sci. U.S.A.* **1994**, *91*, 1163−1167.
(54) Ghosh, S.; Padmanabhan, B.; Anand, C.; Nagaraja, V. Lysine acetylation of theMycobacterium tuberculosisHU protein modulates its DNA binding and genome organization. *Mol. Microbiol.* **2016**, *100*, 577−588.
(55) Carabetta, V. J.; Greco, T. M.; Cristea, I. M.; Dubnau, D. YfmK is an Nε-lysine acetyltransferase that directly acetylates the histone-like protein HBsu in Bacillus subtilis. *Proc. Natl. Acad. Sci. U.S.A.* **2019**, *116*, 3752−3757.
(56) Zu, T.; Goyard, S.; Rappuoli, R.; Scarlato, V. DNA Binding of the Bordetella Pertussis H1 Homolog Alters in Vitro DNA Flexibility. *J. Bacteriol.* **1996**, *178*, 2982−2985.
(57) Goyard, S. Identification and Characterization of BpH2, a Novel Histone H1 Homolog in Bordetella Pertussis. *J. Bacteriol.* **1996**, *178*, 3066−3071.
(58) Goyard, S.; Bertin, P. Characterization of BpH3, an H-NS-like Protein in Bordetella Pertussis. *Mol. Microbiol.* **1997**, *24*, 815−823.
(59) Jacquet, M.; Cukier-Kahn, R.; Pla, J.; Gros, F. A Thermostable Protein Factor Acting on in Vitro DNA Transcription. *Biochem. Biophys. Res. Commun.* **1971**, *45*, 1597−1607.
(60) Friedrich, K.; Gualerzi, C. O.; Lammi, M.; Losso, M. A.; Pon, C. L. Proteins from the Prokaryotic Nucleoid. Interaction of Nucleic Acids with the 15 KDa Escherichia Coli Histone-like Protein H-NS. *FEBS Lett.* **1988**, *229*, 197−202.
(61) Balandina, A.; Kamashev, D.; Rouviere-Yaniv, J. The Bacterial Histone-like Protein HU Specifically Recognizes Similar Structures in All Nucleic Acids: DNA, RNA, AND THEIR HYBRIDS. *J. Biol. Chem.* **2002**, *277*, 27622−27628.
(62) Dame, R. T.; Goosen, N. HU: Promoting or Counteracting DNA Compaction? *FEBS Lett.* **2002**, *529*, 151−156.
(63) van Noort, J.; Verbrugge, S.; Goosen, N.; Dekker, C.; Dame, R. T. Dual Architectural Roles of HU: Formation of Flexible Hinges and Rigid Filaments. *Proc. Natl. Acad. Sci.* **2004**, *101*, 6969−6974.
(64) Dilweg, I. W.; Dame, R. T. Post-Translational Modification of Nucleoid-Associated Proteins: An Extra Layer of Functional Modulation in Bacteria? *Biochem. Soc. Trans.* **2018**, *46*, 1381−1392.
(65) Grainger, D. C.; Hurd, D.; Goldberg, M. D.; Busby, S. J. W. Association of Nucleoid Proteins with Coding and Non-Coding Segments of the Escherichia Coli Genome. *Nucleic Acids Res.* **2006**, *34*, 4642−4652.

https://dx.doi.org/10.1021/acs.jproteome.0c00178
J. Proteome Res. 2020, 19, 3680−3696

APPENDIX III

A Mutation Upstream of the *rplN-rpsD* Ribosomal Operon Downregulates *Bordetella pertussis* Virulence Factor Production without Compromising Bacterial Survival within Human Macrophages

Novák J, Jurnečka D, Linhartová I, Holubová J, Staněk O, Štipl D, Dienstbier A, Večerek B, Azevedo N, Provazník J, Beneš V, Šebo P.

mSystems. 2020 Dec 8;5(6):e00612-20. doi: 10.1128/mSystems.00612-20.

AMERICAN SOCIETY FOR MICROBIOLOGY | mSystems®

RESEARCH ARTICLE
Molecular Biology and Physiology

A Mutation Upstream of the *rplN-rpsD* Ribosomal Operon Downregulates *Bordetella pertussis* Virulence Factor Production without Compromising Bacterial Survival within Human Macrophages

Jakub Novák,[a] David Jurnečka,[a] Irena Linhartová,[a] Jana Holubová,[a] Ondřej Staněk,[a] Daniel Štipl,[b] Ana Dienstbier,[b] Branislav Večerek,[b] Nayara Azevedo,[c] Jan Provazník,[c] Vladimír Beneš,[c] Peter Šebo[a]

[a]Laboratory of Molecular Biology of Bacterial Pathogens, Institute of Microbiology of the Czech Academy of Sciences, Prague, Czech Republic
[b]Laboratory of Post-Transcriptional Control of Gene Expression, Institute of Microbiology of the Czech Academy of Sciences, Prague, Czech Republic
[c]Genomics Core Facility, European Molecular Biology Laboratory, Services and Technology Unit, Heidelberg, Germany

ABSTRACT The BvgS/BvgA two-component system controls expression of ~550 genes of *Bordetella pertussis*, of which, ~245 virulence-related genes are positively regulated by the BvgS-phosphorylated transcriptional regulator protein BvgA (BvgA~P). We found that a single G-to-T nucleotide transversion in the 5′-untranslated region (5′-UTR) of the *rplN* gene enhanced transcription of the ribosomal protein operon and of the *rpoA* gene and provoked global dysregulation of *B. pertussis* genome expression. This comprised overproduction of the alpha subunit (RpoA) of the DNA-dependent RNA polymerase, downregulated BvgA and BvgS protein production, and impaired production and secretion of virulence factors by the mutant. Nonetheless, the mutant survived like the parental bacteria for >2 weeks inside infected primary human macrophages and persisted within infected mouse lungs for a longer period than wild-type *B. pertussis*. These observations suggest that downregulation of virulence factor production by bacteria internalized into host cells may enable persistence of the whooping cough agent in the airways.

IMPORTANCE We show that a spontaneous mutation that upregulates transcription of an operon encoding ribosomal proteins and causes overproduction of the downstream-encoded α subunit (RpoA) of RNA polymerase causes global effects on gene expression levels and proteome composition of *Bordetella pertussis*. Nevertheless, the resulting important downregulation of the BvgAS-controlled expression of virulence factors of the whooping cough agent did not compromise its capacity to persist for prolonged periods inside primary human macrophage cells, and it even enhanced its capacity to persist in infected mouse lungs. These observations suggest that the modulation of BvgAS-controlled expression of virulence factors may occur also during natural infections of human airways by *Bordetella pertussis* and may possibly account for long-term persistence of the pathogen within infected cells of the airways.

KEYWORDS *Bordetella pertussis*, host-pathogen interactions, intracellular bacteria, macrophages, two-component regulatory systems, virulence regulation

The Gram-negative coccobacillus *Bordetella pertussis* is an exclusively human pathogen and the major agent of the respiratory infectious disease called pertussis, or whooping cough (1). Pertussis used to be the primary cause of infant mortality in developed countries prior to the introduction of whole-cell pertussis vaccines (wP) in the 1950s (2–5). Despite worldwide vaccination coverage, pertussis still remains the least-controlled vaccine-preventable infectious disease, accounting for more than 12

Citation Novák J, Jurnečka D, Linhartová I, Holubová J, Staněk O, Štipl D, Dienstbier A, Večerek B, Azevedo N, Provazník J, Beneš V, Šebo P. 2020. A mutation upstream of the *rplN-rpsD* ribosomal operon downregulates *Bordetella pertussis* virulence factor production without compromising bacterial survival within human macrophages. mSystems 5:e00612-20. https://doi.org/10.1128/mSystems.00612-20.

Editor Tricia A. Van Laar, California State University, Fresno

Address correspondence to Peter Šebo, sebo@biomed.cas.cz.

Received 1 July 2020
Accepted 6 November 2020
Published 8 December 2020

million whooping cough cases annually worldwide and causing >100,000 pertussis deaths a year (2). Moreover, pertussis recently resurged in the most-developed countries due to the introduction of less-reactogenic acellular pertussis vaccines (aP) that confer shorter-lasting protection and fail to control transmission of the infection in vaccinated populations (6). Furthermore, the generalized pressure of the aP vaccine has promoted emergence of variants of antigens contained in the aP vaccines and has selected for globally spreading pertactin-deficient *B. pertussis* isolates that escape opsonization by the aP vaccine-induced antibodies (7–10).

In the course of adaptation to the human host, the recently evolved *B. pertussis* species lost numerous genes of its *Bordetella bronchiseptica*-like ancestor, and it represents a genetically monomorphic species that exhibits a low diversity of coding sequences and a low degree of antigenic variability between clinical isolates (6, 11). Nonetheless, the genome of *B. pertussis* harbors numerous copies (up to ~240 copies) of the IS*481* insertion element, and recombination events between them generate a highly variable chromosomal architecture of the clinical isolates (12, 13). It remains to be determined whether this fluidity of genome organization and occasional duplication of portions of the genome enhance bacterial fitness and enable the bacterium to dynamically adapt to the selective pressure of the environment within host airways (11, 13–16).

B. pertussis expresses a whole array of virulence factors, producing four known immunomodulatory protein toxins, namely, the pertussis toxin (PT), the adenylate cyclase toxin-hemolysin (CyaA, ACT, or AC-Hly), the dermonecrotic toxin (DNT) and the type III secretion system effector BteA. The bacterium also employs several types of adhesins, such as fimbriae (FIM), filamentous hemagglutinin (FHA), or pertactin (PRN), and produces at least two major complement resistance factors, the autotransporter proteins Vag8 and BrkA (1, 17–20). Intriguingly, *B. pertussis* mutants deficient in expression of PT or PRN are still able to infect humans and can invade epithelial cells (8, 21). The bacterium produces several additional outer membrane autotransporter proteins of unknown function, and it remains to be determined whether additional toxins and virulence factors are to be discovered among the proteins of unknown function encoded in the *B. pertussis* genome.

The transcription of *B. pertussis* virulence factor genes is controlled by the master regulator of *Bordetella* virulence (*vir*), the BvgAS two-component system. This consists of a membrane-inserted BvgS sensor kinase that in the Bvg$^+$ phase phosphorylates the regulatory transcription factor BvgA (22). Binding of phosphorylated BvgA (BvgA~P) to multiple sites in the promoter regions of the so-called "*vir*-activated genes" (*vag*) then activates transcription of ~245 virulence-related genes and indirectly represses expression of ~326 so-called "*vir*-repressed genes" (*vrg*), which get expressed in the Bvg$^-$ phase of *B. pertussis* (23, 24). Variation between the Bvg$^+$ and Bvg$^-$ phases occurs at rather high frequencies (~10^{-6} per generation per cell) due to chromosome replication errors that cause a frameshifting expansion or retraction of a C-rich homopolymeric tract in the *bvgS* open reading frame (25, 26).

The level of activity of the BvgS/BvgA phosphorelay offers a continuum of gene expression adjustments of the BvgAS regulon (24, 27) from the Bvg$^+$ "ON" state, through the intermediate Bvg^i "ON/OFF" state, to the avirulent Bvg$^-$ "OFF" state (28, 29). The signals sensed by the BvgS kinase inside host airways remain unknown, but the levels of phosphorylation of BvgA are downmodulated, albeit incompletely, at lower growth temperatures (e.g., 24°C) (30), or in the presence of millimolar concentrations of nicotinic acid (>2 mM) or sulfate ions (>5 mM) (27, 31). The avirulent Bvg$^-$ phase was found to enable survival of the animal pathogen *B. bronchiseptica* in the environment in association with an amoeba host (32, 33). However, it remains unclear whether modulation of BvgAS activity occurs and plays any role also during the life cycle of *B. pertussis* inside human airways (34). At temperatures occurring in the nasal cavity and nasopharynx of humans (~32 to 34°C), the bacteria might adopt an intermediary Bvg^i phase, reducing expression of some virulence factors and upregulating production of some proteins involved in biofilm formation, such as BipA (29, 35, 36).

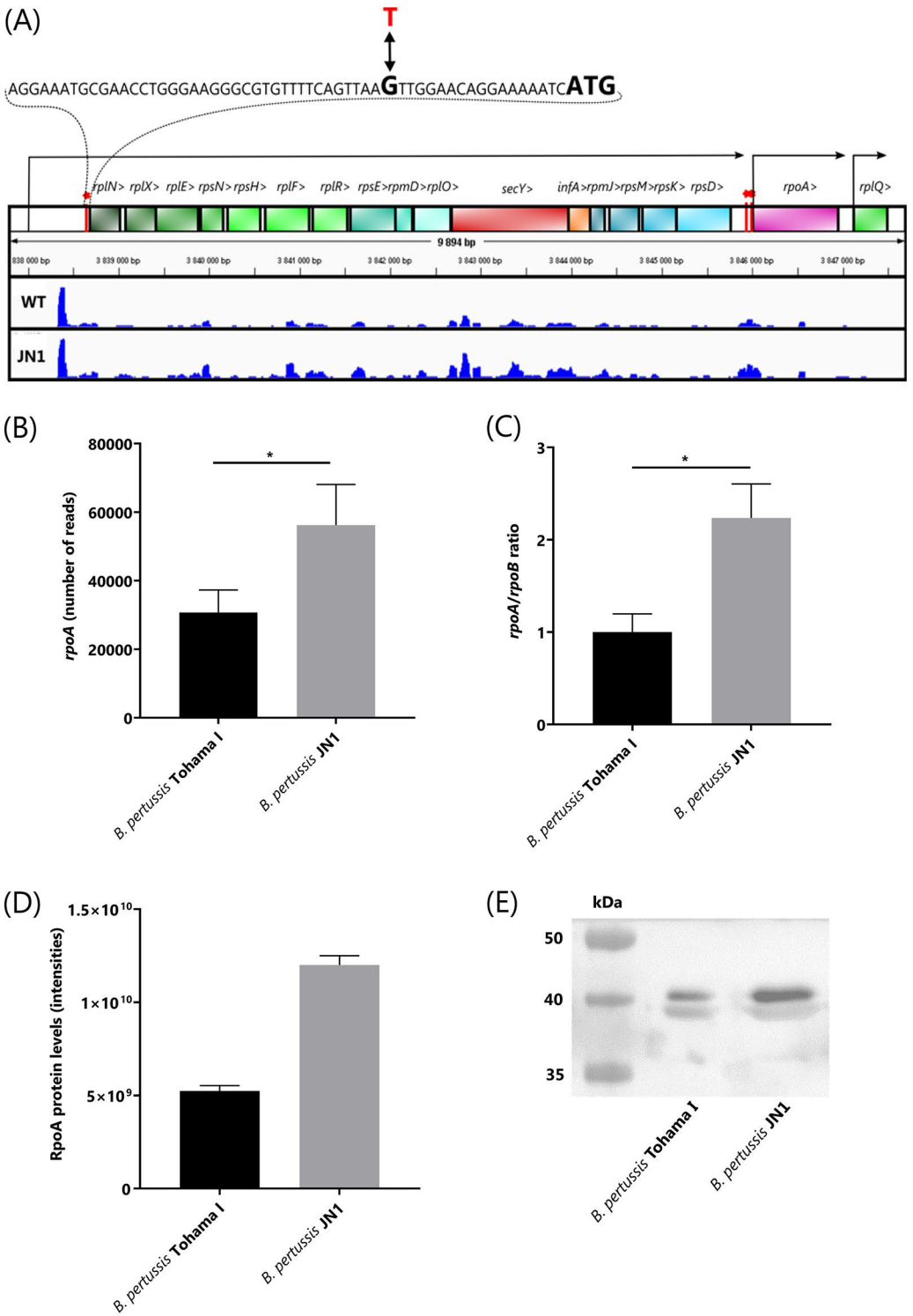

FIG 1 Operon structure downstream of the G-to-T transversion in the JN1 mutant strain and comparison of relative levels of *rpoA* transcript and RpoA protein in JN1 and WT *B. pertussis*. (A) The sequence harboring the G→T transversion SNP at position 3,838,664 of *B. pertussis* Tohama I chromosome in the JN1 mutant is zoomed in, indicating in bold the ATG start codon of the *rplN* gene. The Rockhopper algorithm-predicted promoter positions and transcripts are indicated by arrows. The height of the blue tracks represents the numbers of RNA-seq sequence reads that were aligned to the plus strand of the genome. The RNA-seq result for one representative pair of 4 biological replicates of *B. pertussis* WT and JN1 mutant transcriptomes is shown. The red bars topped by an asterisk indicate the positions at which the mutations increasing RpoA production were found by us in the JN1 mutant (a G→T transversion at position 3,838,664 upstream of *rplN*) and by Carbonetti et al. (61) in the 5′ region of the *rpoA* gene (C→T transition at 48 bp and A→G transition at 9

(Continued on next page)

Moreover, an intriguing observation was made during long-term follow-up of *B. pertussis*-infected mice and primates, where *B. pertussis* persistence in the nasopharynx and accumulation of Bvg$^-$ phase-locked mutants was observed over several months after infection (37, 38). Downregulation of expression of most virulence factors was also recently observed in the course of *B. pertussis* adaptation to an intracellular niche within human THP-1 macrophages (39).

Previous reports provided evidence that the C terminus of BvgA may interact with the C terminus of the α-subunit (RpoA) of the DNA-dependent RNA polymerase during transcriptional activation of the *vag* genes (40, 41). Intriguingly, mutations that upregulated production of RpoA were found to cause a drop in transcription of the pertussis and adenylate cyclase toxin genes by an as-yet-unresolved mechanism (42). In this study, we analyzed the transcriptome and proteome of a spontaneous mutant deficient in production of a number of known virulence factors due to upregulated transcription of the operon coding for ribosomal proteins upstream of the *rpoA* gene. We show that despite a pleiotropic defect on production of known virulence factors under laboratory conditions, the mutant can persist for several weeks within primary human macrophages cultured *in vitro* and in infected mouse lungs *in vivo*.

RESULTS

G-to-T transversion in the 5′-UTR of a ribosomal operon causes a pleiotropic deregulation of gene expression in *B. pertussis*. While deleting the *BP3063* gene from *B. pertussis* Tohama I chromosome, we obtained a Δ*BP3063* clone that was nonhemolytic on Bordet-Gengou agar (BGA). Intriguingly, the absence of adenylate cyclase toxin-hemolysin (ACT) production was not due to deletion of the putative deacetylase gene, since other Δ*BP3063* clones remained hemolytic. Moreover, the nonhemolytic mutant also failed to produce pertactin and pertussis toxin (not shown), whereas PCR resequencing did not reveal any mutation in the *bvgAS* locus that controls expression of *Bordetella* virulence genes (not shown). Therefore, we sequenced the genome of the nonhemolytic mutant at a high coverage (171-fold) using Illumina technology (ENA project PRJEB38438) and aligned the reads to the Tohama I reference genome sequence. This analysis revealed a single G-to-T base transversion at position 3,838,664, hence, in the 5′-untranslated region (5′-UTR) of the *BP3626-rplN* gene of the operon encoding ribosomal proteins (Fig. 1A). To confirm that the G-T transversion located 18 bases upstream of the start codon of *rplN* accounted for the nonhemolytic phenotype, we introduced the point mutation into the chromosome of the parental *B. pertussis* Tohama I strain. Indeed, the generated sequence-confirmed JN1 mutant was nonhemolytic on BGA plates (not shown) and grew slightly faster in standard Stainer-Scholte medium (SSM) (43) than the wild-type bacteria (see Fig. S1 in the supplemental material).

To determine the extent to which the G-T transversion in the 5′-UTR of *rplN* affected virulence factor production, we compared the proteome of the JN1 mutant to that of Tohama I bacteria grown under identical conditions. Altogether 1,466 individual proteins were identified in the proteomic data set generated on 3 replicate culture samples of the two strains (see Table S1). This covered almost 45% of the theoretical proteome of *B. pertussis*. Based on a *t* test, 472 of the identified proteins were differentially expressed between the wild-type and JN1 strains and another 61 proteins were detected in one proteome but not the other (presence/absence). When a secretome analysis was performed using concentrated culture supernatants (see Table S2), 804 proteins were detected in total, and 292 of them were differentially expressed between the wild type and the JN1 mutant, based on *t* test analysis. Sixty-seven other proteins were then reproducibly present/absent in one of the two secretomes. Hence, the G-T

FIG 1 Legend (Continued)
bp upstream of the ATG codon of *rpoA*, respectively). RNA-seq experiment result as total number of *rpoA* reads per equal amount of total bacterial RNA (B) and the *rpoA/rpoB* transcript ratios determined by qPCR analysis (C). Total production of RpoA protein in wild-type and JN1 cells determined by high-throughput proteomics analysis (D) and compared by Western blotting with an anti-RpoA polyclonal serum in equal amounts of total bacterial protein (E). *, $P \leq 0.05$.

TABLE 1 Proteomic and transcriptomic analyses of expression levels of the ribosomal operon genes located downstream to the G-to-T transversion at position 3,838,664 in the JN1 mutant chromosome

		Expression level[a]					
		Transcriptome			Proteome		
Gene	Protein	FC	JN1/WT	*P* value	FC	JN1/WT	*P* value
rplN	50S ribosomal protein L14	2.3	↑	8.1E−26	1.6	NS	2.11E−01
rplX	50S ribosomal protein L24	2.8	↑	5.3E−30	1.0	NS	9.50E−01
rplE	50S ribosomal protein L5	2.5	↑	4.6E−25	1.3	NS	6.43E−02
rpsN	30S ribosomal protein S14	3.1	↑	1.6E−21	ND		ND
rpsH	30S ribosomal protein S8	2.2	↑	1.1E−13	1.3	↑	3.51E−02
rplF	50S ribosomal protein L6	2.5	↑	1.9E−21	1.4	NS	8.43E−01
rplR	50S ribosomal protein L18	2.7	↑	5.4E−36	2.7	↓	5.29E−04
rpsE	30S ribosomal protein S5	2.1	↑	9.3E−09	2.4	↓	7.73E−03
rpmD	50S ribosomal protein L30	2.6	↑	1.8E−35	ND		ND
rplO	50S ribosomal protein L15	3.2	↑	6.3E−74	1.7	NS	8.79E−01
secY	Protein translocase subunit SecY	2.1	↑	8.5E−16	ND		ND
infA2	Translation initiation factor IF-1 2	1.8	↑	1.5E−12	2.6	NS	6.25E−01
rpmJ	50S ribosomal protein L36	2.1	↑	3.5E−28	ND		ND
rpsM	30S ribosomal protein S13	2.7	↑	2.2E−70	2.4	↓	3.56E−05
rpsK	30S ribosomal protein S11	2.2	↑	5.3E−71	2.4	↓	2.64E−03
rpsD	30S ribosomal protein S4	2.9	↑	2.7E−57	1.7	↓	1.33E−02
rpoA	DNA-directed RNA polymerase subunit alpha	1.9	↑	2.0E−44	2.3	↑	5.94E−02
rplQ	50S ribosomal protein L17	1.3	↑	2.6E−10	1.3	NS	1.01E−01

[a]FC, fold change difference represents the absolute ratio of the values of the tested samples. For the transcriptome, it was derived from the "log2FoldChange" value from DESeq2. For the proteome, it was derived as a fold change difference of median values of intensities. ND, not detected. JN1/WT, change trend observed for JN1 mutant compared to the WT, indicated as higher (↑) or lower (↓) mRNA/protein levels in the JN1 mutant compared to that in the wild-type strain. NS, not statistically significantly different.

transversion at position 3,838,664 of the JN1 chromosome had a truly pleiotropic impact on expression of the genome of *B. pertussis*.

Production of most virulence factors is strongly downregulated in the JN1 mutant due to reduced levels of the BvgA protein. Since the G-T transversion did not occur in any known transcriptional regulator gene, we examined if its pleiotropic effect on proteome composition may have resulted from alteration of any potential regulatory small RNA (sRNA) sequence. Towards this aim, we compared the transcriptomes of the wild-type and JN1 strains by unbiased comparative transcriptome sequencing (RNA-seq) analysis (see Tables S3 and S4). To ensure that the maximum number of sRNA molecules shorter than 50 nucleotides was retained, no length restrictions on the size of analyzed RNA molecules were applied, and cDNA libraries were prepared from total RNA of five wild-type and four JN1 strain replicate samples. Upon deep sequencing, the candidate sense and antisense sRNA sequences and the operon structures were identified using the Rockhopper software algorithms (44, 45). As summarized in Table S5, the G-to-T transversion at position 3,838,664 most likely did not affect the sequence of any sRNA transcript, as the most closely located sRNA sequence was identified between bases 3,838,293 and 3,838,561 on the plus strand of the chromosome. The G-T transversion also did not affect transcription of the *BP3624* gene in the opposite direction from the ribosomal operon (Table S4).

However, due to the G-T transversion in the 5′-UTR of *rplN*, transcription of the downstream ribosomal operon genes was increased by a factor of two to three (Table 1). This translated only in part into an alteration of the levels of produced ribosomal proteins (Table 1). For example, the *rplN*-encoded 50S ribosomal protein L14 could not itself be classified as significantly upregulated in JN1. Some of the downstream-encoded proteins then classified as insignificantly upregulated and some as downregulated (Table 1). However, the expression of the immediately downstream-

TABLE 2 Virulence factors significantly deregulated on protein level

		Expression level[a]					
		Transcriptome		Proteome		Secretome	
Gene	Protein	FC	JN1/WT	FC	JN1/WT	FC	JN1/WT
bipA	BipA, *Bordetella* Bvg-intermediate phase outer membrane protein involved in biofilm formation	2.4	↑	2.4	↑	2.1	↑
BP0529	Autotransporter	1.6	↑	4.2	↑	1.6	↓
sphB3	Serine protease	1.1	↑	ND		P/A	↑
bopB	Type III secreted protein B	10.3	↓	P/A	↓	P/A	↓
bopD	Type III secreted protein D	7.7	↓	12.1	↓	3356.8	↓
bopN	Type III secreted protein N	7.5	↓	ND		P/A	↓
BP0499	Uncharacterized protein	7.4	↓	10.1	↓	P/A	↓
BP1251	Putative toxin	5.4	↓	7.6	↓	ND	
BP1252	Putative exported protein	5.8	↓	4.3	↓	4.9	↓
BP2265	Uncharacterized protein	6.0	↓	P/A	↓	ND	
brkA	BrkA autotransporter involved in complement resistance	7.4	↓	3.1	↓	4.7	↓
bscC	Type III secretion system protein C	9.0	↓	P/A	↓	ND	
bscE	Type III secretion system protein E	4.0	↓	24.2	↓	ND	
bscL	Type III secretion system protein L	6.6	↓	P/A	↓	ND	
bscP	Type III secretion system protein P	6.9	↓	P/A	↓	ND	
bscQ	Type III secretion system protein Q	7.2	↓	P/A	↓	ND	
bscU	Type III secretion system protein U	6.7	↓	P/A	↓	ND	
bvgA	*Bordetella* virulence gene regulator protein BvgA	2.4	↓	2.5	↓	2.4	↓
bvgR	*Bordetella* avirulence gene repressor BvgR	1.2	↓	1.5	↓	ND	
bvgS	*Bordetella* virulence gene regulator kinase BvgS	2.2	↓	2.5	↓	ND	
cyaA	Bifunctional adenylate cyclase toxin-hemolysin	5.1	↓	448.9	↓	62.8	↓
dnt	Dermonecrotic toxin	5.9	↓	P/A	↓	2.3	↓
fhaB	Filamentous hemagglutinin	1.6	↓	1.9	↓	3.2	↓
fhaC	Filamentous hemagglutinin transporter protein FhaC	2.8	↓	1.9	↓	2.4	↓
fhaE	Protein FhaE	2.5	↓	1.6	↓	1.8	↓
fhaL	Adhesin	2.4	↓	P/A	↓	6.8	↓
fhaS	Adhesin	2.3	↓	P/A	↓	4.8	↓
fim2	Serotype 2 fimbrial subunit	5.8	↓	2.6	↓	114.1	↓
fimB	Chaperone protein FimB/FhaD	2.6	↓	1.4	↓	ND	
prn	Pertactin autotransporter adhesin	2.7	↓	ND		2.5	↓
ptlC	Type IV secretion system protein PtlC	4.1	↓	P/A	↓	P/A	↓
ptlF	Type IV secretion system protein PtlF	4.9	↓	2.9	↓	2.9	↓
ptlG	Type IV secretion system protein PtlG	4.5	↓	P/A	↓	P/A	↓
ptxA	Pertussis toxin subunit 1	4.4	↓	ND		62.7	↓
ptxB	Pertussis toxin subunit 2	4.0	↓	ND		188.7	↓
ptxC	Pertussis toxin subunit 3	3.8	↓	ND		163.9	↓
ptxD	Pertussis toxin subunit 4	3.8	↓	ND		420.5	↓
sphB1	Autotransporter subtilisin-like protease	4.7	↓	3.4	↓	3.6	↓
tcfA	Tracheal colonization factor	49.8	↓	14.4	↓	27.6	↓
tex	Transcription accessory protein Tex	1.8	↓	5.5	↓	P/A	↓
vag8	Autotransporter protein Vag8, complement resistance	93.8	↓	19.1	↓	119.6	↓

[a]FC, fold change difference represents the absolute ratio of the values of the tested samples. For the transcriptome, it was derived from the "log2FoldChange" value from DESeq2. For the proteome and secretome, it was derived as a fold change difference of median values of intensities. ND, not detected; P/A, significance determined based on presence/absence criterion, otherwise, only proteins with a *P* value of ≤0.05 are shown. JN1/WT, change trend observed for JN1 mutant compared to the WT, indicated as higher (↑) or lower (↓) mRNA/protein levels in the JN1 mutant compared to that in the wild-type strain.

located *rpoA* gene (Fig. 1), encoding the alpha subunit of the DNA-directed RNA polymerase (RpoA), was statistically significantly upregulated 2- to 3-fold on both transcript and protein levels (Table 1), as also verified by quantitative PCR (qPCR) (Fig. 1B and C) and Western blot analysis (Fig. 1D and E), respectively.

Importantly, as assessed by label-free proteomics, the JN1 mutant produced >2-fold smaller relative amounts of the BvgA and BvgS proteins that govern expression of virulence-related genes and the production of the bona fide virulence factors of *B. pertussis* (Table 2). Indeed, the transcriptomic and proteomic examinations confirmed that the relative amounts of the adenylate cyclase toxin-hemolysin (ACT) protein were strongly reduced in the biomass and culture supernatants of the JN1 mutant, explaining its nonhemolytic phenotype (Table 2). Furthermore, a significant downregulation

TABLE 3 Comparison of gene expression and protein levels of selected *vir*-repressed genes (*vrgs*) in wild-type and JN1 strains

			Expression level[a]					
			Transcriptome		Proteome		Secretome	
Gene	Name	Product	FC	JN1/WT	FC	JN1/WT	FC	JN1/WT
BP1311		Membrane protein	4.1	↑	NS	ND	NS	ND
BP2922	*bfrG*	TonB-dependent receptor	3.6	↑	NS	ND	NS	ND
BP3501	*vrg-24*	Hypothetical protein	3.5	↑	4.4	↑	4.9	↑
BP3635	*rplO*	50S ribosomal protein L15	3.2	↑	NS	ND	NS	ND
BP2671		Hypothetical protein	3.1	↑	2.8	↑	4.6	↑
BP1991		Flp pilus assembly membrane protein	3.0	↑	NS	ND	NS	ND
BP3671		Glycosyl transferase family protein	2.9	↑	NS	ND	NS	ND
BP2923		Lipoprotein	2.8	↑	NS	ND	NS	ND
BP3497		Hypothetical protein	2.8	↑	P/A	↑	NS	ND
BP3627	*rplX*	50S ribosomal protein L24	2.8	↑	NS	ND	NS	ND
BP3440		Putative exported protein	2.8	↑	2.6	↑	3.8	↑
BP3498		Hypothetical protein	2.8	↑	2.0	↑	NS	ND
BP3500		FAD-binding dehydrogenase	2.7	↑	NS	ND	NS	ND
BP1996		Putative type II secretion system protein	2.6	↑	NS	ND	NS	ND
BP1996		Putative type II secretion system protein	2.6	↑	NS	ND	NS	ND
BP1532		Amino acid ABC transporter substrate-binding protein	2.5	↑	2.8	↑	2.3	↑

[a]FC, fold change difference represents the absolute ratio of the values of the tested samples. For the transcriptome, it was derived from the "log2FoldChange" value from DESeq2. For the proteome and secretome, it was derived as a fold change difference of median values of intensities. NS, not significantly different; P/A, significance determined based on presence/absence criterion, otherwise, only proteins with a *P* value of ≤0.05 are shown. JN1/WT, change trend observed for JN1 mutant compared to the WT, indicated as higher (↑) or lower (↓) mRNA/protein levels in the JN1 mutant than in the wild-type strain. ND, not detected.

of production of other toxin proteins, adhesins, or of components of the type III and type IV secretion systems was observed in JN1 (Table 2). The extent of downregulation varied between the virulence-related proteins, and even if some of them accumulated at close to wild-type levels in the biomass of bacterial cells, their amounts secreted into culture supernatants of the JN1 mutant were much decreased (Table 2). This was particularly true for pertussis toxin and the strongly reduced amounts of its S1 to S4 subunits in culture supernatants. The low level of PT secretion was likely due to a strong downregulation of the PtlC, -F, and -G protein components of the type IV system involved in pertussis toxin excretion from bacterial periplasm (46). Similarly, the amount of the fimbriae protein Fim2 was strongly reduced, as were the amounts of the autotransporters and complement resistance proteins BrkA and Vag8 anchored in the bacterial outer membrane or of the type III secretion system proteins BopB, BopD, BscC, BscE, BscL, BscP, BscQ, and BscU. Intriguingly, we also observed a significant downregulation of the highly conserved 86-kDa Tex protein involved in the regulation of toxin expression in *B. pertussis* and *Clostridium perfringens* (47, 48). In contrast, proteins encoded by *BP3399* (putative zf-CHCC domain-containing protein), *BP1315* (universal stress family protein), and *BP3501* (putative *Bordetella* uptake gene) were strongly overproduced in the JN1 mutant (Table S1).

Nevertheless, the downregulation of the BvgA, BvgS, and BvgR proteins in JN1 was not sufficient for a full upregulation of transcription of the >300 previously identified *vrg* genes expressed in the Bvg$^-$ phase (23, 49). Transcription of only 144 *vrg* genes was significantly upregulated (fold change [FC] $\geq$ 1.5, adjusted $P < 0.05$) in JN1 (see Table S6), with the most upregulated *vrg* genes (FC $\geq$ 2.5) listed in Table 3. The level of residual transcription of some 36 *vrg* genes in JN1 remained as low as or even lower than in the wild-type strain (Table S6). For example, the *vrg-6* gene was not upregulated in JN1 (Table S6), in line with the rather modest downregulation of the BvgR phosphodiesterase protein that prevents activation of *vrg-6* transcription (34).

JN1 produces small amounts of BvgA~P. It was important to examine whether the generalized decrease of virulence factor production in the JN1 mutant was due to reduced levels of the phosphorylated BvgA (BvgA~P) transcriptional regulator that is crucial for activation of virulence gene transcription. Therefore, we compared the

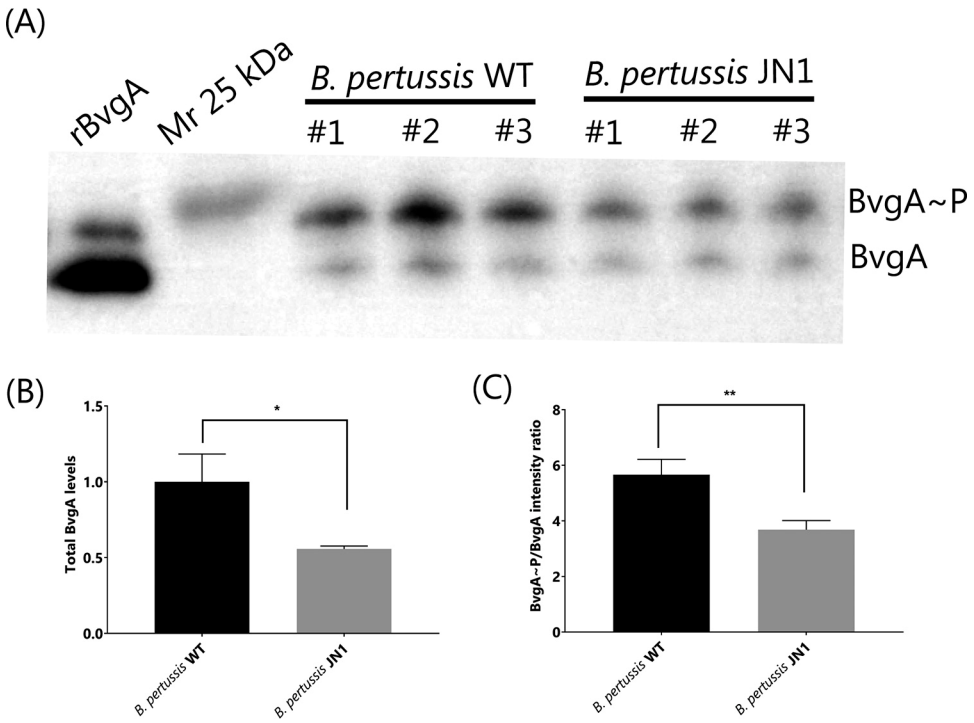

FIG 2 BvgA production and phosphorylation in the JN1 mutant. (A) Production and phosphorylation of BvgA. Equal amounts of total bacterial protein from three independent cultures of wild-type and JN1 strains were separated using a 12.5% SuperSep Phos-tag gel, and the BvgA and BvgA~P proteins were detected by Western blotting using a polyclonal anti-BvgA antibody with chemiluminescence detection; 0.1 μg of purified recombinant 6×His-BvgA protein (rBvgA) was used as a positive control. (B) Total detected amounts of BvgA in the JN1 cells normalized to the total BvgA amount. (C) Ratios of phosphorylated BvgA~P versus nonphosphorylated BvgA amounts, as determined by quantitative luminometric analysis of Western blot signals. *, $P \leq 0.05$; **, $P \leq 0.01$.

relative amounts of BvgA~P protein in the JN1 mutant and in wild-type bacteria using total protein extracts separated on 12.5% SuperSep Phos-tag gels that allow BvgA~P to be resolved from BvgA (50). The two forms of the protein could thus be immunodetected by Western blots with a BvgA-specific antibody (51). As shown in Fig. 2A and B, an approximately 2-fold lower chemiluminescent signal of total BvgA protein was detected for equal amounts of total biomass protein of JN1 cells than for the wild-type *B. pertussis* cells, in agreement with the results of the label-free proteomic analysis (cf. Table 2). Moreover, the ratio of the detected BvgA~P form to the nonphosphorylated BvgA protein was reduced by approximately 30% in the JN1 mutant (Fig. 2C), likely due to a reduced level of the BvgS kinase in JN1 cells (cf. Table 2). Hence, the total cytosolic concentration of BvgA~P can be estimated to have been approximately 3-fold lower in the JN1 cells than in wild-type bacteria cultured under identical conditions.

To test the hypothesis that the overproduced free RpoA deregulated virulence gene expression in JN1 by sequestering BvgA and/or other transcription factors into nonproductive complexes, we immunoprecipitated RpoA from lysates of wild-type or JN1 cells with an anti-RpoA polyclonal serum (52). The spectra of proteins pulled down by RpoA were compared, and due to the extreme sensitivity of mass spectrometric detection, a total of 530 proteins were identified in at least two replicates of the precipitates from either wild-type or JN1 but not in the negative control (see Table S7). Only proteins detected in at least two replicates of a sample set were considered further, and the significance of differences in protein amounts in the immunoprecipitates was assessed by a *t* test and by the presence/absence criterion. This identified 36 RpoA-associated proteins that were significantly enriched in the JN1 samples and 35 proteins

TABLE 4 Transcription-related proteins with significantly different levels of association with immunoprecipitated RpoA

Gene name	Protein name	FC[a]	JN1/WT[b]	ToS[c]	*P* value
BP0737	Putative inner membrane sensor for iron transport	NA	↑	P/A	
BP1315	Universal stress family protein	1.7	↑	*t* test	0.044
BP2216	Putative transcriptional regulator (MarR family)	1.3	↑	*t* test	0.017
fur	Ferric uptake regulation protein	NA	↑	P/A	
infA2	Translation initiation factor IF-1 2	2.2	↑	*t* test	0.002
BP2227	Putative anti-sigma factor	NA	↓	P/A	
BP3138	Putative two-component system response regulator	1.4	↓	*t* test	0.046
brpL	Putative RNA polymerase sigma factor	NA	↓	P/A	
rpoB	DNA-directed RNA polymerase subunit beta	NA	↓	P/A	
bvgA	Transcriptional regulator BvgA	2.4	↓[d]	*t* test[d]	0.166

[a]FC, fold change difference; NA, not applicable, as the protein was not detected in the WT sample.
[b]JN1/WT, trend observed in JN1 mutant compared to that in the wild-type strain. ↑, more protein was immunoprecipitated in JN1 strain; ↓, less protein was immunoprecipitated in JN1 strain.
[c]ToS, type of significance analysis; P/A, significance determined based on presence/absence criterion.
[d]Not statistically significant.

that were present in significantly reduced amounts compared to the composition of the precipitates from wild-type bacteria (Table S7). Among the proteins enriched in the JN1 samples were several proteins involved in transcriptional regulation, such as the BP2216 protein from the MarR family of transcriptional regulators, a universal stress family protein BP1315, and the ferric uptake transcriptional regulator protein (Table 4). Importantly, the RpoB subunit of the RNA polymerase was not detected in the precipitates from JN1 lysates, indicating that the anti-RpoA antibody pulled down preferentially the free overproduced RpoA protein and not the RNA polymerase complexes. Increased relative amounts of RpoA were pulled down from JN1 lysates compared to that from wild-type (WT) lysates (Table S7), whereas reduced amounts of the BvgA protein were detected in the JN1 precipitates compared to that in the wild-type sample, even if the decrease of the BvgA amount was not statistically significant (Table 4). The result, thus, did not enable us to conclude whether the overproduced free RpoA formed complexes with BvgA.

The JN1 mutant is prone to killing in human serum and to autoaggregation but persists inside human macrophage cells and in infected mouse lungs. To corroborate the results of the omics analysis, we next assessed some of the proteome-predicted phenotypes of the JN1 mutant. Among its most downregulated virulence factors were the BrkA and Vag8 autotransporter proteins that account for resistance of *B. pertussis* to complement-mediated killing in human serum (53). Indeed, the JN1 mutant was approximately 10-fold more sensitive to killing in human serum than wild-type bacteria (Fig. 3A).

Conversely, the JN1 mutant exhibited an enhanced production of the Bvg-intermediate phase protein BipA (cf. Table 2) that is involved in *Bordetella* biofilm formation (35, 54) and exhibited a higher autoaggregation index than the wild-type Tohama I strain (Fig. 3B).

Intriguingly, nonopsonized *B. pertussis* bacteria were recently found to survive to some extent the internalization into human macrophages and to adapt to the intracellular niche by downregulating virulence factor production (39, 55, 56). As shown in Fig. 4A, despite the reduced production of adhesins, the JN1 bacteria were internalized at higher levels than the wild-type bacteria by primary human peripheral blood monocyte-derived macrophages (PBDMs), becoming protected from killing by the antibiotic polymyxin B (100 μg/ml) added into culture medium after 2 h of coincubation of bacteria with PBDMs (day 0 [d0]). Moreover, approximately one order of magnitude higher CFU numbers of the JN1 mutant than of the wild-type bacteria (Fig. 4A) were recovered from repeatedly washed macrophages that were cultured for 24 or 48 h after infection in medium containing 10 μg/ml of polymyxin B that kills any noninternalized extracellularly attached bacteria. Intriguingly, at time points beyond 72 h from

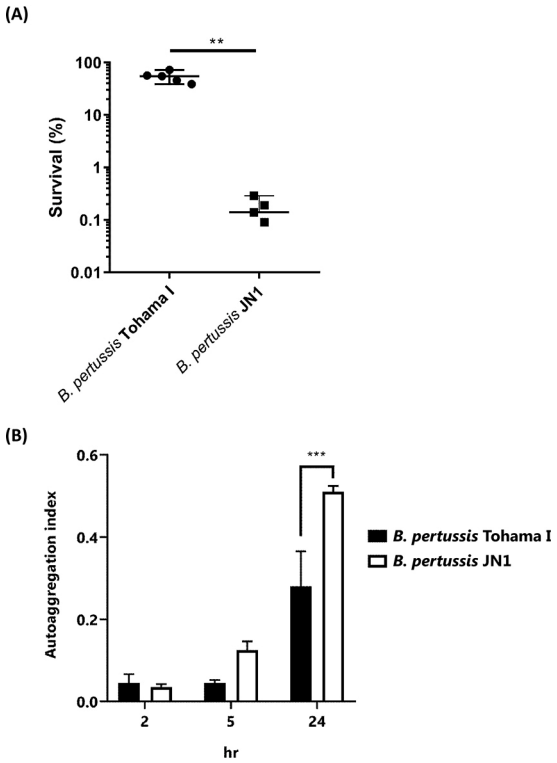

FIG 3 Comparison of serum resistance and autoaggregation capacities between wild-type and JN1 strains of *B. pertussis*. (A) Serum-killing assay with wild-type and JN1 strains of *B. pertussis*; 10^6 CFU/ml were incubated in 2% normal human serum for 1 h at 37°C, and serial dilutions of the suspension were plated for CFU counting. The CFU count of bacterial suspensions incubated with heat-inactivated serum was set as 100%. (B) The autoaggregation index was determined as described in Materials and Methods. The experiments were performed 3 times in triplicates ($n = 9$) and means ± standard deviations (SD) are given. **, $P \leq 0.01$; ***, $P \leq 0.001$.

infection, no bacteria able to form colonies on BGA plates were recovered from the infected macrophages. However, our parallel experiments with mScarlet-expressing fluorescent *B. pertussis* revealed that nonopsonized *B. pertussis* can persist in primary human macrophages grown in medium containing 5% human plasma for many weeks (J. Novak, unpublished data). This suggested that beyond day 3 from infection, the surviving intracellular bacteria adopted a dormant and viable but nonculturable (VBNC) state inside the macrophage cells (57). Therefore, we used a "live/dead" propidium monoazide-based qPCR assay for differential enumeration of the intracellularly surviving or killed bacteria (58). As shown in Fig. 4B, on days 7 and 14 after infection, comparable numbers of total genome equivalents of the JN1 and wild-type (WT) bacteria (live plus dead) were detected in the lysates of infected macrophages. For the fraction of viable bacteria, the JN1/WT ratio was slightly >1 (~1.1). Hence, despite being defective in virulence factor production, the JN1 mutant persisted inside primary human macrophage cells over the prolonged period of 2 weeks as well as the wild-type bacteria.

Since we have recently observed that long-term intracellular persistence of *B. pertussis* bacteria modulates the phenotype of the infected human macrophages (J. Novak, unpublished data), we compared the phenotypic changes elicited in PBDM cells by internalized wild-type and JN1 mutant bacteria (Fig. 5). As shown in Fig. 5A and B and compared to that in noninfected cells, after 7 days of intracellular persistence, both wild-type and JN1 bacteria provoked a strong and comparable (~10-fold) downregulation of surface expression of the CD11b subunit of the complement receptor 3 (Fig. 5A) and of the CD36 class B scavenger receptor (Fig. 5B). In turn, infection by both

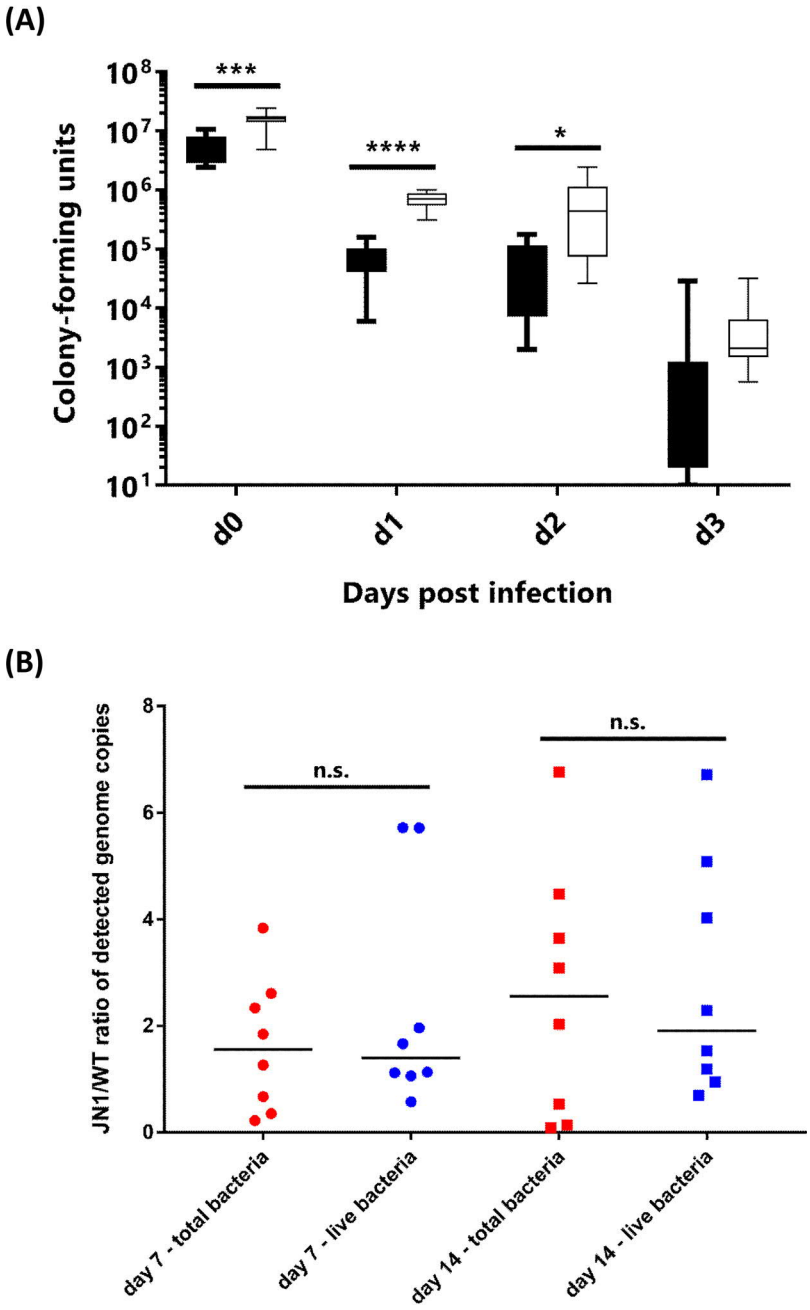

FIG 4 Intracellular survival of wild-type *B. pertussis* and of the JN1 mutant inside primary human macrophages (hPBDMs). (A) CFU counts of bacteria surviving intracellularly in infected hPBDMs for up to 3 days, as determined by plating of equal amounts of macrophage lysates on BGA. Black bars represent wild-type *B. pertussis*, white bars represent *B. pertussis* JN1. (B) Ratios of JN1/WT genome equivalents of intracellular bacteria per equal number of infected macrophage cells after 7 and 14 days of infection were determined by the propidium monoazide-based qPCR assay. Red symbols, total detected genomes; blue symbols, genomes of live bacteria capable of excluding phorbol myristate acetate (PMA). ns, $P > 0.05$; *, $P \leq 0.05$; ***, $P \leq 0.001$; ****, $P \leq 0.0001$.

strains provoked upregulation of cell surface expression of the lipopolysaccharide (LPS) receptor CD14 (Fig. 5C) and of the HLA-DR molecule involved in antigen presentation to T cells (Fig. 5D). The JN1 mutant then triggered exposure of significantly higher levels of CD14 than the wild-type bacteria. Moreover, the level of CD14 remained high over the 2 weeks of intracellular infection. Hence, despite a strongly reduced capacity to produce the known virulence factors in standard laboratory culture media, the JN1 mutant survived inside primary macrophage cells at least as well

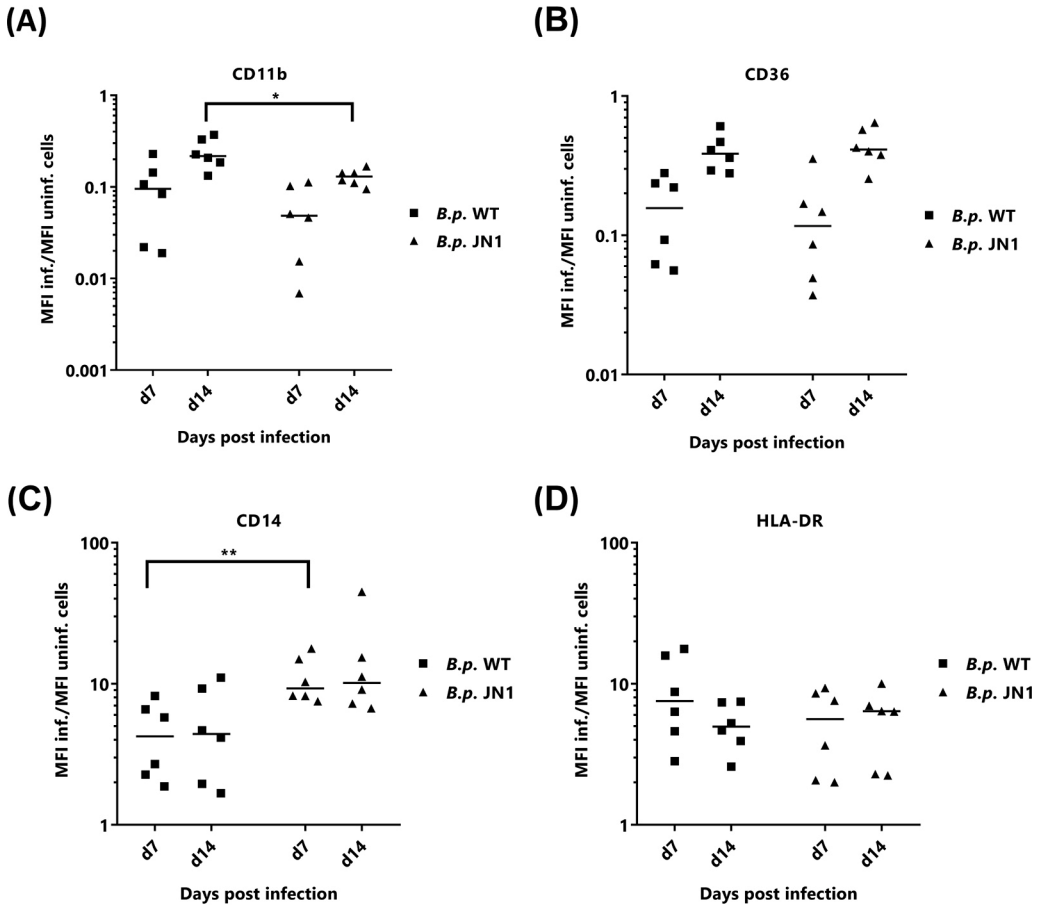

FIG 5 Persisting intracellular infection with wild-type or JN1 mutant *B. pertussis* bacteria alters expression of phenotypic markers of macrophage cells. On days 7 and 14 after infection (MOI, 50:1) of primary human peripheral blood-derived macrophages with the wild-type or JN1 mutant *B. pertussis* bacteria, the expression of surface markers on intracellularly infected and noninfected cells was compared by flow cytometry analysis. Comparison of mean fluorescence intensities (MFIs) of CD11b (A), CD14 (B), CD36 (C), and HLA-DR (D) surface markers are shown as ratios of MFI of infected to MFI of uninfected cells. The relative MFI value found for uninfected cells was set as 1. Differences between samples on days 7 and 14 postinfection were statistically tested by *t* test. *, $P \leq 0.05$; **, $P \leq 0.01$.

as the wild-type *B. pertussis* bacteria, and it triggered similar phenotypic changes of infected macrophage cells as the wild-type bacteria.

This prompted us to test the capacity of the JN1 mutant to colonize mouse lungs. Five-week-old female BALB/cByJ mice were intranasally challenged with 1×10^5 CFU (50 μl) of the wild-type or JN1 bacteria, and lung colonization was followed over 27 days. As shown in Fig. 6, whereas the wild-type *B. pertussis* bacteria proliferated by 2 orders of magnitude within a week from infection before being progressively cleared from the lungs, the JN1 bacteria did not proliferate over the first week of infection but persisted longer and at higher numbers than the wild-type strain. In two independent challenge experiments yielding highly reproducible results, the persisting JN1 bacteria were still isolated from mouse lungs at a low but reliably detectable level even 27 days after infection, when the wild-type bacteria have in the majority of mice been cleared (Fig. 6).

DISCUSSION

We report that a spontaneous G-to-T transversion in the 5′ UTR of the first gene (*rplN*) of a ribosomal operon exerted a pleiotropic effect on the global expression pattern of the *B. pertussis* genome. Moreover, this single G-to-T base transversion located 18 bases upstream of the ATG start codon of *rplN* provoked a generalized defect of virulence factor production, most likely through the downregulation of the levels of the BvgA∼P transcriptional activator of *Bordetella* virulence gene expression.

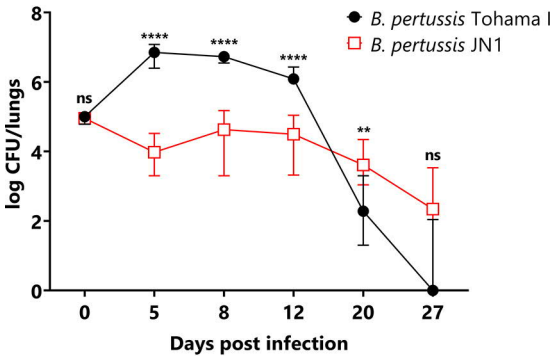

FIG 6 Comparison of lung colonization of infected mice between wild-type and JN1 mutant *B. pertussis*. Mice were inoculated intranasally with 50 μl of suspensions containing 1×10^5 CFU of the *B. pertussis* strains. At the indicated time points, the challenged mice were sacrificed, and lung homogenates were plated on Bordet-Gengou agar for CFU counting after 5 days. The experiment was repeated twice with groups of 3 mice per time point, yielding very similar results. Therefore, the values from two experiments were pooled, and the medians ($n = 6$ for day postinfection [dpi] 0 to 27) with 95% confidence intervals (CIs) are shown. ns, not significant; *, $P \leq 0.05$; ****, $P \leq 0.0001$.

RNA-seq analysis revealed that the point mutation enhanced, by an as-yet-undefined mechanism, the steady-state abundance of transcripts of the *rplN-rpsD* operon and of the *rpoA* gene located immediately downstream (cf. Fig. 1). Recent analysis of the primary transcriptome of *B. pertussis* did not reveal any *rpoA* promoter (59). This raises the hypothesis that the *rpoA* open reading frame (ORF), starting 214 nucleotides downstream of the stop codon of the *rpsD* ORF, is cotranscribed at least to some extent with the strongly expressed ribosomal operon. Alternatively, upregulation of *rpoA* transcription from a putative own promoter or enhanced *rpoA* transcript stability may have accounted for the observed RpoA overproduction in the JN1 mutant. Since it is not obvious by which mechanism such effects could be caused by a G-to-T transversion located some 7.4 kb upstream of *rpoA* in the 5′ UTR of the *rplN* gene, the mechanism by which *rpoA* expression is increased in the JN1 mutant deserves further experimental exploration.

The observed overproduction of RpoA offers a plausible explanation of the mechanism by which the G-to-T transversion in a noncoding region of a housekeeping operon would exert such a pleiotropic effect on gene expression and virulence factor production in *B. pertussis*. Indeed, Carbonetti and coworkers previously observed that overproduction of RpoA due to mutations in the 5′-UTR of the *rpoA* gene resulted in reduced transcription of BvgA-activated virulence genes and could be reversed by inducible overexpression of the *bvgAS* genes in mutants overproducing RpoA (60, 61). Moreover, previous suppressor analyses revealed that the RpoA and BvgA proteins interact through their C-terminal moieties within transcriptional initiation complexes (41, 60, 62). Hence, an initial partial sequestration of the BvgA∼P protein into nonproductive complexes by the overproduced RpoA would reduce, first of all, the transcription of the *bvgAS* locus itself, as this is positively autoregulated by the transcriptional activator BvgA∼P produced by phosphorylation of BvgA by BvgS (23). Hence, the more BvgA∼P is withdrawn from the transcription initiation complexes of RNA polymerase by the excess of RpoA subunit, the smaller are the amounts of the BvgA and BvgS proteins produced *de novo* in the JN1 cells. Hence, the concentration of BvgA∼P in cells will drop further and become limiting for activation of transcription of the BvgA∼P-dependent virulence genes (41, 42, 60–62). Indeed, an approximately 3-fold lower concentration of BvgA∼P was detected in JN1 cells by Western blots of Phos-tag gel-resolved BvgA isoforms (cf. Fig. 2). This result lends support to the operation of a downregulating loop of decreasing activation of *bvgAS* transcription (cf. Table 2).

It remains to be determined by which mechanism the G-T base transversion in the

5′-UTR of the *rplN* gene increases the steady-state abundance of transcripts of the *rplN-rpsD* operon. The G-T transversion occurred at a site where no sRNA molecule sequence was predicted, and the performed RNA-seq analysis did not reveal the existence of any sRNA molecule that would have been affected by the analyzed mutation.

While it is plausible to conclude that the virulence genes were downregulated in the JN1 mutant through downregulation of BvgA∼P production, the G-T transversion in the 5′ UTR of the *rplN* gene exerted a much broader effect on the global expression profile of the *B. pertussis* genome. It is plausible to assume that downregulation of the BvgAS system in the JN1 mutant allowed production of *vrg* proteins that are involved in transcriptional activation of other *B. pertussis* regulons. Nevertheless, the extent of BvgA downregulation in the JN1 mutant was not sufficient for a full upregulation of all of the >300 previously identified *vrg* genes transcribed when *B. pertussis* is in the Bvg$^-$ phase (23, 49, 63). Expression of only 144 *vrg* genes was significantly upregulated (FC $\geq$ 1.5, $P < 0.05$) in JN1, and the already very low residual transcription level of some 37 *vrg* genes was even lower (FC $\geq$ 1.5, $P < 0.05$) in JN1 than in the wild-type strain (see Table S6 in the supplemental material). For example, the *vrg-6* gene was not upregulated in JN1 (Table 3), most likely because of the insufficient downregulation of the BvgR phosphodiesterase that hydrolyzes c-di-GMP and thereby prevents activation of *vrg-6* transcription by the c-di-GMP-activated RisA (34). Furthermore, the mixed pattern of transcription of *vrg* genes in JN1 did not confer a true Bvg$^-$ phenotype. It is plausible to assume that many transcription factors other than BvgA∼P also intervened in the regulation of expression of *vrg* genes.

Indeed, among the transcriptional regulators produced at increased amounts in the JN1 mutant were the proteins encoded by the *BP2216*, *BP2913*, *BP1315*, and *fur* genes. *BP2216* encodes a transcriptional regulator of the MarR family (23, 39), and *BP2913* encodes a predicted anti-sigma factor, similar to the RslA and RskA anti-sigma factors of *Mycobacterium tuberculosis* (64, 65). The *BP1315* gene-encoded protein belongs to the family of universal stress proteins. The ferric uptake regulation (Fur) protein encoded by the *fur* gene primarily serves under iron-replete conditions as a transcriptional repressor of dozens of iron-regulated genes and orchestrates expression of iron acquisition and homeostasis systems of bacteria. In accordance with such a major regulatory role of Fur, and because of its capacity to bind the RNA polymerase (66), it is plausible to assume that its enhanced production contributed to the generalized deregulation of gene expression in the JN1 mutant.

Another layer of gene expression deregulation may have occurred on the posttranscriptional level. For example, overproduction of RpoA was associated with a significant downregulation of a highly conserved 86-kDa protein possessing both RNA and DNA binding domains and initially named as Tex for "toxin expression protein" (Table 2). Tex was previously shown to bind the 5′ regions of target mRNAs and was previously found to positively regulate the production of a set of toxins in *C. perfringens* (47, 67). Moreover, Tex also appears to be involved in the regulation of virulence of *Burkholderia pseudomallei*, and it was initially discovered by Fuchs and coworkers as a dominant antisuppressor that ablated the effect of an as-yet-uncharacterized suppressor mutation that restored PT and CyaA production in *B. pertussis* mutants overproducing RpoA (47, 48). Tex, hence, appears to be somehow involved in regulation of virulence factor production in *B. pertussis*, and its downregulation may have affected the composition of the JN1 proteome.

Somewhat surprisingly, we observed that despite a generalized defect in virulence factor production, the JN1 mutant infected primary human macrophages at least as efficiently as the wild-type bacteria and persisted at comparable levels within macrophages for at least 2 weeks. This goes well with the recent observation that adaptation of *B. pertussis* to the intracellular niche inside human macrophages is accompanied by a downregulation of most of the known virulence factors (39). Indeed, the persistent intracellular infection by the JN1 bacteria with impaired virulence factor production triggered similar alterations of expression of macrophage markers as infection by the

wild-type bacteria capable of producing the virulence factors, with the exception of the significantly higher upregulation of the CD14 marker by JN1 infection.

Moreover, despite the impairment in virulence factor production and despite increased sensitivity to complement-mediated killing in human serum, the JN1 mutant was still able to persistently infect mouse lungs at reduced but well-detectable levels (cf. Fig. 6). It will be of interest to determine if the upregulated expression of the autotransporter protein BatB contributed to the survival of the JN1 mutant in mouse lungs, since a homolog of BatB was found to protect *B. bronchiseptica* from inflammatory clearance from the mouse respiratory tract (68). The persistence of the JN1 mutant further indicates that downregulation of production of the known virulence factors may allow *B. pertussis* low-level colonization of the airway mucosa without harnessing the inflammatory and immune responses of the host. This would go well with the intriguing observation that persistent infection of the airways of primates was accompanied by accumulation of Bvg$^-$ phase-locked *B. pertussis* mutants (37, 38). Moreover, *B. pertussis* antigen was detected inside columnar epithelial cells of the bronchiole and trachea of an infant 8 weeks after a diagnosis of pertussis (69). The sum of these observations raises the possibility that modulation of BvgAS activity or Bvg phase variation may play a role also in the lifestyle of *B. pertussis*, possibly during an intracellular stage of airway infection.

MATERIALS AND METHODS

***B. pertussis* strains and growth conditions.** *B. pertussis* JN1 was derived from the wild-type Tohama I strain obtained from the Institute Pasteur collection (CIP 81.32). The JN1 mutant was constructed by introduction of the G→T base transversion at position 3,838,664 of the *B. pertussis* Tohama I chromosome through markerless allelic exchange, using the pSS4245 vector (gift from Scott Stibitz). Briefly, an SpeI-EcoRI site-flanked upstream DNA fragment, carrying the G→T base transversion, was amplified using the primer pair 5′-ACTAGTGTGGCCCTGGTCGTGCTG-3′ (forward) and 5′-GAATTCCGGCAGCAAGCACACCAGCGTGATGTAAATCGCAA-3′ (reverse). The EcoRI-BamHI site-flanked downstream fragment was amplified using the primers 3′-GAATTCCTGGTGATGCGTTG-3′ (forward) and 5′-GGATCCCACCACGCCGTGACGTTTG-3′. The two PCR products were digested by the corresponding restriction endonucleases and simultaneously ligated into the pSS4245 plasmid linearized by SpeI and BamHI. The construct carrying the mutation was verified by sequencing, and the cloned fragment was next recombined into the bacterial chromosome by double crossing over, according to a previously described procedure (70). The introduction of the mutation into a bacterial chromosome and absence of undesired mutations were then verified by PCR resequencing. Bacteria were grown on Bordet-Gengou (BG) agar plates supplemented with 15% defibrinated sheep blood (LabMedia Servis, Czech Republic) at 37°C and 5% CO_2 for 5 days to visualize hemolysis. Liquid cultures were obtained by growing bacteria in modified Stainer-Scholte medium supplemented with 3 g/liter of Difco Casamino Acids (Thermo) and 1 g/liter of heptakis(2,6-di-*O*-dimethyl)-β-cyclodextrin for 18 h at 37°C.

Genome sequencing, annotation, and SNP detection. The genome of the JN1 strain was sequenced at 171-fold coverage using Illumina MiSeq system, and the adaptor sequences and low-quality bases were removed from the reads using the Trimmomatic tool (71). The reads were mapped to *B. pertussis* Tohama I genome using Burrows-Wheeler Aligner (72). Uniquely mapped reads were selected using SAMtools (73). Single-nucleotide polymorphisms (SNPs) and insertions/deletions in the studied genome compared to that of *B. pertussis* Tohama I were detected with Pilon software (74). The data for this study have been deposited in the European Nucleotide Archive (ENA) at EMBL-EBI under accession number PRJEB38438.

Quantitative PCR analysis of *rpoA* transcription. Reverse transcription-quantitative PCR (RT-qPCR) analysis of the *rpoA* transcript levels was performed as described earlier (75). Samples of total RNA (biological triplicates of RNA isolated from WT and JN1 strains used for RNA-seq analysis) were treated using the TURBO DNA-free kit (Thermo Fisher Scientific). Aliquots of total RNA (1 μg) were reverse transcribed in duplicates into cDNA in a 25-μl reaction mixture using a reverse transcription system (Promega). All primers (see Table S8 in the supplemental material) were designed to anneal at 60°C and were analyzed for secondary structures and for cross-dimers in primer pairs. RT-qPCR analysis of each cDNA sample was performed in technical triplicates on a Bio-Rad CFX96 instrument using SYBR green JumpStart *Taq* ReadyMix (Sigma-Aldrich), 200 nmol of each primer, and 40 ng of reverse transcribed RNA in a 20-μl reaction mixture. The *rpoB* gene was used as the reference gene, and relative gene expression was quantified using amplification efficiency values (76).

Analysis of RpoA protein levels by Western blotting. Wild-type and JN1 *B. pertussis* bacteria were grown in 3 ml of SSM to an optical density at 600 nm (OD_{600}) of approximately 1.1. Cells from 1 ml of culture were harvested by centrifugation at 16,000 $\times$ *g* for 5 min at room temperature, and bacterial pellets were resuspended in 400 μl of TUS buffer (50 mM Tris-HCl [pH 8.0], 8 M urea, 2% [wt/vol] SDS). Samples were heated for 5 min at 95°C, and equal amounts of protein of the JN1 and WT samples were resolved by 10% SDS-PAGE, transferred onto the nitrocellulose membrane, and probed with a 1:3,000 diluted rabbit anti-RpoA serum kindly provided by Linda Doubravova (52). Blots were incubated with a peroxidase-

labeled secondary anti-rabbit antibody at a 1:5,000 dilution, and the RpoA protein was detected using enhanced chemiluminescence (ECL) with a SuperSignal West Femto maximum sensitivity substrate (Thermo Scientific). The chemiluminescent signals were quantified using the Fiji processing package of ImageJ (77).

Infections of primary human PBDMs. Human peripheral blood mononuclear cells from anonymous healthy donors were isolated from buffy coats purchased at Thomayer Hospital (Prague, Czech Republic). The cells were purified using a modified double-gradient centrifugation method, as described by Menck et al. (78), with the modification that fetal calf serum was replaced by heat-inactivated (56°C, 30 min) 5% human AB serum (HS) obtained from pooled plasma from 5 male donors (Thomayer Hospital, Prague). For long-term culture experiments, the medium with HS was systematically sterilized by filtration with 0.22-μm filters before use. Differentiation was performed in Petri dishes for bacterial cultures for six to 7 days in RPMI medium (Sigma) with 5% HS, supplemented with 50 ng/ml recombinant human macrophage colony-stimulating factor (rh M-CSF; ImmunoTools) with antibiotics; half of the medium was changed after 3 to 4 days. The freshly added medium contained 50 ng/ml rh M-CSF but no antibiotics. One day before infection, the cells were washed twice with phosphate-buffered saline (PBS), detached by incubation with 0.02% EDTA solution for 15 min at 37°C, collected by centrifugation at 1,300 rpm for 3 to 5 min, resuspended in Dulbecco's modified Eagle medium (DMEM) without antibiotics (Sigma) and containing 5% HS, counted, and seeded into 12-well plates at ~0.4 $\times$ 10^6 cells per well.

Bacterial inocula were grown as liquid cultures to an OD_{600} of 1.0 to 1.3 (~2 $\times$ 10^9 CFU/ml), diluted in SS medium, and used to infect macrophage cells at a multiplicity of infection (MOI) of 50:1. Culture plates were centrifuged at 640 $\times$ *g* for 5 min to facilitate bacterial attachment to macrophage cells, followed by coincubation for 2 h at 37°C in a humidified 5% CO_2 atmosphere. Unattached bacteria were washed away with prewarmed PBS, and cells were replaced in medium containing 100 μg/ml of polymyxin B for 1 h to kill noninternalized bacteria. The cells were next washed with PBS and either lysed for CFU plating (d0) or cultured for determined times in medium containing 5% HS and 10 μg/ml of polymyxin B to block extracellular bacterial growth. Equal numbers of cells were lysed by resuspension in 900 μl of sterile water, followed by addition of 100 μl of 10$\times$ PBS. The lysates were serially diluted in PBS and plated on BGA for determination of *B. pertussis* CFU after 5 days of growth.

Live/dead quantitative real-time PCR. A modified version of the protocol described by Ramkissoon et al. (58) was used. Macrophage cells grown in 12-well plates were washed with PBS, detached in 1 ml of 0.02% EDTA for 15 min at 37°C, resuspended by scraping, and collected by centrifugation at 2,000 $\times$ *g* for 10 min. Cell pellets were resuspended to equal cell density in PBS, and 500 μl of cell suspensions were split into two 200-μl aliquots. One microliter of 20 mM PMAxx (Biotium, USA) was added to one aliquot, and both aliquots of a sample were incubated in the dark at room temperature on a rocking platform for 10 min. All cell samples were next irradiated for 5 min in the PMA-Lite light-emitting diode (LED) photolysis device (Biotium, USA) and eventually frozen. Genomic DNA from macrophages was isolated using the QIAamp DNA minikit (Qiagen) according to the manufacturer's instructions. For qPCR analysis, the TaqMan gene expression master mix (Applied Biosystems) was used. The 20-μl qPCR mixtures for quantification of the IS*481* target sequence contained 10 μl of TaqMan master mix, 2 μl of each 900 nM primer, 2 μl of the 150 nM probe, and 4 μl of template, using the IS481_fwd ATCAAGCACCGCTTTACCC and IS481_rev TTGGGAGTTCTGGTAGGTGTG primers and the IS*481* probe 6-carboxyfluorescein (FAM)-AATGGCAAGGCCGAACGCTTCA-black hole quencher 1 (BHQ1). Bacterial genomic DNA was used as a positive control, and the total number of detected *B. pertussis* genome copies was calculated as described by Ramkissoon et al. (58). Bacterial survival at the time points 7 and 14 days of infection was calculated as a ratio between the numbers of genomes detected in macrophages after the infection with JN1 mutant strain compared to that with wild-type *B. pertussis*.

Flow cytometry analysis. Cells were stained with specific antibodies or isotype controls (Table S8) in 96-well plates on ice and analyzed by flow cytometry using a BD LSR II instrument with high-throughput sampler and evaluated using FlowJo V10 software.

Analysis of BvgA and BvgA~P protein levels. Wild-type and JN1 *B. pertussis* bacteria were cultured in SSM to an OD_{600} of ~1, cells from 1 ml were collected by centrifugation, and whole bacterial cell lysates were prepared and analyzed as described by Chen at al. (50). Based on the individual OD_{600} values of each culture, the sample volumes were adjusted to load equal amounts of total bacterial protein onto 12.5% SuperSep Phos-tag gels (Wako). The resolved BvgA and BvgA~P isoforms were detected by Western blotting using a rabbit polyclonal anti-BvgA antibody (51) with chemiluminescence detection. The total amount of BvgA protein was calculated by summing up the signal of both bands (phosphorylated and unphosphorylated) from densitometry analysis. To determine the ratio of the phosphorylated and unphosphorylated forms of BvgA, the chemiluminescent signal from the upper band was divided by the chemiluminescent signal from the lower band in the given lane.

Proteomic analysis. *Bordetella pertussis* Tohama I and JN1 strains grown on BGA plates for 3 days at 37°C with 5% CO_2 were used to inoculate 5 ml of liquid cultures in SS medium to a final OD_{600} of 0.2. Bacterial cultures were grown overnight at 37°C and eventually inoculated 1:10 into 50 ml of SSM. After reaching the late-exponential phase (OD of ~1), the cultures were centrifuged at 20,000 $\times$ *g* for 20 min at 4°C, and for the analysis of the secretome, 35 ml of the upper portion of the supernatant was carefully withdrawn from each tube. The remaining bacteria were removed by passage of the supernatants through a 0.22-μm filter, and trichloroacetic acid was added to a final concentration of 10%. The proteins were precipitated overnight at 4°C and collected at 20,000 $\times$ *g* for 20 min at 4°C, and the precipitate was washed with ice-cold acetone. For proteomic analysis of whole bacterial cells, bacterial pellets were washed in PBS. Both washed cells and the precipitates of the supernatants were resuspended by 8 M urea in 50 mM ammonium bicarbonate buffer, pH 8.3 (UA buffer). Three biological replicates of each

sample were subjected to liquid chromatography tandem mass spectrometry (LC-MS/MS) proteomic analysis.

For analysis of composition of RpoA complexes, ~3×10^{10} *B. pertussis* cells were lysed in 0.5 ml of buffer, and immunoprecipitation was performed with a rabbit anti-RpoA serum kindly provided by Linda Doubravova (52), using a Pierce co-immunoprecipitation (Co-IP) kit (catalog number 26149; Thermo Scientific), according to the manufacturer's instructions. Pierce control agarose resin was used as a negative control. Three biological replicates of each sample were analyzed by LC-MS/MS.

Briefly, 70 μg of total protein of whole bacterial cells, from culture supernatant precipitate, or of immunoprecipitate was applied to a 30-kDa-cutoff membrane filter and processed using a modified protocol for filter-aided sample preparation (FASP) (79). Briefly, proteins were washed twice by UA buffer and then by 50 mM ammonium bicarbonate buffer, pH 8.3 (AB buffer). Reduction of disulfide bonds was carried out by 100 mM dithiothreitol (DTT) in AB buffer (reduction buffer) on a shaker for 30 min at 60°C at 200 rpm followed by alkylation of sulfhydryl groups by the addition of chloroacetamide (CAA) to final 50 mM concentration for 30 min at room temperature in the dark. Solutions were discarded, and mass spectrometry-grade trypsin in AB buffer was added onto the filter at a protein/enzyme ratio of 35:1. The overnight incubation on a shaker at 37°C and 200 rpm then followed. Afterwards, peptides were eluted by three consecutive centrifugations with AB buffer at 14,000 $\times$ *g* for 20 min and acidified by 2% trifluoroacetic acid (TFA) to reach a final concentration of 0.2% TFA. Peptides were then desalted using C_{18} extraction disks (Empore, USA) and filled ZipTip tips and vacuum dried. Prior to LC-MS/MS analysis, samples were resuspended in 2% acetonitrile (ACN) in 0.1% TFA.

A nano reversed-phase column (EASY-Spray column, 50 cm, 75-μm inside diameter [i.d.], PepMap C_{18}, 2-μm particles, 100 Å pore size) was used for LC-MS analysis. Mobile phase buffer A was composed of water and 0.1% formic acid. Mobile phase B was composed of acetonitrile and 0.1% formic acid. Samples were loaded onto the trap column (Acclaim PepMap300, C_{18}, 5 μm, 300 Å wide pore, 300 μm by 5 mm) at a flow rate of 15 μl/min. Loading buffer was composed of water, 2% acetonitrile, and 0.1% trifluoroacetic acid. Peptides were eluted with gradient of B from 4% to 35% over 60 min at a flow rate of 300 nl/min. Eluting peptide cations were converted to gas-phase ions by electrospray ionization and analyzed on a Thermo Orbitrap Fusion (Q-OT-qIT). Survey scans of peptide precursors from 350 to 1,400 *m/z* were performed at 120,000 resolution (at 200 *m/z*) with a 5×10^5 ion count target. Tandem MS was performed by isolation at 1.5 Th with the quadrupole higher-energy collisional dissociation (HCD) fragmentation with normalized collision energy of 30, and rapid scan MS analysis in the ion trap. The MS 2 ion count target was set to 104, and the max injection time was 35 ms. Only those precursors with a charge state of 2 to 6 were sampled for MS 2. The dynamic exclusion duration was set to 45 s with a 10-ppm tolerance around the selected precursor and its isotopes. Monoisotopic precursor selection was turned on. The instrument was run in top speed mode with 2-s cycles (80). The data were analyzed and quantified with label-free quantification (LFQ) algorithms in MaxQuant v1.6.3.3 (81) and the Andromeda search engine (82). Extracted ion current ratios of every detected peptide were calculated, and peptide ion signals were normalized to the dominant population of proteins that varied minimally within our experimental data sets (83). The false-discovery rate (FDR) parameter was set to 1% for both proteins and peptides. The enzyme specificity of trypsin was set as C terminal to Arg and Lys. Carbamidomethylation was set as the fixed modification, while N-terminal protein acetylation and methionine oxidation were variable modifications. Maximal number of missed cleavages was set to 2. All hits identified in searches as contaminants were filtered out. The data were searched against *Bordetella pertussis* reference proteome database (strain Tohama I/ATCC BAA-589/NCTC 13251).

Statistical testing of proteomics data. For analysis of composition of the immunoprecipitates, all proteins detected in the negative control were subtracted. Only proteins detected in at least two replicates of at least one of the strain samples were considered. Differentially regulated proteins in wild-type and JN1 mutant samples were identified by Student's two-sample *t* test (s0 = 0.1, permutation-based FDR $\leq$ 0.05) applied on signal intensities. Testing was performed in Perseus ver. 1.6.5 (84). Only proteins quantified in at least two biological replicates of the wild-type or JN1 samples were tested. Proteins quantified in at least two replicates of samples from one strain but consistently absent across all three replicates of the sample from the other strain were evaluated as significantly regulated. For proteins that were significantly differentially regulated, fold change differences (FC) were calculated from the median values as $FC = 2^{(median\_WT - median\_JN1)}$.

RNA-seq analysis. Liquid bacterial cultures (15 ml) were grown overnight as stated above. Eight-milliliter cultures at an OD of 1 to 1.5 were mixed with 2 ml of STOP solution (5% phenol in ethanol [EtOH]) and centrifuged (15 min, 8,000 rpm, 4°C), and cell pellets were frozen at −80°C until use. The pellets were thawed, lysed in 300 μl of Tris-EDTA (TE) buffer with lysozyme for 5 min at room temperature, and dissolved with 0.9 ml of the TRI reagent for 5 min at room temperature. The samples were centrifuged (10 min, 12,000 rpm, 4°C), the supernatants (1 ml) were extracted with 200 μl of chloroform, and 500 μl of the water phase was precipitated with 500 μl of isopropanol for 45 min at 4°C. Precipitates were washed twice with 900 μl of 75% EtOH and resuspended in 50 μl of RNase-free water.

rRNA was removed from 400 ng of total RNA with NEBNext rRNA depletion kit (*Escherichia coli*) (New England Biolabs, Ipswich, MA). Subsequently, stranded total RNA-seq libraries were prepared from rRNA-free RNA samples using the NEBNext Ultra II directional RNA library prep kit for Illumina (New England Biolabs). Small RNA-Seq libraries were prepared manually from 200 ng of total RNA using the NEBNext Multiplex small RNA library prep kit (New England Biolabs).

Obtained libraries that passed the quality control (QC) step assessed on the Agilent Bioanalyzer system were pooled in equimolar amounts. Each pool of libraries was loaded on the Illumina sequencer

HiSeq 2500 and sequenced unidirectionally, generating ~180 million reads per lane, each at 62 bases long. Raw data were deposited as project PRJEB39011 in the European Nucleotide Archive (ENA).

The adapter sequence AGATCGGAAGA and reads shorter than 10 nucleotides were removed with Cutadapt (85). The analysis was performed in R programming language using Bioconductor (86). FASTQ files were aligned using the Rsubread package version 1.34.7 (87). Reads were counted with the featureCounts software (88) that is part of the Rsubread package and *Bordetella pertussis* Tohama I genome assembly ASM19571v1.45. Differential expression analysis was performed with DESeq2 (89). For identification of novel and existing sRNAs, transcript boundaries, and operons, data were analyzed by Rockhopper (44, 45).

Infection of mice. All animal experiments were approved by the Animal Welfare Committee of the Institute of Microbiology of the ASCR, v. v. i., in Prague, Czech Republic. Handling of animals was performed according to the Guidelines for the care and use of laboratory animals, the Act of the Czech National Assembly, collection of laws numbers 246/1992. Five-week-old female BALB/cByJ (Charles River, France) were used in this study. Mice were anesthetized by intraperitoneal (i.p.) injection of ketamine (80 mg/kg of body weight) and xylazine (8 mg/kg of body weight) in saline and were inoculated intranasally with 1×10^5 CFU of *B. pertussis* cells in 50 μl. Viable CFU were determined by plating on BG agar plates.

Infected mice were euthanized 2 h after exposure to challenge suspension (day 0 plus 2 h) and on the indicated days thereafter (days 5, 8, 12, 21, and 27). The lungs were aseptically removed and homogenized in physiological solution with tissue grinders. Serial dilutions of lung homogenates were plated on BG agar plates supplemented with 15% defibrinated sheep blood, and CFU were counted after 5 days of incubation at 37°C. Three mice per time point were used, and this experiment was repeated 2 times for data points D5 to D20 and 3 times for data point D27. The average value of the results obtained with a challenge dose of 10^5 CFU is shown.

Autoaggregation assay. The autoaggregation assay was performed according to Cattelan et al. (90). Bacteria were cultured in 3 ml of SS medium with heptakis(2,6-di-*O*-methyl-β-cyclodextrin) (1 g/liter) and supplement for 24 h. Cells were harvested by centrifugation (5,000 rpm, 10 min) and resuspended in 3 ml of SS medium (with supplement, no cyclodextrin) at an OD_{650} of 1.0, followed by static incubation at room temperature. After 2, 5, and 24 h of incubation, 200 μl of the medium was taken from the top layer of the suspension, and the absorbance at 650 nm was measured. The autoaggregation index (AI) represents the fraction of aggregated cells relative to the total cell population and was calculated as follows: $(ODt_0 - OD_t)/ODt_0$, where ODt_0 is the initial OD measurement and OD_t is the OD measured at a designated time point t (2, 5, and 24 h).

Serum resistance assay. Precultures of liquid bacterial cultures were grown in modified SSM medium to an OD of ~0.8 in a total volume of 20 ml, and 1 ml of cultures at an OD of 0.05 were prepared and diluted 10 times in a total volume of 1 ml of SSM. Fifty microliters of each diluted culture was then mixed with 440 μl of SSM and either 10 μl of normal human serum (Merck/Sigma-Aldrich, H4522) or 10 μl of heat-inactivated (56°C, 30 min) serum. Samples were incubated for 1 h at 37°C with shaking (300 rpm), and 50 μl was withdrawn and mixed with 450 μl of PBS containing 10 mM EDTA to inhibit the complement. Serial dilutions were plated on BG blood agar plates, and CFU were counted after 5 days of incubation.

Data availability. The genome sequence data of the nonhemolytic mutant have been deposited in the European Nucleotide Archive (ENA) at EMBL-EBI under accession number PRJEB38438. Data from RNA-seq analyses are deposited as the project PRJEB39011 in the European Nucleotide Archive (ENA). The mass spectrometry proteomics data have been deposited to the ProteomeXchange Consortium via the PRIDE (91) partner repository with the data set identifier PXD020023.

SUPPLEMENTAL MATERIAL

Supplemental material is available online only.

FIG S1, TIF file, 0.3 MB.

TABLE S1, XLSX file, 0.4 MB.

TABLE S2, XLSX file, 0.3 MB.

TABLE S3, XLSX file, 0.3 MB.

TABLE S4, XLSX file, 0.4 MB.

TABLE S5, XLSX file, 0.5 MB.

TABLE S6, XLSX file, 0.1 MB.

TABLE S7, XLSX file, 0.2 MB.

TABLE S8, XLSX file, 0.1 MB.

ACKNOWLEDGMENTS

We thank Roy Gross, David Hot, Loic Coutte, Camille Locht, and Andrew Preston for stimulating discussions, Hana Lukeova, Iva Marsikova, and Mireia Osuna for excellent technical assistance, and Karel Harant and Pavel Talacko from Laboratory of Mass Spectrometry, BIOCEV, Charles University, Faculty of Science, for help with mass spectrometry.

This work was supported by the grants 19-27630X (to P.S.) and 19-12338S (to B.V.) from the Czech Science Foundation.

J.N. designed the study, performed research, analyzed the data, prepared figures, and wrote the initial manuscript, D.J. performed the proteomics analyses, I.L. performed the flow cytometry experiments and analyzed the data, J.H. and O.S. performed the mouse experiments, D.S. performed the serum resistance assay and qPCR analysis, A.D. analyzed the genome sequencing data, B.V. contributed to the study design and manuscript editing, J.P., N.A., and V.B. performed the RNA-seq analysis, and P.S. contributed to study design, interpreted the results, and wrote the paper.

REFERENCES

1. Melvin JA, Scheller EV, Miller JF, Cotter PA. 2014. *Bordetella pertussis* pathogenesis: current and future challenges. Nat Rev Microbiol 12:274–288. https://doi.org/10.1038/nrmicro3235.
2. WHO. 2015. Pertussis vaccines: WHO position paper - September 2015. Wkly Epidemiol Rec 90:433–458.
3. Yeung KHT, Duclos P, Nelson EAS, Hutubessy RCW. 2017. An update of the global burden of pertussis in children younger than 5 years: a modelling study. Lancet Infect Dis 17:974–980. https://doi.org/10.1016/S1473-3099(17)30390-0.
4. Kuchar E, Karlikowska-Skwarnik M, Han S, Nitsch-Osuch A. 2016. Pertussis: history of the disease and current prevention failure, p 77–82. *In* Pokorski M (ed), Pulmonary dysfunction and disease. Springer International Publishing, Cham, Switzerland.
5. Cherry JD. 2013. Pertussis: challenges today and for the future. PLoS Pathog 9:e1003418. https://doi.org/10.1371/journal.ppat.1003418.
6. Mooi FR. 2010. Bordetella pertussis and vaccination: the persistence of a genetically monomorphic pathogen. Infect Genet Evol 10:36–49. https://doi.org/10.1016/j.meegid.2009.10.007.
7. Bouchez V, Hegerle N, Strati F, Njamkepo E, Guiso N. 2015. New data on vaccine antigen deficient *Bordetella pertussis* isolates. Vaccines (Basel) 3:751–770. https://doi.org/10.3390/vaccines3030751.
8. Bouchez V, Brun D, Cantinelli T, Dore G, Njamkepo E, Guiso N. 2009. First report and detailed characterization of *B. pertussis* isolates not expressing pertussis toxin or pertactin. Vaccine 27:6034–6041. https://doi.org/10.1016/j.vaccine.2009.07.074.
9. Hegerle N, Guiso N. 2014. *Bordetella pertussis* and pertactin-deficient clinical isolates: lessons for pertussis vaccines. Expert Rev Vaccines 13:1135–1146. https://doi.org/10.1586/14760584.2014.932254.
10. van der Lee S, Hendrikx LH, Sanders EAM, Berbers GAM, Buisman A-M. 2018. Whole-cell or acellular pertussis primary immunizations in infancy determines adolescent cellular immune profiles. Front Immunol 9:51. https://doi.org/10.3389/fimmu.2018.00051.
11. Belcher T, Preston A. 2015. *Bordetella pertussis* evolution in the (functional) genomics era. Pathog Dis 73:ftv064. https://doi.org/10.1093/femspd/ftv064.
12. Parkhill J, Sebaihia M, Preston A, Murphy LD, Thomson N, Harris DE, Holden MTG, Churcher CM, Bentley SD, Mungall KL, Cerdeño-Tárraga AM, Temple L, James K, Harris B, Quail MA, Achtman M, Atkin R, Baker S, Basham D, Bason N, Cherevach I, Chillingworth T, Collins M, Cronin A, Davis P, Doggett J, Feltwell T, Goble A, Hamlin N, Hauser H, Holroyd S, Jagels K, Leather S, Moule S, Norberczak H, O'Neil S, Ormond D, Price C, Rabbinowitsch E, Rutter S, Sanders M, Saunders D, Seeger K, Sharp S, Simmonds M, Skelton J, Squares R, Squares S, Stevens K, Unwin L, et al. 2003. Comparative analysis of the genome sequences of *Bordetella pertussis*, *Bordetella parapertussis* and *Bordetella bronchiseptica*. Nat Genet 35:32–40. https://doi.org/10.1038/ng1227.
13. Weigand MR, Peng Y, Batra D, Burroughs M, Davis JK, Knipe K, Loparev VN, Johnson T, Juieng P, Rowe LA, Sheth M, Tang K, Unoarumhi Y, Williams MM, Tondella ML. 2019. Conserved patterns of symmetric inversion in the genome evolution of *Bordetella* respiratory pathogens. mSystems 4:e00702-19. https://doi.org/10.1128/mSystems.00702-19.
14. Weigand MR, Peng Y, Loparev V, Batra D, Bowden KE, Burroughs M, Cassiday PK, Davis JK, Johnson T, Juieng P, Knipe K, Mathis MH, Pruitt AM, Rowe L, Sheth M, Tondella ML, Williams MM. 2017. The history of *Bordetella pertussis* genome evolution includes structural rearrangement. J Bacteriol 199:e00806-16. https://doi.org/10.1128/JB.00806-16.
15. Dienstbier A, Pouchnik D, Wildung M, Amman F, Hofacker IL, Parkhill J, Holubova J, Sebo P, Vecerek B. 2018. Comparative genomics of Czech vaccine strains of *Bordetella pertussis*. Pathog Dis 76:fty071. https://doi.org/10.1093/femspd/fty071.
16. Abrahams JS, Weigand MR, Ring N, MacArthur I, Peng S, Williams MM, Bready B, Catalano AP, Davis JR, Kaiser MD, Oliver JS, Sage JM, Bagby S, Tondella ML, Gorringe AR, Preston A. 7 February 2020. Duplications drive diversity in Bordetella pertussis on an underestimated scale. BioRxiv https://doi.org/10.1101/2020.02.06.937284.
17. Cerny O, Kamanova J, Masin J, Bibova I, Skopova K, Sebo P. 2015. *Bordetella pertussis* adenylate cyclase toxin blocks induction of bactericidal nitric oxide in macrophages through cAMP-dependent activation of the SHP-1 phosphatase. J Immunol 194:4901–4913. https://doi.org/10.4049/jimmunol.1402941.
18. Cerny O, Anderson KE, Stephens LR, Hawkins PT, Sebo P. 2017. cAMP signaling of adenylate cyclase toxin blocks the oxidative burst of neutrophils through Epac-mediated inhibition of phospholipase C activity. J Immunol 198:1285–1296. https://doi.org/10.4049/jimmunol.1601309.
19. Hasan S, Kulkarni NN, Asbjarnarson A, Linhartova I, Osicka R, Sebo P, Gudmundsson GH. 2017. *Bordetella pertussis* adenylate cyclase toxin disrupts functional integrity of bronchial epithelial layers. Infect Immun 86:e00445-17. https://doi.org/10.1128/IAI.00445-17.
20. Ahmad JN, Cerny O, Linhartova I, Masin J, Osicka R, Sebo P. 2016. cAMP signalling of *Bordetella* adenylate cyclase toxin through the SHP-1 phosphatase activates the BimEL-Bax pro-apoptotic cascade in phagocytes. Cell Microbiol 18:384–398. https://doi.org/10.1111/cmi.12519.
21. Bassinet L, Gueirard P, Maitre B, Housset B, Gounon P, Guiso N. 2000. Role of adhesins and toxins in invasion of human tracheal epithelial cells by *Bordetella pertussis*. Infect Immun 68:1934–1941. https://doi.org/10.1128/iai.68.4.1934-1941.2000.
22. Uhl MA, Miller JF. 1994. Autophosphorylation and phosphotransfer in the Bordetella pertussis BvgAS signal transduction cascade. Proc Natl Acad Sci U S A 91:1163–1167. https://doi.org/10.1073/pnas.91.3.1163.
23. Moon K, Bonocora RP, Kim DD, Chen Q, Wade JT, Stibitz S, Hinton DM. 2017. The BvgAS Regulon of *Bordetella pertussis*. mBio 8:e01526-17. https://doi.org/10.1128/mBio.01526-17.
24. Cummings CA, Bootsma HJ, Relman DA, Miller JF. 2006. Species- and strain-specific control of a complex, flexible regulon by *Bordetella* BvgAS. J Bacteriol 188:1775–1785. https://doi.org/10.1128/JB.188.5.1775-1785.2006.
25. Stibitz S, Aaronson W, Monack D, Falkow S. 1989. Phase variation in *Bordetella pertussis* by frameshift mutation in a gene for a novel two-component system. Nature 338:266–269. https://doi.org/10.1038/338266a0.
26. Gogol EB, Cummings CA, Burns RC, Relman DA. 2007. Phase variation and microevolution at homopolymeric tracts in *Bordetella pertussis*. BMC Genomics 8:122. https://doi.org/10.1186/1471-2164-8-122.
27. Lacey BW. 1960. Antigenic modulation of *Bordetella pertussis*. J Hyg (Lond) 58:57–93. https://doi.org/10.1017/s0022172400038134.
28. Cotter PA, Miller JF. 1994. BvgAS-mediated signal transduction: analysis of phase-locked regulatory mutants of *Bordetella bronchiseptica* in a rabbit model. Infect Immun 62:3381–3390. https://doi.org/10.1128/IAI.62.8.3381-3390.1994.
29. Mason E, Henderson MW, Scheller EV, Byrd MS, Cotter PA. 2013. Evidence for phenotypic bistability resulting from transcriptional interference of bvgAS in *Bordetella bronchiseptica*. Mol Microbiol 90:716–733. https://doi.org/10.1111/mmi.12394.
30. Seydlova G, Beranova J, Bibova I, Dienstbier A, Drzmisek J, Masin J, Fiser R, Konopasek I, Vecerek B. 2017. The extent of the temperature-induced membrane remodeling in two closely related *Bordetella* species reflects their

adaptation to diverse environmental niches. J Biol Chem 292:8048–8058. https://doi.org/10.1074/jbc.M117.781559.
31. Melton AR, Weiss AA. 1989. Environmental regulation of expression of virulence determinants in *Bordetella pertussis*. J Bacteriol 171:6206–6212. https://doi.org/10.1128/jb.171.11.6206-6212.1989.
32. Taylor-Mulneix DL, Bendor L, Linz B, Rivera I, Ryman VE, Dewan KK, Wagner SM, Wilson EF, Hilburger LJ, Cuff LE, West CM, Harvill ET. 2017. *Bordetella bronchiseptica* exploits the complex life cycle of *Dictyostelium discoideum* as an amplifying transmission vector. PLoS Biol 15:e2000420. https://doi.org/10.1371/journal.pbio.2000420.
33. Linz B, Ma L, Rivera I, Harvill ET. 2019. Genotypic and phenotypic adaptation of pathogens: lesson from the genus *Bordetella*. Curr Opin Infect Dis 32:223–230. https://doi.org/10.1097/QCO.0000000000000549.
34. Merkel TJ, Stibitz S, Keith JM, Leef M, Shahin R. 1998. Contribution of regulation by the *bvg* locus to respiratory infection of mice by *Bordetella pertussis*. Infect Immun 66:4367–4373. https://doi.org/10.1128/IAI.66.9.4367-4373.1998.
35. Stockbauer KE, Fuchslocher B, Miller JF, Cotter PA. 2001. Identification and characterization of BipA, a *Bordetella* Bvg-intermediate phase protein. Mol Microbiol 39:65–78. https://doi.org/10.1046/j.1365-2958.2001.02191.x.
36. Williams CL, Boucher PE, Stibitz S, Cotter PA. 2005. BvgA functions as both an activator and a repressor to control Bvg^i phase expression of *bipA* in *Bordetella pertussis*: *bipA* transcription in *B. pertussis*. Mol Microbiol 56:175–188. https://doi.org/10.1111/j.1365-2958.2004.04526.x.
37. Karataev GI, Sinyashina LN, Medkova AYu, Semin EG, Shevtsova ZV, Matua AZ, Kondzariya IG, Amichba AA, Kubrava DT, Mikvabia ZYa. 2016. Insertional inactivation of virulence operon in population of persistent *Bordetella pertussis* bacteria. Russ J Genet 52:370–377. https://doi.org/10.1134/S102279541603008X.
38. Medkova AI, Siniashina LN, Rumiantseva IP, Voronina OL, Kunda MS, Karataev GI. 2013. Accumulation of the *bvg*- *Bordetella pertussis* a virulent mutants in the process of experimental whooping cough in mice. Mol Gen Mikrobiol Virusol 2013:22–26. (In Russian.)
39. Petráčková D, Farman MR, Amman F, Linhartová I, Dienstbier A, Kumar D, Držmíšek J, Hofacker I, Rodriguez ME, Večerek B. 2020. Transcriptional profiling of human macrophages during infection with Bordetella pertussis. RNA Biol 17:731–742. https://doi.org/10.1080/15476286.2020.1727694.
40. Boucher PE, Maris AE, Yang M-S, Stibitz S. 2003. The response regulator BvgA and RNA polymerase α subunit C-terminal domain bind simultaneously to different faces of the same segment of promoter DNA. Mol Cell 11:163–173. https://doi.org/10.1016/s1097-2765(03)00007-8.
41. Boucher PE, Murakami K, Ishihama A, Stibitz S. 1997. Nature of DNA binding and RNA polymerase interaction of the *Bordetella pertussis* BvgA transcriptional activator at the *fha* promoter. J Bacteriol 179:1755–1763. https://doi.org/10.1128/jb.179.5.1755-1763.1997.
42. Carbonetti NH, Khelef N, Guiso N, Gross R. 1993. A phase variant of *Bordetella pertussis* with a mutation in a new locus involved in the regulation of pertussis toxin and adenylate cyclase toxin expression. J Bacteriol 175:6679–6688. https://doi.org/10.1128/jb.175.20.6679-6688.1993.
43. Stainer DW, Scholte MJ. 1970. A simple chemically defined medium for the production of phase I *Bordetella pertussis*. J Gen Microbiol 63:211–220. https://doi.org/10.1099/00221287-63-2-211.
44. McClure R, Balasubramanian D, Sun Y, Bobrovskyy M, Sumby P, Genco CA, Vanderpool CK, Tjaden B. 2013. Computational analysis of bacterial RNA-Seq data. Nucleic Acids Res 41:e140. https://doi.org/10.1093/nar/gkt444.
45. Tjaden B. 2015. *De novo* assembly of bacterial transcriptomes from RNA-seq data. Genome Biol 16:1. https://doi.org/10.1186/s13059-014-0572-2.
46. Locht C, Coutte L, Mielcarek N. 2011. The ins and outs of pertussis toxin. FEBS J 278:4668–4682. https://doi.org/10.1111/j.1742-4658.2011.08237.x.
47. Fuchs TM, Deppisch H, Scarlato V, Gross R. 1996. A new gene locus of Bordetella pertussis defines a novel family of prokaryotic transcriptional accessory proteins. J Bacteriol 178:4445–4452. https://doi.org/10.1128/jb.178.15.4445-4452.1996.
48. Moule MG, Spink N, Willcocks S, Lim J, Guerra-Assunção JA, Cia F, Champion OL, Senior NJ, Atkins HS, Clark T, Bancroft GJ, Cuccui J, Wren BW. 2015. Characterization of new virulence factors involved in the intracellular growth and survival of *Burkholderia pseudomallei*. Infect Immun 84:701–710. https://doi.org/10.1128/IAI.01102-15.
49. Coutte L, Huot L, Antoine R, Slupek S, Merkel TJ, Chen Q, Stibitz S, Hot D, Locht C. 2016. The multifaceted RisA regulon of *Bordetella pertussis*. Sci Rep 6:32774. https://doi.org/10.1038/srep32774.
50. Chen Q, Boulanger A, Hinton DM, Stibitz S. 2013. Separation and detection of phosphorylated and nonphosphorylated BvgA, a *Bordetella pertussis* response regulator, *in vivo* and *in vitro*. Bio Protoc 3:e970. https://doi.org/10.21769/BioProtoc.970.
51. Keidel K, Amman F, Bibova I, Drzmisek J, Benes V, Hot D, Vecerek B. 2018. Signal transduction-dependent small regulatory RNA is involved in glutamate metabolism of the human pathogen *Bordetella pertussis*. RNA 24:1530–1541. https://doi.org/10.1261/rna.067306.118.
52. Novakova L, Bezouskova S, Pompach P, Spidlova P, Saskova L, Weiser J, Branny P. 2010. Identification of multiple substrates of the StkP Ser/Thr protein kinase in *Streptococcus pneumoniae*. J Bacteriol 192:3629–3638. https://doi.org/10.1128/JB.01564-09.
53. Marr N, Shah NR, Lee R, Kim EJ, Fernandez RC. 2011. *Bordetella pertussis* autotransporter Vag8 binds human C1 esterase inhibitor and confers serum resistance. PLoS One 6:e20585. https://doi.org/10.1371/journal.pone.0020585.
54. de Gouw D, Serra DO, de Jonge MI, Hermans PW, Wessels HJ, Zomer A, Yantorno OM, Diavatopoulos DA, Mooi FR. 2014. The vaccine potential of *Bordetella pertussis* biofilm-derived membrane proteins. Emerg Microbes Infect 3:1–9. https://doi.org/10.1038/emi.2014.58.
55. Lamberti YA, Hayes JA, Perez Vidakovics ML, Harvill ET, Rodriguez ME. 2010. Intracellular trafficking of *Bordetella pertussis* in human macrophages. Infect Immun 78:907–913. https://doi.org/10.1128/IAI.01031-09.
56. Lamberti Y, Cafiero JH, Surmann K, Valdez H, Holubova J, Večerek B, Sebo P, Schmidt F, Völker U, Rodriguez ME. 2016. Proteome analysis of *Bordetella pertussis* isolated from human macrophages. J Proteomics 136:55–67. https://doi.org/10.1016/j.jprot.2016.02.002.
57. Li L, Mendis N, Trigui H, Oliver JD, Faucher SP. 2014. The importance of the viable but non-culturable state in human bacterial pathogens. Front Microbiol 5:258. https://doi.org/10.3389/fmicb.2014.00258.
58. Ramkissoon S, MacArthur I, Ibrahim M, de Graaf H, Read RC, Preston A. 2020. A qPCR assay for *Bordetella pertussis* cells that enumerates both live and dead bacteria. PLoS One 15:e0232334. https://doi.org/10.1371/journal.pone.0232334.
59. Amman F, D'Halluin A, Antoine R, Huot L, Bibova I, Keidel K, Slupek S, Bouquet P, Coutte L, Caboche S, Locht C, Vecerek B, Hot D. 2018. Primary transcriptome analysis reveals importance of IS elements for the shaping of the transcriptional landscape of *Bordetella pertussis*. RNA Biol 15:967–975. https://doi.org/10.1080/15476286.2018.1462655.
60. Carbonetti NH, Romashko A, Irish TJ. 2000. Overexpression of the RNA polymerase alpha subunit reduces transcription of Bvg-activated virulence genes in *Bordetella pertussis*. J Bacteriol 182:529–531. https://doi.org/10.1128/jb.182.2.529-531.2000.
61. Carbonetti NH, Fuchs TM, Patamawenu AA, Irish TJ, Deppisch H, Gross R. 1994. Effect of mutations causing overexpression of RNA polymerase alpha subunit on regulation of virulence factors in Bordetella pertussis. J Bacteriol 176:7267–7273. https://doi.org/10.1128/jb.176.23.7267-7273.1994.
62. Stibitz S. 1998. Mutations affecting the alpha subunit of *Bordetella pertussis* RNA polymerase suppress growth inhibition conferred by short C-terminal deletions of the response regulator BvgA. J Bacteriol 180:2484–2492. https://doi.org/10.1128/JB.180.9.2484-2492.1998.
63. Coutte L, Antoine R, Slupek S, Solans L, Derop J, Bonnefond A, Hot D, Locht C. 2020. Combined RNAseq and ChIPseq analyses of the BvgA virulence regulator of *Bordetella pertussis*. mSystems 5:e00208-20. https://doi.org/10.1128/mSystems.00208-20.
64. Hahn M-Y, Raman S, Anaya M, Husson RN. 2005. The *Mycobacterium tuberculosis* extracytoplasmic-function sigma factor SigL regulates polyketide synthases and secreted or membrane proteins and is required for virulence. J Bacteriol 187:7062–7071. https://doi.org/10.1128/JB.187.20.7062-7071.2005.
65. Shukla J, Gupta R, Thakur KG, Gokhale R, Gopal B. 2014. Structural basis for the redox sensitivity of the *Mycobacterium tuberculosis* SigK–RskA σ–anti-σ complex. Acta Crystallogr D Biol Crystallogr 70:1026–1036. https://doi.org/10.1107/S1399004714000121.
66. Seo SW, Kim D, Latif H, O'Brien EJ, Szubin R, Palsson BO. 2014. Deciphering Fur transcriptional regulatory network highlights its complex role beyond iron metabolism in *Escherichia coli*. Nat Commun 5:4910. https://doi.org/10.1038/ncomms5910.
67. Abe K, Obana N, Nakamura K. 2010. Effects of depletion of RNA-binding protein Tex on the expression of toxin genes in *Clostridium perfringens*. Biosci Biotechnol Biochem 74:1564–1571. https://doi.org/10.1271/bbb.100135.
68. Williams CL, Haines R, Cotter PA. 2008. Serendipitous discovery of an immunoglobulin-binding autotransporter in *Bordetella* species. Infect Immun 76:2966–2977. https://doi.org/10.1128/IAI.00323-08.

69. Paddock CD, Sanden GN, Cherry JD, Gal AA, Langston C, Tatti KM, Wu K-H, Goldsmith CS, Greer PW, Montague JL, Eliason MT, Holman RC, Guarner J, Shieh W-J, Zaki SR. 2008. Pathology and pathogenesis of fatal *Bordetella pertussis* infection in infants. Clin Infect Dis 47:328–338. https://doi.org/10.1086/589753.
70. Skopova K, Tomalova B, Kanchev I, Rossmann P, Svedova M, Adkins I, Bibova I, Tomala J, Masin J, Guiso N, Osicka R, Sedlacek R, Kovar M, Sebo P. 2017. Cyclic AMP-elevating capacity of adenylate cyclase toxin-hemolysin is sufficient for lung infection but not for full virulence of *Bordetella pertussis*. Infect Immun 85:e00937-16. https://doi.org/10.1128/IAI.00937-16.
71. Bolger AM, Lohse M, Usadel B. 2014. Trimmomatic: a flexible trimmer for Illumina sequence data. Bioinformatics 30:2114–2120. https://doi.org/10.1093/bioinformatics/btu170.
72. Li H, Durbin R. 2009. Fast and accurate short read alignment with Burrows-Wheeler transform. Bioinformatics 25:1754–1760. https://doi.org/10.1093/bioinformatics/btp324.
73. Li H, Handsaker B, Wysoker A, Fennell T, Ruan J, Homer N, Marth G, Abecasis G, Durbin R, 1000 Genome Project Data Processing Subgroup. 2009. The Sequence Alignment/Map format and SAMtools. Bioinformatics 25:2078–2079. https://doi.org/10.1093/bioinformatics/btp352.
74. Walker BJ, Abeel T, Shea T, Priest M, Abouelliel A, Sakthikumar S, Cuomo CA, Zeng Q, Wortman J, Young SK, Earl AM. 2014. Pilon: an integrated tool for comprehensive microbial variant detection and genome assembly improvement. PLoS One 9:e112963. https://doi.org/10.1371/journal.pone.0112963.
75. Bibova I, Skopova K, Masin J, Cerny O, Hot D, Sebo P, Vecerek B. 2013. The RNA chaperone Hfq is required for virulence of *Bordetella pertussis*. Infect Immun 81:4081–4090. https://doi.org/10.1128/IAI.00345-13.
76. Pfaffl MW. 2001. A new mathematical model for relative quantification in real-time RT-PCR. Nucleic Acids Res 29:e45. https://doi.org/10.1093/nar/29.9.e45.
77. Schindelin J, Arganda-Carreras I, Frise E, Kaynig V, Longair M, Pietzsch T, Preibisch S, Rueden C, Saalfeld S, Schmid B, Tinevez J-Y, White DJ, Hartenstein V, Eliceiri K, Tomancak P, Cardona A. 2012. Fiji: an open-source platform for biological-image analysis. Nat Methods 9:676–682. https://doi.org/10.1038/nmeth.2019.
78. Menck K, Behme D, Pantke M, Reiling N, Binder C, Pukrop T, Klemm F. 2014. Isolation of human monocytes by double gradient centrifugation and their differentiation to macrophages in Teflon-coated cell culture bags. J Vis Exp 2014:51554. https://doi.org/10.3791/51554.
79. Wiśniewski JR, Zougman A, Nagaraj N, Mann M. 2009. Universal sample preparation method for proteome analysis. Nat Methods 6:359–362. https://doi.org/10.1038/nmeth.1322.
80. Hebert AS, Richards AL, Bailey DJ, Ulbrich A, Coughlin EE, Westphall MS, Coon JJ. 2014. The one hour yeast proteome. Mol Cell Proteomics 13:339–347. https://doi.org/10.1074/mcp.M113.034769.
81. Cox J, Hein MY, Luber CA, Paron I, Nagaraj N, Mann M. 2014. Accurate proteome-wide label-free quantification by delayed normalization and maximal peptide ratio extraction, termed MaxLFQ. Mol Cell Proteomics 13:2513–2526. https://doi.org/10.1074/mcp.M113.031591.
82. Cox J, Neuhauser N, Michalski A, Scheltema RA, Olsen JV, Mann M. 2011. Andromeda: a peptide search engine integrated into the MaxQuant environment. J Proteome Res 10:1794–1805. https://doi.org/10.1021/pr101065j.
83. Cox J, Mann M. 2008. MaxQuant enables high peptide identification rates, individualized p.p.b.-range mass accuracies and proteome-wide protein quantification. Nat Biotechnol 26:1367–1372. https://doi.org/10.1038/nbt.1511.
84. Tyanova S, Temu T, Sinitcyn P, Carlson A, Hein MY, Geiger T, Mann M, Cox J. 2016. The Perseus computational platform for comprehensive analysis of (prote)omics data. Nat Methods 13:731–740. https://doi.org/10.1038/nmeth.3901.
85. Martin M. 2011. Cutadapt removes adapter sequences from high-throughput sequencing reads. EMBnet J 17:10. https://doi.org/10.14806/ej.17.1.200.
86. Huber W, Carey VJ, Gentleman R, Anders S, Carlson M, Carvalho BS, Bravo HC, Davis S, Gatto L, Girke T, Gottardo R, Hahne F, Hansen KD, Irizarry RA, Lawrence M, Love MI, MacDonald J, Obenchain V, Oleś AK, Pagès H, Reyes A, Shannon P, Smyth GK, Tenenbaum D, Waldron L, Morgan M. 2015. Orchestrating high-throughput genomic analysis with Bioconductor. Nat Methods 12:115–121. https://doi.org/10.1038/nmeth.3252.
87. Liao Y, Smyth GK, Shi W. 2019. The R package Rsubread is easier, faster, cheaper and better for alignment and quantification of RNA sequencing reads. Nucleic Acids Res 47:e47. https://doi.org/10.1093/nar/gkz114.
88. Liao Y, Smyth GK, Shi W. 2014. featureCounts: an efficient general purpose program for assigning sequence reads to genomic features. Bioinformatics 30:923–930. https://doi.org/10.1093/bioinformatics/btt656.
89. Love MI, Huber W, Anders S. 2014. Moderated estimation of fold change and dispersion for RNA-seq data with DESeq2. Genome Biol 15:550. https://doi.org/10.1186/s13059-014-0550-8.
90. Cattelan N, Jennings-Gee J, Dubey P, Yantorno OM, Deora R. 2017. Hyperbiofilm formation by *Bordetella pertussis* strains correlates with enhanced virulence traits. Infect Immun 85:e00373-17. https://doi.org/10.1128/IAI.00373-17.
91. Perez-Riverol Y, Csordas A, Bai J, Bernal-Llinares M, Hewapathirana S, Kundu DJ, Inuganti A, Griss J, Mayer G, Eisenacher M, Pérez E, Uszkoreit J, Pfeuffer J, Sachsenberg T, Yilmaz S, Tiwary S, Cox J, Audain E, Walzer M, Jarnuczak AF, Ternent T, Brazma A, Vizcaíno JA. 2019. The PRIDE database and related tools and resources in 2019: improving support for quantification data. Nucleic Acids Res 47:D442–D450. https://doi.org/10.1093/nar/gky1106.

APPENDIX IV

Review

Structure-Function Relationships Underlying the Capacity of *Bordetella* Adenylate Cyclase Toxin to Disarm Host Phagocytes

Novak J, Cerny O, Osickova A, Linhartova I, Masin J, Bumba L, Sebo P, Osicka R.

Toxins (Basel). 2017 Sep 24;9(10):300. doi: 10.3390/toxins9100300.

toxins

MDPI

Review

Structure–Function Relationships Underlying the Capacity of *Bordetella* Adenylate Cyclase Toxin to Disarm Host Phagocytes

Jakub Novak [1,2], Ondrej Cerny [1,†], Adriana Osickova [1,2], Irena Linhartova [1], Jiri Masin [1], Ladislav Bumba [1], Peter Sebo [1] and Radim Osicka [1,*]

[1] Institute of Microbiology of the CAS, v.v.i., 142 20 Prague, Czech Republic; jakub.novak@biomed.cas.cz (J.N.); o.cerny@imperial.ac.uk (O.C.); osickova@biomed.cas.cz (A.O.); linhart@biomed.cas.cz (I.L.); masin@biomed.cas.cz (J.M.); bumba@biomed.cas.cz (L.B.); sebo@biomed.cas.cz (P.S.)

[2] Faculty of Science, Charles University in Prague, 128 43 Prague, Czech Republic

* Correspondence: osicka@biomed.cas.cz; Tel.: +420-241-062-770

† Present address: MRC Centre for Molecular Bacteriology and Infection, Imperial College London, London SW7 2AZ, UK

Academic Editor: Alexandre Chenal

Received: 29 August 2017; Accepted: 21 September 2017; Published: 24 September 2017

Abstract: *Bordetellae*, pathogenic to mammals, produce an immunomodulatory adenylate cyclase toxin–hemolysin (CyaA, ACT or AC-Hly) that enables them to overcome the innate immune defense of the host. CyaA subverts host phagocytic cells by an orchestrated action of its functional domains, where an extremely catalytically active adenylyl cyclase enzyme is delivered into phagocyte cytosol by a pore-forming repeat-in-toxin (RTX) cytolysin moiety. By targeting sentinel cells expressing the complement receptor 3, known as the CD11b/CD18 ($\alpha_M\beta_2$) integrin, CyaA compromises the bactericidal functions of host phagocytes and supports infection of host airways by *Bordetellae*. Here, we review the state of knowledge on structural and functional aspects of CyaA toxin action, placing particular emphasis on signaling mechanisms by which the toxin-produced 3′,5′-cyclic adenosine monophosphate (cAMP) subverts the physiology of phagocytic cells.

Keywords: adenylate cyclase toxin; *Bordetella*; β_2 integrins; cAMP; CD11b/CD18; cell signaling; complement receptor 3; innate immunity; membrane pores; repeats-in-toxin

1. Introduction

Three species of the Gram-negative aerobic coccobacilli of the genus *Bordetellae*, *B. pertussis*, *B. parapertussis* and *B. bronchiseptica*, are pathogenic to mammals. Of them, the species *B. pertussis* is one of the few human-adapted pathogens and causes the respiratory infectious disease called pertussis, or whooping cough [1]. Despite global vaccination coverage, pertussis remains the least-controlled vaccine preventable infectious disease. A recently published model estimates that, in 2014, the global pertussis burden in children younger than five years was ~24 million cases, accounting for more than 160,000 deaths, predominantly of infants [2]. *B. pertussis* infections are often complicated by secondary infections and pneumonia [3], because of a predisposing immunosuppressive action of the numerous virulence factors produced by the pathogen [1]. Among them, the adenylate cyclase toxin–hemolysin (known as CyaA, ACT or AC-Hly) excels in subversion of multiple host immune defense mechanisms [4,5].

CyaA belongs to the large family of repeat-in-toxin (RTX) cytotoxins that harbor the characteristic C-terminal calcium-binding aspartate and glycine-rich nonapeptide repeats of a consensus sequence G-G-X-G-X-D-X-X-X (X, any amino acid residue) [6–8]. The toxin is a 1706 residue-long polypeptide

(Figure 1) consisting of an N-terminal ~400 residue-long adenylate cyclase (AC) enzyme that is linked to a characteristic RTX hemolysin (Hly) moiety of ~1300 residues [9]. The Hly moiety itself consists of four functional subdomains [7,10], comprising: (i) a hydrophobic pore-forming domain [11]; (ii) an activation domain, with the two posttranslationally acylated lysine residues [12,13]; (iii) a receptor-binding RTX domain consisting of ~40 typical calcium-binding RTX nonapeptide repeats [14]; and (iv) a non-processed C-terminal secretion signal recognized by a bacterial type I secretion system (T1SS) [15,16], respectively.

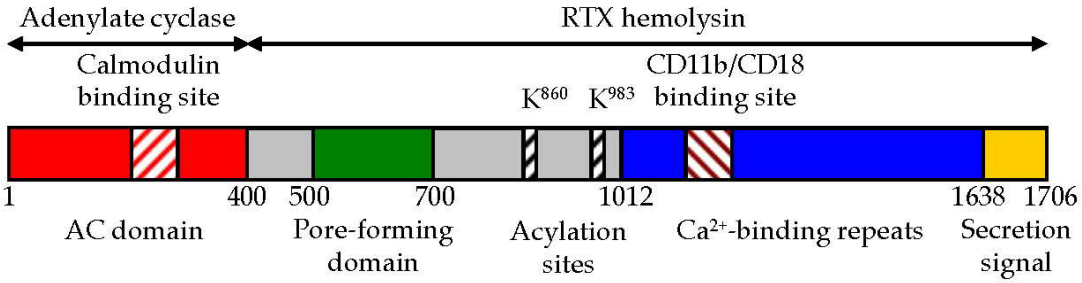

Figure 1. Schematic representation of CyaA. CyaA is a 1706 residue-long polypeptide that consists of an N-terminal AC enzyme domain (~400 residues) and a C-terminal Hly moiety (~1300 residues) that are linked together with a ~100 residue-long segment (residues 400 to 500). The Hly portion of CyaA itself harbors several functional subdomains: (i) a hydrophobic pore-forming domain (residues 500 to 700); (ii) an activation domain (residues 800 and 1000), where the posttranslational acylation at two lysine residues (K860 and K983) occurs; (iii) a typical calcium-binding RTX domain with the nonapeptide repeats binding calcium ions and with the CD11b/CD18-binding segment (residues 1166–1287); and (iv) a C-terminal secretion signal.

The Hly moiety of CyaA mediates toxin binding to the CD11b/CD18 heterodimer that serves as the complement receptor 3 (CR3) on myeloid phagocytes, and is also known as the $\alpha_M\beta_2$ integrin or Mac-1 [17,18]. Upon insertion into the target cell membrane, the Hly moiety delivers the catalytic AC domain of CyaA directly into the cytosol of cells by a poorly understood mechanism that requires proper calcium-induced folding, acylation and structural integrity of the Hly moiety [10,19–21]. In the cytosol, the AC domain binds calmodulin (CaM) [22] and hijacks cellular signaling by unregulated conversion of cytosolic adenosine triphosphate (ATP) to the key signaling molecule, 3′,5′-cyclic adenosine monophosphate (cAMP) [4,23,24]. The Hly moiety of CyaA is functionally independent of the AC domain and can itself form small cation-selective membrane pores that permeabilize target cell membrane and can provoke colloid-osmotic (oncotic) lysis of cells [11,19,25–27].

Once inserted across the membrane of target cells, CyaA acts as a swift multifunctional saboteur that ablates phagocyte functions by at least three parallel and synergic cytotoxic activities that hijack cellular signaling. Membrane insertion of CyaA mediates: (i) influx of calcium ions into cytosol of cells [28]; (ii) translocation of the AC domain that subverts cellular signaling pathways by an extremely rapid and uncontrolled elevation of cytosolic cAMP concentration [18,23,29–31]; and (iii) formation of the oligomeric CyaA pores that permeabilize cellular membrane and activate MAPK signaling by mediating potassium ion efflux from cells [26,32–36]. Depending on the encountered toxin amount, the phagocyte then undergoes apoptotic or necrotic cell death [27,37–39].

Here, we summarize the current knowledge of structure–function relationships that underlie the action of CyaA toxin. We next discuss the recent advances in deciphering of the signaling pathways through which the action of CyaA abrogates the sentinel functions of phagocytic cells and enables *Bordetellae* to overcome the innate immune defense of the host.

2. CyaA Structure

2.1. The AC Domain of CyaA

The AC domain of CyaA belongs to the class II of adenylyl cyclase enzymes [EC 4.6.1.1] that convert ATP to cAMP, a "second messenger" and key intracellular signaling molecule [40]. The AC of CyaA of *Bordetellae* [5,8], the edema factor (EF) of *Bacillus anthracis* [41,42] and the ExoY effector of *Pseudomonas aeruginosa* [43,44] play an important role in virulence of these pathogenic bacteria. These AC enzymes exhibit a very low catalytic activity inside bacterial cytosol and are only activated upon delivery into cytosol of host eukaryotic cells, where ExoY is activated by filamentous actin [45], while the EF and the AC domain of CyaA are activated upon binding of eukaryotic CaM in a 1:1 stoichiometry [22,41,46]. Binding to CaM increases the catalytic activity of the AC enzyme by a factor of ~100–1000-fold [22,47] and the CaM-activated AC enzyme produces a pathologic level of cytosolic cAMP that hijacks cellular signaling [4,24]. CyaA catalyzes not only the formation of cAMP but also the formation of cCMP and cUMP and these multiple cNMP-forming enzyme activities involve a single catalytic site [48]. Two functional subdomains of the catalytic AC domain, T25 and T18, were identified by limited proteolysis, which are still able to assemble with CaM into a fully active ternary complex [46]. By using residue modification and mutagenesis, the catalytic site of the AC was located within the T25 subdomain (residues 1–224), while the main CaM-binding site was located on the T18 fragment (residues 225–399) [49,50].

Several residues play a critical role in the catalytic activity of the AC enzyme of CyaA. Two lysine residues at positions 58 and 65 (K58 and K65) within segment I (residues 54 to 77) were found to be part of the AC catalytic site and their replacements resulted in an important decrease, or total loss, of AC enzymatic activity [49]. In addition, a histidine residue at position 63 (H63) in segment I has been identified as the general acid/base catalyst in a predicted charge-relay system proposed to be involved in the reaction mechanism of adenylyl cyclization [51]. In segment II (residues 184 to 196), two aspartate residues D188 and D190 appear to be required for binding of the Mg^{2+}-ATP complex [52]. Finally, substitutions of residues H298 and E301 in segment III (residues 294 to 314) also affect the nucleotide binding properties of AC, albeit to a lesser degree [52]. These early observations were confirmed and corroborated upon solving of the crystal structure of the AC enzyme-C-terminal domain of CaM (C-CaM) complex with adefovir diphosphate (Figure 2), a metabolite of an anti-viral drug tightly binding into the catalytic site and thereby mimicking binding of ATP [53]. This study revealed that D188, D190 and H298 residues are crucial for binding of the catalytic Mg^{2+} metal ions, while D304 is involved in positioning of ribose, and R37, K58, K65 and K84 residues are required for binding of the triphosphate of the ATP substrate [53]. Deprotonation of 3′ OH of ATP is then accomplished by H63, the central catalytic residue of the AC enzyme that is further involved in the reaction mechanism of adenylyl cyclization [51].

The crystal structure of the AC enzyme-C-CaM complex (Figure 2) revealed that four discrete regions of the AC enzyme bind calcium-loaded CaM with a large buried contact surface [53]. Of those, the W242 residue within an α-helix of the T18 subdomain makes extensive contacts with the calcium-induced hydrophobic pocket of CaM [54]. Amino acid substitutions of the W242 residue have yielded AC enzymes with a full catalytic activity and up to 1000-fold reduced affinity for CaM [49,50]. It was further confirmed that all four regions of the AC domain contribute to CaM binding and that the CaM-induced conformational change of CyaA is crucial for catalytic activation [49,50,54]. Biochemical and molecular modeling studies revealed that the β-hairpin (residues 259 to 273) of the AC domain interacts with the N-terminal domain of CaM (N-CaM) [55]. Site-specific mutations in the β-hairpin resulted in conformational perturbations in metal binding sites I and II of N-CaM, while no significant structural modifications were observed in C-CaM [56]. Intriguingly, when the AC domain interacts with intact CaM, the metal-binding sites I and II of CaM bind Mg^{2+} ions, while the sites III and IV of CaM are loaded with Ca^{2+} ions [57]. Mg^{2+} ions are present in millimolar concentrations in the cytosol of cells and the action of CyaA and cAMP signaling induces entry of Ca^{2+} ions into cells [28,58,59].

The competition of Ca^{2+} and Mg^{2+} ions for the metal binding sites I and II offers space for fine-tuning of the catalytic activity of the AC enzyme, which starts to be inhibited already at >100 nM free Ca^{2+} [60].

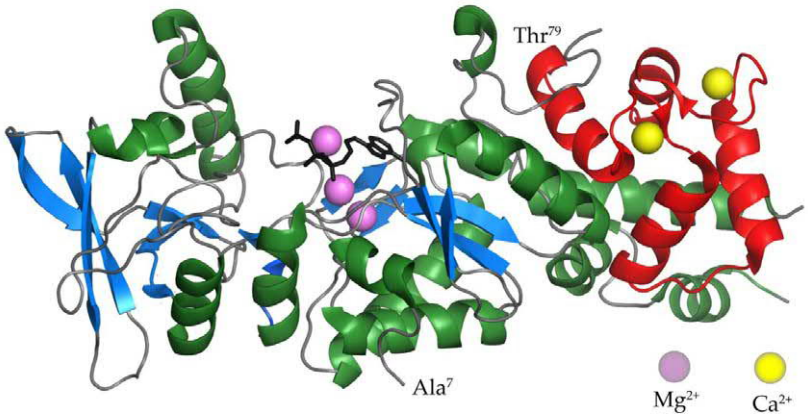

Figure 2. The crystal structure of the AC domain of CyaA in the complex with the C-terminal domain of CaM [53]. α-helices and β-strands of the AC domain are colored in green and blue, respectively. The C-terminal domain of CaM is colored in red. Calcium and magnesium ions are represented by yellow and violet balls. The structure of the ATP analog adefovir diphosphate is represented by black lines.

2.2. The AC to Hly-Linking Segment

A ~100-residue-long segment, located between residues 400 and 500 of CyaA (Figure 1), links the AC enzyme to the Hly moiety. It has no homologs in the other proteins of the RTX family and only little is known about its structure and function in CyaA activities. A synthetic peptide comprising residues 454 to 484 of CyaA was shown to possess a lipid bilayer interacting and destabilizing capacity [61]. Mass spectrometry combined with circular dichroism revealed that the linker segment consisting of residues 411 to 490 forms α-helical secondary structures and inserts into the liposomal membrane [62]. In line with the obvious assumption that the AC-to-Hly-linking segment is involved in translocation of the AC domain across the cell membrane, deletion of the residues 375 to 485 abolished the capacity of CyaA to translocate the AC domain across the membrane of erythrocytes [63]. Moreover, this segment is rich in arginine residues proposed to be involved in target membrane destabilization and individual alanine substitutions of four of them (R435A, R443A, R461A and R487A) decreased the capacity of CyaA to translocate the AC domain across target cell membrane [62]. The AC-to-Hly-linking segment further appears to play a role in restricting the propensity of CyaA to form pores in target cell membranes. The CyaA variant lacking the N-terminal residues 6 to 489 exhibits, indeed, a strongly enhanced cell-permeabilizing and pore-forming activity [64,65]. Furthermore, combined substitution of three negatively charged residues clustered within the N-terminal half of the linker segment of CyaA by neutral residues (D445N + D446N + E448Q) provoked a dramatic increase of the specific pore-forming capacity of the toxin without altering its specific capacity to translocate the AC domain across target cell membrane [62]. Thus, the presence and clustering of negative charges in the AC-to-Hly-linking segment of CyaA appear to account for the relatively modest cell-permeabilizing capacity of CyaA pores, as compared to typical hemolysins of the RTX family [62].

2.3. The Pore-Forming Domain of CyaA

The hydrophobic pore-forming domain of CyaA, comprised between residues 500 to 700 (Figure 1), consists of several predicted amphipathic and hydrophobic α-helical structures. These play a key role both in AC domain translocation, as well as in the formation of cation-selective oligomeric CyaA pores within target membranes [11,19,25,66–69]. By using the method of osmotic solute exclusion, the size of the pore formed by CyaA in the cell membrane was estimated to be between 0.6 to 0.8 nm in diameter [26]. Very similar size of CyaA pores was derived also from planar lipid bilayer

measurements [11]. The CyaA pores can permeabilize cell membranes for small cations [34] and can provoke colloid-osmotic (oncotic) lysis of erythrocytes, thus accounting for the hemolytic halo that surrounds *Bordetella* colonies grown on blood agar plates [70]. However, compared to typical RTX hemolysins, the specific hemolytic activity of CyaA is rather low [19,26,65,71,72]. This suggests that the pore-forming domain of CyaA evolved towards a function in delivery of the invasive AC domain across target cell membrane, at the expense of its pore-forming capacity. However, the CyaA pore is too small in diameter to allow passage of even an unfolded AC domain polypeptide across the membrane. Moreover, mutant CyaA variants (e.g., E570Q + K860R) that are essentially unable to form pores and permeabilize cellular membrane for monovalent cations, are still fully capable to translocate the AC domain across the lipid bilayer of cell membrane [69] by an as yet enigmatic mechanism, which likely involves formation of a protein–lipid interface by membrane-inserted CyaA monomers. The cation-selective CyaA pores mediate potassium ion efflux from nucleated cells [32,69] and this cell-permeabilizing activity of CyaA contributes to its overall cytotoxicity towards phagocytic cells [27,38,69].

The pore-forming domain can mediate insertion of CyaA into naked lipid bilayers of liposomes on its own [73]. Indeed, truncated CyaA constructs lacking the entire RTX domain and the C-terminal secretion signal (residues 1007 to 1706) can also insert into artificial planar lipid bilayers with applied membrane potential and form pores that exhibit similar characteristics as the pores formed by the entire CyaA toxin [11]. However, the calcium-loaded and folded RTX domain appears to play a key structural role in the pore-forming activity of CyaA as well [7]. The exceedingly cooperative calcium-dependent folding of the RTX domain [7,15,74,75] was found to yield a steep (~50-fold) increase of the propensity of CyaA to form pores in artificial lipid bilayers as the concentration of free calcium ions crosses a very narrow threshold of 0.7 to 0.8 mM Ca^{2+} [76]. CyaA can further insert into and perturb the structure and integrity of lipid bilayer membranes that are devoid of membrane potential and it mediates the release of marker substances from liposomes [20,73,77,78]. However, it is highly questionable whether in the absence of membrane potential the CyaA protein adopts the same transmembrane topology inside lipid bilayer and forms the same types of pores, permeabilizing the lipid bilayer by the same mechanism, as in the presence of membrane potential. This is rather unlikely, as the phenotypes of charge-reversing substitutions of the E509 and E516 residues within the pore-forming domain of CyaA, which significantly alter the hemolytic and pore-forming activities of CyaA on membranes bearing potential [68], are not at all reproduced on liposomal membranes that are devoid of membrane potential [73]. Moreover, CyaA pores were shown to exhibit voltage dependence and the type and characteristics of pores formed by CyaA were found to depend on the level and orientation of the electrical potential across the membranes [79]. Therefore, interpretation of results obtained with CyaA on liposomal membranes is highly prone to generate artifactual and biologically irrelevant conclusions.

2.4. The Activation Domain of CyaA

Production of the biologically active CyaA toxin requires covalent posttranslational fatty-acyl modification of proCyaA by the co-expressed protein toxin acyltransferase CyaC [80,81]. Initially, the native CyaA purified from *B. pertussis* (BP338) was found to be activated by amide-linked palmitoylation of only the ε-amino group of the lysine residue 983 [12]. However, the recombinant CyaA produced in *E. coli* in the presence of CyaC was found to be acylated also on the lysine residue 860 [13]. A double modification of both conserved lysine residues (K860 and K983) was then found also on CyaA secreted by the recombinant *B. pertussis* strain 18323/pHSP9, which produces increased CyaC and CyaA amounts due to expression of the *cyaCABDE* locus from a low copy number plasmid [82]. It remains to be determined whether CyaA produced by clinical isolates is doubly acylated or mono-acylated.

Ablation of either of the acylation sites by an arginine substitution yielded monoacylated CyaA-K860R and CyaA-K983R toxins that exhibited importantly reduced toxin activities on erythrocytes that lack the CD11b/CD18 integrin receptor of CyaA [83,84]. However, subsequent

production of CyaA with both K860 and K983 residues intact, but preferentially acylated on either the K860 or the K983 residue by co-expressed mutated variants of CyaC, allowed concluding that the K860 residue plays a structural role in toxin activity that is independent of its acylation status [85]. Use of such incompletely acylated CyaA variants allowed to demonstrate that acylation of the K860 residue alone does not confer a substantial cell-invasive activity on CyaA. In contrast, acylation of K983 was found to be necessary and sufficient for toxin activities on erythrocytes [85]. This was confirmed also for toxin activities on myeloid phagocytic cells that bear the CD11b/CD18 receptor of CyaA [84]. Acylation of the K860 residue alone conferred on the monoacylated CyaA-K983R toxin an almost full capacity to bind the receptor and tightly associate with the CD11b/CD18-expressing J774A.1 mouse macrophage cells but the capacity of CyaA-K983R toxin to penetrate cells and translocate the AC domain was largely impaired [84]. In contrast, the monoacylated CyaA-K860R was as active in CD11b/CD18 binding and AC domain delivery into the macrophage cells as the intact CyaA, demonstrating that the acylation of K860 is dispensable, whereas the acylation of the K983 residue is necessary and sufficient for the capacity of CyaA to bind and penetrate the membrane of myeloid phagocytes [84].

Of note, the non-acylated pro-CyaA forms pores in planar lipid bilayers with a lower propensity than the fully acylated toxin, but the proCyaA pores have similar properties as pores formed by the acylated CyaA [84]. It appears, hence, that the presence of acyl residues on CyaA is not crucial for the structure of the formed pores. However, pores formed in lipid bilayers by the monoacylated CyaA-K983R toxin exhibited importantly reduced selectiveness for cations than pores formed by intact CyaA, revealing that the K983 residue may also play an important role in toxin structure independently of its acylation status [84].

2.5. The RTX Domain of CyaA

The RTX domain of CyaA consists of five distinct RTX blocks (I to V) located between residues 1012 and 1638 that harbor the typical RTX nonapeptide repeats [14]. Recently, we solved the 3D structure of the segment encompassing residues 1529 to 1681 of CyaA and comprising the block V with its C-terminal folding-initiating structure (Figure 3) [15]. The nonapeptide tandem repeats within this structure are arranged in a regular right-handed helix consisting of parallel β-strands, forming a β-roll structure with eight calcium ions bound within the turns connecting the β-strands [15]. Similar β-roll arrangement was observed for 3D structures of other RTX proteins, such as proteases and lipases of *Pseudomonas aeruginosa* and *Serratia marcescens* [86–88]. In these typical RTX β-rolls, the first six residues of the nonapeptide RTX motif (G-G-X-G-X-D) constitute a turn with a bound calcium ion, while the last three residues form a short β-strand. Calcium ions are then periodically coordinated by carboxyl groups of the side chains of aspartic acid residues and the carbonyl groups of the polypeptide backbone of the nonapeptide RTX motifs.

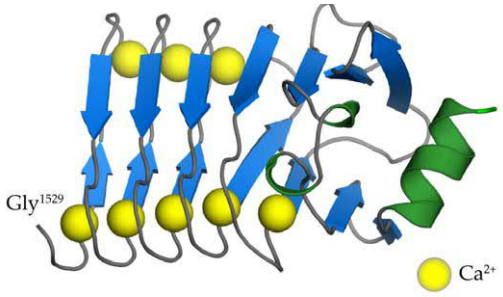

Figure 3. The crystal structure of the segment 1529–1681 of CyaA [15]. The consecutive nonapeptide tandem repeats (G-G-X-G-X-D-X-X-X) are arranged in a regular right-handed helix of parallel β-strands (β-roll). β-strands and the C-terminal α-helix are colored in blue and green, respectively. Calcium ions are represented by yellow balls.

The five β-roll blocks of the RTX domain are connected by segments of variable lengths and their Ca^{2+}-dependent folding proceeds in an extremely cooperative manner and results in dehydration and compaction of the RTX domain [7,15,74,75,79]. As recently revealed by a low-resolution SAXS structure of the entire monomeric CyaA holotoxin molecule, the N-terminal ~1000 residue-long portion of the CyaA molecule then can fold back onto this RTX domain "scaffold" to form a rather compact and quite stable structure [89]. Finally, the blocks II and III of the RTX domain form the major CD11b/CD18-binding structure of CyaA [18,90,91].

2.6. The C-Terminal Secretion Signal of CyaA

The Hly moiety of CyaA harbors within the last 74 residues an unprocessed secretion signal that is recognized by the T1SS apparatus formed by the CyaBDE proteins across the bacterial cell wall [16,92]. Led by the C-terminal sequence, the toxin is extruded through the T1SS conduit in an unfolded state, directly from the calcium-depleted bacterial cytosol into the host body fluids containing millimolar concentrations of free calcium ions [9,15,93,94]. At the low concentrations of calcium ions inside the bacterial cytosol, the RTX domain remains intrinsically disordered and highly hydrated [75,95–97]. In the course of extrusion from bacterial cells, the binding of calcium ions from body fluids triggers folding of the emerging C-terminal segment [98]. This forms a capping structure and scaffolds the calcium-driven co-secretional folding of the translocating RTX domain, which proceeds vectorially from the C-terminus towards the N-terminal end and ratchets and accelerates toxin translocation out of the bacterial cell [15].

3. Binding Interaction of CyaA with the Complement Receptor 3 on the Surface of Phagocytic Cells

Due to the extremely high specific enzymatic activity of the AC domain of CyaA, the toxin was found early on to bind and penetrate at low but well detectable levels a variety of eukaryotic cell types originating from diverse mammalian species [24,71,99,100]. This non-saturable and unspecific cell binding is likely to be mediated by a low affinity interaction of the toxin with abundant cell surface glycoproteins, or glycosylated lipid molecules, such as certain gangliosides that accumulate in lipid microdomains of the plasma membrane of cells [20,101]. Indeed, pre-incubation of the toxin with gangliosides, such as >1 μM G_{T1b}, strongly reduced the capacity of CyaA to penetrate into Chinese hamster ovary (CHO) cells [20]. However, CyaA was observed to act particularly efficiently, at very low toxin concentrations, on myeloid phagocytic cells, such as neutrophils, monocytes and macrophages [23,102]. This indicated the existence of a proteinaceous and leukocyte-specific receptor of CyaA. Indeed, respiratory infection experiments with *Bordetella* species in mice revealed that CyaA specifically targets neutrophils and other phagocytes without provoking much damage of the airway epithelial cells [103,104]. Moreover, other members of the RTX toxin family were previously found to bind β_2 integrin receptors of leukocytes [105–108]. Guermonprez and coworkers demonstrated in 2001 that CyaA specifically binds target cells through interaction with the integrin CD11b/CD18 that serves as complement receptor 3 (CR3) on myeloid phagocytic cells [17].

The CD11b/CD18 heterodimer (Figure 4a) binds a large variety of physiological ligands and is involved in numerous leukocyte functions. These include adherence of monocytes and neutrophils to vascular endothelium, phagocytosis of complement-opsonized microorganisms, respiratory burst or degranulation of neutrophils, cell spreading, chemotaxis and other functions [109]. CD11b/CD18 belongs to the β_2 family of integrins restricted to leukocytes, comprising four heterodimeric transmembrane glycoproteins sharing the same β_2 subunit that pairs with four distinct α subunits [109,110] to form the $\alpha_L\beta_2$ (CD11a/CD18, LFA-1), $\alpha_M\beta_2$ (CD11b/CD18, Mac-1, CR3), $\alpha_X\beta_2$ (CD11c/CD18, p150/195), and $\alpha_D\beta_2$ (CD11d/CD18) heterodimers, respectively. Despite high level of sequence homology between the α subunits of the four β_2 integrins, CyaA was found to specifically bind only to dendritic cells (DCs) and macrophages expressing the CD11b/CD18 molecule, but not to B cells or T cells expressing only the CD11a/CD18 molecule [17]. Moreover, cell-binding and penetration of these cells is selectively blocked by certain CD11b-specific antibodies

and dose-dependent saturable binding of CyaA is observed only with CHO cells transfected to express CD11b/CD18, but not with CHO cells expressing CD11a/CD18 or CD11c/CD18 integrins [17,18]. At less than 1 nM CyaA concentrations, mimicking the physiological situation in vivo [111], the binding of CyaA to CD11b/CD18 was shown to be a prerequisite for efficient toxin penetration into cells and high levels of intoxication of cells by cAMP, leading to CyaA-induced cell death [27,38,112].

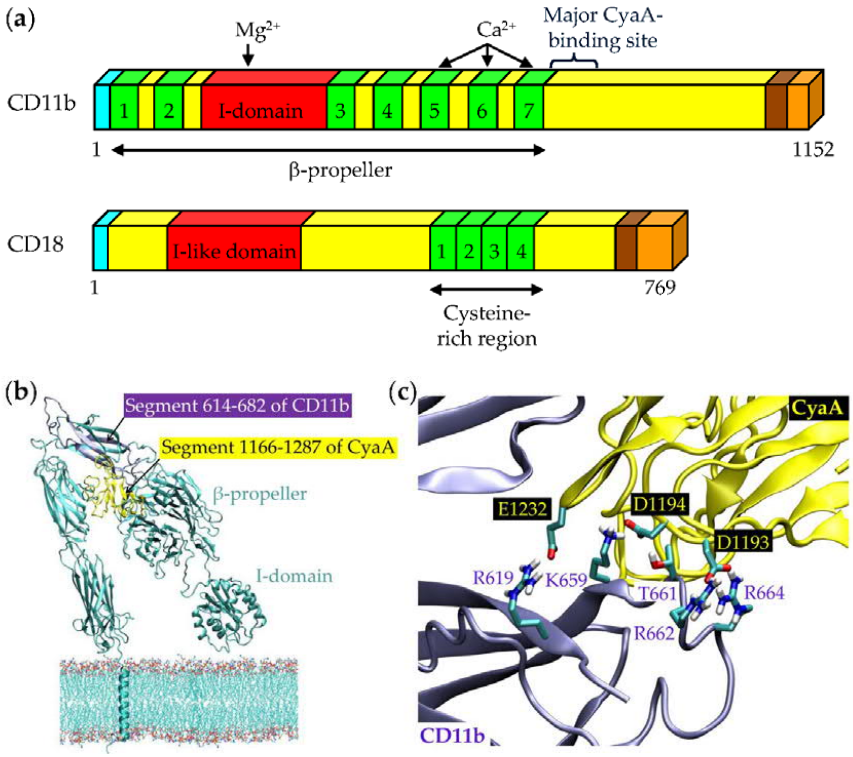

Figure 4. Schematic representation of the CD11b/CD18 heterodimer and its interaction with CyaA. (**a**) The 1152 residues long CD11b subunit contains an N-terminal secretion signal (16 residues; cyan), an N-terminal extracellular domain (1088 residues; yellow), a transmembrane segment (24 residues; brown) and a C-terminal cytoplasmic tail (24 residues; beige) [113,114]. The N-terminal part of CD11b consists of seven β-sheet repeats (1 to 7, from 52 to 79 residues; green), which have been predicted to fold into a β-propeller domain and a region of 187 residues, called the inserted or I-domain, that is localized between repeats 2 and 3 of the β-propeller (red) [115,116]. The I domain contains an Mg^{2+}/Mn^{2+} coordination site at its surface (MIDAS) that is critical for ligand binding [115,117,118]. Repeats 5 to 7 of CD11b have EF hand-like Ca^{2+}-binding motifs [116]. CyaA primarily recognizes the CD11b segment containing residues 614 to 682. The CD18 subunit is a 769 residues long polypeptide chain harboring an N-terminal secretion signal (22 residues; cyan), an N-terminal extracellular domain (678 residues; yellow), a transmembrane segment (23 residues; brown) and a C-terminal cytoplasmic domain (46 residues; beige) [119]. The extracellular domain contains the I-like domain (residues 124 to 363; red) and 56 cysteine residues forming the Cys-rich region localized near the membrane and composed of four repeat units of approximately 40 residues (green). These fold into small, very compact domains and are parts of the long stalk. The CD11b and CD18 subunits harbor several potential N-glycosylation sites (N-X-S/T), most of them modified by oligosaccharide chains linked to asparagine residues [120,121]. (**b**) 3D model of the CD11b subunit of CR3 (generated with the Modeler suite of programs) with the highlighted segment 614–682 (violet) that interacts with the segment 1166–1287 of CyaA (yellow; modeled using the structure prediction server I-TASSER) [18]. (**c**) The negatively charged residues of the 1166–1287 segment of CyaA are involved in the interaction with the positively charged and hydrophilic residues of the 614–682 segment of CD11b [18]. Reproduced and modified from [18], 2015, eLife Sciences Publications.

We showed that the initial interaction of CyaA with CD11b/CD18 depends on the recognition of N-linked oligosaccharide chains of the integrin receptor, where a significant reduction of CyaA binding is observed upon removal of the peripheral sialic acid residues from the cell surface glycoproteins by neuraminidase treatment [122]. Moreover, CyaA binding was completely abolished when sugar chains were entirely removed by PNGase F and a complete inhibition of CyaA binding to the CD11b/CD18-expressing cells was observed when N-glycosylation of de novo synthesized proteins was blocked by tunicamycin, while the CD11b/CD18 heterodimer still formed and was presented on cell surface [122]. In addition, CyaA binding to the integrin receptor was specifically and efficiently inhibited in the presence of free saccharides that are found as building units of the oligosaccharide chains of CD11b/CD18 [122].

The CD11b subunit harbors 19 predicted canonical N-glycosylation sites (N-X-S/T) and the CD18 subunit has 6 such sites [109]. To analyze the relative importance of individual N-glycans of CD11b/CD18 for binding and biological activity of CyaA, we substituted one-by-one the asparagine residues of each of the consensus N-glycosylation sites of CD11b/CD18 with a glutamine residue that cannot be glycosylated [120]. Examination of the CD11b/CD18 mutant variants and mass spectrometry analysis of the N-glycosylation pattern of the integrin revealed that N-linked oligosaccharide chains located in the C-terminal portion of the CD11b subunit are involved in CyaA binding and penetration into cells [120]. The initial interaction of CyaA with CD11b/CD18, hence, appears to depend on a multivalent interaction of CyaA with multiple oligosaccharide chains located in the C-terminal portion of the CD11b subunit. These multivalent contacts with glycan chains then would enhance both the specificity and the affinity of the initial interaction of CyaA with its receptor.

The weak lectin-like capacity of CyaA to bind sugar structures offers an attractive hypothesis for explaining the previous observation that CyaA may bind gangliosides on cells lacking the CD11b/CD18 receptor [20,101]. Gangliosides are acidic lipids composed of a ceramide linked to an oligosaccharide chain containing one or more sialic acid residues [123]. CyaA might thus potentially recognize an oligosaccharide moiety of gangliosides, including negatively charged sialic acid residues, similarly as it recognizes oligosaccharide chains of the β_2 integrin CD11b/CD18.

Upon a weak primary interaction of CyaA with the N-linked glycans, the selectivity of CyaA binding to CD11b/CD18 is dictated by a subsequent highly specific protein–protein interaction. It involves the segment 1166–1287 of CyaA [90] and a segment containing residues 614 to 682 of the CD11b subunit of CR3 (Figure 4b) [18]. Detailed analysis of the binding interaction revealed that negatively charged glutamate and aspartate residues of the 1166–1287 segment of CyaA would interact with positively charged and hydrophilic residues within the 614–682 segment of CD11b (Figure 4c) [18]. However, the interaction may be more complex, as additional segments of CD11b appear to be contributing to CyaA binding to the CD11b/CD18 heterodimer, to some extent [18]. This suggests that the toxin binds the integrin through a multivalent interaction also at the protein–protein level. Engagement of other CD11b segments may facilitate or stabilize/position the toxin for higher-affinity interaction with the principal binding site located within the 614–682 segment of CD11b. Moreover, binding of CyaA to CD11b required proper folding of the CD11b subunit on the scaffold of the CD18 subunit, as CyaA bound CD11b only when this was associated and presented in a complex with CD18 on cell surface [18]. Most importantly, unlike fibrinogen, iC3b, the intercellular adhesion molecule 1 (ICAM-1) and other proteinaceous ligands of CR3, the CyaA toxin did not bind the integrin through the conserved I (inserted)-domain of CD11b (Figure 4) [18,115].

These data allowed us to propose that the segment between residues 614 to 682 and the adjacent N-linked oligosaccharide chains located in the C-terminal portion of CD11b may cooperate in forming a highly organized structure that accounts for specific binding of CyaA to CD11b, supporting its subsequent penetration across cellular membrane and biological activities. The structural integrity of this CyaA-binding site could be destabilized by deglycosylation of CD11b [122], by the removal of some of the individual N-linked glycans [120], or by point substitutions introduced into the 614–682 segment [18]. We further demonstrated that the transmembrane α-helical segments of CD11b/CD18

are not directly involved in AC domain translocation and/or pore formation by the toxin but serve in maintaining of a proper conformation of the integrin, required for efficient toxin binding and action [124].

4. Phagocyte Membrane Penetration and Permeabilization by CyaA

The highly specific interaction with the CD11b subunit of CD11b/CD18 facilitates insertion of CyaA into the lipid bilayer of cellular membrane and translocation of the AC domain across it into the cytosol of phagocytic cells (Figure 5). The irreversible insertion of the toxin into cell membrane shifts the toxin–receptor binding equilibrium to the right and would account for the very high apparent affinity (in the nanomolar range) of CyaA binding to CD11b/CD18-expressing cells [17,18]. Indeed, an about two orders of magnitude lower affinity is observed for the mere binding interaction of CyaA with the isolated CD11b/CD18 heterodimer that is not anchored in a biological membrane [17,18].

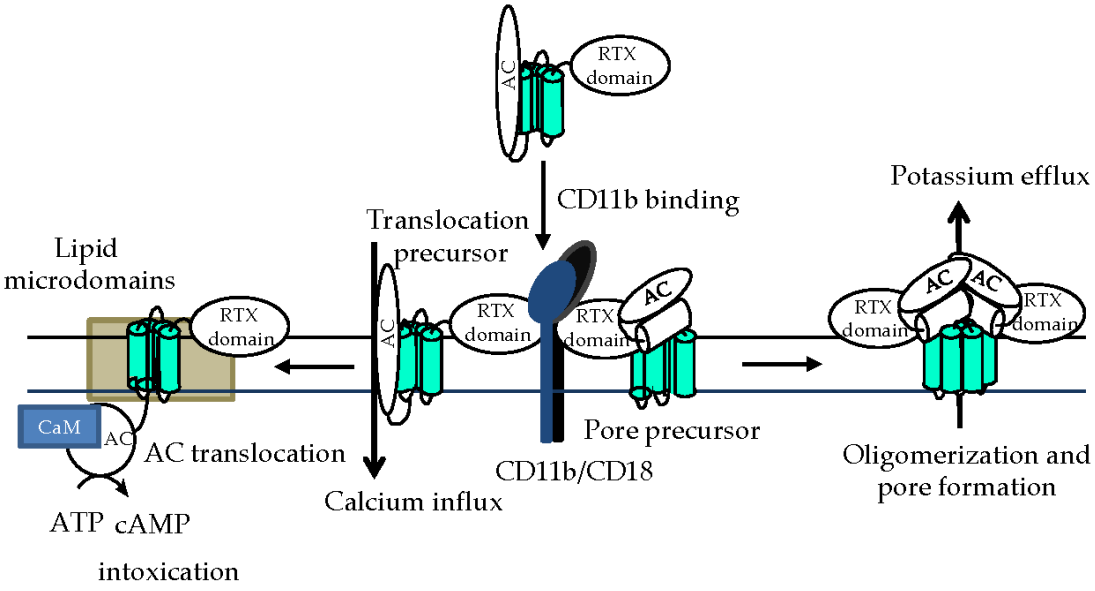

Figure 5. Schematic model of CyaA action on target membrane. After binding to CD11b/CD18 on myeloid cells [17,18], CyaA penetrates the cytoplasmic membrane and employs two distinct conformers to exert its multiple activities [68]. One would be the translocation precursor that would account for delivery of the invasive AC domain across the lipid bilayer [69] and provoke a concomitant influx of calcium ions into cell cytosol [28]. The other conformer would form a pore precursor that would oligomerize into CyaA pores [11,66,68], provoking potassium efflux from target cells [34]. Not drawn to scale.

The AC domain of the toxin crosses the cellular membrane in two steps (Figure 5). First, the initial insertion of the AC domain into the membrane with the rest of the CyaA molecule creates a transient conduit for calcium and permeabilizes cells for influx of extracellular calcium ions [28]. This activates calpain-mediated cleavage of the talin tether that anchors CD11b/CD18 to actin cytoskeleton and mobilizes the CyaA-integrin complex for recruitment into cholesterol-rich lipid microdomains. There, the specific packing of membrane lipids allows completion of the second step of AC domain translocation across membrane into cell cytosol [58]. AC translocation across the lipid bilayer is driven and controlled by the gradient of electrical potential across the membrane [59,125] and exhibits a very short half-time of dozens of seconds [71].

In parallel to translocation of the AC domain, the hydrophobic pore-forming domain of CyaA is critical for the second activity of the toxin in target membranes (Figure 5), namely for its ability to form oligomeric cation-selective transmembrane pores [9,11,66,68,69,126]. While translocation of the

AC domain into cell cytosol appears to be a linear function of toxin concentration, the pore-forming activity of CyaA is a higher order function of toxin concentration and exhibits a Hill cooperativity number higher than 3 [25,34,68,127,128]. This suggests that monomers of CyaA can deliver the AC domain across membrane, bypassing the CyaA pore [69], while oligomerization of several toxin molecules is required for formation of cation-conducting pores. Indeed, pores formed by CyaA in artificial membranes behave as frequently opening and closing membrane channels that exhibit a short lifetime, suggestive of association-dissociation equilibrium between the non-conducting CyaA monomers and the conducting CyaA oligomers [11,66]. Moreover, pairs of inactive CyaA constructs with non-overlapping deletions complemented each other in vitro and exhibited a partially restored cytotoxic activity [10]. Active CyaA complexes were then obtained through association of an inactive CyaA variant, lacking a conserved sequence located between residues 1636 and 1650 (block A), with the C-terminal CyaA fragment (residues 1490 to 1706) carrying the block A [129]. The ability of CyaA to form the oligomeric membrane pores appears to be selectively modulated by the acylation status of the toxin, as only the pore-forming (hemolytic) activity of CyaA, but not its membrane penetration and AC delivery capacities, appear to be differentially affected upon covalent modification of the K860 and K983 residues by different fatty-acyl chains [11,13,83,127]. The rate of formation, as well as the cation selectiveness and size of the CyaA pores can further be altered by charge-reversing substitutions of glutamate residues in the predicted amphipathic transmembrane α-helical segments of the pore-forming domain of CyaA [66,68,130].

Importantly, the influx of extracellular calcium ions into cell cytosol, provoked by toxin insertion into cell membrane, decelerates recycling of cellular membrane and the uptake of membrane-inserted CyaA pores [33]. Persistence of CyaA pores within the cytoplasmic membrane exacerbates pore-mediated efflux of potassium ions from cells, which further decelerates clathrin-dependent endocytic uptake of the membrane-inserted CyaA pores [33]. Cell permeabilization, hence, exacerbates in a positive feedback loop, where enhanced cell permeabilization further decreases toxin pore removal from the membrane and enables the escape of membrane-inserted toxin pores from proteolytic destruction in the endosomes [33].

5. Subversion of Spleen Tyrosine Kinase (Syk)-Mediated Signaling by CyaA-Produced cAMP

Like other integrins, also the CyaA receptor CD11b/CD18 is involved in bi-directional signaling across cellular membrane [131,132]. Upon activation by intracellular signals, the inside-out signaling is triggered through rearrangement of the integrin molecule from an inactive (closed, bent, low-affinity) conformation to an active (open, extended, high-affinity) conformation, which enhances the avidity of the integrin for ligands [133,134]. While the endogenous ligands preferentially bind the I-domain of activated CD11b/CD18 [135], CyaA preferentially binds the inactive integrin that is in the bent conformation [18]. By difference to endogenous ligands binding to the I-domain, the I-domain-independent mode of CyaA binding does not trigger outside-in signaling through the canonical Src-ITAM-Syk signaling pathway in human monocytes [18,136–140]. Moreover, the intracellular signaling of cAMP produced by the translocated AC enzyme of CyaA prevents by an as yet unknown mechanism the activation of Syk by the outside-in signaling, resulting from binding of the complement activation product iC3b to CD11b/CD18. Furthermore, CyaA/cAMP signaling can near-instantly inactivate also Syk that has been pre-activated by iC3b binding to CD11b/CD18 [18]. This unprecedented mode of binding and action distinguishes CyaA from all other known ligands of the I-domain-containing integrins and it has numerous implications for our understanding of the potent immunosubversive capacity of CyaA on myeloid phagocytes. Indeed, Syk signaling plays a key role in triggering both FcR- and CR3-mediated phagocytic pathways upon immunoglobulin or iC3b binding to opsonin receptors [141–143]. Besides inactivation of Syk, CyaA/cAMP signaling was found to rapidly and selectively decrease also the activity of the small GTP-ase RhoA [31], which acts downstream of Syk [144]. The inhibitory action of CyaA at the two different signaling levels (Syk and RhoA) would thus synergize in bringing about a rapid and complete inhibition

of opsonophagocytic uptake and killing of bacteria [23,31,145]. Besides FcR- and CR3-mediated phagocytosis, the Syk tyrosine kinase also regulates other cellular processes involved in the control of bacterial infections by the sentinel cells of the immune system, such as phagocyte chemotaxis, neutrophil extracellular trap (NET) formation, generation of reactive oxygen intermediates and degranulation of phagocytes [137,146–149]. All these phagocyte activities were previously found to be suppressed by the cAMP-elevating activity of CyaA [23,102,150,151]. The observed disruption of Syk signaling by CyaA/cAMP, hence, impairs a broad range of host innate immune defense mechanisms that are critical for control of *Bordetella* infection.

6. Subversion of Airway Sentinel Cell Functions by CyaA

6.1. Alveolar Macrophages

Alveolar macrophages (AMs) serve as major sentinel and antigen-presenting cells of the lower airways and their phenotype resembles in many respects that of DCs. In the steady state, the AMs express low levels of the CyaA receptor CD11b/CD18 and upregulate its expression to higher levels upon pro-inflammatory activation in response to infection [152]. While nothing is known about the outcome of CyaA/cAMP intoxication of AMs, this is likely to play a role in modulation of host immunity at least in the course of the critical pneumonia phase of pertussis in infants. At this stage, *B. pertussis* bacteria are massively present in the alveoli, the AMs are activated and CyaA can target them through binding to CR3. It is not known whether *B. pertussis* bacteria reach lung alveoli in any significant numbers, or whether CyaA action on AMs plays any important role in modulation of host immunity, in the course of a typical uncomplicated whooping cough illness in older children or adults. This could occur for example during the catarrhal phase of the disease, when bacteria proliferate vigorously on the mucosa of the upper airways. Moreover, even quiescent AMs express increased levels of pro-inflammatory genes, being ready to initiate a prompt innate immune response [153]. Hence, a potential immunomodulatory action of CyaA on AMs might be involved in dampening of host immune response to *B. pertussis* infection, the hallmark of which is the absence of fever and of any massive pro-inflammatory host response. It is thus plausible to speculate that CyaA subverts the immune signaling initiated by AMs in response to infection and restricts the release of soluble mediators, such as interferons, IL-1β, IL-8, TNF-α, and CXCL5, which attract and activate neutrophils and stimulate their proliferation in bone marrow [154,155]. AM-produced signaling also leads to activation of intraepithelial DCs (IAE-DCs) interspersed between columnar epithelial cells of the airway mucosa, which are another likely target of subversive action of CyaA.

6.2. Modulation of Macrophage Functions by CyaA/cAMP Signaling

As introduced above, it remains unknown whether and how does the CyaA toxin subvert the immune functions of AMs. However, there is little doubt on the relevance of CyaA toxin action on monocytes and lung interstitial macrophages attracted to *B. pertussis*-infected airway mucosa [156]. Confer and Eaton in 1982 and Pearson and co-workers in 1987 have shown that CyaA action on primary human monocytes subverts their capacity to respond by reactive oxygen species (ROS) production to diverse stimuli [23,102]. We showed in 2008 that the CyaA-produced cAMP signaling instantly inhibits CR3-mediated opsonophagocytic uptake of particles into mouse macrophages exposed to as little as <0.1 nM purified CyaA toxin [31]. The FcγR-mediated phagocytic uptake of antibody-opsonized particles was less sensitive to interference of CyaA/cAMP signaling. However, CyaA action rapidly inhibited macropinocytic fluid phase uptake and provoked massive actin cytoskeleton rearrangements and unproductive membrane ruffling, due to selective inactivation of the small GTPase RhoA in the absence of any detectable activation of Rac1, Rac2 or RhoG [31].

CyaA activity was found to extend survival of non-opsonized *B. pertussis* bacteria within human macrophages under conditions of high multiplicity of infection [157,158]. Using murine RAW264.7 macrophages, we found that CyaA/cAMP signaling through the protein kinase A (PKA) pathway

activates by an as yet unknown mechanism the Src homology domain 2 containing protein tyrosine phosphatase (SHP) 1 that plays an important role in regulation of numerous receptor signaling processes in leukocytes [29]. PKA signaling and activation of SHP-1, but not of SHP-2, inactivated the AP-1 transcription factor through dephosphorylation of its c-Fos subunit and inhibited LPS-inducible expression of the NO synthase (iNOS) and production of bactericidal NO. As a result, the CyaA/cAMP signaling-induced activation of SHP-1 extended the survival of internalized *B. pertussis* bacteria inside murine macrophages [29]. Moreover, CyaA action provoked activation and nuclear translocation of the NF-κB transcription factor, while decreasing the phosphorylation of STAT1 and the protein levels of the IRF1 transcription factor [29]. This is likely to modulate the transcriptional program in macrophages towards immunomodulatory cytokine signaling and M2 polarization.

6.3. CyaA/cAMP-Triggered Reprogramming of Gene Expression in Macrophages

Recently, the analysis of global gene expression profiles of CyaA-treated murine bone marrow-derived macrophages (BMDMs) exposed to 100 pM CyaA for 24 h revealed that sustained CyaA-cAMP signaling altered expression of more than 2000 genes. Most of the upregulated ones were coding for proteins involved in immune responses and inflammation, such as genes for DC markers or for chemokines involved in chemoattraction of neutrophils (*Cxcl5* and *Cxcl7*) [159]. Such CyaA activity effects on lung AMs would go well with the observation that a synergy between cAMP signaling and pore-forming activities of CyaA accounts for massive neutrophil infiltration into *B. pertussis*-infected mouse lungs [156].

Among the down-regulated genes were the ones for proteins involved in cell proliferation, such as cyclins B1 and B2 and their CDK1 partner [159]. This would go well with the observation that a single in vitro exposure of murine J774A.1 macrophage cells to non-lethal (picomolar) concentrations of CyaA provokes cell cycle arrest in the G_1/G_0 phase, which lasts for 3 to 6 days. This appears to be due to inhibition of phosphorylation of the ERK 1/2 kinase and of cyclin D1, with concomitant increase of levels of the CDK inhibitor p27kip1 and of phospho-CREB [160].

Deeper analysis of gene expression alterations induced in BMDMs by exposure to 100 pM CyaA revealed modulation of several pathways that regulate systemic and local inflammatory responses and chromatin remodeling, such as Smarcc1 (or SRG3). This chromatin remodeling factor was recently implicated in promoting of a Th2 response by reprogramming of DCs or macrophages [161] and in the shift from classical "proinflammatory" (M1) to alternative "immunoregulatory" (M2) activation of macrophages [162]. The decision between the "classical" M1 and "alternative" M2 activation states of macrophages is driven by various mechanisms, of which one includes modulation of subcellular localization and activities of the SIK family of kinases. In line with that, we have recently observed by a phosphoproteomic analysis that CyaA/cAMP signaling triggers posttranslational regulation of SIK kinases and eventually also of their downstream target CRTC3 in murine bone marrow-derived dendritic cells (BMDCs) [163]. This is consistent with the known outcomes of CyaA action on DCs, as SIK1 and SIK3 were shown to negatively regulate the response to TLR4 stimulation [164]. Inhibition of SIK kinases, followed by CRTC3 dephosphorylation, was then shown to promote production of the anti-inflammatory cytokine IL-10, which drives tolerogenic polarization of M2 macrophages [165,166]. Further analysis of the impact on gene expression profiles of BMDMs [159] indicates that CyaA/cAMP signaling triggers atypical activation of macrophages that includes markers characteristic for both M1 and M2 activation states. Experimental testing of this hypothesis is currently underway in our laboratory.

6.4. Induction of Macrophage Apoptosis by CyaA

In addition to blocking bactericidal functions of phagocytes, CyaA is also able to induce macrophage apoptosis both in vivo and in vitro [103,167]. First apoptotic cells can be observed after 2 h of incubation of macrophages with the *B. pertussis* 18323 bacteria at multiplicity of infection ratio of 100:1, which in 6 to 8 h yields apoptotic death of almost 100% of infected macrophages [167].

Triggering of apoptotic cell death does not depend on engulfment of *B. pertussis* bacteria [167] and depends on toxin activity of CyaA, but not of pertussis toxin [103,167]. We have recently demonstrated that cAMP-induced PKA signaling results in stabilization of the pro-apoptotic Bcl-2 family protein BimEL [112], most likely through direct phosphorylation of BimEL by PKA at the serine 83 residue [168]. In parallel, PKA by an unknown mechanism causes activation of the SHP-1 tyrosine phosphatase [29] that can dephosphorylate ERK1/2 [169] and thus inhibit its capacity to phosphorylate BimEL and commit it for degradation by the proteasome [170]. Accumulation of BimEL then leads to activation of the Bax protein and its permeabilizing association with outer mitochondrial membrane and release of cytochrome c [112]. In parallel, CyaA-produced cAMP signaling provokes dephosphorylation of threonine 308 and serine 473 residues of the pro-survival kinase PKB/AKT and inhibition of its activity. As a result, the FoxO3a transcription factor becomes dephosphorylated and eventually translocates into cell nucleus, where it up-regulates transcription of the *Bim* gene, yielding a persistent increase of pro-apoptotic BimEL levels in cell cytosol [112].

6.5. Intraepithelial Dendritic Cells

IAE-DCs of myeloid origin are found in both the epithelium and submucosa of conducting airways, as well as on the alveolar surfaces [171,172]. During the response to infection, these bona fide DCs are further replenished by monocyte-derived DCs (mo-DCs) [173] and upon activation by TLR ligands, the IAE-DCs and mo-DCs mature and migrate to the lung-draining lymph nodes to trigger the T cell response.

To get a grasp of the complexity of the subversive CyaA/cAMP signaling in host DCs, we have performed a global and unbiased phosphoproteomic analysis of the early phases of cAMP intoxication of mouse BMDCs by CyaA [163]. Among others, this complex approach revealed a cAMP signaling-dependent inhibition of mTOR and of the SIK family kinases-dependent signaling pathways. cAMP-dependent activation of mTOR inhibitors like tuberin [174] or PRAS40 [175] yielded, among others, a hypophosphorylation of 4E-BP1, which likely causes repression of cap-dependent protein translation [176]. Moreover, mTOR is an important regulator of immune responses and its inhibition has numerous pleiotropic effects [177–179]. Among others, mTOR inhibition would impact on a number of key processes of DC biology, including maturation, migration or cytokine production [179]. Hijacking of these processes by CyaA/cAMP signaling then likely enables *Bordetellae* to favorably shape the host immune response towards immune evasion. Another highly relevant effect of CyaA/cAMP signaling in BMDCs appears to be the cAMP-dependent manipulation of the phosphorylation state of the SIK family of kinases and dephosphorylation of their downstream target CRTC3/TORC3 [163]. This was previously shown to enhance CREB-dependent transcription of the gene for the anti-inflammatory IL-10 cytokine [165]. In this model, the cAMP-activated PKA (and/or eventually other kinases) would phosphorylate SIK1-3 kinases in a cAMP-dependent manner and inhibit their capacity to phosphorylate CRTC3. Dephosphorylated CRTC3 would be next liberated from the complex with the 14-3-3 protein, would translocate into cell nucleus and would bind CREB, which is itself activated via a CyaA/cAMP-activated cAMP-PKA-dependent pathway [180]. CRTC3 would then act as a transcriptional coactivator of phospho-CREB, promoting IL-10 production in phagocytes and M1 to M2b (regulatory) phenotype shift in macrophages [165].

6.6. CyaA Action on Neutrophils

Infection-elicited activation of cytokine and chemokine secretion by TLR-activated IAE-DCs, AMs and infected epithelial cells of the airway mucosa provokes chemotaxis of neutrophils patrolling in the pulmonary vasculature. Neutrophils are the first sentinel cells that enter the infected airways [181,182] and are the most plausible target of the subversive CyaA toxin action, fooling the release of antimicrobial peptides and hydrolytic enzymes from granules of neutrophils and inhibiting assembly of the NADPH oxidase complex and ROS release by oxidative burst of neutrophils [183]. Subversion of the bactericidal activities of neutrophils would thus appear as the primary role of the CyaA toxin in

subversion of host immune defense in the early stages of airway infection by *Bordetellae* [23,104,183]. Indeed, even before the exact nature of the CyaA toxin was characterized, Confer and Eaton discovered that urea extracts of *B. pertussis* bacteria elevate cAMP levels in primary human neutrophils and AMs and thereby paralyze their capacity to produce ROS and kill serum-opsonized bacteria [23]. Friedman and coworkers then described the inhibition of chemotaxis and superoxide production by human neutrophils exposed to CyaA, but failed to observe any changes in their phagocytic capacities by using light microscopy [150]. Inhibition of opsonophagocytosis by CyaA-treated neutrophils was, however, observed by Weingart and Weiss, who showed that upon opsonization with human immune serum a *B. pertussis* mutant lacking CyaA was approximately 10 times more efficiently phagocytosed by human neutrophils than the wild-type bacteria [184,185]. Moreover, addition of purified CyaA to human neutrophils incubated with the mutant bacteria led to impairment of their opsonophagocytic capacity [184]. Furthermore, addition of CyaA-neutralizing monoclonal antibodies, or a human convalescent serum containing such antibodies, restored the phagocytic capacity of human neutrophils exposed to CyaA [184]. More specifically, CyaA action was found to inhibit CR3-mediated phagocytosis by human neutrophils [186], showing that CyaA inhibits a broad spectrum of bactericidal activities of neutrophils.

We have recently addressed the mechanism by which CyaA/cAMP signaling inhibits the oxidative burst of human neutrophils [30]. Two converging mechanisms that interfere with NADPH oxidase activation and ROS production were identified. One appears to involve cAMP/PKA–mediated activation of SHP-1, which limits activation of the ERK and p38 kinases required for assembly of the NADPH oxidase complex. In parallel, activation of the exchange protein directly activated by cAMP (Epac) provokes, by an as yet unknown mechanism, the inhibition of phospholipase C (PLC). By inhibiting PLC-mediated production of the protein kinase C–activating lipid, diacylglycerol, the cAMP/Epac signaling thus blocks the bottleneck step of the converging pathways of oxidative burst triggering [30].

This helps to understand why CyaA plays an important role in the early stages of airway colonization by *B. pertussis*, at least in the mouse model of infection [187–191]. Indeed, no CyaA-deficient clinical isolates of *B. pertussis* have been reported yet, by difference to the massive spread of *B. pertussis* strains defective in production of pertactin, or to occasional isolation of strains deficient in production of filamentous hemagglutinin or pertussis toxin. Further, the 5 kb-large *cyaA* gene exhibits a particularly high degree of sequence conservation across the global population of clinical *B. pertussis* strains [192,193], indicating a high selective pressure for conservation of function of the toxin.

CyaA activity accounts for numerous pathological effects elicited by *B. pertussis* infection in mouse lungs, such as the recruitment of inflammatory leukocytes and the induction of pathological lesions [70,103,156,194]. *B. pertussis* mutants, unable to secrete CyaA, or producing an enzymatically inactive but still hemolytic CyaA-AC^{-} toxoid, were found to be impaired in proliferation in mouse airways [156,187,188,195]. We could recently construct the first non-hemolytic *B. pertussis* mutant that secretes a non-hemolytic CyaA toxin (e.g., CyaA–E570Q + K860R) that is intact for delivery of the AC enzyme into CD11b/CD18-expressing myeloid phagocytes, such as neutrophils, macrophages and DCs [69]. Mouse infection experiments with this mutant then revealed that the cell-permeabilizing (hemolytic) activity of the CyaA toxin is not required for the capacity of *B. pertussis* to proliferate in infected mouse lungs [156]. However, the permeabilization of host cells by CyaA synergizes with the AC enzyme activity of the toxin and importantly contributes to the overall virulence and lethality of *B. pertussis* infection. It is particularly involved in the eliciting of signaling that triggers massive neutrophil infiltration into infected lung tissue and thereby contributes to its subsequent inflammatory damage [156].

Somewhat controversial conclusions were previously reached on whether neutrophils are the main target cells of CyaA during *Bordetella* infections. Harvill and coworkers (1999) showed that CyaA was required for *B. bronchiseptica* infections of SCID-Beige mice lacking the B, T and NK lymphocytes,

suggesting that CyaA acts on neutrophils, or on phagocytes of the monocyte/macrophage lineage [104]. Moreover, neutropenic mice were equally susceptible to lethal infection by wild-type or CyaA-deficient strains, suggesting that neutrophil depletion removed the main target cell on which CyaA needs to exert its biological activity and CyaA was, hence, not required for successful infection of neutropenic mice [104]. However, upon infection of neutropenic mice with *B. pertussis* strains, Andreasen and Carbonetti observed a role for CyaA action on neutrophils only in the immune (convalescent or passively immunized by serum) mice but not in the naive mice [104,196]. This indicates that neutrophils are not the only CR3-expressing target on which CyaA has to act in the mouse airway to support a successful infection of this non-natural host of *B. pertussis*. To which extent these results reflect the limitation of the mouse model in reproducing the protective immune mechanisms operating in human airways remains unknown. Nevertheless, these results are consistent with the finding that CyaA-neutralizing antibodies can restore phagocytic uptake of serum-opsonized *B. pertussis* by human neutrophils [184,186]. Indeed, CyaA is able to efficiently abolish the bactericidal functions of neutrophils and besides of blocking oxidative burst, it can also inhibit NET formation and neutrophil apoptosis [151]. The same conclusion was recently reached also for the interaction of *B. parapertussis* with human neutrophils [197].

7. Conclusions

The rise of whooping cough incidence in the last two decades is due to several factors. Among them, the rapid waning of protection conferred by the current acellular pertussis (aP) vaccines, and the limited spectrum of antigens in these vaccines, appears as most worrisome [5]. This situation calls for development of a next generation of pertussis vaccines that would not only confer protection against the severe pulmonary disease caused by pertussis toxin in infants, but would also prevent bacterial infection and more-or-less asymptomatic colonization, which accounts for the current massive transmission rates of *B. pertussis* in highly aP-vaccinated populations of older children and adults. The detailed characterization of the structure–function relationships and mechanisms of action of key virulence factors, such as CyaA, offers the potential of their use as protective antigens in new vaccines. As reviewed here and summarized in Figure 6, CyaA activity interferes with a broad range of functions of phagocytes that are the sentinel cells of innate immunity. CyaA-caused paralysis of opsonophagocytic killing of the bacteria appears to play a key role in the early stages of colonization by *B. pertussis*. This makes CyaA toxoid to a leading antigen candidate for inclusion into the next generation of aP vaccines. Induction of CyaA-neutralizing antibodies by future aP vaccines is expected to enable neutrophils and macrophages in the airway of vaccinated subjects to fully deploy their bactericidal opsonophagocytic killing activities. Such maximizing of the protective potential of the opsonizing antibodies against bacterial surface antigens, comprised in the aP vaccine, is then expected to enhance also protection against *B. pertussis* infection and not only against the clinical disease.

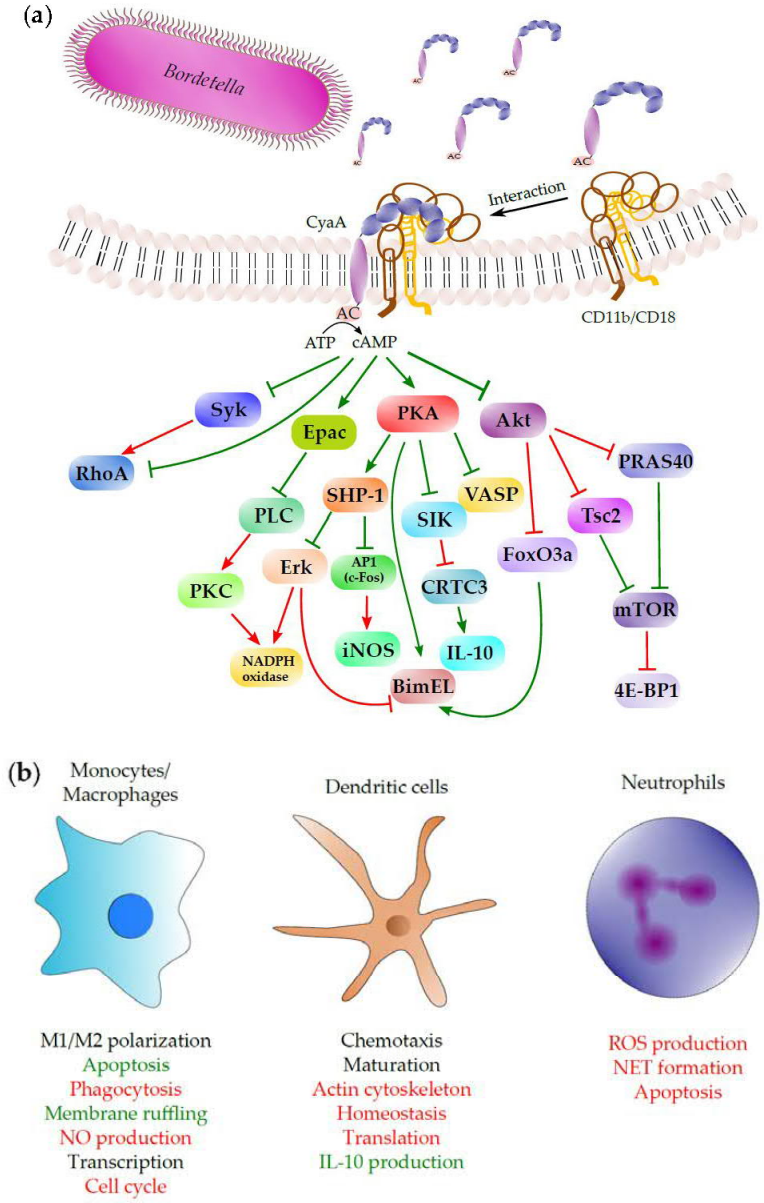

Figure 6. Schematic depiction of CyaA interaction with target cells: cAMP-dependent signaling and its impact on epithelial cells and phagocytes. (**a**) CyaA toxin molecules secreted by the T1SS of *Bordetella* bind specifically to the integrin CD11b/CD18 (CR3, or $\alpha_M\beta_2$) on the surface of phagocytes (monocytes, macrophages, DCs or neutrophils), or interact nonspecifically with the surfaces of other cell types, including epithelial cells. Following insertion into cytoplasmic membrane, CyaA translocates its enzymatic AC domain into the cytosol. In parallel, membrane-inserted CyaA molecules can oligomerize into cell-permeabilizing pores (not shown). Inside cell cytosol, the AC domain is activated by binding of calmodulin and catalyzes an extremely rapid and unregulated conversion of cytoplasmic ATP into cAMP, a key second messenger that hijacks the different cellular signaling pathways schematically delineated in the drawing (see the text for more detailed description of these pathways). The pointed arrowheads in the drawing indicate an activating effect and the flat arrowheads indicate an inhibitory effect under normal physiological conditions. The red color of the arrowhead indicates an inhibitory effect, or interference, elicited by the cAMP signaling of the CyaA toxin and the green color indicates an enhancing effect of CyaA/cAMP-triggered signaling action. (**b**) The outcomes of CyaA/cAMP signaling are shown together with the cell type for which they were originally described. Green color represents stimulation of particular interaction or process by CyaA action, while red color represents inhibition.

Acknowledgments: This work was supported by grants GA15-09157S (R.O.) and 16-05919S (J.M.) from the Grant Agency of the Czech Republic, by project LM2015064 from Ministry of Education, Youth and Sports of the Czech Republic (R.O.), by project UNCE204025/2012 of the Charles University in Prague (A.O.), by grant 228216 from the Grant Agency of the Charles University in Prague (J.N.) and by grant NV16-28126A from Ministry of Health of the Czech Republic (P.S.).

Conflicts of Interest: P.S., R.O., A.O., J.M. and L.B. are co-inventors of patents protecting use of CyaA toxoids and CyaA fragments as pertussis vaccine antigens. P.S. is founder and shareholder of Revabiotech SE that develops a next generation of whole cell pertussis vaccine.

References

1. Melvin, J.A.; Scheller, E.V.; Miller, J.F.; Cotter, P.A. *Bordetella pertussis* pathogenesis: Current and future challenges. *Nat. Rev. Microbiol.* **2014**, *12*, 274–288. [CrossRef] [PubMed]
2. Yeung, K.H.T.; Duclos, P.; Nelson, E.A.S.; Hutubessy, R.C.W. An update of the global burden of pertussis in children younger than 5 years: A modelling study. *Lancet Infect. Dis.* **2017**, *17*, 974–980. [CrossRef]
3. Cherry, J.D. Pertussis in young infants throughout the world. *Clin. Infect. Dis.* **2016**, *63*, S119–S122. [CrossRef] [PubMed]
4. Vojtova, J.; Kamanova, J.; Sebo, P. *Bordetella* adenylate cyclase toxin: A swift saboteur of host defense. *Curr. Opin. Microbiol.* **2006**, *9*, 69–75. [CrossRef] [PubMed]
5. Sebo, P.; Osicka, R.; Masin, J. Adenylate cyclase toxin-hemolysin relevance for pertussis vaccines. *Expert Rev. Vaccines* **2014**, *13*, 1215–1227. [CrossRef] [PubMed]
6. Linhartova, I.; Bumba, L.; Masin, J.; Basler, M.; Osicka, R.; Kamanova, J.; Prochazkova, K.; Adkins, I.; Hejnova-Holubova, J.; Sadilkova, L.; et al. RTX proteins: A highly diverse family secreted by a common mechanism. *FEMS Microbiol. Rev.* **2010**, *34*, 1076–1112. [CrossRef] [PubMed]
7. Rose, T.; Sebo, P.; Bellalou, J.; Ladant, D. Interaction of calcium with *Bordetella pertussis* adenylate cyclase toxin. Characterization of multiple calcium-binding sites and calcium-induced conformational changes. *J. Biol. Chem.* **1995**, *270*, 26370–26376. [CrossRef] [PubMed]
8. Masin, J.; Osicka, R.; Bumba, L.; Sebo, P. *Bordetella* adenylate cyclase toxin: A unique combination of a pore-forming moiety with a cell-invading adenylate cyclase enzyme. *Pathog. Dis.* **2015**, *73*, ftv075. [CrossRef] [PubMed]
9. Glaser, P.; Sakamoto, H.; Bellalou, J.; Ullmann, A.; Danchin, A. Secretion of cyclolysin, the calmodulin-sensitive adenylate cyclase-haemolysin bifunctional protein of *Bordetella pertussis*. *EMBO J.* **1988**, *7*, 3997–4004. [PubMed]
10. Iwaki, M.; Ullmann, A.; Sebo, P. Identification by in vitro complementation of regions required for cell-invasive activity of *Bordetella pertussis* adenylate cyclase toxin. *Mol. Microbiol.* **1995**, *17*, 1015–1024. [CrossRef] [PubMed]
11. Benz, R.; Maier, E.; Ladant, D.; Ullmann, A.; Sebo, P. Adenylate cyclase toxin (CyaA) of *Bordetella pertussis*. Evidence for the formation of small ion-permeable channels and comparison with HlyA of *Escherichia coli*. *J. Biol. Chem.* **1994**, *269*, 27231–27239. [PubMed]
12. Hackett, M.; Guo, L.; Shabanowitz, J.; Hunt, D.F.; Hewlett, E.L. Internal lysine palmitoylation in adenylate cyclase toxin from *Bordetella pertussis*. *Science* **1994**, *266*, 433–435. [CrossRef] [PubMed]
13. Hackett, M.; Walker, C.B.; Guo, L.; Gray, M.C.; Van Cuyk, S.; Ullmann, A.; Shabanowitz, J.; Hunt, D.F.; Hewlett, E.L.; Sebo, P. Hemolytic, but not cell-invasive activity, of adenylate cyclase toxin is selectively affected by differential fatty-acylation in *Escherichia coli*. *J. Biol. Chem.* **1995**, *270*, 20250–20253. [CrossRef] [PubMed]
14. Osicka, R.; Osickova, A.; Basar, T.; Guermonprez, P.; Rojas, M.; Leclerc, C.; Sebo, P. Delivery of CD8(+) T-cell epitopes into major histocompatibility complex class I antigen presentation pathway by *Bordetella pertussis* adenylate cyclase: Delineation of cell invasive structures and permissive insertion sites. *Infect. Immun.* **2000**, *68*, 247–256. [PubMed]
15. Bumba, L.; Masin, J.; Macek, P.; Wald, T.; Motlova, L.; Bibova, I.; Klimova, N.; Bednarova, L.; Veverka, V.; Kachala, M.; et al. Calcium-driven folding of RTX domain beta-rolls ratchets translocation of RTX proteins through type I secretion ducts. *Mol. Cell* **2016**, *62*, 47–62. [CrossRef] [PubMed]

16. Sebo, P.; Ladant, D. Repeat sequences in the *Bordetella pertussis* adenylate cyclase toxin can be recognized as alternative carboxy-proximal secretion signals by the *Escherichia coli* alpha-haemolysin translocator. *Mol. Microbiol.* **1993**, *9*, 999–1009. [CrossRef] [PubMed]
17. Guermonprez, P.; Khelef, N.; Blouin, E.; Rieu, P.; Ricciardi-Castagnoli, P.; Guiso, N.; Ladant, D.; Leclerc, C. The adenylate cyclase toxin of *Bordetella pertussis* binds to target cells via the alpha(M)beta(2) integrin (CD11b/CD18). *J. Exp. Med.* **2001**, *193*, 1035–1044. [CrossRef] [PubMed]
18. Osicka, R.; Osickova, A.; Hasan, S.; Bumba, L.; Cerny, J.; Sebo, P. *Bordetella* adenylate cyclase toxin is a unique ligand of the integrin complement receptor 3. *eLife* **2015**, *4*, e10766. [CrossRef] [PubMed]
19. Bellalou, J.; Sakamoto, H.; Ladant, D.; Geoffroy, C.; Ullmann, A. Deletions affecting hemolytic and toxin activities of *Bordetella pertussis* adenylate cyclase. *Infect. Immun.* **1990**, *58*, 3242–3247. [PubMed]
20. Gordon, V.M.; Young, W.W., Jr.; Lechler, S.M.; Gray, M.C.; Leppla, S.H.; Hewlett, E.L. Adenylate cyclase toxins from *Bacillus anthracis* and *Bordetella pertussis*. Different processes for interaction with and entry into target cells. *J. Biol. Chem.* **1989**, *264*, 14792–14796. [PubMed]
21. Holubova, J.; Kamanova, J.; Jelinek, J.; Tomala, J.; Masin, J.; Kosova, M.; Stanek, O.; Bumba, L.; Michalek, J.; Kovar, M.; et al. Delivery of large heterologous polypeptides across the cytoplasmic membrane of antigen-presenting cells by the *Bordetella* RTX hemolysin moiety lacking the adenylyl cyclase domain. *Infect. Immun.* **2012**, *80*, 1181–1192. [CrossRef] [PubMed]
22. Wolff, J.; Cook, G.H.; Goldhammer, A.R.; Berkowitz, S.A. Calmodulin activates prokaryotic adenylate cyclase. *Proc. Natl. Acad. Sci. USA* **1980**, *77*, 3841–3844. [CrossRef] [PubMed]
23. Confer, D.L.; Eaton, J.W. Phagocyte impotence caused by an invasive bacterial adenylate cyclase. *Science* **1982**, *217*, 948–950. [CrossRef] [PubMed]
24. Ladant, D.; Ullmann, A. *Bordetella pertussis* adenylate cyclase: A toxin with multiple talents. *Trends Microbiol.* **1999**, *7*, 172–176. [CrossRef]
25. Szabo, G.; Gray, M.C.; Hewlett, E.L. Adenylate cyclase toxin from *Bordetella pertussis* produces ion conductance across artificial lipid bilayers in a calcium- and polarity-dependent manner. *J. Biol. Chem.* **1994**, *269*, 22496–22499. [PubMed]
26. Ehrmann, I.E.; Gray, M.C.; Gordon, V.M.; Gray, L.S.; Hewlett, E.L. Hemolytic activity of adenylate cyclase toxin from *Bordetella pertussis*. *FEBS Lett.* **1991**, *278*, 79–83. [PubMed]
27. Basler, M.; Masin, J.; Osicka, R.; Sebo, P. Pore-forming and enzymatic activities of *Bordetella pertussis* adenylate cyclase toxin synergize in promoting lysis of monocytes. *Infect. Immun.* **2006**, *74*, 2207–2214. [CrossRef] [PubMed]
28. Fiser, R.; Masin, J.; Basler, M.; Krusek, J.; Spulakova, V.; Konopasek, I.; Sebo, P. Third activity of *Bordetella* adenylate cyclase (AC) toxin-hemolysin. Membrane translocation of AC domain polypeptide promotes calcium influx into CD11b+ monocytes independently of the catalytic and hemolytic activities. *J. Biol. Chem.* **2007**, *282*, 2808–2820. [CrossRef] [PubMed]
29. Cerny, O.; Kamanova, J.; Masin, J.; Bibova, I.; Skopova, K.; Sebo, P. *Bordetella pertussis* adenylate cyclase toxin blocks induction of bactericidal nitric oxide in macrophages through cAMP-dependent activation of the SHP-1 phosphatase. *J. Immunol.* **2015**, *194*, 4901–4913. [CrossRef] [PubMed]
30. Cerny, O.; Anderson, K.E.; Stephens, L.R.; Hawkins, P.T.; Sebo, P. cAMP signaling of adenylate cyclase toxin blocks the oxidative burst of neutrophils through Epac-mediated inhibition of phospholipase C activity. *J. Immunol.* **2017**, *198*, 1285–1296. [CrossRef] [PubMed]
31. Kamanova, J.; Kofronova, O.; Masin, J.; Genth, H.; Vojtova, J.; Linhartova, I.; Benada, O.; Just, I.; Sebo, P. Adenylate cyclase toxin subverts phagocyte function by RhoA inhibition and unproductive ruffling. *J. Immunol.* **2008**, *181*, 5587–5597. [CrossRef] [PubMed]
32. Dunne, A.; Ross, P.J.; Pospisilova, E.; Masin, J.; Meaney, A.; Sutton, C.E.; Iwakura, Y.; Tschopp, J.; Sebo, P.; Mills, K.H. Inflammasome activation by adenylate cyclase toxin directs Th17 responses and protection against *Bordetella pertussis*. *J. Immunol.* **2010**, *185*, 1711–1719. [CrossRef] [PubMed]
33. Fiser, R.; Masin, J.; Bumba, L.; Pospisilova, E.; Fayolle, C.; Basler, M.; Sadilkova, L.; Adkins, I.; Kamanova, J.; Cerny, J.; et al. Calcium influx rescues adenylate cyclase-hemolysin from rapid cell membrane removal and enables phagocyte permeabilization by toxin pores. *PLoS Pathog.* **2012**, *8*, e1002580. [CrossRef] [PubMed]
34. Gray, M.; Szabo, G.; Otero, A.S.; Gray, L.; Hewlett, E. Distinct mechanisms for K+ efflux, intoxication, and hemolysis by *Bordetella pertussis* AC toxin. *J. Biol. Chem.* **1998**, *273*, 18260–18267. [CrossRef] [PubMed]

35. Svedova, M.; Masin, J.; Fiser, R.; Cerny, O.; Tomala, J.; Freudenberg, M.; Tuckova, L.; Kovar, M.; Dadaglio, G.; Adkins, I.; et al. Pore-formation by adenylate cyclase toxoid activates dendritic cells to prime CD8+ and CD4+ T cells. *Immunol. Cell Biol.* **2016**, *94*, 322–333. [CrossRef] [PubMed]
36. Wald, T.; Petry-Podgorska, I.; Fiser, R.; Matousek, T.; Dedina, J.; Osicka, R.; Sebo, P.; Masin, J. Quantification of potassium levels in cells treated with *Bordetella* adenylate cyclase toxin. *Anal. Biochem.* **2014**, *450*, 57–62. [CrossRef] [PubMed]
37. Bachelet, M.; Richard, M.J.; Francois, D.; Polla, B.S. Mitochondrial alterations precede *Bordetella pertussis*-induced apoptosis. *FEMS Immunol. Med. Microbiol.* **2002**, *32*, 125–131. [CrossRef] [PubMed]
38. Hewlett, E.L.; Donato, G.M.; Gray, M.C. Macrophage cytotoxicity produced by adenylate cyclase toxin from *Bordetella pertussis*: More than just making cyclic amp! *Mol. Microbiol.* **2006**, *59*, 447–459. [CrossRef] [PubMed]
39. Khelef, N.; Guiso, N. Induction of macrophage apoptosis by *Bordetella pertussis* adenylate cyclase-hemolysin. *FEMS Microbiol. Lett.* **1995**, *134*, 27–32. [CrossRef] [PubMed]
40. Barzu, O.; Danchin, A. Adenylyl cyclases: A heterogeneous class of ATP-utilizing enzymes. *Prog. Nucleic Acid Res. Mol. Biol.* **1994**, *49*, 241–283. [PubMed]
41. Shen, Y.; Zhukovskaya, N.L.; Guo, Q.; Florian, J.; Tang, W.J. Calcium-independent calmodulin binding and two-metal-ion catalytic mechanism of anthrax edema factor. *EMBO J.* **2005**, *24*, 929–941. [CrossRef] [PubMed]
42. Tang, W.J.; Guo, Q. The adenylyl cyclase activity of anthrax edema factor. *Mol. Asp. Med.* **2009**, *30*, 423–430. [CrossRef] [PubMed]
43. Morrow, K.A.; Frank, D.W.; Balczon, R.; Stevens, T. The *Pseudomonas aeruginosa* exoenzyme Y: A promiscuous nucleotidyl cyclase edema factor and virulence determinant. *Handb. Exp. Pharmacol.* **2017**, *238*, 67–85. [PubMed]
44. Yahr, T.L.; Vallis, A.J.; Hancock, M.K.; Barbieri, J.T.; Frank, D.W. ExoY, an adenylate cyclase secreted by the *Pseudomonas aeruginosa* type III system. *Proc. Natl. Acad. Sci. USA* **1998**, *95*, 13899–13904. [CrossRef] [PubMed]
45. Belyy, A.; Raoux-Barbot, D.; Saveanu, C.; Namane, A.; Ogryzko, V.; Worpenberg, L.; David, V.; Henriot, V.; Fellous, S.; Merrifield, C.; et al. Actin activates *Pseudomonas aeruginosa* ExoY nucleotidyl cyclase toxin and ExoY-like effector domains from MARTX toxins. *Nat. Commun.* **2016**, *7*, 13582. [CrossRef] [PubMed]
46. Ladant, D. Interaction of *Bordetella pertussis* adenylate cyclase with calmodulin. Identification of two separated calmodulin-binding domains. *J. Biol. Chem.* **1988**, *263*, 2612–2618. [PubMed]
47. Rogel, A.; Schultz, J.E.; Brownlie, R.M.; Coote, J.G.; Parton, R.; Hanski, E. *Bordetella pertussis* adenylate cyclase: Purification and characterization of the toxic form of the enzyme. *EMBO J.* **1989**, *8*, 2755–2760. [PubMed]
48. Gottle, M.; Dove, S.; Kees, F.; Schlossmann, J.; Geduhn, J.; Konig, B.; Shen, Y.; Tang, W.J.; Kaever, V.; Seifert, R. Cytidylyl and uridylyl cyclase activity of *Bacillus anthracis* edema factor and *Bordetella pertussis* CyaA. *Biochemistry* **2010**, *49*, 5494–5503. [CrossRef] [PubMed]
49. Glaser, P.; Elmaoglou-Lazaridou, A.; Krin, E.; Ladant, D.; Barzu, O.; Danchin, A. Identification of residues essential for catalysis and binding of calmodulin in *Bordetella pertussis* adenylate cyclase by site-directed mutagenesis. *EMBO J.* **1989**, *8*, 967–972. [PubMed]
50. Ladant, D.; Michelson, S.; Sarfati, R.; Gilles, A.M.; Predeleanu, R.; Barzu, O. Characterization of the calmodulin-binding and of the catalytic domains of *Bordetella pertussis* adenylate cyclase. *J. Biol. Chem.* **1989**, *264*, 4015–4020. [PubMed]
51. Munier, H.; Bouhss, A.; Krin, E.; Danchin, A.; Gilles, A.M.; Glaser, P.; Barzu, O. The role of histidine 63 in the catalytic mechanism of *Bordetella pertussis* adenylate cyclase. *J. Biol. Chem.* **1992**, *267*, 9816–9820. [PubMed]
52. Glaser, P.; Munier, H.; Gilles, A.M.; Krin, E.; Porumb, T.; Barzu, O.; Sarfati, R.; Pellecuer, C.; Danchin, A. Functional consequences of single amino acid substitutions in calmodulin-activated adenylate cyclase of *Bordetella pertussis*. *EMBO J.* **1991**, *10*, 1683–1688. [PubMed]
53. Guo, Q.; Shen, Y.; Lee, Y.S.; Gibbs, C.S.; Mrksich, M.; Tang, W.J. Structural basis for the interaction of *Bordetella pertussis* adenylyl cyclase toxin with calmodulin. *EMBO J.* **2005**, *24*, 3190–3201. [CrossRef] [PubMed]
54. Bouhss, A.; Krin, E.; Munier, H.; Gilles, A.M.; Danchin, A.; Glaser, P.; Barzu, O. Cooperative phenomena in binding and activation of *Bordetella pertussis* adenylate cyclase by calmodulin. *J. Biol. Chem.* **1993**, *268*, 1690–1694. [PubMed]

55. Guo, Q.; Jureller, J.E.; Warren, J.T.; Solomaha, E.; Florian, J.; Tang, W.J. Protein-protein docking and analysis reveal that two homologous bacterial adenylyl cyclase toxins interact with calmodulin differently. *J. Biol. Chem.* **2008**, *283*, 23836–23845. [CrossRef] [PubMed]
56. Springer, T.I.; Goebel, E.; Hariraju, D.; Finley, N.L. Mutation in the beta-hairpin of the *Bordetella pertussis* adenylate cyclase toxin modulates N-lobe conformation in calmodulin. *Biochem. Biophys. Res. Commun.* **2014**, *453*, 43–48. [CrossRef] [PubMed]
57. Springer, T.I.; Emerson, C.C.; Johns, C.W.; Finley, N.L. Interaction with adenylate cyclase toxin from *Bordetella pertussis* affects the metal binding properties of calmodulin. *FEBS Open Bio* **2017**, *7*, 25–34. [CrossRef] [PubMed]
58. Bumba, L.; Masin, J.; Fiser, R.; Sebo, P. *Bordetella* adenylate cyclase toxin mobilizes its beta2 integrin receptor into lipid rafts to accomplish translocation across target cell membrane in two steps. *PLoS Pathog.* **2010**, *6*, e1000901. [CrossRef] [PubMed]
59. Otero, A.S.; Yi, X.B.; Gray, M.C.; Szabo, G.; Hewlett, E.L. Membrane depolarization prevents cell invasion by *Bordetella pertussis* adenylate cyclase toxin. *J. Biol. Chem.* **1995**, *270*, 9695–9697. [CrossRef] [PubMed]
60. Shen, Y.; Lee, Y.S.; Soelaiman, S.; Bergson, P.; Lu, D.; Chen, A.; Beckingham, K.; Grabarek, Z.; Mrksich, M.; Tang, W.J. Physiological calcium concentrations regulate calmodulin binding and catalysis of adenylyl cyclase exotoxins. *EMBO J.* **2002**, *21*, 6721–6732. [CrossRef] [PubMed]
61. Subrini, O.; Sotomayor Perez, A.C.; Hessel, A.; Spiaczka-Karst, J.; Selwa, E.; Sapay, N.; Veneziano, R.; Pansieri, J.; Chopineau, J.; Ladant, D.; et al. Characterization of a membrane-active peptide from the *Bordetella pertussis* CyaA toxin. *J. Biol. Chem.* **2013**, *288*, 32585–32598. [CrossRef] [PubMed]
62. Masin, J.; Osickova, A.; Sukova, A.; Fiser, R.; Halada, P.; Bumba, L.; Linhartova, I.; Osicka, R.; Sebo, P. Negatively charged residues of the segment linking the enzyme and cytolysin moieties restrict the membrane-permeabilizing capacity of adenylate cyclase toxin. *Sci. Rep.* **2016**, *6*, 29137. [CrossRef] [PubMed]
63. Karst, J.C.; Barker, R.; Devi, U.; Swann, M.J.; Davi, M.; Roser, S.J.; Ladant, D.; Chenal, A. Identification of a region that assists membrane insertion and translocation of the catalytic domain of *Bordetella pertussis* CyaA toxin. *J. Biol. Chem.* **2012**, *287*, 9200–9212. [CrossRef] [PubMed]
64. Gray, M.C.; Lee, S.J.; Gray, L.S.; Zaretzky, F.R.; Otero, A.S.; Szabo, G.; Hewlett, E.L. Translocation-specific conformation of adenylate cyclase toxin from *Bordetella pertussis* inhibits toxin-mediated hemolysis. *J. Bacteriol.* **2001**, *183*, 5904–5910. [CrossRef] [PubMed]
65. Masin, J.; Fiser, R.; Linhartova, I.; Osicka, R.; Bumba, L.; Hewlett, E.L.; Benz, R.; Sebo, P. Differences in purinergic amplification of osmotic cell lysis by the pore-forming RTX toxins *Bordetella pertussis* CyaA and *Actinobacillus pleuropneumoniae* ApxIA: The role of pore size. *Infect. Immun.* **2013**, *81*, 4571–4582. [CrossRef] [PubMed]
66. Basler, M.; Knapp, O.; Masin, J.; Fiser, R.; Maier, E.; Benz, R.; Sebo, P.; Osicka, R. Segments crucial for membrane translocation and pore-forming activity of *Bordetella* adenylate cyclase toxin. *J. Biol. Chem.* **2007**, *282*, 12419–12429. [CrossRef] [PubMed]
67. Masin, J.; Roderova, J.; Osickova, A.; Novak, P.; Bumba, L.; Fiser, R.; Sebo, P.; Osicka, R. The conserved tyrosine residue 940 plays a key structural role in membrane interaction of *Bordetella* adenylate cyclase toxin. *Sci. Rep.* **2017**, *7*, 9330. [CrossRef] [PubMed]
68. Osickova, A.; Osicka, R.; Maier, E.; Benz, R.; Sebo, P. An amphipathic alpha-helix including glutamates 509 and 516 is crucial for membrane translocation of adenylate cyclase toxin and modulates formation and cation selectivity of its membrane channels. *J. Biol. Chem.* **1999**, *274*, 37644–37650. [PubMed]
69. Osickova, A.; Masin, J.; Fayolle, C.; Krusek, J.; Basler, M.; Pospisilova, E.; Leclerc, C.; Osicka, R.; Sebo, P. Adenylate cyclase toxin translocates across target cell membrane without forming a pore. *Mol. Microbiol.* **2010**, *75*, 1550–1562. [CrossRef] [PubMed]
70. Weiss, A.A.; Hewlett, E.L.; Myers, G.A.; Falkow, S. Pertussis toxin and extracytoplasmic adenylate cyclase as virulence factors of *Bordetella pertussis*. *J. Infect. Dis.* **1984**, *150*, 219–222. [CrossRef] [PubMed]
71. Rogel, A.; Hanski, E. Distinct steps in the penetration of adenylate cyclase toxin of *Bordetella pertussis* into sheep erythrocytes. Translocation of the toxin across the membrane. *J. Biol. Chem.* **1992**, *267*, 22599–22605. [PubMed]
72. Rogel, A.; Meller, R.; Hanski, E. Adenylate cyclase toxin from *Bordetella pertussis*. The relationship between induction of cAMP and hemolysis. *J. Biol. Chem.* **1991**, *266*, 3154–3161. [PubMed]

73. Masin, J.; Konopasek, I.; Svobodova, J.; Sebo, P. Different structural requirements for adenylate cyclase toxin interactions with erythrocyte and liposome membranes. *Biochim. Biophys. Acta* **2004**, *1660*, 144–154. [CrossRef] [PubMed]
74. Bauche, C.; Chenal, A.; Knapp, O.; Bodenreider, C.; Benz, R.; Chaffotte, A.; Ladant, D. Structural and functional characterization of an essential RTX subdomain of *Bordetella pertussis* adenylate cyclase toxin. *J. Biol. Chem.* **2006**, *281*, 16914–16926. [CrossRef] [PubMed]
75. Chenal, A.; Guijarro, J.I.; Raynal, B.; Delepierre, M.; Ladant, D. RTX calcium binding motifs are intrinsically disordered in the absence of calcium: Implication for protein secretion. *J. Biol. Chem.* **2009**, *284*, 1781–1789. [CrossRef] [PubMed]
76. Knapp, O.; Maier, E.; Polleichtner, G.; Masin, J.; Sebo, P.; Benz, R. Channel formation in model membranes by the adenylate cyclase toxin of *Bordetella pertussis*: Effect of calcium. *Biochemistry* **2003**, *42*, 8077–8084. [CrossRef] [PubMed]
77. Fiser, R.; Konopasek, I. Different modes of membrane permeabilization by two RTX toxins: HlyA from *Escherichia coli* and CyaA from *Bordetella pertussis*. *Biochim. Biophys. Acta* **2009**, *1788*, 1249–1254. [CrossRef] [PubMed]
78. Martin, C.; Requero, M.A.; Masin, J.; Konopasek, I.; Goni, F.M.; Sebo, P.; Ostolaza, H. Membrane restructuring by *Bordetella pertussis* adenylate cyclase toxin, a member of the RTX toxin family. *J. Bacteriol.* **2004**, *186*, 3760–3765. [CrossRef] [PubMed]
79. Knapp, O.; Maier, E.; Masin, J.; Sebo, P.; Benz, R. Pore formation by the *Bordetella* adenylate cyclase toxin in lipid bilayer membranes: Role of voltage and pH. *Biochim. Biophys. Acta* **2008**, *1778*, 260–269. [CrossRef] [PubMed]
80. Barry, E.M.; Weiss, A.A.; Ehrmann, I.E.; Gray, M.C.; Hewlett, E.L.; Goodwin, M.S. *Bordetella pertussis* adenylate cyclase toxin and hemolytic activities require a second gene, *cyaC*, for activation. *J. Bacteriol.* **1991**, *173*, 720–726. [CrossRef] [PubMed]
81. Sebo, P.; Glaser, P.; Sakamoto, H.; Ullmann, A. High-level synthesis of active adenylate cyclase toxin of *Bordetella pertussis* in a reconstructed *Escherichia coli* system. *Gene* **1991**, *104*, 19–24. [CrossRef]
82. Havlicek, V.; Higgins, L.; Chen, W.; Halada, P.; Sebo, P.; Sakamoto, H.; Hackett, M. Mass spectrometric analysis of recombinant adenylate cyclase toxin from *Bordetella pertussis* strain 18323/pHSP9. *J. Mass Spectrom. JMS* **2001**, *36*, 384–391. [CrossRef] [PubMed]
83. Basar, T.; Havlicek, V.; Bezouskova, S.; Halada, P.; Hackett, M.; Sebo, P. The conserved lysine 860 in the additional fatty-acylation site of *Bordetella pertussis* adenylate cyclase is crucial for toxin function independently of its acylation status. *J. Biol. Chem.* **1999**, *274*, 10777–10783. [CrossRef] [PubMed]
84. Masin, J.; Basler, M.; Knapp, O.; El-Azami-El-Idrissi, M.; Maier, E.; Konopasek, I.; Benz, R.; Leclerc, C.; Sebo, P. Acylation of lysine 860 allows tight binding and cytotoxicity of *Bordetella* adenylate cyclase on CD11b-expressing cells. *Biochemistry* **2005**, *44*, 12759–12766. [CrossRef] [PubMed]
85. Basar, T.; Havlicek, V.; Bezouskova, S.; Hackett, M.; Sebo, P. Acylation of lysine 983 is sufficient for toxin activity of *Bordetella pertussis* adenylate cyclase. Substitutions of alanine 140 modulate acylation site selectivity of the toxin acyltransferase CyaC. *J. Biol. Chem.* **2001**, *276*, 348–354. [CrossRef] [PubMed]
86. Baumann, U. Crystal structure of the 50 kda metallo protease from *Serratia marcescens*. *J. Mol. Biol.* **1994**, *242*, 244–251. [CrossRef] [PubMed]
87. Baumann, U.; Wu, S.; Flaherty, K.M.; McKay, D.B. Three-dimensional structure of the alkaline protease of *Pseudomonas aeruginosa*: A two-domain protein with a calcium binding parallel beta roll motif. *EMBO J.* **1993**, *12*, 3357–3364. [PubMed]
88. Meier, R.; Drepper, T.; Svensson, V.; Jaeger, K.E.; Baumann, U. A calcium-gated lid and a large beta-roll sandwich are revealed by the crystal structure of extracellular lipase from *Serratia marcescens*. *J. Biol. Chem.* **2007**, *282*, 31477–31483. [CrossRef] [PubMed]
89. Cannella, S.E.; Ntsogo Enguene, V.Y.; Davi, M.; Malosse, C.; Sotomayor Perez, A.C.; Chamot-Rooke, J.; Vachette, P.; Durand, D.; Ladant, D.; Chenal, A. Stability, structural and functional properties of a monomeric, calcium-loaded adenylate cyclase toxin, CyaA, from *Bordetella pertussis*. *Sci. Rep.* **2017**, *7*, 42065. [CrossRef] [PubMed]
90. El-Azami-El-Idrissi, M.; Bauche, C.; Loucka, J.; Osicka, R.; Sebo, P.; Ladant, D.; Leclerc, C. Interaction of *Bordetella pertussis* adenylate cyclase with CD11b/CD18: Role of toxin acylation and identification of the main integrin interaction domain. *J. Biol. Chem.* **2003**, *278*, 38514–38521. [CrossRef] [PubMed]

91. Wang, X.; Stapleton, J.A.; Klesmith, J.R.; Hewlett, E.L.; Whitehead, T.A.; Maynard, J.A. Fine epitope mapping of two antibodies neutralizing the *Bordetella* adenylate cyclase toxin. *Biochemistry* **2017**, *56*, 1324–1336. [CrossRef] [PubMed]
92. Masure, H.R.; Au, D.C.; Gross, M.K.; Donovan, M.G.; Storm, D.R. Secretion of the *Bordetella pertussis* adenylate cyclase from *Escherichia coli* containing the hemolysin operon. *Biochemistry* **1990**, *29*, 140–145. [CrossRef] [PubMed]
93. Holland, I.B.; Peherstorfer, S.; Kanonenberg, K.; Lenders, M.; Reimann, S.; Schmitt, L. Type I protein secretion-deceptively simple yet with a wide range of mechanistic variability across the family. *EcoSal Plus* **2016**, *7*. [CrossRef]
94. Thomas, S.; Holland, I.B.; Schmitt, L. The type 1 secretion pathway—The hemolysin system and beyond. *Biochim. Biophys. Acta* **2014**, *1843*, 1629–1641. [CrossRef] [PubMed]
95. O'Brien, D.P.; Hernandez, B.; Durand, D.; Hourdel, V.; Sotomayor-Perez, A.C.; Vachette, P.; Ghomi, M.; Chamot-Rooke, J.; Ladant, D.; Brier, S.; et al. Structural models of intrinsically disordered and calcium-bound folded states of a protein adapted for secretion. *Sci. Rep.* **2015**, *5*, 14223. [CrossRef] [PubMed]
96. Sotomayor-Perez, A.C.; Ladant, D.; Chenal, A. Disorder-to-order transition in the CyaA toxin RTX domain: Implications for toxin secretion. *Toxins* **2014**, *7*, 1–20. [CrossRef] [PubMed]
97. Szilvay, G.R.; Blenner, M.A.; Shur, O.; Cropek, D.M.; Banta, S. A fret-based method for probing the conformational behavior of an intrinsically disordered repeat domain from *Bordetella pertussis* adenylate cyclase. *Biochemistry* **2009**, *48*, 11273–11282. [CrossRef] [PubMed]
98. Lenders, M.H.; Weidtkamp-Peters, S.; Kleinschrodt, D.; Jaeger, K.E.; Smits, S.H.; Schmitt, L. Directionality of substrate translocation of the hemolysin A type I secretion system. *Sci. Rep.* **2015**, *5*, 12470. [CrossRef] [PubMed]
99. Gray, M.C.; Ross, W.; Kim, K.; Hewlett, E.L. Characterization of binding of adenylate cyclase toxin to target cells by flow cytometry. *Infect. Immun.* **1999**, *67*, 4393–4399. [PubMed]
100. Hanski, E. Invasive adenylate cyclase toxin of *Bordetella pertussis*. *Trends Biochem. Sci.* **1989**, *14*, 459–463. [CrossRef]
101. Vojtova, J.; Kofronova, O.; Sebo, P.; Benada, O. *Bordetella* adenylate cyclase toxin induces a cascade of morphological changes of sheep erythrocytes and localizes into clusters in erythrocyte membranes. *Microsc. Res. Tech.* **2006**, *69*, 119–129. [CrossRef] [PubMed]
102. Pearson, R.D.; Symes, P.; Conboy, M.; Weiss, A.A.; Hewlett, E.L. Inhibition of monocyte oxidative responses by *Bordetella pertussis* adenylate cyclase toxin. *J. Immunol.* **1987**, *139*, 2749–2754. [PubMed]
103. Gueirard, P.; Druilhe, A.; Pretolani, M.; Guiso, N. Role of adenylate cyclase-hemolysin in alveolar macrophage apoptosis during *Bordetella pertussis* infection in vivo. *Infect. Immun.* **1998**, *66*, 1718–1725. [PubMed]
104. Harvill, E.T.; Cotter, P.A.; Yuk, M.H.; Miller, J.F. Probing the function of *Bordetella bronchiseptica* adenylate cyclase toxin by manipulating host immunity. *Infect. Immun.* **1999**, *67*, 1493–1500. [PubMed]
105. Ambagala, T.C.; Ambagala, A.P.; Srikumaran, S. The leukotoxin of *Pasteurella haemolytica* binds to beta(2) integrins on bovine leukocytes. *FEMS Microbiol. Lett.* **1999**, *179*, 161–167. [PubMed]
106. Jeyaseelan, S.; Hsuan, S.L.; Kannan, M.S.; Walcheck, B.; Wang, J.F.; Kehrli, M.E.; Lally, E.T.; Sieck, G.C.; Maheswaran, S.K. Lymphocyte function-associated antigen 1 is a receptor for *Pasteurella haemolytica* leukotoxin in bovine leukocytes. *Infect. Immun.* **2000**, *68*, 72–79. [CrossRef] [PubMed]
107. Lally, E.T.; Kieba, I.R.; Sato, A.; Green, C.L.; Rosenbloom, J.; Korostoff, J.; Wang, J.F.; Shenker, B.J.; Ortlepp, S.; Robinson, M.K.; et al. RTX toxins recognize a beta2 integrin on the surface of human target cells. *J. Biol. Chem.* **1997**, *272*, 30463–30469. [CrossRef] [PubMed]
108. Li, J.; Clinkenbeard, K.D.; Ritchey, J.W. Bovine CD18 identified as a species specific receptor for *Pasteurella haemolytica* leukotoxin. *Vet. Microbiol.* **1999**, *67*, 91–97. [CrossRef]
109. Arnaout, M.A. Structure and function of the leukocyte adhesion molecules CD11/CD18. *Blood* **1990**, *75*, 1037–1050. [PubMed]
110. Mazzone, A.; Ricevuti, G. Leukocyte CD11/CD18 integrins: Biological and clinical relevance. *Haematologica* **1995**, *80*, 161–175. [PubMed]
111. Eby, J.C.; Gray, M.C.; Warfel, J.M.; Paddock, C.D.; Jones, T.F.; Day, S.R.; Bowden, J.; Poulter, M.D.; Donato, G.M.; Merkel, T.J.; et al. Quantification of the adenylate cyclase toxin of *Bordetella pertussis* in vitro and during respiratory infection. *Infect. Immun.* **2013**, *81*, 1390–1398. [CrossRef] [PubMed]

112. Ahmad, J.N.; Cerny, O.; Linhartova, I.; Masin, J.; Osicka, R.; Sebo, P. cAMP signalling of *Bordetella* adenylate cyclase toxin through the SHP-1 phosphatase activates the BimEL-Bax pro-apoptotic cascade in phagocytes. *Cell. Microbiol.* **2016**, *18*, 384–398. [CrossRef] [PubMed]
113. Corbi, A.L.; Kishimoto, T.K.; Miller, L.J.; Springer, T.A. The human leukocyte adhesion glycoprotein Mac-1 (complement receptor type 3, CD11b) alpha subunit. Cloning, primary structure, and relation to the integrins, von Willebrand factor and factor B. *J. Biol. Chem.* **1988**, *263*, 12403–12411. [PubMed]
114. Hickstein, D.D.; Hickey, M.J.; Ozols, J.; Baker, D.M.; Back, A.L.; Roth, G.J. cDNA sequence for the alpha M subunit of the human neutrophil adherence receptor indicates homology to integrin alpha subunits. *Proc. Natl. Acad. Sci. USA* **1989**, *86*, 257–261. [CrossRef] [PubMed]
115. Diamond, M.S.; Garcia-Aguilar, J.; Bickford, J.K.; Corbi, A.L.; Springer, T.A. The I domain is a major recognition site on the leukocyte integrin Mac-1 (CD11b/CD18) for four distinct adhesion ligands. *J. Cell Biol.* **1993**, *120*, 1031–1043. [CrossRef] [PubMed]
116. Oxvig, C.; Springer, T.A. Experimental support for a beta-propeller domain in integrin alpha-subunits and a calcium binding site on its lower surface. *Proc. Natl. Acad. Sci. USA* **1998**, *95*, 4870–4875. [CrossRef] [PubMed]
117. Lee, J.O.; Rieu, P.; Arnaout, M.A.; Liddington, R. Crystal structure of the A domain from the alpha subunit of integrin CR3 (CD11b/CD18). *Cell* **1995**, *80*, 631–638. [CrossRef]
118. Michishita, M.; Videm, V.; Arnaout, M.A. A novel divalent cation-binding site in the a domain of the beta 2 integrin cr3 (cd11b/cd18) is essential for ligand binding. *Cell* **1993**, *72*, 857–867. [CrossRef]
119. Gahmberg, C.G.; Tolvanen, M.; Kotovuori, P. Leukocyte adhesion-structure and function of human leukocyte beta2-integrins and their cellular ligands. *Eur. J. Biochem.* **1997**, *245*, 215–232. [CrossRef] [PubMed]
120. Hasan, S.; Osickova, A.; Bumba, L.; Novak, P.; Sebo, P.; Osicka, R. Interaction of *Bordetella* adenylate cyclase toxin with complement receptor 3 involves multivalent glycan binding. *FEBS Lett.* **2015**, *589*, 374–379. [CrossRef] [PubMed]
121. Asada, M.; Furukawa, K.; Kantor, C.; Gahmberg, C.G.; Kobata, A. Structural study of the sugar chains of human leukocyte cell adhesion molecules CD11/CD18. *Biochemistry* **1991**, *30*, 1561–1571. [CrossRef] [PubMed]
122. Morova, J.; Osicka, R.; Masin, J.; Sebo, P. RTX cytotoxins recognize beta2 integrin receptors through N-linked oligosaccharides. *Proc. Natl. Acad. Sci. USA* **2008**, *105*, 5355–5360. [CrossRef] [PubMed]
123. Hirai, M.; Iwase, H.; Hayakawa, T.; Koizumi, M.; Takahashi, H. Determination of asymmetric structure of ganglioside-DPPC mixed vesicle using SANS, SAXS, and DLS. *Biophys. J.* **2003**, *85*, 1600–1610. [CrossRef]
124. Wald, T.; Osickova, A.; Masin, J.; Liskova, P.M.; Petry-Podgorska, I.; Matousek, T.; Sebo, P.; Osicka, R. Transmembrane segments of complement receptor 3 do not participate in cytotoxic activities but determine receptor structure required for action of *Bordetella* adenylate cyclase toxin. *Pathog. Dis.* **2016**, *74*. [CrossRef] [PubMed]
125. Veneziano, R.; Rossi, C.; Chenal, A.; Devoisselle, J.M.; Ladant, D.; Chopineau, J. *Bordetella pertussis* adenylate cyclase toxin translocation across a tethered lipid bilayer. *Proc. Natl. Acad. Sci. USA* **2013**, *110*, 20473–20478. [CrossRef] [PubMed]
126. Powthongchin, B.; Angsuthanasombat, C. Effects on haemolytic activity of single proline substitutions in the *Bordetella pertussis* CyaA pore-forming fragment. *Arch. Microbiol.* **2009**, *191*, 1–9. [CrossRef] [PubMed]
127. Betsou, F.; Sebo, P.; Guiso, N. CyaC-mediated activation is important not only for toxic but also for protective activities of *Bordetella pertussis* adenylate cyclase-hemolysin. *Infect. Immun.* **1993**, *61*, 3583–3589. [PubMed]
128. Vojtova-Vodolanova, J.; Basler, M.; Osicka, R.; Knapp, O.; Maier, E.; Cerny, J.; Benada, O.; Benz, R.; Sebo, P. Oligomerization is involved in pore formation by *Bordetella* adenylate cyclase toxin. *FASEB J.* **2009**, *23*, 2831–2843. [CrossRef] [PubMed]
129. Bejerano, M.; Nisan, I.; Ludwig, A.; Goebel, W.; Hanski, E. Characterization of the C-terminal domain essential for toxic activity of adenylate cyclase toxin. *Mol. Microbiol.* **1999**, *31*, 381–392. [CrossRef] [PubMed]
130. Kurehong, C.; Powthongchin, B.; Thamwiriyasati, N.; Angsuthanasombat, C. Functional significance of the highly conserved Glu(570) in the putative pore-forming helix 3 of the *Bordetella pertussis* haemolysin toxin. *Toxicon* **2011**, *57*, 897–903. [CrossRef] [PubMed]
131. Anthis, N.J.; Campbell, I.D. The tail of integrin activation. *Trends Biochem. Sci.* **2011**, *36*, 191–198. [CrossRef] [PubMed]

132. Tan, S.M. The leucocyte beta2 (CD18) integrins: The structure, functional regulation and signalling properties. *Biosci. Rep.* **2012**, *32*, 241–269. [CrossRef] [PubMed]
133. Kinashi, T. Adhere upright: A switchblade-like extension of beta2 integrins. *Immunity* **2006**, *25*, 521–522. [CrossRef] [PubMed]
134. Luo, B.H.; Springer, T.A. Integrin structures and conformational signaling. *Curr. Opin. Cell Biol.* **2006**, *18*, 579–586. [CrossRef] [PubMed]
135. Yalamanchili, P.; Lu, C.; Oxvig, C.; Springer, T.A. Folding and function of I domain-deleted Mac-1 and lymphocyte function-associated antigen-1. *J. Biol. Chem.* **2000**, *275*, 21877–21882. [CrossRef] [PubMed]
136. Jakus, Z.; Fodor, S.; Abram, C.L.; Lowell, C.A.; Mocsai, A. Immunoreceptor-like signaling by beta 2 and beta 3 integrins. *Trends Cell Biol.* **2007**, *17*, 493–501. [CrossRef] [PubMed]
137. Mocsai, A.; Zhou, M.; Meng, F.; Tybulewicz, V.L.; Lowell, C.A. Syk is required for integrin signaling in neutrophils. *Immunity* **2002**, *16*, 547–558. [CrossRef]
138. Mocsai, A.; Abram, C.L.; Jakus, Z.; Hu, Y.; Lanier, L.L.; Lowell, C.A. Integrin signaling in neutrophils and macrophages uses adaptors containing immunoreceptor tyrosine-based activation motifs. *Nat. Immunol.* **2006**, *7*, 1326–1333. [CrossRef] [PubMed]
139. Mocsai, A.; Ruland, J.; Tybulewicz, V.L. The Syk tyrosine kinase: A crucial player in diverse biological functions. *Nat. Rev. Immunol.* **2010**, *10*, 387–402. [CrossRef] [PubMed]
140. Schymeinsky, J.; Mocsai, A.; Walzog, B. Neutrophil activation via beta2 integrins (CD11/CD18): Molecular mechanisms and clinical implications. *Thromb. Haemost.* **2007**, *98*, 262–273. [PubMed]
141. Crowley, M.T.; Costello, P.S.; Fitzer-Attas, C.J.; Turner, M.; Meng, F.; Lowell, C.; Tybulewicz, V.L.; DeFranco, A.L. A critical role for Syk in signal transduction and phagocytosis mediated by Fcgamma receptors on macrophages. *J. Exp. Med.* **1997**, *186*, 1027–1039. [CrossRef] [PubMed]
142. Kiefer, F.; Brumell, J.; Al-Alawi, N.; Latour, S.; Cheng, A.; Veillette, A.; Grinstein, S.; Pawson, T. The Syk protein tyrosine kinase is essential for Fcgamma receptor signaling in macrophages and neutrophils. *Mol. Cell Biol.* **1998**, *18*, 4209–4220. [CrossRef] [PubMed]
143. Shi, Y.; Tohyama, Y.; Kadono, T.; He, J.; Miah, S.M.; Hazama, R.; Tanaka, C.; Tohyama, K.; Yamamura, H. Protein-tyrosine kinase Syk is required for pathogen engulfment in complement-mediated phagocytosis. *Blood* **2006**, *107*, 4554–4562. [CrossRef] [PubMed]
144. Caron, E.; Hall, A. Identification of two distinct mechanisms of phagocytosis controlled by different Rho GTPases. *Science* **1998**, *282*, 1717–1721. [CrossRef] [PubMed]
145. Lenz, D.H.; Weingart, C.L.; Weiss, A.A. Phagocytosed *Bordetella pertussis* fails to survive in human neutrophils. *Infect. Immun.* **2000**, *68*, 956–959. [CrossRef] [PubMed]
146. Willeke, T.; Schymeinsky, J.; Prange, P.; Zahler, S.; Walzog, B. A role for Syk-kinase in the control of the binding cycle of the beta2 integrins (CD11/CD18) in human polymorphonuclear neutrophils. *J. Leukoc. Biol.* **2003**, *74*, 260–269. [CrossRef] [PubMed]
147. Gevrey, J.C.; Isaac, B.M.; Cox, D. Syk is required for monocyte/macrophage chemotaxis to CX3CL1 (fractalkine). *J. Immunol.* **2005**, *175*, 3737–3745. [CrossRef] [PubMed]
148. Forsberg, M.; Lofgren, R.; Zheng, L.; Stendahl, O. Tumour necrosis factor-alpha potentiates CR3-induced respiratory burst by activating p38 MAP kinase in human neutrophils. *Immunology* **2001**, *103*, 465–472. [CrossRef] [PubMed]
149. Van Ziffle, J.A.; Lowell, C.A. Neutrophil-specific deletion of Syk kinase results in reduced host defense to bacterial infection. *Blood* **2009**, *114*, 4871–4882. [CrossRef] [PubMed]
150. Friedman, R.L.; Fiederlein, R.L.; Glasser, L.; Galgiani, J.N. *Bordetella pertussis* adenylate cyclase: Effects of affinity-purified adenylate cyclase on human polymorphonuclear leukocyte functions. *Infect. Immun.* **1987**, *55*, 135–140. [PubMed]
151. Eby, J.C.; Gray, M.C.; Hewlett, E.L. Cyclic AMP-mediated suppression of neutrophil extracellular trap formation and apoptosis by the *Bordetella pertussis* adenylate cyclase toxin. *Infect. Immun.* **2014**, *82*, 5256–5269. [CrossRef] [PubMed]
152. Guth, A.M.; Janssen, W.J.; Bosio, C.M.; Crouch, E.C.; Henson, P.M.; Dow, S.W. Lung environment determines unique phenotype of alveolar macrophages. *Am. J. Physiol. Lung Cell. Mol. Physiol.* **2009**, *296*, L936–L946. [CrossRef] [PubMed]
153. Gordon, S. Alternative activation of macrophages. *Nat. Rev. Immunol.* **2003**, *3*, 23–35. [CrossRef] [PubMed]

154. Pinilla-Vera, M.; Xiong, Z.; Zhao, Y.; Zhao, J.; Donahoe, M.P.; Barge, S.; Horne, W.T.; Kolls, J.K.; McVerry, B.J.; Birukova, A.; et al. Full spectrum of LPS activation in alveolar macrophages of healthy volunteers by whole transcriptomic profiling. *PLoS ONE* **2016**, *11*, e0159329. [CrossRef] [PubMed]
155. Craig, A.; Mai, J.; Cai, S.; Jeyaseelan, S. Neutrophil recruitment to the lungs during bacterial pneumonia. *Infect. Immun.* **2009**, *77*, 568–575. [CrossRef] [PubMed]
156. Skopova, K.; Tomalova, B.; Kanchev, I.; Rossmann, P.; Svedova, M.; Adkins, I.; Bibova, I.; Tomala, J.; Masin, J.; Guiso, N.; et al. Cyclic AMP-elevating capacity of adenylate cyclase toxin-hemolysin is sufficient for lung infection but not for full virulence of *Bordetella pertussis*. *Infect. Immun.* **2017**, *85*. [CrossRef] [PubMed]
157. Friedman, R.L.; Nordensson, K.; Wilson, L.; Akporiaye, E.T.; Yocum, D.E. Uptake and intracellular survival of *Bordetella pertussis* in human macrophages. *Infect. Immun.* **1992**, *60*, 4578–4585. [PubMed]
158. Valdez, H.A.; Oviedo, J.M.; Gorgojo, J.P.; Lamberti, Y.; Rodriguez, M.E. *Bordetella pertussis* modulates human macrophage defense gene expression. *Pathog. Dis.* **2016**, *74*. [CrossRef] [PubMed]
159. Cheung, G.Y.; Dickinson, P.; Sing, G.; Craigon, M.; Ghazal, P.; Parton, R.; Coote, J.G. Transcriptional responses of murine macrophages to the adenylate cyclase toxin of *Bordetella pertussis*. *Microb. Pathog.* **2008**, *44*, 61–70. [CrossRef] [PubMed]
160. Gray, M.C.; Hewlett, E.L. Cell cycle arrest induced by the bacterial adenylate cyclase toxins from *Bacillus anthracis* and *Bordetella pertussis*. *Cell. Microbiol.* **2011**, *13*, 123–134. [CrossRef] [PubMed]
161. Lee, S.W.; Park, H.J.; Jeon, S.H.; Lee, C.; Seong, R.H.; Park, S.H.; Hong, S. Ubiquitous over-expression of chromatin remodeling factor SRG3 ameliorates the T cell-mediated exacerbation of EAE by modulating the phenotypes of both dendritic cells and macrophages. *PLoS ONE* **2015**, *10*, e0132329. [CrossRef] [PubMed]
162. Sica, A.; Mantovani, A. Macrophage plasticity and polarization: In vivo veritas. *J. Clin. Investig.* **2012**, *122*, 787–795. [CrossRef] [PubMed]
163. Novak, J.; Fabrik, I.; Linhartova, I.; Link, M.; Cerny, O.; Stulik, J.; Sebo, P. Phosphoproteomics of cAMP signaling of *Bordetella* adenylate cyclase toxin in mouse dendritic cells. *Sci. Rep.* under revision.
164. Yong Kim, S.; Jeong, S.; Chah, K.H.; Jung, E.; Baek, K.H.; Kim, S.T.; Shim, J.H.; Chun, E.; Lee, K.Y. Salt-inducible kinases 1 and 3 negatively regulate Toll-like receptor 4-mediated signal. *Mol. Endocrinol.* **2013**, *27*, 1958–1968. [CrossRef] [PubMed]
165. Clark, K.; MacKenzie, K.F.; Petkevicius, K.; Kristariyanto, Y.; Zhang, J.; Choi, H.G.; Peggie, M.; Plater, L.; Pedrioli, P.G.; McIver, E.; et al. Phosphorylation of CRTC3 by the salt-inducible kinases controls the interconversion of classically activated and regulatory macrophages. *Proc. Natl. Acad. Sci. USA* **2012**, *109*, 16986–16991. [CrossRef] [PubMed]
166. MacKenzie, K.F.; Clark, K.; Naqvi, S.; McGuire, V.A.; Nöehren, G.; Kristariyanto, Y.; van den Bosch, M.; Mudaliar, M.; McCarthy, P.C.; Pattison, M.J.; et al. PGE(2) induces macrophage IL-10 production and a regulatory-like phenotype via a protein kinase A-SIK-CRTC3 pathway. *J. Immunol.* **2013**, *190*, 565–577. [CrossRef] [PubMed]
167. Khelef, N.; Zychlinsky, A.; Guiso, N. *Bordetella pertussis* induces apoptosis in macrophages: Role of adenylate cyclase-hemolysin. *Infect. Immun.* **1993**, *61*, 4064–4071. [PubMed]
168. Moujalled, D.; Weston, R.; Anderton, H.; Ninnis, R.; Goel, P.; Coley, A.; Huang, D.C.; Wu, L.; Strasser, A.; Puthalakath, H. Cyclic-AMP-dependent protein kinase A regulates apoptosis by stabilizing the BH3-only protein Bim. *EMBO Rep.* **2011**, *12*, 77–83. [CrossRef] [PubMed]
169. Palen, D.I.; Belmadani, S.; Lucchesi, P.A.; Matrougui, K. Role of SHP-1, Kv.1.2, and cGMP in nitric oxide-induced ERK1/2 map kinase dephosphorylation in rat vascular smooth muscle cells. *Cardiovasc. Res.* **2005**, *68*, 268–277. [CrossRef] [PubMed]
170. Ley, R.; Ewings, K.E.; Hadfield, K.; Howes, E.; Balmanno, K.; Cook, S.J. Extracellular signal-regulated kinases 1/2 are serum-stimulated "Bim(EL) kinases" that bind to the BH3-only protein Bim(EL) causing its phosphorylation and turnover. *J. Biol. Chem.* **2004**, *279*, 8837–8847. [CrossRef] [PubMed]
171. Van Haarst, J.M.; de Wit, H.J.; Drexhage, H.A.; Hoogsteden, H.C. Distribution and immunophenotype of mononuclear phagocytes and dendritic cells in the human lung. *Am. J. Respir. Cell Mol. Biol.* **1994**, *10*, 487–492. [CrossRef] [PubMed]
172. Baharom, F.; Rankin, G.; Blomberg, A.; Smed-Sorensen, A. Human lung mononuclear phagocytes in health and disease. *Front. Immunol.* **2017**, *8*, 499. [CrossRef] [PubMed]
173. Guilliams, M.; Lambrecht, B.N.; Hammad, H. Division of labor between lung dendritic cells and macrophages in the defense against pulmonary infections. *Mucosal Immunol.* **2013**, *6*, 464–473. [CrossRef] [PubMed]

174. Tee, A.R.; Fingar, D.C.; Manning, B.D.; Kwiatkowski, D.J.; Cantley, L.C.; Blenis, J. Tuberous sclerosis complex-1 and -2 gene products function together to inhibit mammalian target of rapamycin (mTOR)-mediated downstream signaling. *Proc. Natl. Acad. Sci. USA* **2002**, *99*, 13571–13576. [CrossRef] [PubMed]
175. Sancak, Y.; Thoreen, C.C.; Peterson, T.R.; Lindquist, R.A.; Kang, S.A.; Spooner, E.; Carr, S.A.; Sabatini, D.M. PRAS40 is an insulin-regulated inhibitor of the mTORC1 protein kinase. *Mol. Cell* **2007**, *25*, 903–915. [CrossRef] [PubMed]
176. Gingras, A.C.; Gygi, S.P.; Raught, B.; Polakiewicz, R.D.; Abraham, R.T.; Hoekstra, M.F.; Aebersold, R.; Sonenberg, N. Regulation of 4E-BP1 phosphorylation: A novel two-step mechanism. *Genes Dev.* **1999**, *13*, 1422–1437. [CrossRef] [PubMed]
177. Schmitz, F.; Heit, A.; Dreher, S.; Eisenächer, K.; Mages, J.; Haas, T.; Krug, A.; Janssen, K.P.; Kirschning, C.J.; Wagner, H. Mammalian target of rapamycin (mTOR) orchestrates the defense program of innate immune cells. *Eur. J. Immunol.* **2008**, *38*, 2981–2992. [CrossRef] [PubMed]
178. Weichhart, T.; Costantino, G.; Poglitsch, M.; Rosner, M.; Zeyda, M.; Stuhlmeier, K.M.; Kolbe, T.; Stulnig, T.M.; Hörl, W.H.; Hengstschläger, M.; et al. The TSC-mTOR signaling pathway regulates the innate inflammatory response. *Immunity* **2008**, *29*, 565–577. [CrossRef] [PubMed]
179. Thomson, A.W.; Turnquist, H.R.; Raimondi, G. Immunoregulatory functions of mTOR inhibition. *Nat. Rev. Immunol.* **2009**, *9*, 324–337. [CrossRef] [PubMed]
180. Perkins, D.J.; Gray, M.C.; Hewlett, E.L.; Vogel, S.N. *Bordetella pertussis* adenylate cyclase toxin (ACT) induces cyclooxygenase-2 (COX-2) in murine macrophages and is facilitated by act interaction with CD11b/CD18 (Mac-1). *Mol. Microbiol.* **2007**, *66*, 1003–1015. [CrossRef] [PubMed]
181. Kreisel, D.; Nava, R.G.; Li, W.; Zinselmeyer, B.H.; Wang, B.; Lai, J.; Pless, R.; Gelman, A.E.; Krupnick, A.S.; Miller, M.J. In Vivo two-photon imaging reveals monocyte-dependent neutrophil extravasation during pulmonary inflammation. *Proc. Natl. Acad. Sci. USA* **2010**, *107*, 18073–18078. [CrossRef] [PubMed]
182. Pechous, R.D. With friends like these: The complex role of neutrophils in the progression of severe pneumonia. *Front. Cell. Infect. Microbiol.* **2017**, *7*, 160. [CrossRef] [PubMed]
183. Eby, J.C.; Hoffman, C.L.; Gonyar, L.A.; Hewlett, E.L. Review of the neutrophil response to *Bordetella pertussis* infection. *Pathog. Dis.* **2015**, *73*, ftv081. [CrossRef] [PubMed]
184. Weingart, C.L.; Mobberley-Schuman, P.S.; Hewlett, E.L.; Gray, M.C.; Weiss, A.A. Neutralizing antibodies to adenylate cyclase toxin promote phagocytosis of *Bordetella pertussis* by human neutrophils. *Infect. Immun.* **2000**, *68*, 7152–7155. [CrossRef] [PubMed]
185. Weingart, C.L.; Weiss, A.A. *Bordetella pertussis* virulence factors affect phagocytosis by human neutrophils. *Infect. Immun.* **2000**, *68*, 1735–1739. [CrossRef] [PubMed]
186. Mobberley-Schuman, P.S.; Connelly, B.; Weiss, A.A. Phagocytosis of *Bordetella pertussis* incubated with convalescent serum. *J. Infect. Dis.* **2003**, *187*, 1646–1653. [CrossRef] [PubMed]
187. Goodwin, M.S.; Weiss, A.A. Adenylate cyclase toxin is critical for colonization and pertussis toxin is critical for lethal infection by *Bordetella pertussis* in infant mice. *Infect. Immun.* **1990**, *58*, 3445–3447. [PubMed]
188. Gross, M.K.; Au, D.C.; Smith, A.L.; Storm, D.R. Targeted mutations that ablate either the adenylate cyclase or hemolysin function of the bifunctional cyaa toxin of *Bordetella pertussis* abolish virulence. *Proc. Natl. Acad. Sci. USA* **1992**, *89*, 4898–4902. [CrossRef] [PubMed]
189. Guiso, N.; Rocancourt, M.; Szatanik, M.; Alonso, J.M. *Bordetella* adenylate cyclase is a virulence associated factor and an immunoprotective antigen. *Microb. Pathog.* **1989**, *7*, 373–380. [CrossRef]
190. Guiso, N.; Szatanik, M.; Rocancourt, M. Protective activity of *Bordetella* adenylate cyclase-hemolysin against bacterial colonization. *Microb. Pathog.* **1991**, *11*, 423–431. [CrossRef]
191. Weiss, A.A.; Hewlett, E.L.; Myers, G.A.; Falkow, S. Tn5-induced mutations affecting virulence factors of *Bordetella pertussis*. *Infect. Immun.* **1983**, *42*, 33–41. [PubMed]
192. Chenal-Francisque, V.; Caro, V.; Boursaux-Eude, C.; Guiso, N. Genomic analysis of the adenylate cyclase-hemolysin C-terminal region of *Bordetella pertussis*, *Bordetella parapertussis* and *Bordetella bronchiseptica*. *Res. Microbiol.* **2009**, *160*, 330–336. [CrossRef] [PubMed]
193. Bart, M.J.; Harris, S.R.; Advani, A.; Arakawa, Y.; Bottero, D.; Bouchez, V.; Cassiday, P.K.; Chiang, C.S.; Dalby, T.; Fry, N.K.; et al. Global population structure and evolution of *Bordetella pertussis* and their relationship with vaccination. *mBio* **2014**, *5*, e01074. [CrossRef] [PubMed]

194. Khelef, N.; Bachelet, C.M.; Vargaftig, B.B.; Guiso, N. Characterization of murine lung inflammation after infection with parental *Bordetella pertussis* and mutants deficient in adhesins or toxins. *Infect. Immun.* **1994**, *62*, 2893–2900. [PubMed]
195. Khelef, N.; Sakamoto, H.; Guiso, N. Both adenylate cyclase and hemolytic activities are required by *Bordetella pertussis* to initiate infection. *Microb. Pathog.* **1992**, *12*, 227–235. [CrossRef]
196. Andreasen, C.; Carbonetti, N.H. Role of neutrophils in response to *Bordetella pertussis* infection in mice. *Infect. Immun.* **2009**, *77*, 1182–1188. [CrossRef] [PubMed]
197. Gorgojo, J.; Scharrig, E.; Gomez, R.M.; Harvill, E.T.; Rodriguez, M.E. *Bordetella parapertussis* circumvents neutrophil extracellular bactericidal mechanisms. *PLoS ONE* **2017**, *12*, e0169936. [CrossRef] [PubMed]